Marine Vessel Wave Wake:
Focus on Vessel Operations within Sheltered Waterways

Gregor J Macfarlane, B.Eng. (Hons), M.Phil.

Submitted in fulfilment of the
requirements for the Degree of
Doctor of Philosophy

Australian Maritime College, University of Tasmania

5 June 2012

Declarations

Declaration of Originality

This thesis contains no material which has been accepted for a degree or diploma by the University or any other institution, except by way of background information and duly acknowledged in the thesis, and to the best of my knowledge and belief no material previously published or written by another person except where due acknowledgement is made in the text of the thesis, nor does the thesis contain any material that infringes copyright.

Authority of Access

This thesis may be made available for loan and limited copying and communication in accordance with the *Copyright Act 1968*.

Gregor J Macfarlane
5 June 2012

Abstract

This thesis reports on an investigation into the characteristics of the wave wake generated by vessels that typically operate within sheltered waterways. It is well known that these waves can result in issues for other users of the waterway and the surrounding environment. These issues include erosion of the surrounding banks, damage or nuisance to moored vessels and other maritime structures and endanger people working or enjoying activities in small craft or close to the shore.

A review of the wave patterns generated at sub-critical, trans-critical and super-critical depth Froude numbers has been conducted, with an emphasis on those craft that commonly utilise sheltered waterways, namely small commercial vessels and recreational craft. Particular attention was given to planing and wakeboarding vessels, given the large and increasing number of these craft. One of the major issues often confronted is that of bank erosion and a study was conducted to determine which measures of erosion potential are the most descriptive in these circumstances.

Over recent decades it has been common to quantify a vessel's wave wake using the characteristics of just a single wave within the entire wave train, usually the highest. However, in this study it has been shown that this is generally inadequate when considering craft operating at trans-critical or super-critical speeds. Three significant waves of interest were described and quantified in this study.

A comprehensive set of model scale experiments was conducted to investigate the effect that water depth, hull form and vessel speed has on the waves generated by nineteen different hull forms, including a mixture of typical monohulls and catamarans. Four primary measures were quantified for each of the three key waves, including wave height, wave period, decay rate and wave angle.

The results from the experiments were used to develop an empirical tool to provide wave wake predictions and to investigate the effect that water depth, hull form and vessel speed has on each of the four primary wave measures. Predictions from the tool were validated against measured data from several independent full scale trials.

A wave wake regulatory criterion, suitable for the operation of typical recreational craft and small commercial vessels operating in sheltered waterways, was proposed and incorporated within the prediction tool.

Acknowledgements

Many people provided assistance during the course of this study, but special thanks are due to:

Prof. Neil Bose, supervisor of both my PhD research and my ‘day job’, firstly for his encouragement and support that has allowed me to undertake this project and for his valuable guidance along the way.

Dr. Jonathan Duffy, not just for his valuable experience and contribution as co-supervisor, but also for the splendid job he did while taking over my day job for over 12 months to allow me the opportunity to undertake this rewarding challenge.

My colleagues within the team at the AMC Towing Tank and Model Test Basin, especially Tim Lilienthal, Kirk Meyer, Drew Honeychurch, Liam Honeychurch and Shaun Denehy, for their assistance while my attention regularly strayed between my day job and PhD.

My colleagues and fellow post-graduates within the AMC National Centre for Maritime Engineering and Hydrodynamics. A special thank you goes to Prof. Martin Renilson for over 20 years of encouragement and advice.

Friend and fellow PhD candidate, Dr.* Alex Robbins, for countless discussions related to boats and wave wake, most of which ended off-topic and in fits of laughter. (**to be confirmed in the near future!*).

Various key participants from industry for their valued input, especially naval architect Greg Cox, geomorphologist Jason Bradbury and cruise vessel owner/operators Troy and Guy Grining.

My wife, Leanne, and children, Lachlan, Callum, Bethany and Ainsley, for their support, encouragement and understanding over the past few years while I have tried (and often failed) to find the right balance between work, study and family. Special thanks also to my mother, father and two sisters – for similar reasons, but over a much longer timeframe.

Table of Contents

List of Figures

List of Tables

Nomenclature

A	Constant
B	Waterline beam
B_{OA}	Beam overall
c_g	Group velocity
c_p	Phase velocity
C_{wp}	Wave probe calibration factor
d	Vessel draught
E	Wave energy per wavelength
E_t	Transmitted wave energy
$\overline{E}$	Wave energy density
f	Wave frequency
F	Fetch
Fr_h	Depth Froude number
Fr_L	Length Froude number
Fr_∇	Volumetric Froude number
g	Acceleration due to gravity
h	Water depth
H	Wave height
H_A	Wave height for Wave A
H_B	Wave height for Wave B
H_C	Wave height for Wave C
H_b	Wave height (benchmark)
H_c	Wave height (conventional vessels)
H_{HSC}	Wave height (high speed craft)
H_n	Height of half-wavelength wave
i_E	Half angle of entry
L	Waterline length
L_{OA}	Length overall
n	Wave decay rate exponent
n_A	Wave decay rate exponent for Wave A
n_B	Wave decay rate exponent for Wave B
n_C	Wave decay rate exponent for Wave C
$\overline{P}$	Average wave power
$\overline{P_n}$	Power of half-wavelength wave
R	Scale factor

s	Demihull spacing (centreline to centreline)
$S(f)$	Spectral ordinate
T	Wave period
T_A	Wave period for Wave A
T_B	Wave period for Wave B
T_C	Wave period for Wave C
T_b	Wave period (benchmark)
T_c	Wave period (conventional vessels)
T_{HSC}	Wave period (high speed craft)
T_n	Period of half-wavelength
T'	Normalised wave period ($T/\sqrt{L}$)
T_A'	Normalised wave period for Wave A ($T/\sqrt{L}$)
T_B'	Normalised wave period for Wave B ($T/\sqrt{L}$)
T_C'	Normalised wave period for Wave C ($T/\sqrt{L}$)
u	Velocity
u_m	Velocity (model)
u_s	Velocity (ship)
U_A	Wind stress factor
V_{wp}	Wave probe voltage
y	Lateral distance between the sailing line and measurement point
α	Angle between wave crests and shoreline
β	Propagation angle of diverging waves to the sailing line of the vessel
γ	Wave height constant
γ_A	Wave height constant for Wave A
γ_B	Wave height constant for Wave B
γ_C	Wave height constant for Wave C
Δ	Vessel displacement
∇	Volume
θ	Wave angle (between the cusp locus line and the sailing line of the vessel)
θ_A	Wave angle of Wave A
θ_B	Wave angle of Wave B
θ_C	Wave angle of Wave C
λ	Wavelength
π	Pi, constant
ρ	Water density
σ	Uncertainty

Abbreviations

AIAA	American Institute of Aeronautics and Astronautics
AMC	Australian Maritime College
ASCE	American Society of Civil Engineers
ASME	American Society of Mechanical Engineers
CFD	Computational Fluid Dynamics
CIP	Constrained Interpolation Profile method
DPIPWE	Department of Primary Industry, Parks, Water and Environment
DTMB	David Taylor Model Basin
FFT	Fast Fourier Transform
GPS	Global Positioning System
HRW	Hydraulics Research Wallingford
HSC	High Speed Craft
IAHR	International Association for Hydro-Environment Engineering and Research
IMarEST	The Institute of Marine Engineering, Science and Technology
ITTC	International Towing Tank Conference
KdV	Korteweg-de Vries equation
KP	Kadomtsev-Petviashvili equations
MCA	Maritime and Coastguard Agency
NTU	Non-dimensional Turbidity Unit
PIANC	Permanent International Association of Navigation Congresses
RANS	Reynolds Averaged Navier Stokes equations
RAPP	Risk Assessment Passage Plan
RINA	Royal Institution of Naval Architects
RPM	Rankine Panel Method
RTK	Real Time Kinematics
SNAME	Society of Naval Architects and Marine Engineers
URANS	Unsteady Reynolds Averaged Navier Stokes equations
USACERC	U.S. Army Coastal Engineering Research Center
WP	Wave probe
WSF	Washington State Ferries

Chapter 1

Introduction

1.1 Definition of the Problem

It is well understood that all vessels generate a pattern of waves when travelling at speed (Lighthill 1978). But since the 1980s the wave wake generated by high-speed marine vessels (also commonly referred to as wash or wake wash) has seen a variety of new issues arise for other users of the waterway and the surrounding environment (PIANC 2003; Murphy *et al*. 2006). These include:

- shoreline (or bank) erosion and/or accretion;
- damage or nuisance to moored vessels;
- damage to jetties and other marine structures;
- endangering people working or enjoying activities in small craft or close to the shore;
- destruction of fragile water plants;
- disturbance of silt;
- damage to the ecology of intertidal and shallow sub-tidal habitat.

The waves generated by large high-speed craft have been blamed for causing several serious accidents, including some fatalities, as was experienced in a well-publicised incident in the United Kingdom in July 1999 where a shoaling wave from a 122 m long high-speed ferry grew to a reported 4 m in height close to shore, swamping a recreational fishing vessel and drowning one person (Fresco 1999; Hamer 1999; Marine Accident Investigation Branch 2000).

Another well documented example of the consequences of the generation of wave wake from large high speed marine craft occurred in the mid-late 1990s in the Canadian province of British Columbia (BC Ferries 2000; Fissel *et al*. 2001; Wikipedia 2010). The provincial government at the time decided to use the provincial Crown corporation BC Ferries to advance its economic (and political) goal of supporting the local shipbuilding industry by creating a fleet of three large custom-designed high-speed catamaran passenger/vehicle ferries, with the eventual goal of exporting additional vessels on the international market. This was an attempt to emulate the success of Australian shipbuilders (such as Incat Tasmania and Austal Ships) in the global fast ferry market. The vessels, referred to as *PacifiCats*, were

supposed to reduce the travel time of the ferry services between the Canadian mainland and Vancouver Island by 30 minutes when compared to the existing conventional ferries. This required that the new vessels operate at a service speed of about 37 knots. Due to various blunders by the government, BC Ferries, design bureaus, and the shipyards, the cost of the program more than doubled from US$210 million to almost US$460 million and final delivery was almost 3 years behind schedule. When operating at design speed, the *PacifiCat* fleet created a large wave wake which was found to have damaged waterfront wharves and property in coastal areas. Subsequently, the fleet were forced to reduce speed when not operating in open seas (up to a third of their route) and alter their route to minimise the time spent close to sensitive shorelines, resulting in a substantial increase in fuel consumption. All these factors combined such that the intended speed advantage offered by these vessels was negated. Following various other problems with the design and operation, as well as bowing to political pressure, the government auctioned off the *PacifiCat* fleet in 2003 for less than US$20 million. At the time of writing, the vessels were being converted into luxury motor yachts at the Abu Dhabi Mar Shipyard in Abu Dhabi (Wikipedia 2010).

The introduction of large high speed ferries passing through the Marlborough Sounds, New Zealand, also caused significant safety and environmental problems during the 1990s. Action by local community groups eventually resulted in a maximum speed limit of 18 knots being imposed in 2000 which eventually led to the removal of high speed craft from this route (Parnell *et al*. 2007). Similar problems have also been published for several other locations, including Denmark (Kofoed-Hansen 1996; Parnell and Kofoed-Hansen 2001), Puget Sound, Washington USA (Fox *et al*. 1993; Stumbo *et al*. 1999), San Francisco Bay, USA (Austin 1999), Sweden (Strom and Ziegler 1998; Allenström *et al*. 2003), and Estonia (Soomere and Rannat 2003).

To address these issues maritime authorities in several regions have imposed regulations on marine traffic (Kofoed-Hansen and Mikkelsen 1997; Kirkegaard *et al*. 1998; Stumbo *et al*. 1999; Whittaker *et al*. 2000a; Albright 2000; Kirk and Single 2000; Croad and Morris 2003). In some specific regions the restrictions have been severe enough that the operation of high-speed vessels is now considered not to be viable, as was the case with the *PacifiCats* and the high speed craft operating in Marlborough Sounds. Situations such as this have resulted in the cancellation of a number of high-speed ferry operations, with some industry experts predicting that this

may lead to the demise of the high-speed ferry industry. The effect of this on the Australian shipbuilding industry would be substantial.

As a result, the wave wake generated by large vessels has received costly and high-profile research programs and regulatory responses to address the operation of these vessels over the past ten to fifteen years. Conversely, the wave wake from small commercial vessels and recreational craft can impact significantly on sheltered waterways, yet the sector receives little research funding and is often regulated with simplistic criteria.

There have been many cases internationally where problems have been attributed to vessel wave wake as a result of the introduction of high-speed recreational and small commercial vessels on sheltered waterways since the mid 1980s. Some of these waterways have been used successfully for transportation and trade for thousands of years, but the introduction of the potentially more damaging waves created by high-speed craft has seen a notable increase in wave wake related issues (Kogoy 1998; Cox 2000; Murphy *et al*. 2006, Cartwright *et al*. 2008).

Sheltered waterways within Australia have certainly not been immune from these issues, resulting in a number of investigations, including the Gordon River (Nanson *et al*. 1994; Bradbury *et al*. 1995), Parramatta River (Smith 1990; Patterson Britton and Partners 1995), Brisbane River (Macfarlane and Cox 2005), Swan and Canning Rivers (Pattiaratchi and Hegge 1990; Macfarlane and Gourlay 2009), Hawkesbury River (Lesleighter 1964; Scholer 1974), Noosa River (Queensland Environmental Protection Agency 2002; Macfarlane and Cox 2003), Maroochy River (Todd 2004; Macfarlane and Cox 2005), Williams River (GHD 2006; Worley Parsons 2010) and Wandandian Creek (O'Reilly 2009).

The demonstrated inability of the shorelines bordering these sheltered, or fetch-limited, waterways to achieve a new dynamic equilibrium condition over the past two decades has led to the increasing need to implement at least one or more of the following remedial measures, Dand *et al*. (1999b):

- regulate vessel operations (vessel speed and/or route) within these regions to minimise or eliminate the generation of damaging waves,
- optimise the vessel design to minimise or eliminate the generation of damaging waves; or,
- implement remedial measures on shore.

It appears that the most commonly adopted of these remedial measures for documented cases in sheltered waterways is to regulate vessel operations through the implementation of suitable criteria (Dand *et al*. 1999b; Croad and Parnell 2002; PIANC 2003; Glamore *et al*. 2005; Phillips and Hook 2006; Bradbury 2007; Osborne *et al*. 2009). Regardless of the actions adopted, there is a demonstrated need to understand the phenomenon and to develop the means to minimise its effect through design and operation.

This requires the development and validation of suitable predictive tools that quantify the characteristics of the waves generated by a wide variety of vessel hull forms under all practical operational conditions at an early stage when planning ferry and other services, including the design of vessels and waterway infrastructure. Developing such prediction tools is a task that has proven to be difficult when attempting to accurately predict the far-field wave wake from near-field measurements due to the very complex array of variables involved (Dand *et al*. 1999a; Campana *et al*. 2005). This is partly because many of the problems associated with vessel-generated waves occur in shallow and/or restricted water and because the pattern of waves generated in shallow water is very different to that generated in deep water (Havelock 1908; Sorensen 1973; Lighthill 1978). There are also additional complexities to take into consideration when the vessel generating the waves is at one water depth and the waves propagate into regions where the water depth and the bathymetry vary. The many factors that need to be considered can be summarised as follows:

- characteristics of the vessel (speed, hull form, waterline length, beam, draught, displacement, etc),
- characteristics of the waterway (water depth, bathymetry, width, bank type and details),
- the distance between the sailing line of the vessel and the shore (or other point of interest) within the waterway, and;
- the rate of decay of the generated waves.

Both the International Towing Tank Conference (Stern *et al*. 2002; Campana *et al*. 2005; Campana *et al*. 2008) and Murphy *et al*. (2006) have conducted reviews of publicly available methodologies for predicting far-field vessel generated waves. Each of these reviews identified that this process has been significantly hampered by a lack of appropriate benchmark data available in the public domain for researchers to undertake comparisons. A common opinion (Campana *et al*. 2008) is that it is still necessary to validate the numerical models in use based on experimental

measurements (either/both model scale or in-situ) before they can be used for managing wave wake in a particular situation, regardless of what type of technique is deemed the most appropriate.

It is also required that regulatory criteria appropriate for the operation of recreational and small commercial vessels operating in sheltered waterways need to be identified. Australia has a relatively large recreational boating population that utilises the limited sheltered waterways available. This is not dissimilar to the USA, where the majority of recreational boating is enjoyed on fresh water lakes and rivers, as well as sheltered coastal waterways, rather than the open ocean. It therefore makes sense to attempt to develop guidelines for vessel wave wake that allow for the sustainable use of these waterways.

To date, the development of vessel operating criteria for mitigating foreshore impacts has been largely vessel and/or site-specific, making transposition of operating criteria between different sites almost impossible. This is thought to be due to the response of research and regulatory bodies being highly reactive in their approach to wave wake and erosion and as such has been characterised by pockets of site-specific research with little attempt at standardisation (Macfarlane and Cox 2007). A partial exception are the Gordon River cruise services in Tasmania which, operating within a National Park and World Heritage Area, are regulated by a land management rather than maritime agency. There the initial response in the early 1990s was reactive, but became proactive with the implementation of a long-term monitoring and vessel certification process that is on-going today (Bradbury *et al*. 1995; Bradbury 2007).

In order to develop wave wake criteria, certain simplified parameters that characterise a vessel's wave wake must be used; otherwise the total range of variables may prove too large to be of practical use (Nanson *et al*. 1994; Macfarlane and Cox 2004). However, many existing wave wake criteria are based on over-simplified concepts and may provide only limited protection against foreshore erosion. From a review of wave wake criteria in use worldwide, older methods that relied on wave height alone are being superseded by measures involving wave power or energy (Macfarlane and Cox 2007). This reflects the growing understanding that wave period and not just wave height is a major determinant of wave wake severity.

1.2 Hypothesis and Research Questions

Hypothesis:

It is hypothesised that bank erosion and other issues caused by vessel generated waves can be avoided, or at least minimised, if (a) the causes of the phenomenon are identified and generally understood, (b) a technique for quantifying the primary characteristics of the waves generated by a wide range of marine vessels, under varying operating conditions, is developed and validated, (c) the resultant predictions of vessel wave wake are assessed using appropriate regulatory criteria, and (d) appropriate remedial actions are undertaken.

Research Questions:

The following questions were posed to enable the above hypotheses to be tested:

- What is the background to this phenomenon?
- Can a wave wake prediction tool be developed based on physical scale model experimental data?
- Can the wave wake prediction tool cover vessel operations at sub-critical, trans-critical and super-critical vessel speeds?
- Can the wave wake prediction tool be used to investigate the effect of vessel hull form?
- Can the wave wake prediction tool be validated against full scale experimental data?
- What are appropriate wave wake criteria for vessel operations on sheltered waterways with sensitive shorelines?
- Can the combined application of the wave wake prediction tool and regulatory criteria be used to determine appropriate remedial measures?

1.3 Overview of Thesis Structure

The primary objective of this study is to develop a technique to assess the wave wake of vessels that operate within sheltered waterways that possess sensitive shorelines. This involves the following three key tasks: (1) describe the background and issues related to this issue, (2) develop a prediction tool that can quantify the characteristics of the waves generated by a wide variety of vessel hull forms under practical operational conditions and (3) propose the adoption of suitable regulatory criteria for vessel operations on sheltered waterways. The combined use of the prediction tool and criteria will provide the means to identify any potential wave wake issues very

early in planning and design stages. In order to achieve this objective, a clear understanding of wave wake issues is required, covering several disciplines.

A summary of the thesis structure is provided below.

Chapter 1 ***Introduction*****:** provides background information and defines the problem. Several research questions and objectives of this research are posed.

Chapter 2 ***Vessel Generated Waves*****:** provides general background information on vessel generated waves. This includes a review of the wave patterns generated at sub-critical, trans-critical, critical and super-critical flow regimes. The regimes are a function of depth Froude number, blockage and the three primary vessel speed regimes: displacement, semi-displacement and high-speed (planing). Particular attention is given to planing vessels due to the large numbers of these vessels used for activities such as water skiing, wakeboarding and fishing within sheltered waterways. Some specific wave wake issues related to wakeboarding are also discussed. Several other relevant topics are also briefly reviewed, such as propagating wave phenomena (dispersion and attenuation), restricted channel effects and basic characteristics of wind generated waves. In addition, background information on some issues related to wave wake when vessels operate within sheltered waterways is covered. This includes an outline of the distinct regions where wave wake issues have occurred in recent decades and identifies those regions where bank erosion is of primary interest, including a brief description of the various types of banks.

Chapter 3 ***Quantifying Vessel Wave Wake and Bank Erosion*****:** reviews the basic requirements of wave wake measures and provides background on the effect that vessel speed, principal particulars, displacement and water depth have on the wave patterns and characteristics of the waves generated. The specific measures adopted within this study are stated, including justification for selecting these measures over other techniques. The use of quantities such as wave energy and wave power (often adopted within regulatory criteria) is also discussed. A brief review of previous and current work on the quantification of shoreline (bank) erosion due to vessel wave wake is undertaken. Particular attention is given to some of the most recent work conducted on the lower Gordon River in South-West Tasmania, which includes an investigation into the most common parameters used to quantify bank erosion due to vessel wave wake.

Chapter 4 ***Wave Wake Prediction Techniques*****:** provides a review of previous work on the prediction of vessel wave wake, using both experimental and numerical techniques.

Chapter 5 ***Wave Wake Experiments*****:** presents and discusses the results from a series of physical scale model experiments designed to quantify the wave wake from many different hull forms operating over a wide range of water depths and vessel speeds.

Chapter 6 ***Wave Wake Prediction Tool*****:** outlines the development of a tool for predicting the relevant wave wake characteristics generated by a wide range of recreational and small commercial vessels operating at sub-critical, trans-critical and super-critical speeds. The wave wake prediction tool is validated by comparing predictions against measurements from full scale experiments. The prediction tool is also used to determine key hull form parameters for minimising bank erosion and other wave wake issues.

Chapter 7 ***Wave Wake Regulatory Criteria*****:** provides a brief review of wave wake criteria for regulating vessel operations. A specific criterion is proposed that is believed to be appropriate to the operation of typical recreational craft and small commercial vessels operating in sheltered waterways. This criterion is incorporated within the prediction tool. Examples are provided that outline the application of the prediction tool and proposed regulatory criteria.

Chapter 8 ***Conclusions, Recommendations and Further Work*****:** contains a summary, conclusions and brief details on potential future work.

Chapter 2

Vessel Generated Waves

As noted in Chapter 1, this section has been included to provide background information on relevant boat wave wake issues with a particular focus on the operation of commercial and recreational vessels on sheltered waterways.

2.1 Vessel Wave Patterns

2.1.1 Introduction

The general wave pattern generated by a vessel is largely independent of vessel form, but it is affected by water depth and vessel speed. Traditionally, naval architects and maritime engineers have adopted the length Froude number, Fr_L, as defined in Equation 2.1, to non-dimensionalise vessel speed.

$$Fr_L = \frac{u}{\sqrt{gL}} \tag{2.1}$$

Vessel wave wake is often divided into three categories, depending on vessel speed and water depth. The defining parameter is depth Froude number, Fr_h, a non-dimensional relationship between vessel speed and water depth, as defined in Equation 2.2.

$$Fr_h = \frac{u}{\sqrt{gh}} \tag{2.2}$$

Discussion within Section 2.1 generally refers to cases where the waterway is of infinite width. The effect of waterway width is discussed in Section 2.5.3.

Depth Froude number has its greatest effect when the water depth is less than about one-quarter the vessel's waterline length; it has moderate influence at depths up to one-half the waterline length and has little influence at depths greater than the waterline length.

The water depth limits the speed at which a wave can travel in shallow water, such that the maximum speed will be reached when the depth Froude number equals one.

At a vessel speed below a depth Froude number of one, the speed is said to be sub-critical. A depth Froude number of one is termed the critical speed and speeds leading up to the critical speed are sometimes referred to as trans-critical speeds (approximately $0.75 \leq Fr_h \leq 1.0$). The position of the lower bound of the trans-critical range can vary according to vessel and waterway conditions and between reference texts on the subject. Speeds above a depth Froude number of one are said to be super-critical.

2.1.2 Sub-Critical Speeds ($Fr_h < 0.75$)

For cases where the depth Froude number is less than 1 (more importantly, when the depth Froude number is less than about 0.75), all vessels produce a wave pattern termed the Kelvin wave pattern, named after Lord Kelvin (then Sir William Thomson), an early pioneer of vessel wave theory (Thomson 1887). A typical Kelvin wave pattern is presented in Figure 2.1. It is characterised by two wave types - transverse and divergent waves.

Transverse Waves
These waves are commonly referred to as stern waves and propagate parallel to the vessel's sailing line. The height of these waves is largely a function of vessel length-displacement ratio, with a heavy, short vessel producing higher waves. The period of the transverse waves is a function of vessel speed, as they effectively travel along with the vessel.

Divergent Waves
Commonly referred to as bow waves, the divergent waves propagate obliquely to the vessel’s sailing line at an angle of approximately 55 degrees. This wave formation, referred to as the Kelvin wedge, subtends an angle of slightly less than 20 degrees to the sailing line, which is constant for all vessel forms. Many vessels also create stern divergent waves, though this additional wave train usually melds into the bow divergent system at some point aft of the vessel. Divergent waves are generally steep and close together near the vessel - carrying as much energy as possible for their wavelength. An exception to this can occur at very low length Froude numbers.

The point of intersection of the transverse and divergent wave trains is termed the cusp and represents a localised wave height peak. At successive cusps, the divergent waves decay in height slower than the transverse waves, such that a vessel wake

measured far from the sailing line will feature divergent waves more prominently. The transverse and divergent waves do not actually meet at the Kelvin wedge due to a phase difference of one-quarter of a period (Wehausen and Laitone 1960). However, superposition of the two wave trains does occur, resulting in localised wave height peaks of 'cusp-like' nature, often referred to as cusp points or the cusp locus line. Here, the term 'cusp' is used for its practical and descriptive simplicity.

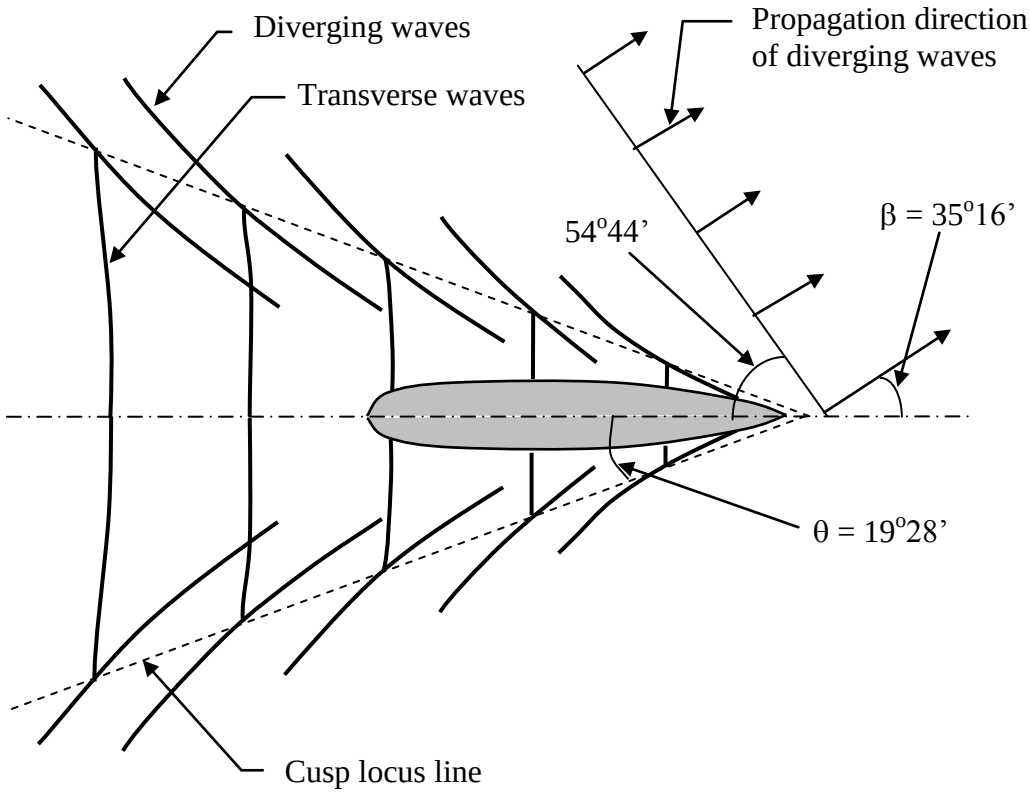

Figure 2.1 Kelvin wave pattern

The waves attenuate (decay) in height with increasing lateral distance from the vessel sailing line. The oblique propagation angle of the divergent system compared with the transverse system means that the divergent system is usually of greater interest when assessing bank erosion, as these waves propagate towards the shore.

There are exceptions to this. If a vessel producing a significant transverse wave system, such as a heavy vessel, changes course, the transverse waves created prior to the course change will continue to propagate along the original course and may eventually reach the shore. This is commonly noted when slow speed displacement vessels traverse a narrow river at cruising speed. The river traps the transverse waves and does not allow them to diffract (spread their energy by growing sideways in crest

length), greatly reducing their height decay. These waves may be evident for several minutes after the vessel has passed.

The theoretical point at which vessel generated waves will start to become depth-affected is at a depth Froude number of approximately 0.57 (Sorensen 1969), although this effect is generally negligible until the depth Froude number increases to around 0.75.

2.1.3 Trans-critical Speeds ($0.75 < Fr_h < 1.0$)

When the depth Froude number enters the trans-critical speed zone ($0.75 < Fr_h < 1.0$) the wave pattern changes. This can be as a result of the water depth shoaling or the vessel's speed changes relative to the water depth.

As the waves reach their depth-limited speed, the divergent waves increase their angle to the sailing line, propagating more in line with the stern transverse waves, as shown in Figure 2.2 (b).

2.1.4 Critical Speed ($Fr_h = 1.0$)

At the critical speed, when the depth Froude number equals one, a vessel will experience a peak in resistance. The relative magnitude of the resistance peak is dependent on the ratio of the water depth to vessel waterline length, with very shallow water for a given waterline length producing the most pronounced increase in resistance.

The wave pattern generated may consist of only one long-period wave, termed a wave of translation, propagating parallel to the sailing line, as shown in Figure 2.2 (c). This single wave travels with the vessel and so does not radiate from it. It does, however, grow in crest length - the vessel transfers energy into this wave that is initially accommodated as a height increase, but once height stabilises the wave grows in crest length. The speed of this crest length growth equals the vessel speed. If banks bound the water at the sides, limiting energy growth in the single wave, a train of several waves, termed *solitons*, may then propagate forward of the vessel if the conditions are conducive to their formation.

(a) Sub-Critical
$Fr_h < 0.75$

- Short-crested divergent waves
- Transverse waves present
- The well-known Kelvin deep water wave pattern

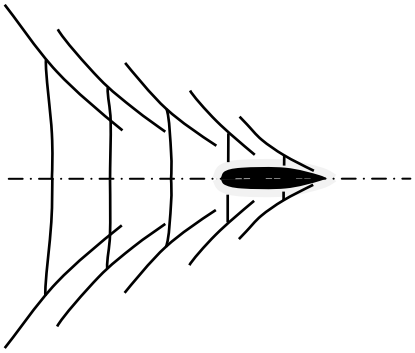

(b) Trans-Critical
$0.75 < Fr_h < 1.0$

- Divergent wave angle increases
- Period of leading waves increases

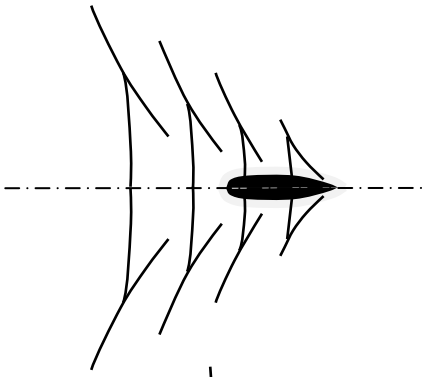

(c) Critical
$Fr_h = 1.0$

- One or more waves perpendicular to the sailing line
- Crest length grows (laterally) at a rate equal to the vessel speed

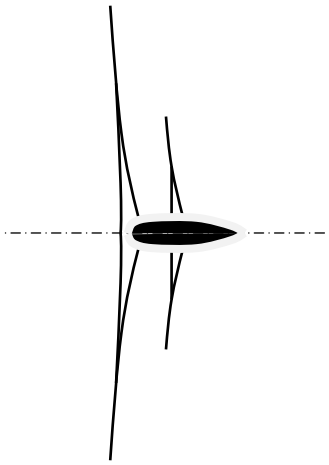

(d) Super-Critical
$Fr_h > 1.0$

- No transverse waves
- Long-crested divergent waves
- Long-period leading waves

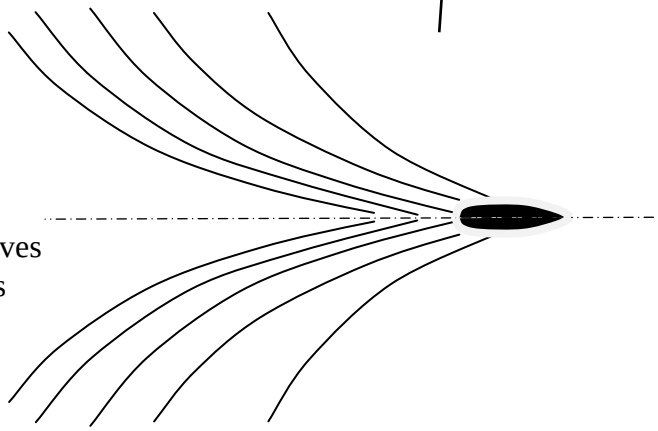

Figure 2.2 Wave wake patterns

These waves of translation are particularly damaging and are to be avoided. Not only are they difficult to see, having a long period but low height, they are hard to maintain

under real-life conditions. It is common for vessels operating in shallow water to operate at speeds that may be depth-critical at times and the Master needs to be aware of this and avoid the critical speed or pass through it quickly. The damaging effects are a non-linear function of vessel displacement, so larger vessels are of more concern than smaller vessels (Cox 2000; Macfarlane 2002).

2.1.5 Super-Critical Speeds ($Fr_h > 1.0$)

At speeds above the depth-critical speed, a vessel's wave pattern changes again, refer Figure 2.2 (d).

The transverse waves, which travel at the speed of the vessel, are no longer able to travel at the vessel speed due to the limiting relationship between maximum wave speed and water depth. As the vessel accelerates from a sub-critical to a super-critical speed, the transverse waves fall behind the vessel and disappear altogether. The lack of a transverse wave train reduces vessel wavemaking resistance, which explains why many vessels go faster in very shallow water.

The divergent waves also re-appear in their more usual form, but propagate at an angle to the sailing line that is dependent on the vessel's speed, such that the velocity vector parallel to the vessel's sailing line is not more than the critical speed. The higher the super-critical vessel speed, the less acute the propagation angle becomes. For very high-speed craft operating in relatively shallow water, it often appears that the divergent waves propagate almost perpendicular to the sailing line.

When viewed from above (Figure 2.2 (d)), the super-critical divergent wave pattern looks different to the sub-critical wave pattern. The super-critical pattern consists of long-crested waves, whereas the sub-critical pattern consists of a series of shorter-crested waves.

2.1.6 Wave Height Constant

Macfarlane and Renilson (1999) discussed the merits of developing a standard numerical measure for quantifying vessel generated waves. It was suggested that any proposed measure meet the requirements listed in Table 2.1. The reasons behind each of these requirements were discussed and a suitable measure was proposed.

In the late 1980s, Renilson and Lenz (1989) developed a technique for predicting the wave height at a given lateral distance from a vessel using a limited number of physical model experiments. Prior to this it was impossible to directly and fairly compare different vessels operating in deep water since the interaction of the transverse and divergent components of the sub-critical wave pattern made such comparisons meaningless. This interaction results in vertical fluctuations in the plot of wave height against lateral distance from the sailing line, as can be seen in Figure 2.3.

The method to predict the wave height at different lateral distances is based on the decay rate of the divergent waves (discussed in more detail in Section 2.2.2). The technique is to obtain a number of longitudinal wave cuts, and to plot the wave height against lateral distance as shown in Figure 2.3. A curve of the power form of Equation 2.3 is then fitted to the experimental data (as shown in the figure).

$$H = \gamma . y^{n} \qquad (2.3)$$

1	Independent of the length of the data sample
2	Able to be used to compare one vessel against another vessel
3	Relatively easy to understand
4	Representative of wave wake problems
5	Easy to measure
6	Independent of the exact distance from vessel sailing line

Table 2.1 Requirements of measure(s) used in regulatory criteria (Macfarlane and Renilson 1999)

Macfarlane and Renilson (1999 and 2000) show that the wave height constant γ can be obtained with good accuracy provided a number of measurements are made in what they have referred to as the 'medium' field – a distance close to the vessel, but outside the so called 'local wave effect'. It is suggested that measurements be made at a minimum of four lateral locations within the region between 1.5L to 3.0L (Macfarlane 2002). Once γ is obtained from the experimental results, Equation 2.3 can be used to predict the wave height at any given lateral distance from the sailing line. Therefore, the wave height constant γ is independent of this distance and can thus be used to directly and fairly compare one vessel against another.

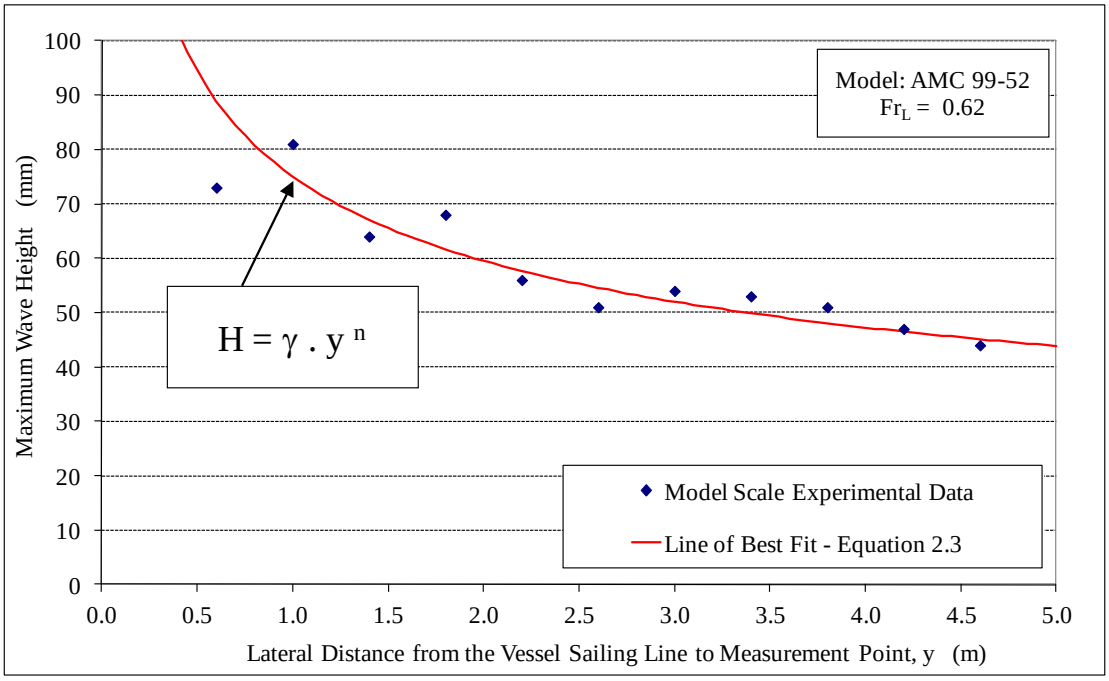

Figure 2.3 Wave height as a function of lateral distance from the sailing line

2.1.7 Wave Angles

The previous sub-sections provided a general description of the large changes in the characteristics of a vessel's wave pattern as it moves from sub-critical speeds through trans-critical to critical and onto super-critical. One of the most obvious changes is in the wave angle, which is thus deserving of further discussion. Firstly, it is useful to clearly define 'wave angle' in this context, as there are often (at least) two wave angles of interest (refer Figure 2.1), namely:

(a) the angle between the cusp locus line and the sailing line of the vessel (θ),
(b) the propagation angle of diverging waves to the sailing line of the vessel (β)

For sub-critical speeds, where the Kelvin wave pattern is generated, the angle between the cusp locus line and sailing line of the vessel is 19°28' and the propagation angle of the diverging waves is 35°16', as shown in Figure 2.1. Note that in some texts (for example, Whittaker *et al*. 1999; Doyle 2001) the angle between the cusp locus line and the sailing line of the vessel is referred to as the wave boundary, which may be a more appropriate description when considering super-critical speeds where there is strictly no identifiable cusp locus, therefore this angle refers to that of the crest of the outer long-crested divergent wave.

Havelock (1908) described how the cusp locus, or wave boundary, angle changes with increasing depth Froude number, as shown in Figure 2.4. Johnson (1958) is believed to be the first to prove this experimentally. More recent experiments by Robbins *et al*. (2009) suggest that the peak wave angle occurs slightly prior to critical speed, closer to $Fr_h = 0.9$.

The change in wave propagation angle with increasing depth Froude number was also described by Havelock (1908), as shown in Figure 2.5, and proven using physical model experiments by others, including Weggel and Sorensen (1986); MCA (1998) and Kofoed-Hansen *et al*. (1999).

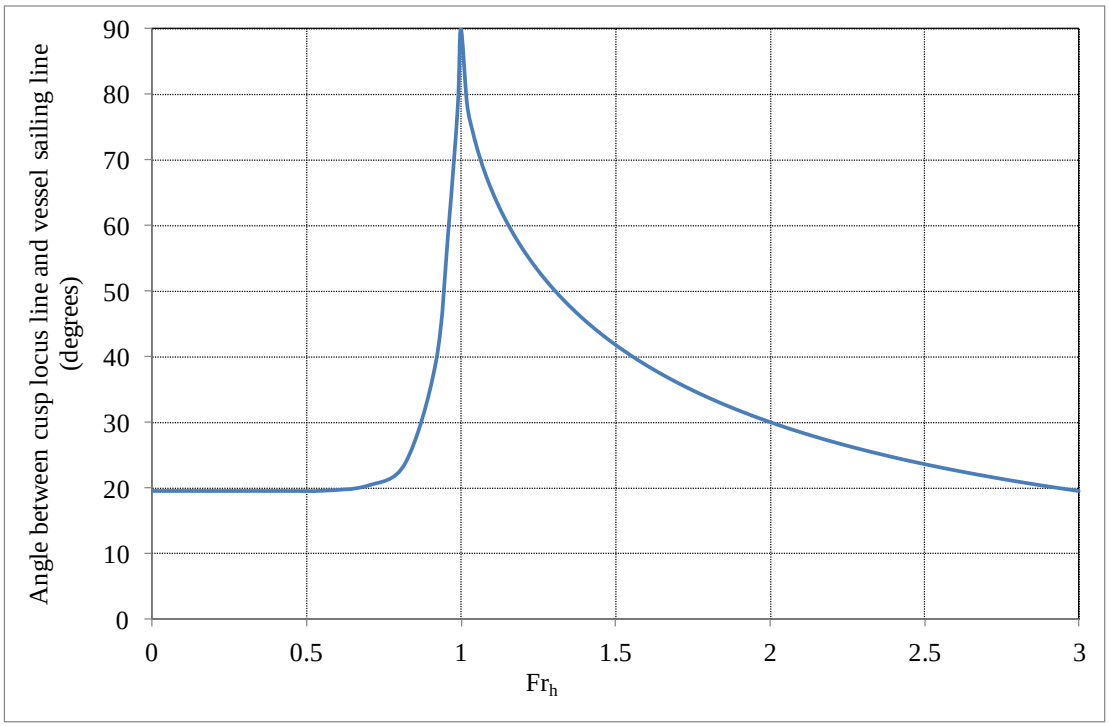

Figure 2.4 Wave angle θ as a function of Fr_h (Havelock 1908)

Following preliminary analysis of physical model experimental data for the present study, it became apparent that further consideration was required when determining the wave angle within high sub-critical and trans-critical speeds. The process adopted also has implications on the appropriate determination of other characteristics, such as the wave height constant and period. This is discussed in more detail below.

It is well known and understood that at intermediate sub-critical depth Froude numbers the dominant waves of the Kelvin wave pattern will consist of a series of diverging waves along the cusp-locus line (which are dispersive in nature). This

series of waves will start with a wave at the bow of the vessel followed by other waves arranged in such a way that each wave is stepped back behind the one in front in echelon and is of quite short length along its crest line (Lighthill 1978). Thus, as the lateral distance from the vessel's sailing line increases it is likely that different waves will be measured. This is clearly the case in the example provided by the aerial photograph in Figure 2.6 where each of the vertical white lines, representing longitudinal cuts of the wave pattern, cuts a different divergent wave (note that there are many more divergent waves than vertical lines displayed).

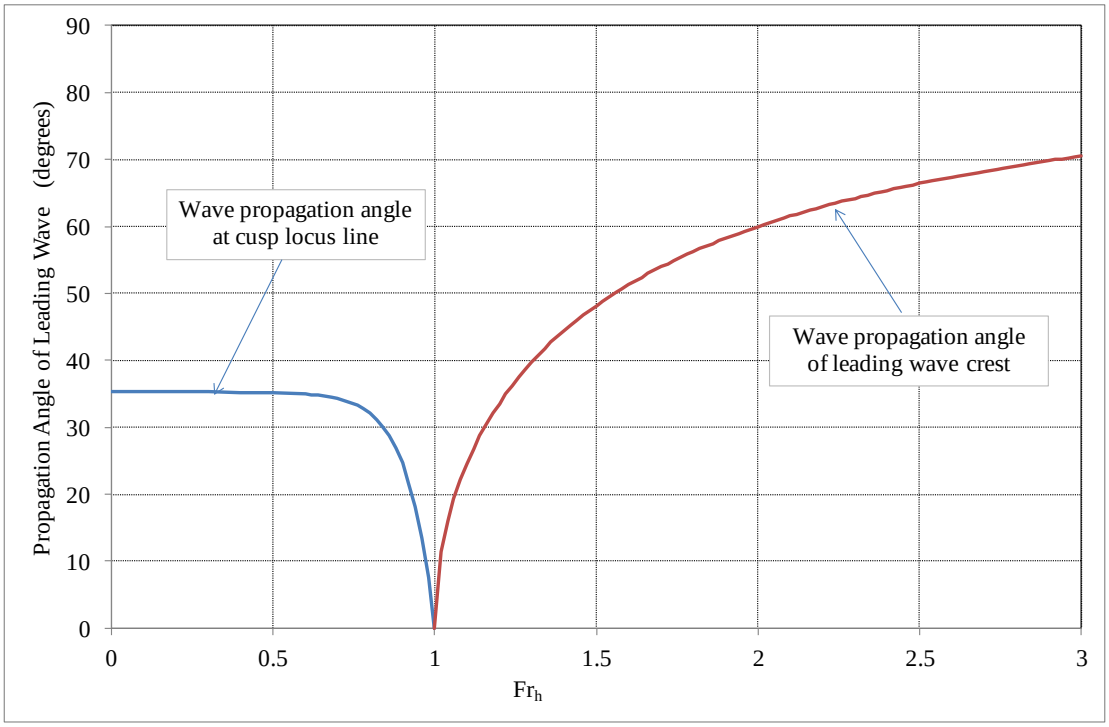

Figure 2.5 Wave propagation angle β as a function of Fr_h (Havelock 1908)

In contrast, it is much easier to identify the leading wave for super-critical vessel speeds (and high trans-critical speeds) as these waves have significantly longer crest lengths, making it a simpler task to track the same wave as it propagates away from the vessel's sailing line.

Where most confusion can occur is at trans-critical speeds when the Kelvin-like wave pattern is still present, however the angle between the cusp locus line and the sailing line of the vessel is increasing rapidly, as was shown in Figure 2.2(b) and Figure 2.4.

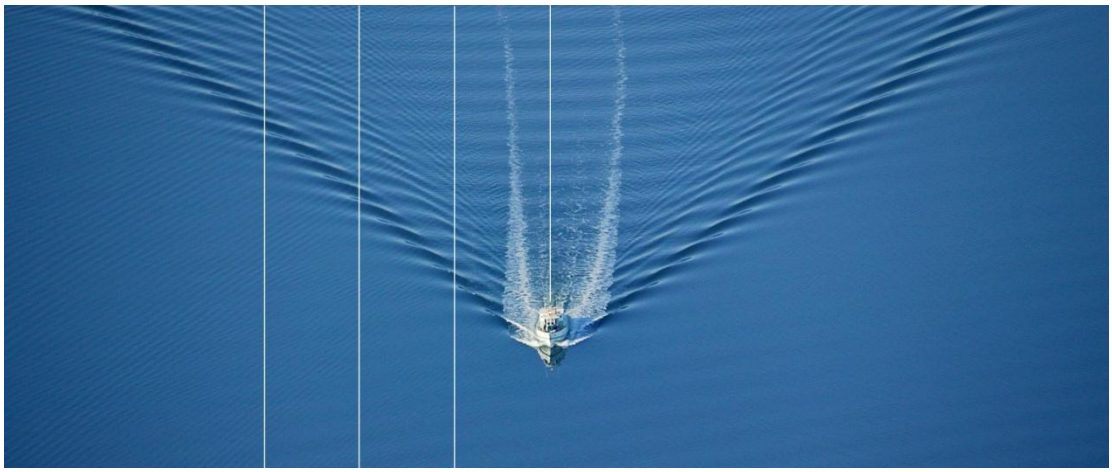

Figure 2.6 Aerial photograph of Kelvin wave pattern (Airview Aerial Photography)

In Figure 2.7, an equivalent "aerial view" of the crests of the leading waves has been generated using experimental data on a scale model of a generic monohull ($L/\nabla^{1/3}$ = 5.89) from a range of depth Froude numbers. Starting with a sub-critical speed, for example Fr_h = 0.50 (red curve, square data points), it is possible to identify the crests of at least two divergent waves, the first just a short distance (~0.2 m) downstream of the bow of the ship model. This crest extends laterally between 1 and 2 m from the sailing line of the ship model (represented by the three data points in a row at y = 1.0, 1.5 and 2.0 m). The second clearly identifiable crest occurs at a downstream distance of about 6.5 m and extends laterally between 3.5 and 4.0 m. There are other wave crests in this lateral range, as indicated by the other 'singular' data points in this curve (for example at downstream distances of approximately 2.0 m and 4.8 m), however spacing between the wave probes is too great to pick up the relatively short lateral lengths of these wave crests.

At the next highest speed increment, Fr_h = 0.78, the wave angle θ has increased and the wave crests are clearly longer (green curve, triangular data points in Figure 2.7). For example, the first crest (about 3 m downstream) extends laterally between the wave probes at y = 1.5 to 3.5 m. The next wave crest occurs about 6.5 m downstream. Insufficient lateral distance prevented the entire length of this crest to be identified.

As expected, only a single long wave crest, with a very high angle to the sailing line, is found at speeds close to the critical speed (Fr_h of both 0.95 and 1.06). It is a similar story for the two super-critical cases of Fr_h = 1.80 and 1.99, however the wave angle to the sailing line is predictably reduced compared to those close to the critical speed.

From the data presented in Figure 2.7, it is obvious that it is a relatively straightforward process to determine the wave angle relative to the sailing line for the leading waves at sub-critical, near-critical and super-critical speeds. However, the same cannot be claimed for the trans-critical speeds where multiple waves having long crest lengths occur, as it is not immediately obvious exactly how this angle should be measured. According to Havelock the angle is defined by the cusp locus line, but for some few cases in the trans-critical speed region when the wave angle and crest length is increasing – and measurements are only available over a limited lateral distance – then it is likely that the cusp locus line may be difficult to clearly identify due to only a single whole wave crest being identified, as was the case in the example at $Fr_h = 0.78$ in Figure 2.7. Note that the use of less wave probes, or increased spacing between probes, could also influence the determination of wave characteristics in the trans-critical speed zone.

For the present study, in these instances extra care was taken to ensure the wave angle was estimated as accurately as possible. This involved creation of similar plots to that shown in Figure 2.7 and comparison against the results for the speeds either side of the one in question. However, it is clear that the angle of the leading wave changes very rapidly in the trans-critical region and as such an appropriately increased level of uncertainty should be applied.

Another factor to consider with operation at trans-critical speeds is potential unsteadiness in the wave wake over time. Results from model scale experiments presented by Robbins *et al*. (2011) show that there is little or no evidence of any unsteadiness with the angle of the leading wave at trans-critical speeds. However, this is not the case for the height of the leading waves. The authors present data from a longitudinal array of seven wave probes by plotting the standard deviation to indicate the level of variation from the average of the measured wave heights. The greatest level of growth in wave height is found at the lowest water depth investigated ($h/L = 0.08$), with this growth detected at speeds between $0.8 < Fr_h < 1.0$.

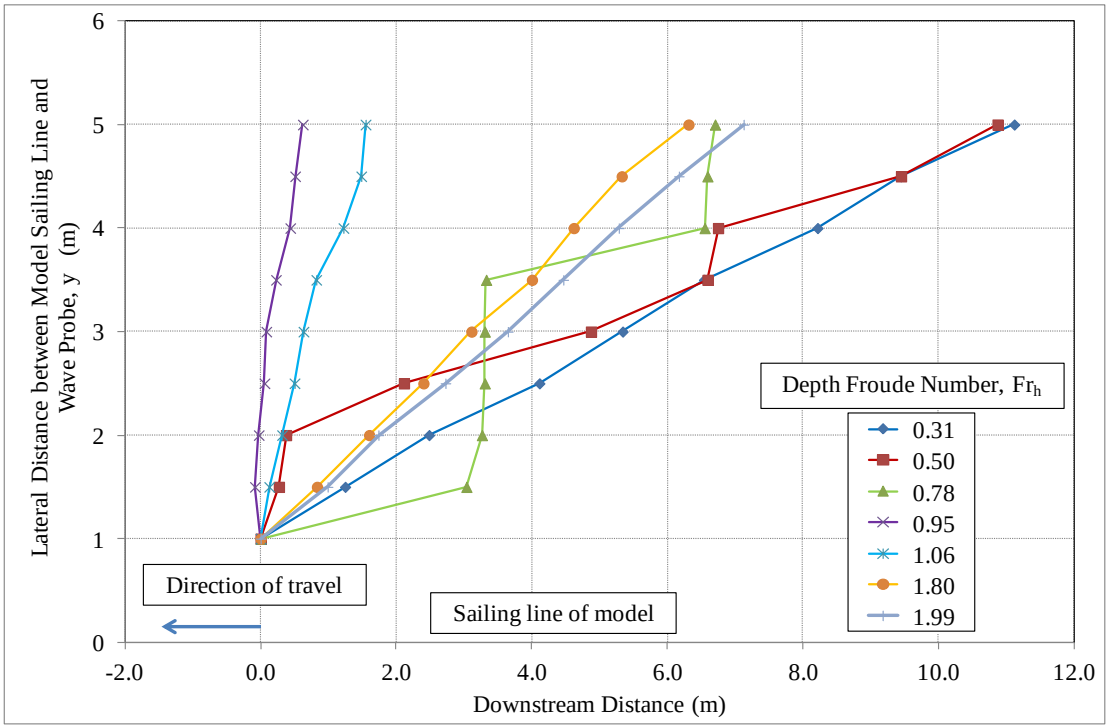

Figure 2.7 Experimental results for leading wave angles

2.1.8 The Effect of Manoeuvring (Turning)

Wave wake generated when vessels turn (or manoeuvre) can be a major contributor to recreational vessel wave wake problems. In general, only generic statements appear to have been made – that the waves are focussed on the inside of a turn and spread on the outside of a turn (Macfarlane and Cox 2004; Schmied *et al*. 2011).

The absolute measurement of wave wake generated during manoeuvring is practically impossible due to the number of variables involved, such as vessel speed and deceleration during the manoeuvre, rate of turn, steadiness of the turn and change in vessel attitude during the turn (banking, trimming etc). Then there is the issue of the required location for measuring the generated waves to record what may be regarded as the characteristic manoeuvring wave wake, remembering that it is inevitable that there will be interference from multiple wave trains.

Advice given by several ski boat owners is that typical high-speed turns used in water skiing activities (by experienced water skiers) can generally be as tight as 2 to 3 times the waterline length of the vessel.

The author has conducted some full scale experiments which have helped to develop the following general conclusions regarding the waves generated while ski boats manoeuvre (Macfarlane and Cox, 2005):

- The height of the primary waves on the outside of a turn are less than the equivalent straight line condition due to wave spreading, so in general these results are of less interest.
- The waves measured on the inside of a tight turn comprise just those generated continuously during the turn. These waves propagate towards the centre of the turn and will come together at various points inside the vessel sailing line. This will create momentary localised interference and some energy will be dissipated, but the waves will eventually continue to propagate past the sailing line and beyond. The disturbance generated by the turn is therefore localised and the medium to far-field wave energy should dissipate rapidly due to diffraction.
- Once the waves on the inside of a turn pass through their nominal focus point somewhere near the centre of the turn, the waves then diffract as they propagate away from the focus point. A tight turn is therefore potentially more preferable than a wide turn in terms of reducing wave energy that reaches the shoreline.

2.1.9 The Effect of Propulsors

The contribution that the propulsion system can have on the wave wake of a vessel has been considered by several researchers. For example, Taato *et al*. (1998) conducted an experimental study to investigate the effect that both conventional propellers and water-jets have on the height of the wave wake generated by a generic high speed monohull. Their model tests considered three cases: towed, self propelled by water-jets and self-propelled by propellers. They concluded that the propulsion systems do not change the general pattern of waves generated, however both propulsion methods may cause an increase in wave amplitude. For example, conventional propellers may cause a 5-10% increase in wave height as compared to the towed case. This is in general agreement with Leer-Andersen and Lundgren (2001) who conducted both towed and self-propelled (using propellers) scale model experiments on a high-speed catamaran operating in both deep and finite water depths. Leer-Andersen and Lundgren also concluded that this increase in wave height may be affected by water depth, with the increase in height being greater the shallower the water depth.

Taato *et al*. (1998) also claim that an increase in wave height of between 20-40% may be expected when the same monohull model is self-propelled using water-jet units. This is a considerably greater increase than the findings of Werenskiold and Stansberg (2011) who conducted scale model experiments on a catamaran, both towed and self-propelled using two stock water-jet units. Werenskiold and Stansberg found an increase in (maximum) wave height of up to 10% for the model propelled by water-jets. The authors assumed that the difference between their towed and water-jet propelled models were due to known differences in trim of each model.

The large increase in height found by Taato *et al*. for their water-jet propelled model is potentially due to experimental error and/or changes in dynamic trim, when compared to the towed ship model. To investigate this further, it is useful to review the time histories of the wave profiles presented by Taato *et al*. where it is evident that the amplitude of almost all waves for the water-jet case, including the leading waves, are higher than the towed model case. In the author's view, it is unlikely that the propulsion system alone will affect all waves in the wave train in a similar manner. It may be more likely that the effect of the propulsors on the leading (bow) waves may be minimal, given that the propulsion system is usually located well aft in most vessels. For the leading waves to have also been affected suggests that it is likely that something else has changed, such as a significant difference in running trim, and/or experimental error, to result in such large differences in wave height.

In conclusion, it is generally accepted that a vessel's propulsion system, regardless of type, is likely to contribute to the height of some of the waves generated. An increase in height of the maximum waves of up to 10% appears to be a reasonable approximation, however further research is required to provide a more precise estimation.

The potential impact of slipstream wash from propulsors on the marine environment has also been investigated. For example, both Atlar *et al*. (2006) and Wang *et al*. (2002) conducted experiments in a cavitation tunnel using laser Doppler anemometry to quantify the wash velocities generated by propellers and podded propulsors. Results indicate that the most significant impact of the slipstream wash on the surrounding environment will occur when the vessel is operating in confined waterways, where under-keel clearance is low and the shore is in close proximity to the stern of the vessel.

2.2 Propagating Wave Phenomena

2.2.1 Dispersion

As the propagation of deep-water divergent waves is unaffected by water depth, the waves will propagate at speeds dependent on their individual wavelengths (Newman 1977). The longer period waves will travel faster and the shorter period waves will travel slower. If a wave trace is taken at different distances away from the sailing line, the trace will show the wave packet to be lengthening further from the sailing line as the individual waves spread out. This phenomenon is termed dispersion and deep-water waves are considered to be dispersive. Figure 2.8 illustrates dispersion, where the width of the first group of waves on the left hand side of each trace increases with increasing lateral distance. The wavelength and wave direction are related by the dispersion relation (Lighthill 1978).

There is also a weak relationship between wave speed and wave height – for a given wavelength the higher waves travel slightly faster and therefore disperse (USACERC 1977). Amplitude dispersion is ignored in wave wake studies as the effect is generally negligible.

As the period of the transverse waves is dependent on vessel speed, the transverse waves will all have the same period when the vessel is travelling at a constant speed. Therefore, there will be no dispersion evident (in practice there is weak dispersion, probably due to amplitude dispersion caused by height attenuation away from the vessel).

If the divergent waves propagate from deep to shallow water, or are created in shallow water to begin with, the waves will be influenced by the bottom. When the speed of each wave is depth-critical, that is, the depth Froude number for each wave equals unity, the maximum speed of propagation becomes limited to the depth-critical speed. A wave packet will then stop dispersing and the waves will travel at the same depth-limited speed. Shallow water waves are therefore termed non-dispersive.

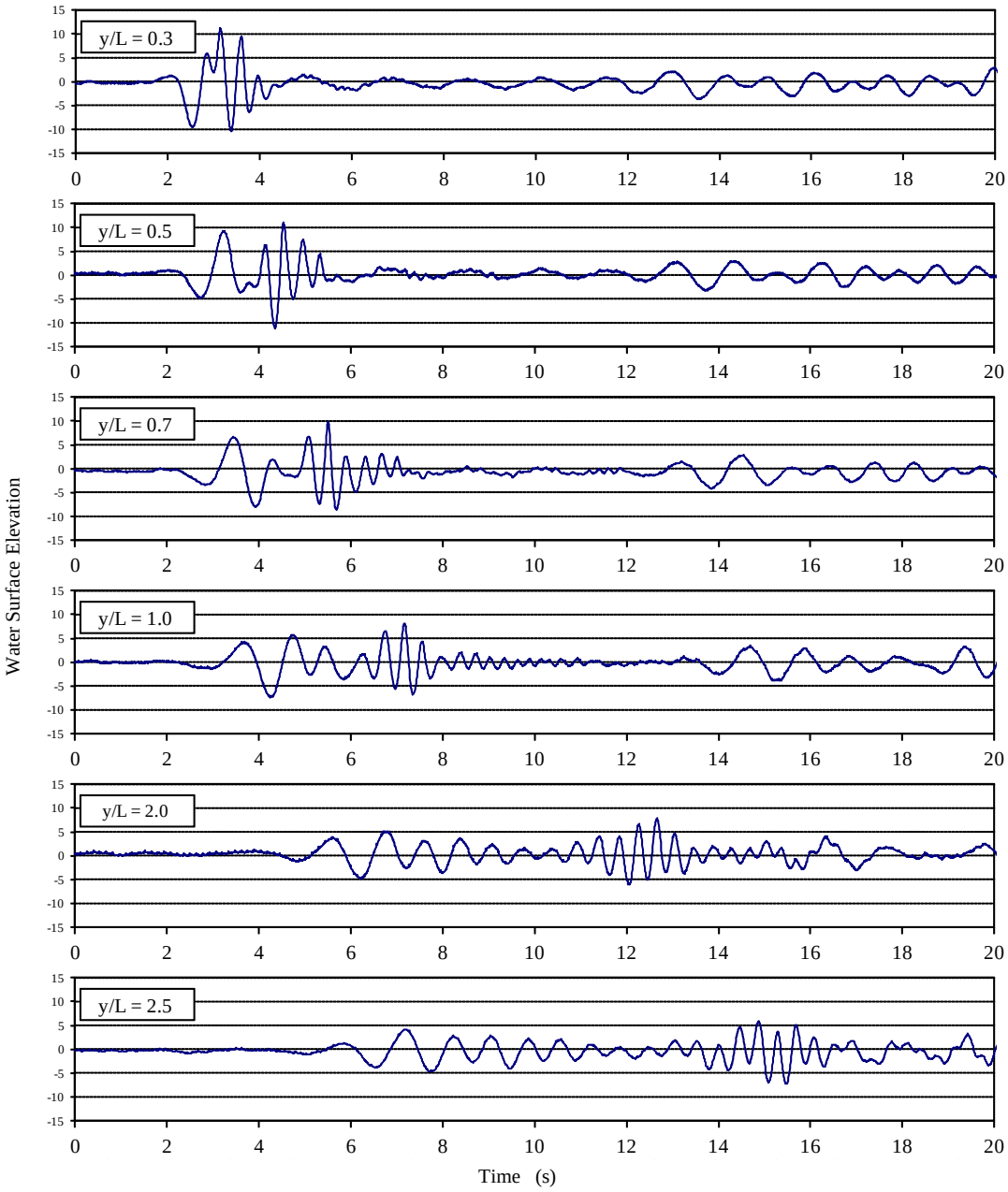

Figure 2.8 Deep water wave dispersion, for different lateral probe positions

This is not exactly the case for vessel waves in shallow water. With the divergent wave packet being comprised of many waves with different wavelengths, the waves with long wavelengths will become speed limited and therefore non-dispersive before those slower waves with shorter wavelengths. Also, in reality there is some leakage of wave energy in a non-dispersive packet, but this is only evident over several ship lengths of shallow water wave propagation.

Dispersion can create difficulties when assessing wave traces obtained through the conduct of physical experiments. Where a trace taken close to a vessel (within, say, half a boat length), the trace may appear to consist of only a few waves, when in fact these waves represent many more waves of differing wavelength superimposed. It takes approximately one to two boat lengths for waves to disperse sufficiently such that the period of individual waves can be measured with certainty (as was seen in the example provided in Figure 2.8). Wave height is affected to a lesser degree.

2.2.2 Attenuation

As the distance abreast of the sailing line increases, the wave height decreases. This height attenuation is due to diffraction – spreading the wave energy along the wave crest. Therefore, in order to determine the potential impact of wave wake on a shoreline, the attenuation, or decay, rate of the waves with distance from the sailing line must be known.

Havelock (1908) extended the work of Thomson (1887) at sub-critical speeds to show that the wave heights at the so-called cusp points (the point of interaction of the transverse and divergent wave systems) decrease at a rate inversely proportional to the cube root of the distance from the vessel. Havelock also showed that the transverse waves generally decrease at a rate inversely proportional to the square root of the distance from the vessel, a fact that applies to all waves that appear behind the cusp locus line. Therefore, transverse waves tend to decay at a faster rate than the higher waves that occur along the cusp locus line. Thus, it is reasonable to conclude that the waves along the cusp locus line (typically the highest divergent waves in a propagating wave packet) will become even more prominent to the observer as the distance from the vessel increases. Several studies have shown this to be true, including Sorensen (1969), Sorensen (1973) and Renilson and Lenz (1989).

According to Havelock's deep-water vessel wave theory, the attenuation measured at the cusp is:

For divergent waves:

$$H = \gamma y^{-\frac{1}{3}} \qquad (2.4)$$

For transverse waves:

$$H = \gamma y^{-\frac{1}{2}} \qquad (2.5)$$

Both Equations 2.4 and 2.5 are of the power form seen in Equation 2.3 and γ is a wave height constant, as discussed in Section 2.1.6. All literature cited within this thesis generally use equations of this general (power) form to describe the wave decay rate, although there is some discussion as to the most appropriate value of the exponent, n.

The wave trace from a single probe is not guaranteed of cutting exactly at the cusp (where the transverse and divergent waves intersect), so the attenuation exponents ($-^1/_3$ and $-^1/_2$) may vary. However, analysis of experimental data by several authors supports the use of these exponents for sub-critical speeds (Sorensen 1967 and 1969; Gadd 1994; Cox 2000; Macfarlane 2002). Previous work by the author concluded that there is some variation, with typical decay exponents ranging between -0.2 to -0.45, however the use of -1/3 was considered a good engineering approximation. As part of a numerical study using Michell-type theory into the generation and decay of waves created by high-speed vessels, Doctors and Day (2001) found that the deep water decay exponent is generally around -0.33 to -0.5. However, they also found a relatively large spike can occur at low speeds, where values between -0.7 to -1.06 may be expected.

The topic of divergent wave attenuation for vessels operating in finite (shallow) water does not yet appear to be anywhere near as conclusive. Several studies have investigated this issue, with the main common thread that decay rates in finite water depths definitely vary from those for deep water. It is safe to say that the increased number of shallow water variables complicates the assessment of shallow water wave attenuation.

Sorensen (1973) conducted a limited series of experiments in finite water where he concluded that “cusp wave amplitudes decay at an ever increasing rate with distance from the vessel for increasing depth Froude numbers. Further research is needed in this area”.

Data acquired during full scale measurements of the wave wake from several vessels travelling at super-critical speed was analysed by Kofoed-Hansen (1996) and Kofoed-Hansen and Mikkelsen (1997) from which it was concluded that decay exponents around -0.4 were generally appropriate for the limited number of cases investigated.

An experimental study by Doyle (2001) into the decay of waves generated by high speed vessels operating at trans-critical and super-critical speeds found similar results at super-critical speeds, although much lower decay rates, around -0.2 can also be observed. Doyle also found that the rate of decay of the waves generated at the critical speed (Fr_h = 1.0) are substantially different to those at super-critical speeds. It was observed that the wave heights are substantially greater around the ship's hull, but decay much faster with lateral distance from the sailing line. Doyle suggests that an equation of exponential form, such as that shown in Equation 2.6, may provide a better description of this decay (where A is a constant). It should also be noted that unsteady conditions can occur at the critical speed, thus both the wave height and decay rate are dependent upon the length of time that the vessel spends at critical speed.

$$H = y.e^{-An} \qquad (2.6)$$

Robbins *et al*. (2007 and 2009) investigated wave decay by conducting model scale experiments on two different catamaran hulls at three very shallow finite water depths (h/L of 0.075, 0.10, 0.15) over a range of Fr_h. The effect of load condition (draught) was also investigated for each of the two models. The authors plotted the decay rate exponent as a function of Fr_h and fitted a trendline through the data. Their results are shown in Figure 2.9. The trendline for the decay exponent can be seen to vary between -0.2 to -1.0 with the peak (-1.0) occurring just prior to the critical Fr_h of 1.0. The authors conclude that the decay coefficient appears to be independent of hull form and vessel displacement, however it should be noted that this study only involved two catamarans with $L/\nabla^{1/3}$ of 8.48 and 11.14. The present study will consider a much wider range of hull forms.

One aim of the present study is to shed some further light on this topic. As the principal interest is in the operation of small commercial vessels and recreational craft within sheltered waterways such as rivers, harbours and estuaries, the current focus is on the characteristics of the waves within the medium field, which in this context includes lateral distances in the order of 2 to 4 boat lengths from the vessel's sailing line.

As was seen in Figure 2.8, there is generally insufficient dispersion within one boat length to clearly define the periods of the key waves within this near field. It is also very rare (and potentially dangerous) for vessels to operate this closely to sensitive shorelines or maritime structures, therefore the near field is generally not of interest in

most wave wake studies. In the case of most large high speed vessels operating in coastal and semi-sheltered waterways where wave wake is of interest the focus is generally on lateral distances in the order of ten ship lengths and beyond, which is considered to be within the far field.

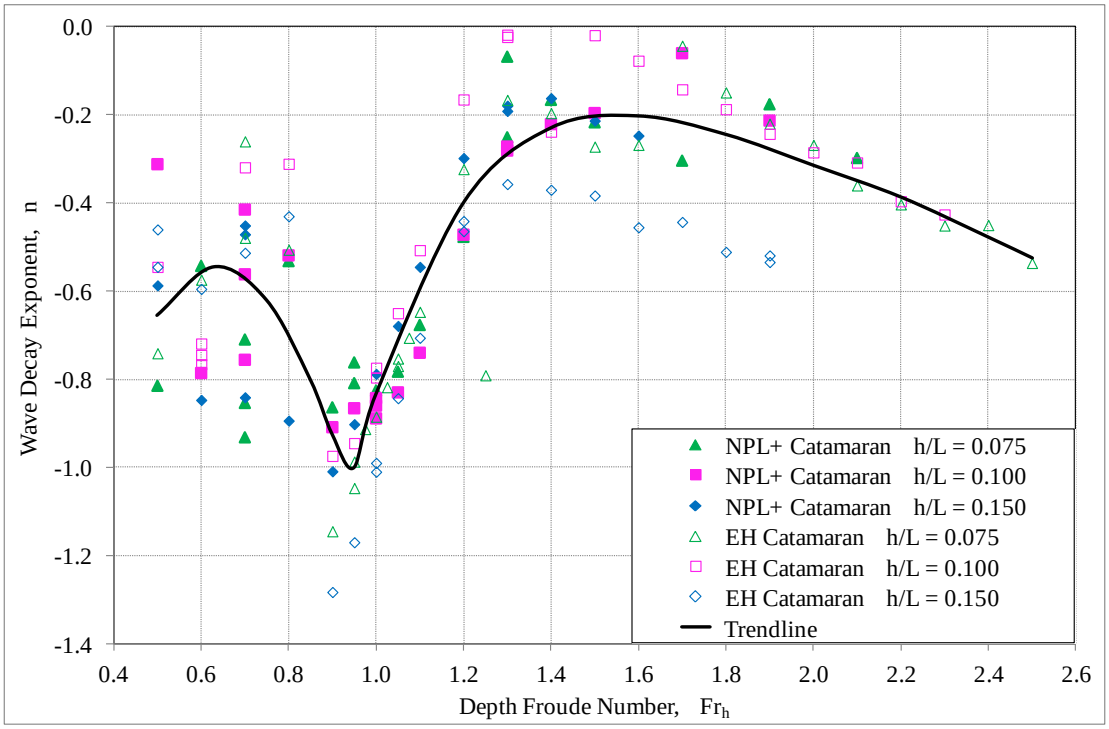

Figure 2.9 Wave decay exponent as a function of Fr_h (Robbins *et al*. 2007)

2.2.3 Wave Energy and Power

Wave energy is the sum of a wave's potential energy and kinetic energy. Wave energy density per square metre of water surface is calculated using (USACERC 1977):

$$\overline{E} = \frac{\rho g H^2}{8} \qquad (2.7)$$

The wave energy density can be multiplied by the wavelength λ to obtain the energy E in each wavelength (per unit width of wave crest):

$$E = \frac{\rho g H^2 \lambda}{8} \qquad (2.8)$$

For waves whose length is less than twice the water depth, the "deep-water" assumption can be used to relate wave length and period. This is often the case for

wind waves when considering very sheltered waterways. Therefore the wavelength can be found from:

$$\lambda = \frac{gT^2}{2\pi} \tag{2.9}$$

Thus, the energy E in each wavelength (per unit width of wave crest) can be calculated using:

$$E = \frac{\rho g^2 H^2 T^2}{16\pi} \tag{2.10}$$

When considering wind-generated waves, most interest is in the energy per unit area, thus energy is a function of just the wave height, not the period of the waves (as shown in Equation 2.7). However, for vessel generated waves, which are more discrete events, it has become commonplace to consider the energy *per wave*. It is in this scenario that the period of the wave becomes important, as seen in Equation 2.10.

Wave power is the rate at which wave energy is transmitted in the direction of wave propagation. The average wave power per unit width of wave crest is (USACERC 1977):

$$\bar{P} = \bar{E} c_g \tag{2.11}$$

c_g is the group velocity, which for deep water is given (when the wavelength is less than twice the water depth, USACERC 1977) by:

$$c_g = \frac{\lambda}{2T} \tag{2.12}$$

Hence the wave power in open water is:

$$\bar{P} = \frac{\rho g^2 H^2 T}{32\pi} \tag{2.13}$$

When waves are impacting directly onto a shoreline, the power calculated above is that which impacts onto the shoreline. When the wave crests are at an angle α to the shoreline, the wave power transmitted per metre of shoreline is:

$$\bar{P} = \bar{E} c_g \cos\alpha = \frac{\rho g^2 H^2 T}{32\pi} \cos\alpha \tag{2.14}$$

Energy density is transmitted at the group velocity (c_g), not phase velocity (c_p), and in deep water $c_g = c_p/2$. But, in cases where finite water depths exist (when the wavelength is greater than twice the water depth), the group velocity is given according to linear theory:

$$c_g = \frac{\lambda}{2T}\left(1 + \frac{4\pi h/\lambda}{\sinh\left(4\pi h/\lambda\right)}\right) \qquad (2.15)$$

Wave energy and wave power are both commonly used in coastal engineering. Assuming a simplified, sinusoidal wave form, wave energy (per wavelength and unit crest width) is proportional to H^2T^2 and wave power (derived from energy density) is proportional to H^2T (as can be seen in Equations 2.10 and 2.14 respectively).

Power is a useful descriptor of wave energy over a period of time, such as may be found in the statistical analysis of an incident wave field acting over a long timeframe. In the case of the wave wake of a passing vessel, the waves generated are discrete events and so do not necessarily lend themselves to description on a statistical time basis. It is felt that wave energy may be a better measure for such discrete events (refer to Section 7.1.4 for further discussion).

2.3 Vessel Speed Regimes

Wave wake is directly related to a vessel's wavemaking resistance. When contemplating the hull resistance of a vessel, naval architects often refer to three distinct speed ranges where the waves generated by a moving vessel will change in magnitude, namely: displacement speed, semi-displacement speed and high speed (also known simply as planing). As described earlier, there are also three depth-related wave wake regimes: sub-critical, trans-critical and super-critical. Certain combinations of vessel speed regime with depth-related regime can result in the most damaging of waves being generated. Thus a knowledge and understanding of vessel speed regimes will benefit any study into vessel wave wake. Each of the vessel speed regimes are shown graphically in terms of Fr_L in Figure 2.10.

In practical terms, the first regime (displacement speed) is best observed in slow, heavy vessels. These vessels experience a practical upper limit of their speed, termed *hull speed*, which can only be exceeded with a substantial increase in engine power. High-speed craft, which have a power-to-weight ratio such that they can travel faster than their hull speed, first experience a resistance hump just above *hull speed* before settling into the high-speed regime. For a planing hull, this will be the onset of planing.

When the waterline length changes notably with speed it can sometimes be more appropriate to use the volumetric Froude number:

$$Fr_v = \frac{u}{\sqrt{g\nabla^{1/3}}} \qquad (2.16)$$

2.3.1 Displacement Speed

All vessels have a displacement speed range where the length of the transverse waves generated is less than the waterline length. The upper limit of this speed range is when the length Froude number, Fr_L, equals 0.399 (Lewis, 1988), which reduces Equation 2.1 to:

$$u = 2.43\sqrt{L} \qquad (2.17)$$

This maximum displacement speed, or hull speed, represents the condition where the longest wave generated equals the waterline length of the vessel. To travel faster than this, the vessel must begin to climb its own bow wave (a common analogy).

Wavemaking resistance in the displacement region is proportional to u^6, so small changes in speed cause large changes in resistance and wave wake.

In the displacement speed region, wave periods are modest and wavemaking energy transforms into wave wake height, creating steep waves. In general, operating at speeds up to 75% of the maximum displacement speed (or about $1.82\sqrt{L}$ knots) will produce modest wave wake height and period.

2.3.2 Semi-displacement Speed

As a vessel powers through the displacement speed limit, it's running trim increases as the transverse waves move aft of the transom. Vessel wavemaking resistance is high, peaking at a length Froude number of approximately 0.5 (Lewis 1988).

Wave wake height increases to its maximum and divergent wave periods increase steadily. A particular operating condition to be avoided is at a length Froude number of 0.5 and depth Froude number of 1.0, when maximum specific wavemaking

resistance and depth effects coincide. This condition occurs when h = 0.25 L and u = 3.04√L.

Semi-displacement speeds, often referred to as hump speeds in planing craft terms (when the vessel appears to climb over the hump before planing) create damaging wave wake.

Fr_L < 0.399

- Displacement speed
- Transverse wavelength < L

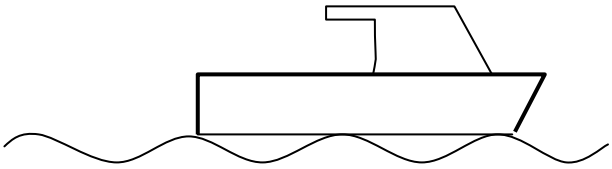

Fr_L = 0.399 (speed = 2.43√L knots)

- Maximum displacement speed ("hull speed")
- Transverse wavelength = L
- Vessel squats and trims by the stern

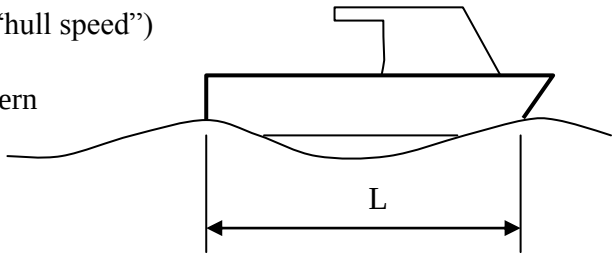

Fr_L = 0.5 (speed = 3.04√L knots)

- Semi-displacement speed
- Transverse wavelength = 1.57L
- Large transverse wave system
- Very high stern trim

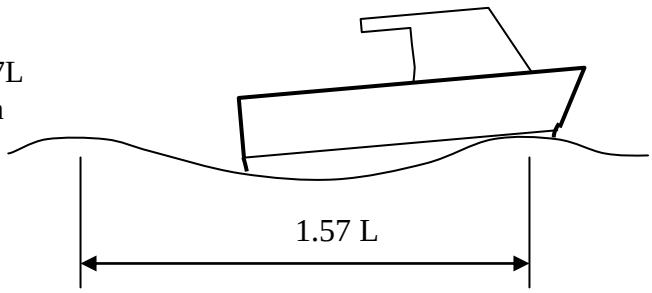

Fr_L > 0.5

- High speed
- Transverse waves reduce in height
- Vessel trim reduces
- Planing hulls begin to lift and plane

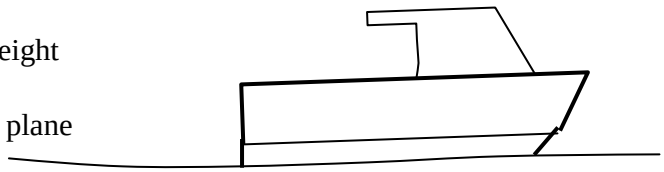

Figure 2.10 Vessel speed regimes

2.3.3 High Speed (Planing)

As the length Froude number increases above 0.5, specific wavemaking resistance slowly reduces. The maximum wave height reduces and maximum wave period levels to a relatively constant value. For a planing hull form, the vessel will be approaching its fully planing condition. Round bilge multihull forms are simply referred to as high-speed displacement forms. Wetted surface area, the basis of frictional hull drag, becomes the principal drag component, hence the drop in total wave wake energy with increasing speed.

It is often said that high-speed vessel wake is preferable to that of the semi-displacement speed, where waves are high and steep. This may appear to be the case, but the high-speed condition produces the longest wave periods, which may have as much or greater effect on shorelines and shoreline structures as wave height. It is important to remember that wave height attenuates with distance from the sailing line but period remains constant.

Given the abundance of vessels operating in the high speed regime on sheltered waterways, and the relative lack of published scientific material specifically on the characteristics of the wave wake they generate, further relevant information is covered in more detail in the following sub-section.

2.4 High Speed Planing Vessels

2.4.1 Introduction

The discussion of vessel wake waves earlier in this section provided a generic overview of wave wake that is applicable to all vessels. However, the overwhelming majority of recreational craft using sheltered waterways are small, high-speed vessels, typically used for water skiing and recreational fishing. There are often a smaller number of slow-speed vessels such as professional fishing vessels, yachts, houseboats and workboats, and some commercial charter and ferry operators. If the vessel length is sufficiently large and it is engaged in a commercial operation, it is not uncommon for case-by-case assessment to approve their operations.

Most high-speed recreational craft are planing monohulls, as monohulls are the cheapest and simplest vessel type to build, and the small recreational boat market is very price sensitive.

When investigating potential bank erosion and other negative impacts from recreational craft, it is helpful to consider the following factors:

1. Recreational boating is not a substantial direct revenue source for marine regulatory authorities, so the sector receives limited attention, hence limited funding.
2. When funding for maritime scientific investigation is limited and a political solution must be found, recreational boaters can be soft targets. It is often easier and cheaper to apply a blanket speed limit to boating activities than to police it.
3. Vessel wave wake complaints are often used to mask other community concerns such as the noise generated by high-speed craft and the loss of amenity. Communities and governments react strongly to tangible evidence such as bank erosion, regardless of the cause, whereas noise and loss of amenity are more subjective, somewhat less tangible, and therefore less likely to attract regulation.
4. Shoreline erosion can very often be the result of land use issues, engineering works, river regulation or climate change and sea level rise.
5. Regulators, builders and owners of small craft have scant information relating to vessel parameters such as displacement, dimensions and hull design. Often only very simplified parameters must be relied upon to determine wave wake potential.
6. Every possible combination of bank type, bank material, riparian vegetation and river bathymetry cannot be covered, and indeed may not need to be.

Small, high-speed planing craft are peculiar in that their resistance components are significantly influenced by the dynamic forces generated by their shape, in turn influencing the generated waves. Some additional discussion is presented to assist with the understanding of these dynamic features.

2.4.2 Hull Resistance Components

All vessels have two primary hydrodynamic resistance (hull drag) components – frictional drag and residuary drag. There are other resistance components such as windage drag (air drag) and appendage drag (drag generated by the underwater appendages such as the shafting and rudder), but these peripheral resistance components have little or no effect on a hull's wavemaking characteristics.

Frictional Resistance

Frictional drag is the drag caused by the friction between the hull bottom and the water. Due to the viscosity (or "thickness") of the water, a layer of water is dragged along by the hull. The very layer next to the hull is dragged along at the hull's forward speed, with successive layers of water dragged at decreasing speeds until there is no effect at some distance away from the hull surface. The thickness of this entrained water, termed the boundary layer, primarily varies with wetted length and speed. For a small planing craft the boundary layer may grow to only about 50mm in thickness by the time it reaches the transom, but for a large ship it can be several metres thick.

The frictional drag of a hull has essentially no influence on the waves the hull generates. It is a viscosity-based drag component.

Residuary Resistance

This resistance component is comprised of several sub-components that vary depending on the hull type, though it literally can be read as "all other hydrodynamic drag components". These components are intended to fall into the category of *gravitational* components, hence having some influence on wavemaking, but some minor components with little or no gravitational context are lumped into this category for convenience.

The largest residuary resistance component is wavemaking drag. Hulls that generate hydrodynamic lift to reduce their overall drag at high speeds also generate a corresponding drag component of that lift. This drag component itself creates waves and reduces the benefit of the wave drag reduction created by the hydrodynamic lift.

2.4.3 Planing Action

The bottom of a planing hull generates its lift in a simple manner. The hull bottom acts like an aircraft wing, except there is flow over only one side. By operating at an angle to the water, termed the trim angle, the bottom surfaces create lift. The magnitude of the lift varies according to:

- the square of the vessel speed, such that doubling speed generates four times the lift;
- the area of the bottom surface;

- the trim angle, such that doubling the trim angle doubles the lift within practical limits;
- the shape of the planing surface, with the optimum being a short, wide planing surface.

As the vessel speed increases, the planing hull is being supported less by buoyancy and more by hydrodynamic planing lift. At a volumetric Froude number of about 3.3 (refer Equation 2.6), the vessel would be fully planing and all of its weight would be supported by lift. The relationship between vessel displacement and fully planing speed is shown in Figure 2.11 (Savitsky 1985).

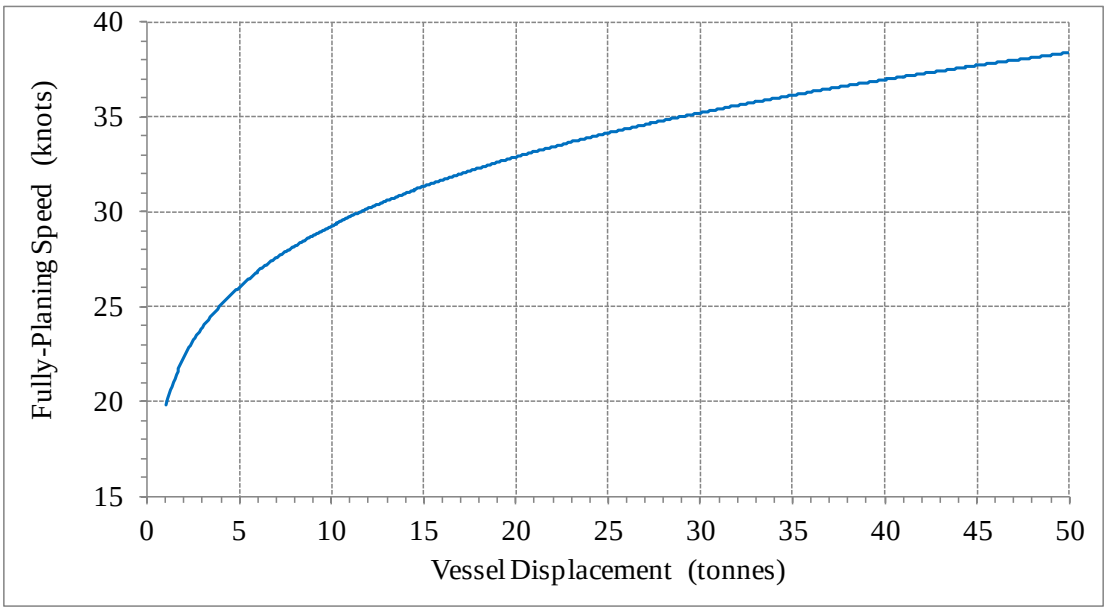

Figure 2.11 Relationship between fully-planing speed and vessel displacement (Savitsky 1985)

The problem for a planing hull comes with the increase of speed above this fully planing speed. The hull cannot keep generating lift greater than its own weight and consequently it would become unstable as it tries to plane on an ever-decreasing bottom area. To overcome this, the hull self-stabilises with increasing speed by reducing its running trim angle.

The reduction in running trim angle pushes the bow down and actually leads to an increase in the wetted surface area. However, the bow area of most vessels is a poor generator of lift due to its deep vee sections, so one doesn't completely offset the other. The re-immersion of the bow with increasing speed creates additional drag,

most of which is viscous and therefore has limited influence on wavemaking. Moreover, the extra waterline length can have a positive effect on wave generation in some instances. Some vessels, including ski boats, employ a gently rising bow profile that does not re-immerse much as speed increases and the trim angle flattens out.

Another consequence of lifting and trimming the hull as speed increases is the change in waterline length. The dynamic waterline length of a planing hull can be much shorter than the static waterline length, shown in Figures 2.12 and 2.13. The standard method of comparing the speed/length ratios is to use length Froude number (Equation 2.1), such that vessels with the same length Froude number are operating in an equivalent dynamic condition.

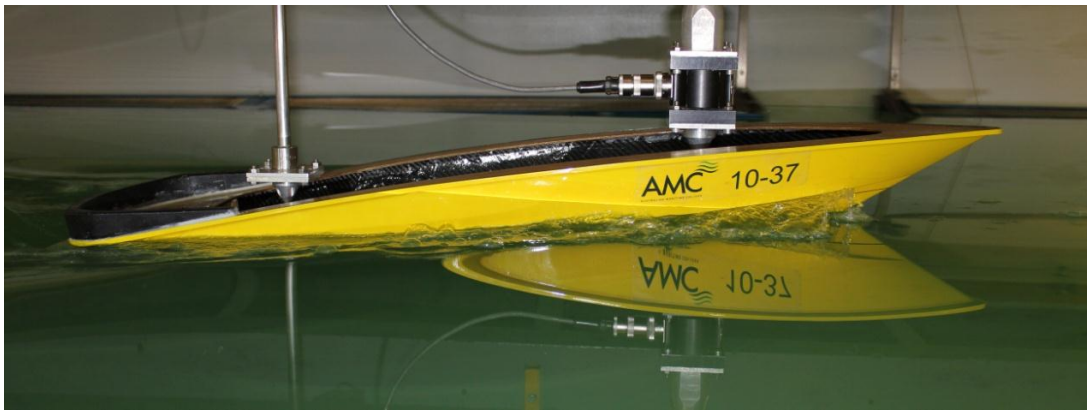

Figure 2.12 Change in dynamic waterline length – pre-planing speed

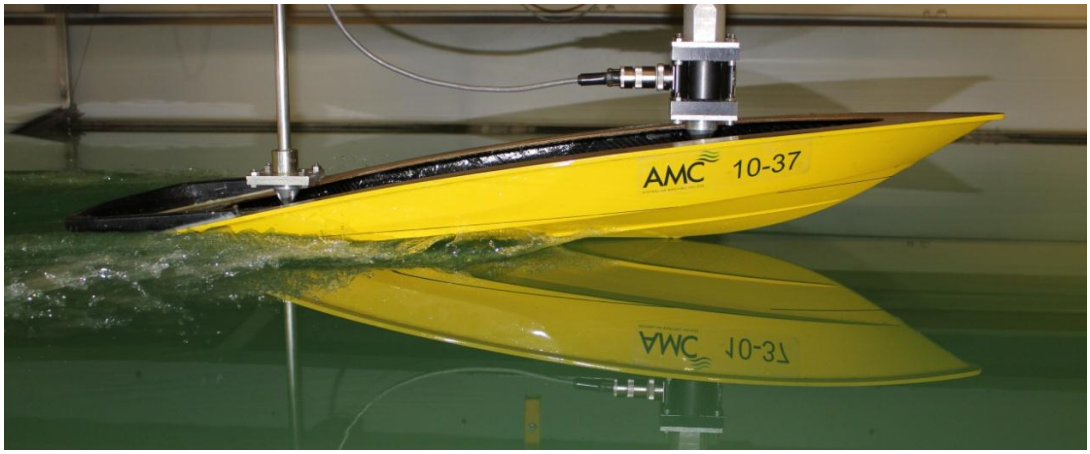

Figure 2.13 Change in dynamic waterline length – planing speed

For instance, a 5 m long waterline vessel travelling at 20 knots experiences the same dynamic conditions as a 10 m long waterline vessel travelling at 28.3 knots. This is

important, as it is not correct to compare vessels of differing waterline lengths at the same speed. However, the use of length Froude number can be misleading where the waterline length is changing with speed. In this instance, it is more appropriate to compare vessels based on volumetric Froude number (Equation 2.16), where the waterline length is replaced by the cube root of displaced underwater volume (hence vessel static weight), as a vessel's weight does not change with speed.

The quantitative relationship between the frictional and wavemaking drag of high-speed craft varies between the three vessel speed regimes. These are further discussed in context with high speed planing craft:

Slow Speeds (displacement)
At low speeds, friction drag can dominate but wave drag for pure displacement hull forms grows according to the sixth power of speed (u^6), so that doubling vessel speed increases wave drag by 64 times (Lewis 1988). In this slow speed range large waves can be created with only small increases in speed, yet waves can be substantially reduced in energy by slowing down slightly.

Pre-planing Speeds
In this region, trim angle can be high as a planing vessel attempts to generate its lift. Wave drag and hence wave wake is high. Wavemaking drag dominates.

Planing Speeds
As the hull reaches fully planing speed and beyond, its wavemaking resistance begins to level out in magnitude and then starts to decrease. The frictional drag component continues to increase and dominates at very high speeds. Planing hulls designed to operate at these very high speeds often employ hull features such as transverse steps or multiple planing surfaces (hydroplane hull forms) to control the growth of frictional drag.

2.4.4 Planing Forms and High-Speed Vessel Wave Generation

Wave energy, being a function of wave height and wave period (covered in Section 2.2.3, Equation 2.10), can be reduced by a reduction in either of these variables, with the reduction being non-linear.

As vessel speed increases and the planing surface is able to generate its lift from a smaller surface area and from a lower trim angle, the wave drag reduces. This is an indication of the efficiency improvement that comes with increasing speed, which also helps to explain why planing hulls have traditionally been viewed as good high-speed load carriers. From this efficient planing surface comes an improving lift/drag ratio, which accounts for the reduction in wave drag. The shorter waterline length can lead to a small reduction in wave period.

Generally, it is accepted that the height of the waves generated by any high-speed vessel is a function of its length to displacement ratio, Macfarlane 2002 (discussed in more detail in Chapter 3). For a given hull form, displacement and speed, a reduction in waterline length will increase wave height and the effect is strongly non-linear. A planing hull that develops a shorter waterline length as speed increases might be viewed as being undesirable, as this would increase wave height. However, the hull is no longer supported by buoyancy - where length-to-displacement ratio is important – it is supported by dynamic lift that produces dynamic drag (hence waves) as a by-product (Savitsky 1985). Shortening the waterline length improves the lift to drag ratio, or planing efficiency, by improving the aspect ratio of the hull surface (width/length ratio). The effect of shortening waterline length may therefore be opposite to that experienced by a high-speed displacement hull form.

With respect to minimising wave wake, in practical terms, the ideal ski boat will have:

- A relatively short length;
- The lightest possible displacement, achieved by keeping hull dimensions small (short length, modest beam and low freeboard), simple outfitting (no unnecessary fitout such as sleeping accommodation) and lightweight petrol engines (outboards preferably due to their slight weight advantage over inboards);
- A low deadrise (shallow vee) bottom. The lift/drag ratio of a planing surface deteriorates with increasing deadrise (depth of the vee), hence increasing wave energy generated;
- No ballast or equivalent effects from hydrofoils;
- A high operating speed, preferably at fully planing speed (Figure 2.11).

At high length Froude numbers, hull forms that generate dynamic lift have wavemaking benefits over those that are not configured to generate such lift,

(Savitsky 1985). Planing hulls can be particularly efficient at high speeds, though in practical terms their efficiency is usually compromised by the need to operate successfully over a wide range of speeds and sea conditions. For instance, the most efficient planing form in terms of hull drag per unit hull weight is a flat bottom hull with a peculiar concave profile, but this shape would not be suitable in anything other than smooth water and it has some dynamic running and turning problems, apart from the fact that it could only be configured to run at one particular condition (weight, weight location and speed). The optimum planing vessel form is shown in Figure 2.14 (Macfarlane and Cox 2005).

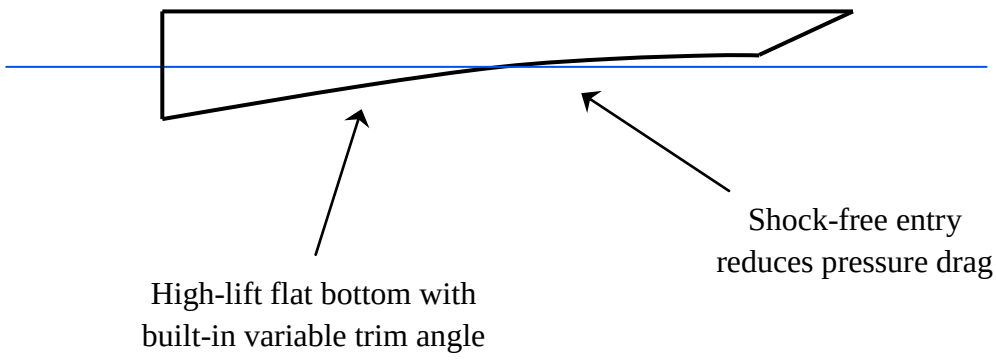

Figure 2.14 Idealised planing hull form for maximum efficiency (Macfarlane and Cox 2005)

2.4.5 Wake Boarding

Wake boarding is a development of water skiing that uses a shorter, wider board, enabling the wake boarder to perform a variety of acrobatic manoeuvres. To assist with the manoeuvres, the wake boarder makes use of the vessel's waves. There are many variations of wake boarding that use a different combination of board size and vessel speed. In general, more intricate and acrobatic manoeuvres are performed at slower vessel speeds than water skiing, where the vessel waves are greatest.

Wave wake height becomes an important factor when undertaking this activity, as well as wave steepness. The waves closest to the vessel will always be the highest and steepest, but there is a practical limit as to how close the wake boarder can manoeuvre from the tow vessel.

As well as varying speed and distance off, the simplest option to increase wave height is to increase the vessel displacement (weight) and running trim angle. This can be done statically through the addition of weight or dynamically by the addition of hydrofoils underneath the tow vessel.

Regardless of how wave wake height is increased, the subsequent wave energy generated is typically higher than a normal ski vessel. When the sport first started in Australia the vessels used were typically little more than modified ski boats or runabouts. However, as the sport has become more popular the vessels have become more developed and are designed to produce a very substantial wave wake.

Water Ballasting

The simplest way of generating a large wake is to increase the weight of the towing vessel. Wake boarders do this by adding water ballast to their vessels, carried in large custom-built bags. This allows the operator to select the appropriate amount of ballast that suits the vessel and the wake boarder without it being a permanent addition to the vessel. At the end of the day, the bag is simply drained to return the vessel to its designed road transportation weight.

This method is regarded as being a static method of increasing wave height, as the weight of the ballast is unaffected by the vessel's speed. The main benefit of this method is its simplicity, requiring only modest cost outlay and with a do-it-yourself option. However, there are some drawbacks:

- The ballast takes up space;
- Its effects are present at all times when the bags are full, unlike dynamic ballasting methods that depend on forward speed;
- It reduces at-rest freeboard that, in some small ski boats, is not large to begin with;
- If the ballast were fitted at main deck level, there would be a slight deterioration in vessel stability.

The ballast is normally positioned at the aft end of the vessel, as this is likely to result in the greatest increase in generated waves. At slow speeds, deep transom immersion increases wave drag, hence wave energy. At higher speeds, weight in the stern increases the running trim angle to generate the additional lift required to carry the ballast, which in turn increases wave drag.

Hydrofoils

Hydrofoils are horizontal fins that are secured beneath the transom of the vessel. They are shaped like an aircraft wing to produce hydrodynamic lift. By orientating the hydrofoil upside down, the lift acts downwards and pulls the aft end of the boat deeper into the water. These foils are fitted to the transom and can be hinged up when not in use. They also have a multiple positioning system that allows for their angle of attack to be adjusted manually. It is quite probable that hydraulic adjustment is also available that would allow adjustment whilst underway.

Unlike ballast bags, hydrofoils are dynamic ballasting devices – their effect being a function of several variables including vessel speed. For a given size and shape of hydrofoil, its downward force is dependent on:

- *Vessel Speed*: The downward force generated varies according to the square of the vessel speed – doubling the vessel speed generates four times the force. If the hydrofoil is low enough to be influenced by the propeller race, the force generated may be higher, but may also be lower if the swirling propeller race has both positive and negative effects on the foil.
- *Angle of Attack*: The force generated varies linearly with the angle of attack – double the angle to the water and the force doubles, though this linearity deteriorates at high angles of attack. Depending on its depth beneath the boat, the force generated by the foil may or may not be affected by the trim angle of the planing hull. The foil would normally be set at a pre-determined angle relative to the hull, but its angle to the water may also depend on the trim angle of the hull, which is normally greater than its at-rest trim angle. However, provided the foil is not very deep (possibly not more than one chord length below the bottom of the vessel, the *chord length* being the foil's fore-and-aft dimension) there would be little or no increase in angle of attack due to hull trim. It is known that hydrofoil vessels with foils operating near the surface start to lose lift when the foils are less than one chord length below the surface. For an inverted hydrofoil generating a downward force the effect may be the same, but possibly to a lesser extent.

There are some significant benefits of these devices:

- The downward force can be varied with speed and angle of attack, though there would be practical limits imposed by ventilation and possibly cavitation;
- The reduced force generated at slower vessel speeds can be partly offset by increasing the angle of attack of the foil;

- The cost is modest, but they need to be made from shaped metal (or high-grade composites) so the manufacture of efficient foils is beyond the do-it-yourself boat owner;
- By generating a downwards force low in the vessel, they give the vessel additional stability when underway;
- They are quick and easy to fit, engage and stow.

Drawbacks are few, the main ones being their decreasing effectiveness at slower speeds and the difficulty installing them on outboard-powered vessels (depending on transom configuration).

As an example of their capacity to generate downward force, a 600 mm span (width) by 150 mm chord (fore-and-aft) foil set at an angle of attack of 6 degrees, 150 mm below the hull bottom, at 10 m/s vessel speed (19.5knots, 22mph), would generate a downward force of 280 kg. This is equivalent to a standard 300 litre ballast bag. The angle of attack is limited only by force breakdown due to ventilation or cavitation.

The overall effect of the hydrofoil on the vessel is more than just to increase the running trim and immersing the transom deeper into the water – there is a two-fold benefit. Firstly, the downward force generated increases the weight of the vessel by a virtual amount, generating what is termed a "virtual displacement". This is the sum of the vessel's actual displacement and the dynamic force generated by the hydrofoil.

Secondly, the downward force produces a stern trim moment, or a lever effect that increases stern sinkage. These two effects are shown in Figure 2.15. In essence, the effect of the hydrofoil is equivalent to the effect of the ballast bag.

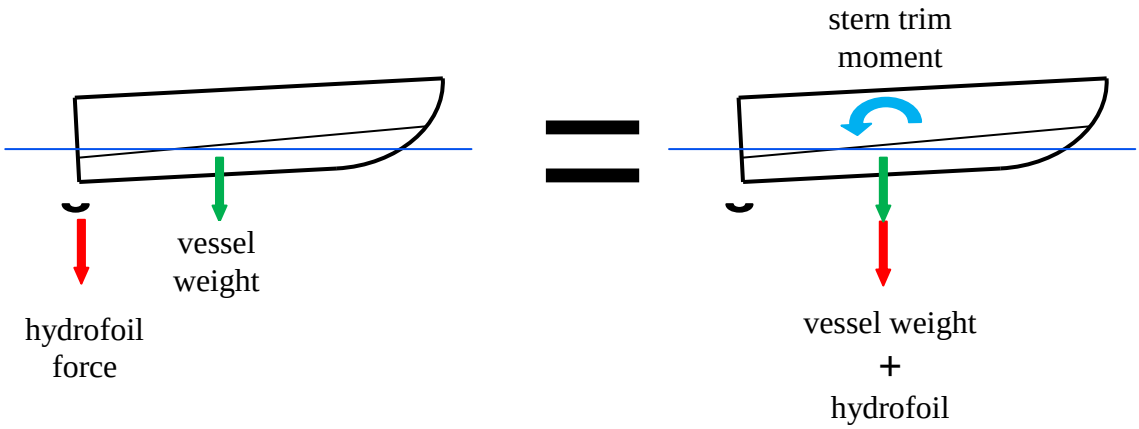

Figure 2.15 Effect of hydrofoil

As previously discussed, wake boarders seek to increase their enjoyment by increasing the height of the waves generated by the tow vessel. There would also be some benefit derived from increasing wave steepness (ratio of wave height to wavelength), but this can only be achieved practically by increasing wave height for a given vessel, rather than wavelength. The definition of ballasting includes the use of foils as well as ballast bags.

As an example of the effects of ballasting, increasing vessel displacement by 25% through ballasting or employing hydrofoils would increase wave height by a similar percentage, but the demonstrated non-linear effect on wave energy (refer Section 3.4) would result in a 56% increase ($1.25^2 = 1.56$). For example, if the vessel generated a (maximum) wave possessing 60 J/m of energy at a lateral distance of 23 m from the sailing line in its un-ballasted condition, the same 60 J/m would be generated at 45 m from the sailing line in the ballasted condition, an increase of almost 100%. Assuming the vessel operated in the centre half of the waterway, the waterway would need to be in the order of double the width of that needed for the un-ballasted condition.

Clearly, wake boarding activities are not recommended in narrow waterways possessing sensitive shorelines and need to be undertaken in more open areas. An additional benefit of this is the likelihood that open waterways with increased fetch are higher energy environments and would be bounded by shorelines more resistant to incident wave energy.

The current level of debate about bank erosion in wake boarding publications suggests that erosion is a contentious issue (for example Watkins 2004; Howden 2004; Glamore 2011). It is quite common within all areas of boating, and probably most other recreational pastimes, that the level of understanding of the issues is fuelled by anecdotal evidence but tempered by limited technical knowledge.

What is needed to address this is user education that will help them to understand the issues so they can take steps to minimise their impact. This will help proponents of wake boarding and water skiing to develop these recreational activities further. Governments, industry associations and sporting bodies must develop partnerships and work towards compromise outcomes.

2.5 Sheltered Waterways

2.5.1 Regions

It is known that wave wake issues can differ considerably depending upon the size and/or speed of the vessel(s) and the location(s) in which they operate. As a result, it is useful to categorise particular scenarios into the following three distinct regions, with reference to examples of rivers and harbours in Australia:

a) *Highly Sensitive Regions* - This region includes very sheltered waterways such as rivers with very limited fetch and/or width. They often have steep, cohesive banks that are highly susceptible to erosion by vessel wave wake. Vessel speeds are likely to be restricted to a small range of sub-critical depth Froude numbers. Vessel operation at trans-critical depth Froude numbers should be avoided and operation at super-critical depth Froude numbers may be limited to only very small craft (less than about 5 m length). Examples in Australia include the lower Gordon River, upper reaches of the Parramatta and Swan Rivers and sections of the Noosa River.
b) *Moderately Sensitive Regions* - This region includes semi-sheltered estuaries such as the lower reaches of large rivers and harbours or areas where shorelines have been artificially armoured to withstand increased wave action. Vessel speeds are likely to be restricted to a range of sub-critical depth Froude numbers. The possible exceptions may include certain small craft and larger wave wake-optimised craft that could operate at some super-critical depth Froude numbers. In such cases, specific criteria may be required to determine acceptable speeds for each vessel type (this is discussed in more detail in Chapter 7). Operation at trans-critical depth Froude numbers should be limited to acceleration and deceleration between the sub and super-critical conditions. Examples include the lower reaches of the Parramatta, Brisbane and Swan Rivers and sheltered areas of Sydney Harbour.
c) *Coastal Regions* - In these more exposed regions, wave wake criteria generally only apply to large high-speed craft operating at trans- or super-critical depth Froude numbers. Minimal problems eventuate from almost all vessels operating at sub-critical speeds. Some existing criteria applied to high-speed vessels are based on acceptable levels from ‘conventional’ (i.e., not high-speed) vessels operating at sub-critical speeds (Parnell and Kofoed-Hansen 2001). Often the criteria are imposed due to adverse safety risks for other users of the waterway (and shoreline)

as a result of large/long vessel waves generated at high speeds. Examples include Scandinavian coastal regions and Marlborough Sounds in New Zealand.

The limited number of regions where wave wake is of concern within Australia (such as those of the Gordon, Parramatta, Brisbane and Swan River ferry services) have been the subject of individual studies that have sought vessel-specific solutions, as opposed to an over-arching methodology that would allow for a desktop evaluation of any vessel in any waterway (refer Macfarlane and Cox, 2007, for a summary of studies conducted).

As discussed in Chapter 1, there is a relatively large recreational boating population in Australia that utilises the limited sheltered waterways available. It therefore makes sense to develop tools and guidelines related to vessel wave wake that allow for the sustainable use of sheltered waterways.

2.5.2 Types of Bank

From discussions with coastal engineers, it is believed that there may only need to be as few as two, but probably three, different bank types considered should a study aim to develop regulatory criteria and suitable threshold criteria to avoid bank erosion due to wave wake. All are natural depositional landforms. Artificial shorelines are more diverse and should be engineered to withstand an appropriate wave climate, although that has not always been the case.

The first is typical of very sheltered waterways that may experience little or no tidal range and do not have a beach structure since the energy climate is not wave dominated. These low-lying banks tend to be characterised by cohesive muds and substantial sediment trapping riparian or saltmarsh vegetation (usually not mangroves). The sediments are fine enough to be transported in suspension by currents and these deposits may represent the accumulation of sediment over extensive (geomorphological) time-scales. Once such natural features are disturbed by erosion the damage is effectively permanent.

The second is characterised by some resemblance to a beach, which usually consists of fine sand and muddy sediment (so-called muddy sands) but may not have formed entirely (or at all) in response to wave driven processes. Cohesive soil banks may lie at the head of the beach, such that the beach represents an adjustment of the bank

which has been exposed to wind wave, tidal and flood influences. These banks can withstand some wave action, but they often do not have the support of riparian vegetation. The upper bank structure can be severely weakened if the riparian vegetation is removed due to anthropogenic intervention such as land development (such as the Brisbane and Parramatta Rivers), cattle grazing and tidal influx (Brisbane River) (University of Nottingham 1996; Todd 2004).

The third possible bank type is what is generally regarded as a sandy beach, with fine to coarse grained sand (sandy mud or clean sand) that extend well above and below the mean waterline. These beaches are normally found in open areas in bays and at estuary mouths where there is a substantial wind wave climate and/or strong tidal flows. It is this third bank type which may be surplus to study requirements, as they are somewhat dynamic by nature and are already reasonably understood by current coastal engineering science (USACERC 1977). These beaches are generally not susceptible to wave wake from small craft although some may be affected by larger, high-speed ferries and shoaling waves may affect the safety of persons close the shore (Parnell *et al*. 2007).

For small craft operating in sheltered waterways, only the first two bank types are considered to be of prime importance.

2.5.3 Restricted Waterway Effects

In rivers and waterways that are shallow and narrow, a vessel may encounter a blockage condition where it effectively begins to push water along with it. This results in a large surge preceding the vessel and a drawdown as the vessel passes. These are often referred to as Bernoulli waves and are particularly common when large ships operate in restricted waters (Pinkster 2009). If the channel is narrow enough, this surge and drawdown impinges on the shoreline and leads to damaging erosion. It is particularly noticeable at speeds around the critical speed and at high speeds.

The most common restricted channel phenomena are:
surge - defined as the rise in surrounding water level preceding an approaching vessel. When a vessel travels in a uniform channel at close to the critical speed (depth Froude number of unity) solitary waves, or solitons, can propagate forward of the vessel almost periodically. Dand *et al* (1999a) concluded that the existence of solitary

waves in open water may explain the "rogue" waves associated with real-world operation of fast craft;

drawdown - sometimes referred to as suction troughs, defined as a lowering of the water level abreast of a passing vessel. It often appears as a recession of water from a beach or bank as a vessel passes close offshore;

backwater flow - defined as the aftwards acceleration of water across a shallow seabed as a vessel passes above.

squat - defined as the mean increase in sinkage and change in dynamic trim when a vessel moves through water. Although present in deep water, squat is considerably aggravated by restrictions in water depth and/or width (Tuck 1967; Ferguson *et al*. 1983; Duffy 2008).

The nett effect of these restricted channel effects is referred to as blockage in ship design. The calculation of blockage is important in the design and operations of canals and ports, as well as in ship scale model testing. There are many references available, though the published methods for calculating blockage can produce widely varying results, depending on the source of the empirical data and/or the water flow assumptions made (Scott 1970; Gross and Watanabe 1972; Millward 1983). What is clear is that a single definitive methodology or set of equations for calculating blockage effects does not exist.

The onset of a blockage condition occurs when the ratio of vessel underwater cross-section against waterway cross-section reaches a particular value. This value is dependent on factors such as the vessel speed and channel width-to-depth ratio. As a guide, if the vessel underwater cross-section is less than 1% of the channel cross-section, blockage will be negligible. Vessels can usually operate with few environmental effects up to a 3-4% ratio (Scott 1970; Robbins *et al*. 2011).

However, blockage effects such as surge and drawdown are localised phenomena that travel along with the vessel. Any vessel passing close to a bank, especially in shallow water, can create a localised blockage effect. This needs to be considered when proposing vessel operating criteria in restricted waterways. The drawdown in particular can be erosive and, if severe enough, will affect people and small craft at the water’s edge.

Several methods exist for predicting water level depression and back flow velocity around large ships operating in restricted waters (Sharp and Fenton 1968; Bouwmeester 1977; Pinkster and Naaijen 2003).

2.5.4 Wind Waves

Waves with different characteristics have different effects on the environment. Wind waves are characterised by low to moderate wave heights, but short periods.

Sheltered waterways generally experience only a wind wave environment. Wind waves of short fetch (and even waves of longer fetch, such as wind-driven ocean seas) exhibit a disproportionate growth relationship between wave height and period, disproportionate in that wave height grows more rapidly than period but both have equal weighting in calculating wave energy (refer Equation 2.10). As an example, the wind wave height and period for varying wind speeds and fetch lengths are shown in Table 2.2. These values are generated by hindcasting - applying a standard set of equations to generate wave data given the wind speed and fetch (the distance the wind has been blowing over water). The formulae used are covered in more detail in the USACERC (1984):

$$\frac{gH}{U_A^2} = 0.283 \tanh\left[0.530\left(\frac{gh}{U_A^2}\right)^{3/4}\right] \tanh\left\{\frac{0.00565\left(\frac{gF}{U_A^2}\right)^{1/2}}{\tanh\left[0.530\left(\frac{gh}{U_A^2}\right)^{3/4}\right]}\right\} \qquad (2.18)$$

$$\frac{gT}{U_A} = 7.54 \tanh\left[0.833\left(\frac{gh}{U_A^2}\right)^{3/8}\right] \tanh\left\{\frac{0.0379\left(\frac{gF}{U_A^2}\right)^{1/3}}{\tanh\left[0.833\left(\frac{gh}{U_A^2}\right)^{3/8}\right]}\right\} \qquad (2.19)$$

It is clear that increasing either fetch or wind speed leads to much faster growth in wave height than wave period. Consequently it can be argued that sheltered waterways experience occasional wind wave height variations of several hundred percent, but with limited accompanying wave period growth.

Sheltered shorelines in a wind wave environment are often dynamically stable. Beach areas, if they exist, adjust in response to the prevailing wave climate and sediment budget. Other landforms in low wave energy environments may typically owe their genesis to processes not associated with waves. When there is a substantial increase in incident wave period beyond what such landforms would normally experience the shoreline may experience erosion. Not only do the longer period waves contain more energy but orbital currents capable of entraining sediment extend to greater depths. Where mud flats are present, shoaling long-period wake waves may form higher breakers more likely to plunge. Small craft traversing at high speeds in sheltered waterways can generate wave periods far longer than those which occur naturally.

Fetch (m)	Wind 5 m/s	Wind 10 m/s	Wind 20 m/s
100 m	26 mm / 0.5 s	62 mm / 0.7 s	144 mm / 0.9 s
500 m	59 mm / 0.8 s	137 mm / 1.1 s	321 mm / 1.5 s
1,000 m	83 mm / 1.0 s	194 mm / 1.4 s	452 mm / 1.9 s
10,000 m	250 mm / 2.0 s	586 mm / 2.8 s	1,304 mm / 3.8 s

Table 2.2 Hindcast wind waves

The geomorphic impact of wind waves is not evenly felt throughout river systems and the greatest impacts occur at the downwind ends of reaches. In contrast, vessel wave wake impacts are more evenly spread throughout the waterway, with diverging waves especially impacting upon shorelines that would not otherwise be subjected to a significant incident wave climate. The wave wakes of high-speed craft, in particular, are dominated by the divergent wave system and, as the depth Froude number becomes super-critical, all waves propagate obliquely to the sailing line (refer Section 2.1).

The example illustrated in Table 2.2, which highlighted the fact that the height of wind waves grows by several hundred percent but the period increases at a much slower rate with increasing wind speed, has three further consequences.

Firstly, wind waves, or chop, cause discomfort to small marine craft. The waves are close together and relatively high, so they are considered to be steep. The wave period is often similar to the roll period of small vessels, causing them to roll synchronously when stationary.

Secondly, the energy in wind waves tends to be more height-dependent than period dependent. As discussed in Section 2.2.3, for wave wake studies wave energy is equally a function of both wave height and period. A shoreline naturally subjected to wind waves may occasionally experience waves with a large height, but the corresponding period will remain relatively low. Similarly, such a shoreline may be able to withstand vessel wave wake, provided the wave wake is characterised by moderate wave height but low corresponding wave period.

Thirdly, shoaling waves tend to increase in height before breaking. However, for waves with periods less than 3 seconds, the shoaling is considered to be negligible (less than 10% height increase), and for waves with periods less than 2 seconds the waves will be close to breaking before any shoaling occurs, USACERC (1984). Wind waves, particularly in sheltered and semi-enclosed waters, tend to maintain their deep-water height before breaking. This can also be seen at a surf beach, where the long-period swells stand up before breaking but the wind-driven chop simply breaks on the shore.

The last point is of particular interest, as it is commonly believed by many people that vessel wave wake height is the primary determinant of erosion potential – wave height is a more visual indicator of wake waves (Lesleighter 1964). However, wave period possibly has a greater effect in sheltered and semi-enclosed waters, particularly on shorelines with sloping beaches (Parnell and Kofoed-Hansen 2001; Macfarlane *et al*. 2008). Such shorelines have natural, dynamic mechanisms to withstand wind waves, but the sudden introduction of vessel wave wake containing much longer-period waves may upset the balance.

Chapter 3

Quantifying Vessel Wave Wake and Bank Erosion

3.1 Introduction

Historically, the height of a single wave has been used as the primary comparative measure for vessel wave wake. It is possibly the simplest parameter to measure and this fulfils another desirable requirement – it is within public perception where subjective visual observation must substitute for engineering measurement. Similar comments were made by Lesleighter (1964) in his analysis of ski boat wave wake on the Hawkesbury River, where he found that inflated anecdotal claims of excessive wave wake height could not be substantiated by measurement.

In the authors' opinion, the historical use of wave height alone, or indeed any single criterion, cannot possibly reflect the true erosion potential of a vessel's wave wake. Wave period is a strong indicator of the potential to move sediment in any shoreline environment, either through the period-dependent orbital velocity below the surface of shallow, but unbroken, waves, or through the gravity driven jets of plunging breakers (USACERC 1984). Period, along with height, is required to calculate both wave energy and wave power of a single wave (refer Section 2.2.3).

In this chapter, the basic requirements of wave wake measures are reviewed and background on the effect that vessel speed, vessel size/displacement and water depth has on the wave patterns and characteristics of the waves generated is provided. The specific measures adopted within this study are stated, including justification for selecting these measures over other techniques.

There is also a brief review of previous and current work on the quantification of shoreline (bank) erosion due to vessel wave wake. Particular attention is given to some of the most recent work conducted on the lower Gordon River in South-West Tasmania.

3.2 Relevant Wave Wake Characteristics

When attempting to quantify vessel generated waves, particularly when considering sheltered waterways, it is necessary to identify the waves of geomorphological

interest and focus upon them. As was discussed in the previous chapter, of the two vessel-generated wave types, transverse and divergent, it is the divergent systems that dominate in high-speed vessel wakes. Transverse waves can be significant when generated by displacement hull forms or heavy, transom-sterned high-speed craft traversing at displacement speeds, and especially where the waterways are very narrow. Transverse wave height (and therefore energy) decays faster than divergent wave height with lateral separation from the sailing line, but this decay becomes bounded by the shoreline. Being more of a concern with slow vessel speeds, transverse waves are best controlled by changes to operating speeds and vessel design.

In analysing vessel wave wakes, the two parameters of maximum wave height and the corresponding wave period for the highest wave (often termed the *maximum* wave) have been commonly adopted as the primary measures over the past decade or two. The importance of quantifying wave wakes with simple measures is critical when assessing small craft wave wake impacts. If the measures were complicated, statistically difficult to represent or costly to collect and collate, regulatory authorities may be reluctant to pursue a path of boating management through scientific understanding. Blanket speed limits might be a typical response but these, which to be effective must be specified for the 'worst offender', are likely to be overly restrictive for other vessel classes.

These primary measures, height of the maximum wave and its corresponding period, appear to exhibit certain predictable relationships at high vessel speeds, which is essential to the development of simple but sound methods for predicting small craft wave wake. Cox (2000) demonstrated for high-speed craft travelling at sub-critical depth Froude numbers that divergent wave height is largely a function of length-displacement ratio of the vessel and the corresponding period is largely a function of vessel waterline length. Analysis by Macfarlane (2002) clearly supports this and confirms that vessel hull form has only a limited bearing on high-speed, deep water wave wake, as demonstrated in Figures 3.1 and 3.2 (data obtained from Macfarlane *et al*., 2008). Both of these figures present deep water experimental results for approximately 80 different monohulls and multihulls. In Figure 3.1, the height of the maximum wave is plotted as a function of length-displacement ratio ($L/\nabla^{1/3}$) for a vessel speed of 13 knots. There is a very clear trend that an increase in $L/\nabla^{1/3}$ (i.e. making the vessel longer and or lighter) will result in a reduction in maximum wave height.

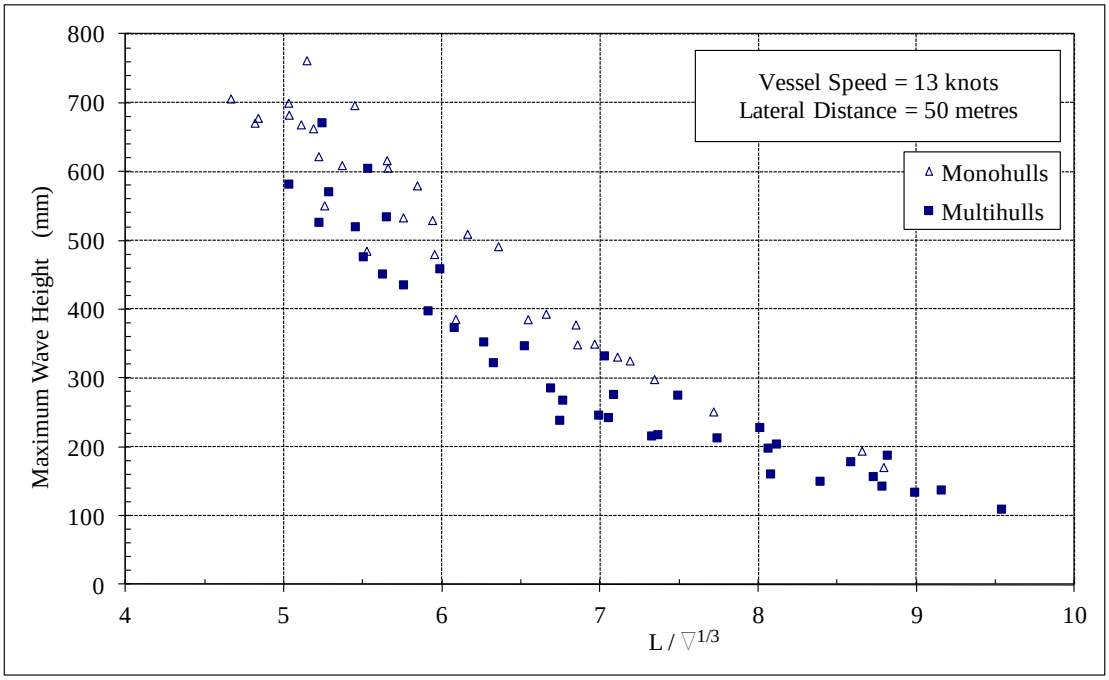

Figure 3.1 Maximum wave height as a function of slenderness ratio (Macfarlane *et al*., 2008)

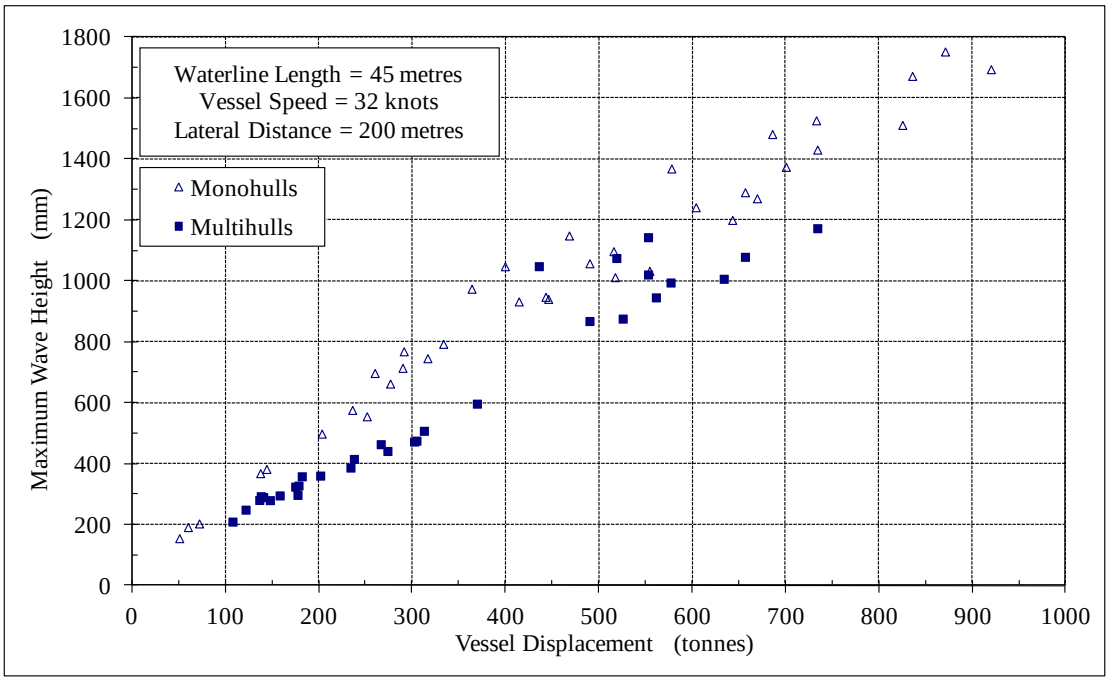

Figure 3.2 Maximum wave height as a function of vessel displacement (Macfarlane *et al*., 2008)

A similar conclusion can be drawn from the data presented in Figure 3.2 where the height of the maximum wave is plotted as a function of vessel displacement. In this case all data sets have been scaled to correspond to a waterline length of 45 m and

speed of 32 knots. It can also be seen in Figures 3.1 and 3.2 that, in general, multihulls generate a lower maximum wave height at an equivalent $L/\nabla^{1/3}$ or displacement.

The data presented in Figure 3.3, taken from field tests on a variety of small commercial vessels and recreational craft, shows how high-speed wave period (normalised by dividing by √L) generally collapses to a narrow, constant band at speeds in excess of $Fr_L > 1.0$ (Macfarlane *et al*., 2008).

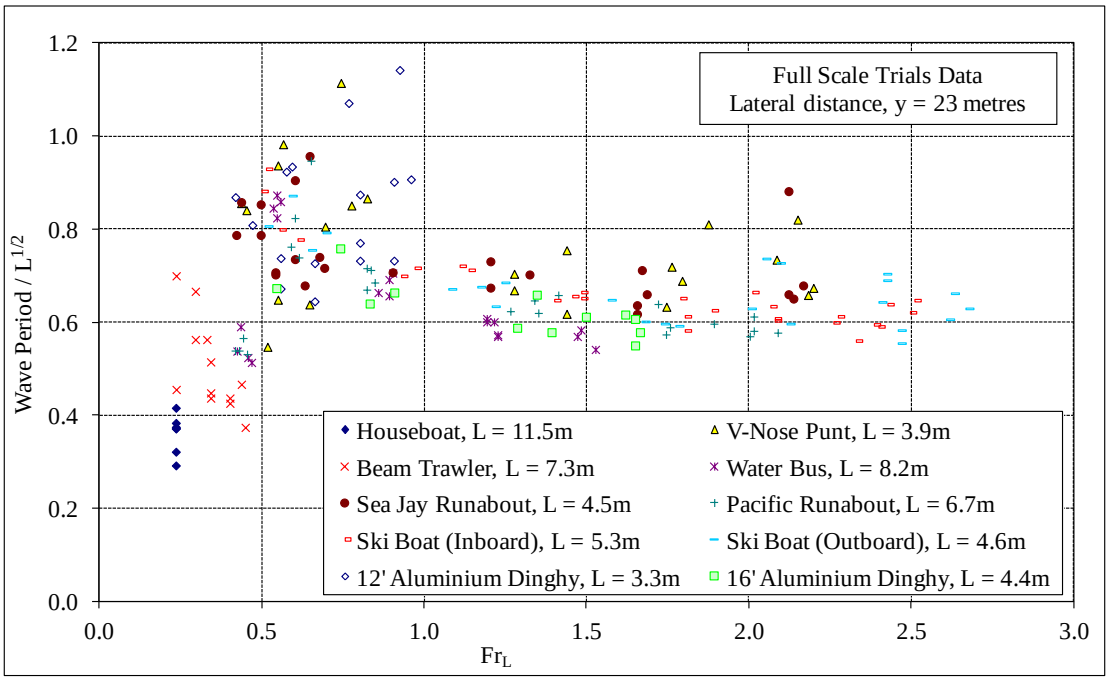

Figure 3.3 Wave period / $L^{1/2}$ as a function of length Froude number (Macfarlane *et al*., 2008)

In Figure 3.4, the most common wave wake parameters, such as height, energy and power, show growing values with increasing vessel speed, peaking at a certain speed (normally about $Fr_L = 0.55$) and then decreasing back to a lower level. Similarly, wave period also grows with increasing vessel speed, peaks, but tends to level off rather than decrease at higher speeds. Regardless of which wave wake parameter is used as an erosion indicator, it is clear that there may be two distinct operating speed ranges – slow speed and high speed, with intermediate transitional speeds to be especially avoided.

As previously discussed, planing craft in particular are burdened by this "transition hump" where resistance and hence wave wake is high. In some sports, such as wake

boarding, this is viewed by the proponents as beneficial. Many boaters will explain anecdotally how they believe it is better to travel at high speeds in sheltered areas because of the 'lower wash' and this reasoning has long been used as a justification for transiting at speed. The current science would not support such a generalisation since the waves from small planing vessels have been demonstrated to be capable of eroding both muddy and sandy banks (Scholer 1974; Todd 2004; Swan River Trust 2009).

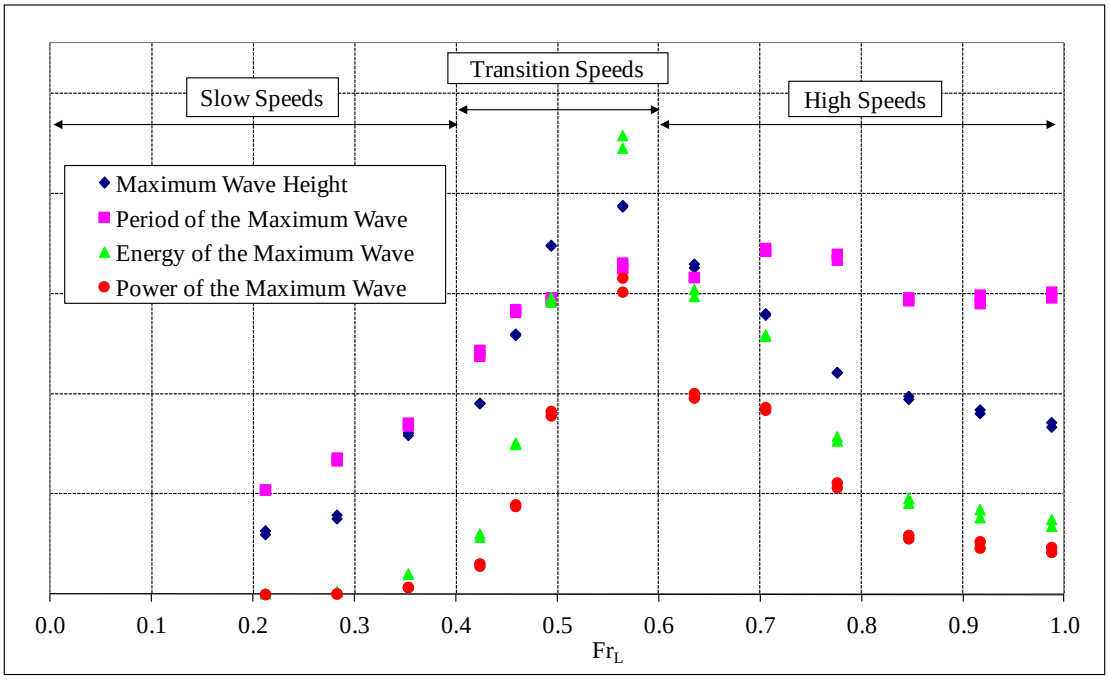

Figure 3.4 Wave height, period, energy and power as a function of Fr_L

An alternative approach to identifying one (or more) individual 'maximum' waves from any longitudinal cut of a vessel's wave wake is to attempt to determine the total energy transmitted by the entire wave packet. Transmitted wave energy E_t is found by integrating the wave power with time (USACERC 1977):

$$E_t = \int \overline{P}\, dt \qquad (3.1)$$

A typical wave profile generated by a vessel, such as the example shown in Figure 2.8, will consist of changing wave height and period so the integral in Equation 3.1 is best evaluated by breaking the surface elevation time history into individual half-wavelengths to account for the varying amplitudes. The total wave energy transmitted is found by summing the contributions for each half-wavelength, as shown in Equation 3.2 (where the subscript *n* indicates each half-wavelength):

$$E_t = \sum_n \bar{P}_n \frac{T_n^2}{2} \quad (3.2)$$

Here $\bar{P}_n$ is calculated from H_n and T_n using the relations given in Equations 2.7, 2.11 and 2.15. For example, in deep water the transmitted wave energy becomes:

$$E_t = \sum_n \frac{\rho g^2 H_n^2 T_n^2}{64\pi} \quad (3.3)$$

This process was used by both Macfarlane and Cox (2003 and 2005) and Gourlay (2010) to obtain the transmitted wave energy from full scale trials data, however, in both cases problems arose in the truncation of the wave train. This can occur due to contamination by either incident wind waves or local wave interference. In the case of Macfarlane and Cox, this was overcome through manual analysis in order to ignore the localised interferences and only select a constant number of 'real' waves, though this leads to sensitivity of the solution and subjectivity. The relative consistency of the transmitted wave energy compared to that of the maximum wave suggests that the contamination in this instance was not substantial.

3.3 Wave Measures used in This Study

As previously discussed, it is very important that the key, or maximum, waves within the overall wave train generated by a vessel are correctly identified and quantified. It has been shown that at sub-critical speeds the maximum (highest) wave generally also possesses the greatest energy of all the waves in the sub-critical wave pattern (Macfarlane 2002). This makes the identification of the single most important wave in the sub-critical wave pattern generally a relatively straightforward task. As part of work done in this study it was concluded that this is often not the case for vessels travelling at trans-critical and super-critical speeds, i.e. the highest wave does not always possess the greatest energy, thus it is likely that waves with greater potential to cause erosion are ignored. Therefore, it is recommended that more than one wave must be identified when attempting to quantify and assess any vessel wave wake where the waves may be depth-affected. As already identified, this includes a large percentage of vessels operating within sheltered waterways.

An investigation has been conducted to determine the minimum number of waves that should be identified and then quantified to ensure all potentially significant waves within a wave train are considered. This investigation involved the careful analysis of

a very large collection of data obtained through the conduct of model and full scale experiments involving all important variables, each over a wide range of typical 'real-life' conditions. It has been found that clearly identifiable packets of waves are often generated, with each packet possessing quite different wave periods. Others have also commented on the existence of such packets of waves, particularly from vessels operating at super-critical speeds (for example, Kofoed-Hansen 1996; Whittaker *et al*. 2000b; Doyle 2001).

Following this investigation, it is suggested that in most finite water depth cases there are a minimum of two key waves within each wave train that must be quantified – in simple terms these waves can be defined as those that contain (a) the greatest height, and (b) the longest period, as it is likely that one of these waves will also possess the greatest energy. However, it has been found that there are also a number of cases where a third significant wave is generated which may contain the greatest energy, but not necessarily possess either the greatest height or period. Therefore, it is recommended that the following three divergent waves be identified then quantified:

Wave A – is defined as the leading diverging wave, which is the wave that will possess the longest period. As previously discussed, it is often the waves with long periods that create the greatest issues within sheltered waterways (particularly bank erosion), which makes the quantification of these waves very important. These leading waves are rarely the highest in the wave train, in fact their height is often relatively low, however there are occasions when their height can be considerable, resulting in the potential for transmitting substantial energy to the shore. A long period wave has a long wavelength, so the energy will be large since the area for the given height is bigger.

As discussed in Section 2.1.7, the wave angle will alter significantly between sub-critical, trans-critical, critical and super-critical speeds. It was shown that it is often easier to identify the leading wave for super-critical vessel speeds (and high trans-critical speeds), compared to sub-critical or trans-critical speeds, as at the higher speeds the leading waves generated have longer crest lengths, making it a simpler task to track the same wave as it propagates away from the vessel's sailing line.

Wave B – is defined as the most significant wave following the leading wave (Wave A). The period will be shorter than the leading wave, but often not by a large margin, whereas the height is very often greater than the leading wave. This wave often

possesses the greatest wave energy, but may not necessarily be either the longest or the highest wave in the wave train. It has been found that the relative heights of Waves A and B can vary markedly between different hull forms, thus it is advantageous to use experience (familiarity with the wave profiles generated by many different hull forms) when attempting to identify Wave B. It is required that the same wave be identified at each lateral location (wave probe), otherwise the properties of the wave may be distorted.

Wave C – it is common for a group of short period divergent waves to be generated and Wave C is defined as being the highest wave within this group. This wave always follows Waves A and B, hence will possess the shortest wave period of these three key waves. In most sub-critical and trans-critical cases this wave also has the lowest wave height of the three waves, or at best a height similar to either Wave A or Wave B (hence also the lowest energy). But what makes this wave significant and worth quantifying is that there are a percentage of occasions, particularly at super-critical speeds, where this wave is the highest generated, and occasionally also contains the greatest energy of all three key waves. However, because of its significantly shorter period, it is very likely that this wave may not be the most significant wave when considering sheltered waterways, as the period may be similar to the local naturally occurring wind wave environment.

The following example is useful to help define each of the above waves and illustrate the need to identify more than one significant wave. A typical time series history of a single wave profile obtained from a model scale experiment is shown in Figure 3.5. In this figure, Waves A, B and C have been identified and the resultant height, period and energy of each wave are provided in Table 3.1 (wave energy is calculated using Equation 2.10). As can be seen, the highest wave in this example is Wave C, but it possesses the shortest period and a significantly lower energy compared to Waves A and B. It is the leading wave (Wave A), with the lowest height but longest period, that possesses the greatest energy.

This example highlights the potential dangers when using the commonly adopted wave wake criterion that only considers the highest wave generated when assessing waves generated at trans-critical or super-critical vessel speeds, as it is likely that at least one or two waves with significantly greater energy and longer period may be ignored (potentially many more as Wave B is often representative of a packet of waves possessing similar period). The consequences of this may result in a significant underestimation of the erosion potential of a particular case, or an unfair comparison

when attempting to assess various different vessels or other variables. The author is aware of several occasions where unscrupulous vessel operators have been known to use similar methods to lower the apparent size of the waves their vessel generates when attempting to meet specific regulatory criteria. This is relatively easy to achieve if only a single 'maximum' wave is identified and assessed against a single criterion.

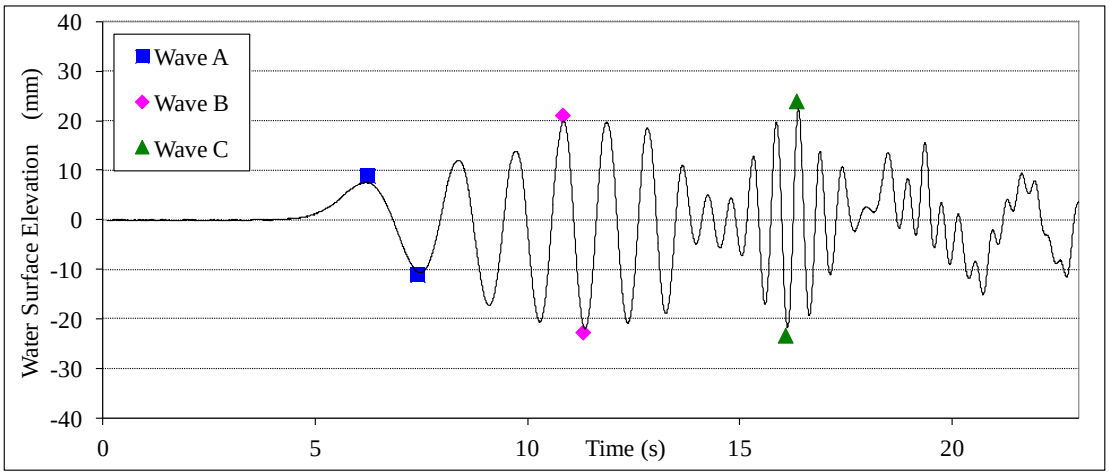

Figure 3.5 Example wave profile time series (Waves A, B and C)

	Wave		
	A	B	C
Wave Height (mm)	18.5	43.0	45.0
Wave Period (s)	2.34	0.96	0.52
Wave Energy (J/m)	3.6	3.3	1.1

Table 3.1 Example wave quantities

Results presented by Macfarlane (2009) identified two distinct packets of waves, each packet with quite differing wave periods, but with the short-period wave being the highest. A time series history example from Macfarlane (2009) has been reproduced in Figure 3.6 showing these two waves. What was not considered in this earlier work was the first (leading) wave, although lower in height is clearly longer (higher period) than all other waves. The present study has considered all three of these waves.

For each of Waves A, B and C it is proposed that the following wave characteristics be quantified: wave height constant (γ), wave period (T), wave decay exponent (n) and wave angle (θ). The precise technique used to identify each of these measures is outlined in detail in Chapter 5.

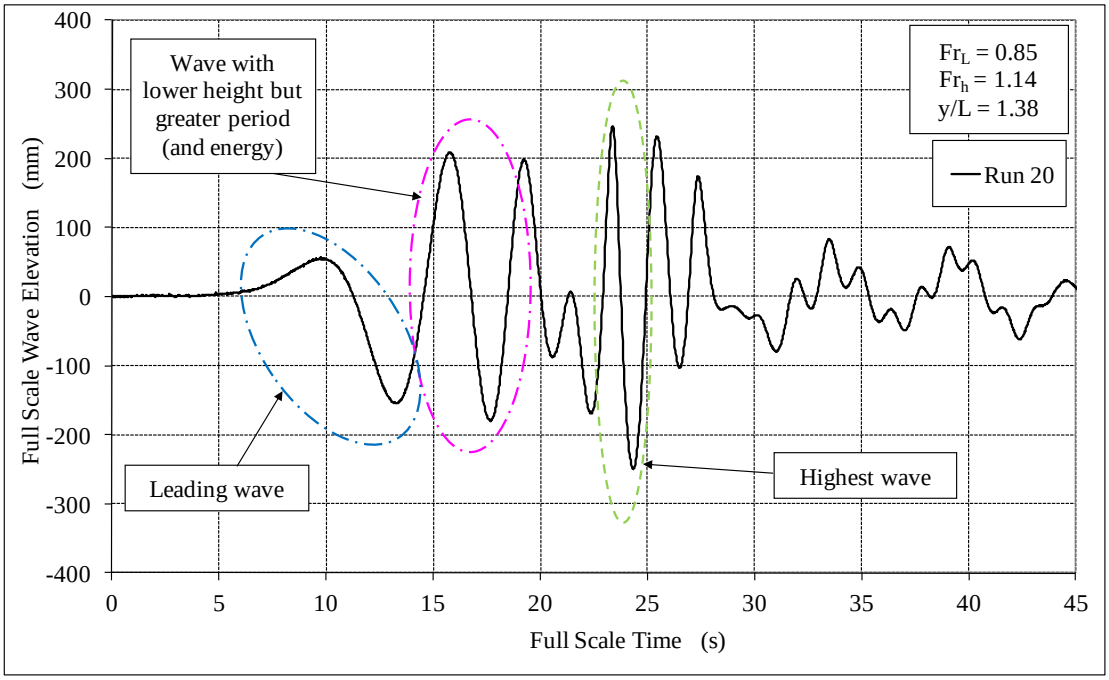

Figure 3.6 Example wave profile time series (Macfarlane 2009)

There are three commonly used methods for determining the period of a wave. These are to determine either:

- The time between consecutive zero up-crossings (or down-crossings) for the defined wave; or,
- The time between the peak and trough (or trough then peak) multiplied by two; or,
- The time between consecutive peaks (or troughs).

For the determination of period of the maximum wave in deep water conditions and preliminary analysis conducted on data from finite water experiments it was found that, in general, there is little difference between the values obtained from these three definitions. Thus, it is considered acceptable to utilise either definition, however it is recommended that the definition remain consistent and be clearly stated wherever possible. In the present study, wave period was determined from the time between consecutive peaks (or troughs).

3.4 Quantifying Bank Erosion due to Vessel Wave Wake

3.4.1 Background

There may never be a rigorous theory that links vessel wave wake and riverbank erosion. This is similarly the case in coastal engineering, where beach erosion is predicted by a number of largely empirical and statistical rules developed over many decades (Kim 2010). Those rules may have a grounding in basic science and engineering, but they are underpinned by empirical equations and a reality that can only be represented statistically, with introduced error as a consequence. The Coastal Engineering Manual (formerly the Shore Protection Manual, 1977 and 1984) by the US Army Corps of Engineers (2008) is weighted heavily with model test results and empirical tables.

Most natural waterways are dynamic environments subject to erosional and/or depositional processes. Not all erosion events can be blamed on vessel wave wake. In many instances local land use practices such as riparian (river bank) vegetation removal and farming, as well as waterway issues such as regulation, channelisation, extractive processes and up- or downstream development (for flood protection or harbours, for instance), can be the root cause of upstream erosion. Boating often simply becomes the focus of attention for an otherwise existing and complex problem.

In contrast to naturally-occurring wave climates, a vessel's wave wake is characterised by short event duration and a broad spectral spread of wave parameters that do not lend themselves to the application of conventional statistical methods. Instead, the principle statistics of concern may well relate to the extent to which certain wave wake parameters exceed those of the existing wave climate in a particular area.

3.4.2 Bank Erosion Studies in Sheltered Waterways

Often, the only way to successfully gather required bank erosion data is to conduct controlled experiments. It is helpful to conduct experiments in the specific waterways being studied, though it is not always necessary to do so if no attempt is made on-site to correlate between the wave wake generated and any erosion that might result.

Experimental programs to provide such correlation are often long-term, high-budget studies (Murphy *et al*. 2006).

The benefits of on-site testing are three-fold. Firstly, there is always benefit in gaining local knowledge of waterway and land use issues, by both interacting with other scientific and regulatory bodies involved as well as speaking with the local waterway users and other stakeholders. Secondly, the science is always made more robust when researching real issues under real conditions. Thirdly, it is important for all concerned, including the researchers and regulatory bodies, to be seen to be doing something with the intention of generating outcomes that balance the environment and the recreational amenity.

In contrast to conducting controlled experiments, incidental measurements of passing vessel traffic is largely useless as a means of gathering data that can be analysed in detail. The testing relies on recording a number of parameters, such as distance between the vessel sailing line and the wave probe, water depths beneath the vessel and the probe, vessel speed and vessel condition, and these parameters cannot be recorded adequately from incidental vessel traffic. The only real uses for incidental data are to collect statistical information on waterway usage and cumulative wave energy.

There exists many publications that document cases of bank erosion due to vessel wave wake in regions outside of Australia, but there is a general lack of any unified theory, see for example Lewis 1956; Johnson 1958; Anderson 1974, 1975 and 1976; Pickrill 1978; Camfield *et al*. 1980; Bhowmik and Demissie 1982 and 1983; Haggerty *et al*. 1983; Kuo 1983; Gadd 1994; Dorava and Moore 1997; Osborne and Boak 1999; McConchie and Toleman 2003; Ten Brinke *et al*. 2004; Hughes *et al*. 2007; Parnell *et al*. 2007; Kelpsaite 2009; Soomere *et al*. 2009; Houser 2010 and 2011; Rapaglia *et al*. 2011. However, only a small number of these studies have made an attempt to quantify the vessel generated waves and relate this to the level of bank erosion. In most cases the issues have been managed by a mix of bank hardening, the application of vessel speed restrictions, or by limiting access. In recent times bank hardening has more often than not involved the use of solid structures, rather than the traditional use of vegetation, which can also attenuate the waves (Bonham 1980 and 1983, Kobayashi *et al*. 1993, Ellis *et al*. 2002).

In Australia there have been several studies that have attempted to measure bank erosion from vessel wave wake (for example: Lesleighter 1964; Pattiaratchi and Hegge 1990; Nanson *et al*. 1994; Bradbury *et al*. 1995; Patterson Britton and Partners 1995; Queensland Environmental Protection Agency 2002; Macfarlane and Cox 2003; Todd 2004; Macfarlane and Cox 2005; GHD 2006; Macfarlane and Gourlay 2009; Worley Parsons 2010). The only long-term, systematic study attempting to quantify a causal relationship between vessel wave wake and bank erosion has been the work undertaken on the Gordon River in Tasmania. This work was instigated in the late 1980s and continues today, though the studies have not always been linear in their progression towards an end.

During the early 2000s, the Queensland Government had a pressing desire to find the causal links between the wave wake of certain vessels and the erosion they may have caused in various rivers in South-East Queensland, including the Noosa, Brisbane, Bremer, Maroochy and Mary Rivers. One aim of the work conducted by Macfarlane and Cox (2003, 2005) was to raise awareness of potential effects of new classes of vessels and activities such as wakeboarding before erosion occurs, so that regulatory bodies are not reliant solely on reactionary measures.

The studies collected wave wake data from controlled field experiments on a range of small craft, but without actually measuring corresponding erosion. Instead, experimental data from erosion studies undertaken on the Gordon River were re-analysed in an attempt to derive relationships between measured small craft wave wake and erosion thresholds in order to develop a set of operating criteria.

The Swan River in Perth, Western Australia, was the topic of a desktop study two decades ago (Pattiarachi and Hegge, 1990), but its analysis technique was rudimentary and the results inconclusive. An increase in regular high-speed commercial ferry services and the growing popularity of high-powered, high-speed recreational craft led to a more comprehensive attempt to quantify the relative contributions of wind and boat generated waves (Macfarlane and Gourlay 2009; Macfarlane 2010; Gourlay 2010). In this study, predictions and full-scale measurements of the waves generated by a selection of identified vessels were undertaken and compared against predicted and measured wind wave characteristics.

Other documented studies within Australia include: Hawkesbury River, NSW (Lesleighter 1964; Scholer 1974), Parramatta River, NSW (Smith 1990; Patterson

Britton & Partners 1995 and 2001; Bishop 2003), Williams River, NSW (GHD 2006; Worley Parsons 2010) and Wandandian Creek, NSW (O'Reilly 2009).

However, it is the large body of work conducted on the lower Gordon River that presents the most comprehensive and useful studies into the relationship between vessel wave wake and bank erosion and as such deserves a more detailed discussion, particularly of the most recent findings (Bradbury 2005b; Macfarlane *et al*. 2008; Bradbury 2010).

3.4.3 Bank Erosion Studies on the Gordon River, Tasmania

The lower Gordon River is a tidal estuary discharging into Macquarie Harbour on Tasmania's West coast. The area is renowned for its scenic attractions and enjoys World Heritage listing for its wilderness values. Several evolutionary stages in the development of the estuary are displayed as one travels upstream past low muddy banks then higher silty banks and finally yet higher sandy levee banks. The last two bank types are of particular significance as they enclose several small meromictic (permanently stratified) lakes that are very rare in a global sense (Worboys *et al*. 2005).

Increasing tourism pressure brought on by a growing number of tour vessels operating on the river over the past 100 years has accelerated erosion well beyond natural regimes. Publicity given to the region by the Gordon below Franklin dam dispute in the early 1980s was followed by the unregulated introduction of larger tourist cruise vessels whose operators traversed the river at high speed in an attempt to reach the upper part of the river where the still water reflects the surrounding cliffs and hills, in turn triggering catastrophic bank erosion (Bradbury 2007). Some of these vessels were up to 32 m in length and capable of speeds of 25 knots. As the banks retreated, the temperate rainforest lining the river toppled into the water, including Huon Pine trees of kiloyear age, significantly degrading the aesthetic qualities of this World Heritage listed area.

Since the late 1980s various forms of regulation have been placed on commercial vessel operations on the river (refer Bradbury 2005a for a summary). The *Lower Gordon River Recreation Zone Plan* by the Tasmanian Parks and Wildlife Service (1998) provides a management policy to conserve the environment and to facilitate environmental sustainability and ecotourism world best practices in accordance with

the significance of the Gordon River environment. The *Plan* acknowledged that further research was required before appropriate regulatory criteria could be determined that will ensure long term sustainability could be specified with confidence. It stated that the Tasmanian Parks and Wildlife Service must continue to conduct, commission and encourage scientific investigation of the river banks and the processes of erosion due to vessel wave wake.

State of the art geomorphology rarely considers waves of such small magnitude and duration associated with those generated by vessels operating at low speeds within sensitive regions such as the lower Gordon River. The focus is very much upon higher energy coastal processes using statistical (spectral) wave characterisation (for example, Miller and Dean 2004; USACERC 1984). As a result, there is less standardisation or agreement upon the specific type of instrumentation and measurements for quantifying river bank erosion within the relevant published literature. However, it appears that the method chosen depends upon the bank form and material properties of interest. The most common methods adopted for quantifying bank erosion due to wave wake is either by surveyed cross-sections, usually using strategically placed erosion pins, or measurement of sediment transport (for example, refer Anderson 1974, 1975 and 1976; Lawler 1993; Bradbury 2010).

For the lower Gordon River scenario the amount of erosion per vessel pass was expected to be less than 0.1 mm for typical experiments. Although of cumulative concern, this degree of erosion per vessel pass (at low speeds) was considered undetectable by measurement of erosion pins in the field (Bradbury 2005b). Therefore, additional measurements of sediment transport were undertaken.

There are three basic techniques applied to the measurement of sediment transport, namely tracers, traps and turbidity. Tracers mimic the size, shape and density of the sediment to be tracked but also possess a distinctive characteristic specifically included to aid tracking, such as colour, fluorescence, radioactivity, magnetism or mineralogy. Sediment traps are devices that intercept sediment in motion and store a sample for later analysis and determination of mass transfer. Turbidity, the degree of suspension of solid material in normally very clear water, is measured using infra-red optical backscatter sensors (Downing *et al*. 1981; Garrard and Hey 1987; Gippel 1995; Bauer *et al*. 2002).

The Gordon River is bounded largely by alluvial and levee bank types with relatively fine sediments (silty sands and cohesive silts) that are easily entrained in the water column (Bradbury *et al*. 1995). In addition to measuring the rate of sediment removal from the bank, turbidity is also considered an appropriate indicator of sediment disturbance (Hilton and Phillips 1982; Erm and Soomere 2006). This approach works well where the sediments are fine enough to be suspended and therefore contain a large proportion of mud rather than sand. It is expected that most coastal river and sheltered waterway systems would fall into this category. Using turbidity as a measure of sediment suspension would be less successful where the banks are predominately composed of sand.

Early series of tests conducted to quantify erosion and sediment transport under different vessel wave wake regimes were conducted by von Krusenstierna (1990) and Nanson *et al*. (1994). Bank erosion, suspended material and swave wake load were measured and compared with different measures of wave wake from passing vessels under controlled test conditions. Swave wake load is defined as a means of assessing the removal of slumped materials by sampling the zone at the base of the bank. It usually involves the strategic placement of a trap on, or close to, the riverbed.

The work of von Krusenstierna and Nanson *et al*. demonstrated that there was a threshold of wave wake values below which the rate of erosion was regarded as less significant, and such thresholds were evident for all the wave wake measures recorded. Around the time of conduct of these experiments the majority of the river was closed to commercial operations and the remainder subject to a blanket speed limit of 9 knots while further research was undertaken.

In some scenarios a degree of vessel induced erosion may be acceptable but this then requires limits to be placed on how much erosion is to be permitted. The work by von Krusenstierna and Nanson *et al*. drew attention to an increase in the rate of erosion as waves became larger (where both height and period may increase) and found that simple measures could explain much of the erosion. However, allowing some erosion is more complicated because one must then consider the cumulative effects of all waves exceeding the erosion threshold.

In these early studies, large passenger ferries were used to generate wave wake, as the trigger for the original study was the erosion being generated by these large vessels travelling at speed on the river (von Krusenstierna 1990; Nanson *et al*. 1994). Whilst

this approach mimics real life, it created some problems with the analysis. Vessel wave wake takes 1-2 boat lengths of travel away from the sailing line to stabilise and some of the results for these long ferries may have been compromised by being long vessels operating in a relatively narrow waterway. Similarly, the measurement of erosion by using erosion pins or swave wake loads can be misleading when the results of a limited number of runs are extrapolated to long periods. Erosion pins are best used where erosion is on-going over a long recording period.

From the mid 1990s further experiments were conducted on cohesive muddy banks lining the Gordon River reaches remaining open to commercial traffic (Bradbury *et al.* 1995). Since the land manager had a pressing need for a criterion to distinguish appropriately 'low wake energy' vessels the suggestion from early (and limited) data of an initial threshold to sediment movement at a wave height of 75 mm was used to define the maximum acceptable wave. This operating criterion, measured at a lateral distance of 50m from the sailing line of the vessel, may appear a simple measure, but it required every commercial vessel seeking a permit to operate on the river to be subjected to wave wake trials and/or ship model experiments. The maximum allowable speed for all vessels presently in service ranges between four and six knots.

In many ways it is somewhat unfortunate that such an extensive test program resulted in an (apparently) over-simplified criterion, though it is extremely unlikely that any of the tourist vessels then operating on the river could produce an acceptable wave wake at high speed, due to their sheer size and displacement. However, it may have been possible for a much smaller vessel being capable of operating at high speed, where the height of the waves generated meet the height-only criteria, but the period of the waves may exceed those of the naturally occurring wind waves by a substantial margin, thus resulting in waves that are very likely to be erosive. This is the dilemma and danger of over-simplified criteria customised to a narrow range of vessels.

Subsequent work demonstrated this criterion to be overly simplistic and that wave period was also an effective influence (Bradbury 2005a). That point was most graphically demonstrated by the extreme turbidity caused by the low but long waves generated by small planing craft (Bradbury 2005b). However limiting wave height and period independently was found overly restrictive in that it excluded many of the wave wake events that did not cause any erosion.

The Tasmanian Government authorities charged with the implementation and monitoring of both vessel operating regimes and erosion studies have initiated a move towards a wave energy/power criterion, based upon both a maximum wave height and a maximum wave period. The authorities are in the unique position of having almost three decades of vessel wave wake studies and erosion monitoring from which to draw their conclusions, combined with the detailed full scale and or model scale wave wake measurements of every tourist vessel certified to operate on the river.

More recent studies on the Gordon River have concentrated on refining the threshold and which of the vessel wave wake parameters are likely to be the best indicators of erosion potential. To do this, small craft were employed to generate the wave wake and a more reliable method of determining erosion was used (Macfarlane *et al*. 2008).

The use of small craft as wave wake generators provides more consistent and predictable wave wake, as the distance from the sailing line to the point of measurement is greater relative to the waterline length of the boat. As the point of the exercise is to find correlation between simple wave parameters and a given measure of erosion, the method of wave generation and hence the size of vessel becomes less important.

For these experiments the quantification of erosion was focussed on the suspension of sediment by measuring turbidity. However, this in itself is not a measure of erosion potential, as there is no reason why the sediment could not precipitate back to its original position. However, there are several key points that strongly favour turbidity as an erosion measure:

- The energy needed to maintain suspension is much lower than the energy needed to initiate suspension; the settling phase may be long and prolonged by naturally occurring energy from wind waves and currents;
- Most rivers would experience some degree of flow, whether tidal or due to run-off. The suspended particles are likely to experience some longshore drift, even if only from the vessel wave wake itself, that most likely would have a longshore component;
- Most river bank materials would have some degree of cohesion. If the cohesion was broken and sediments were suspended and precipitated, the resultant sediments would lack their initial cohesion and be prone to further re-suspension;

- Sediments may be removed from an area above the natural water level as waves wash up the bank. The precipitation of such sediments into their original position would be extremely unlikely.

Elevated turbidity measurements were taken at two water depths of 0.4 m and 1.0 m, with the sensor in the shallower water approximately 0.5 m from the shoreline scarp and the sensor in the deeper water approximately 3 m offshore. Each sensor was fixed at mid-depth. The deeper depth clearly demonstrates the effect of longer period waves, as the influence on the seabed of a passing wave is a function of wave period and not wave height. Any sediment that is entrained in the shallow breaker zone and then settles in slightly deeper water offshore may be re-suspended by long-period waves.

Results from one of several sites used in the on-going study are presented here to illustrate the relationship between commonly used wave parameters and turbidity (Macfarlane *et al,* 2008). These figures show turbidity near the river bank (measured at two different water depths) against the maximum wave parameters of height (Figure 3.7), period (Figure 3.8), energy (Figure 3.9) and power (Figure 3.10). Each wave parameter is discussed in more detail below.

Turbidity as a function of Height of the Maximum Wave – Figure 3.7
Wave height is traditionally the wave parameter that receives the greatest focus, almost certainly because it is the most recognisable wave feature. It was also the basis of the first operating criterion for the Gordon River, which was a maximum wave height of 75 mm at a lateral distance of 50 m from the sailing line. This was not unreasonable, as the criterion was developed for the large tourist vessels operating on the river and none of these vessels could operate at high speeds where long-period waves are generated but still maintain only 75 mm wave height.

The graph clearly shows a degree of scatter, reinforcing the belief that wave height alone is at best only a reasonable indicator of erosion potential. As an example, one data set has a turbidity value of 1 unit and a corresponding wave height of 174 mm, while the second highest recorded turbidity value (211 units) occurs that the same wave height of 174 mm.

The threshold value is unclear, indicating that other wave parameters have an influence on turbidity.

Turbidity as a function of Period of the Maximum Wave – Figure 3.8
The data scatter is marginally reduced compared with wave height (Figure 3.7). As some scatter is always expected with full-scale testing, the results are particularly encouraging. The threshold of turbidity is clear at approximately 1 second and, more importantly, is the same for each of the two sensors at different water depths. This is an important point for any subsequent development of simple operating guidelines, as it removes another variable from the equation. There would appear to be no need to take into account the effect of different incident wave periods and water depths on erosion rates, meaning that bank profile and bank/littoral sediment variations can be ignored.

Turbidity as a function of Power of the Maximum Wave – Figure 3.9
As wave power is a function of height and period (H^2T), it is reasonable to expect that the data scatter shown in the wave height graph (Figure 3.7) would be tempered by the reduced scatter in the wave period graph (Figure 3.8), producing a graph with more predictable trends. The threshold turbidity value of approximately 10 W/m is reasonably clear, below which the values of turbidity at both sites remain essentially negligible.

Turbidity as a function of Energy of the Maximum Wave – Figure 3.10
The trend demonstrated in the wave power graph (Figure 3.9) is even more pronounced in the energy graph (Figure 3.10). Wave energy is also a function of height and period (H^2T^2) but with a greater weighting of period compared to wave power. This further tempers the scatter of the wave height results. The turbidity threshold occurs for both measurement depths at the same energy value of approximately 30 J/m. As with all the graphs, this consistency between the depth at the turbidity measurement site and the inception of turbidity can only be attributed to wave period effects, as the wave height is low compared to the water depth. However, this explains only the bottom disturbance of the approaching wave and not the degree to which the breaking wave may erode the shoreline.

From the results shown in Figures 3.7 to 3.10 several features become apparent:

- All graphs define very definite threshold values below which turbidity is essentially zero (i.e. within the range of instrumental and background noise).
- Wave height is a reasonable indicator of erosion potential.
- There is close correlation between wave period and turbidity.
- There is similarly close correlation between both wave energy and power with turbidity.

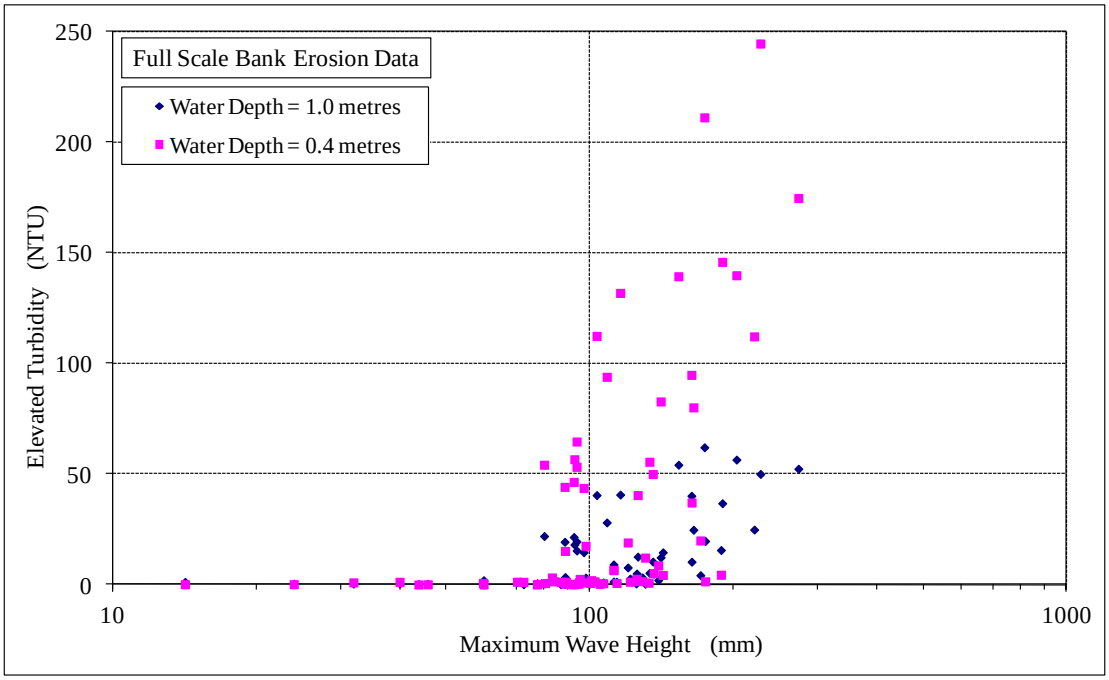

Figure 3.7 Elevated turbidity as a function of maximum wave height (Macfarlane *et al*. 2008)

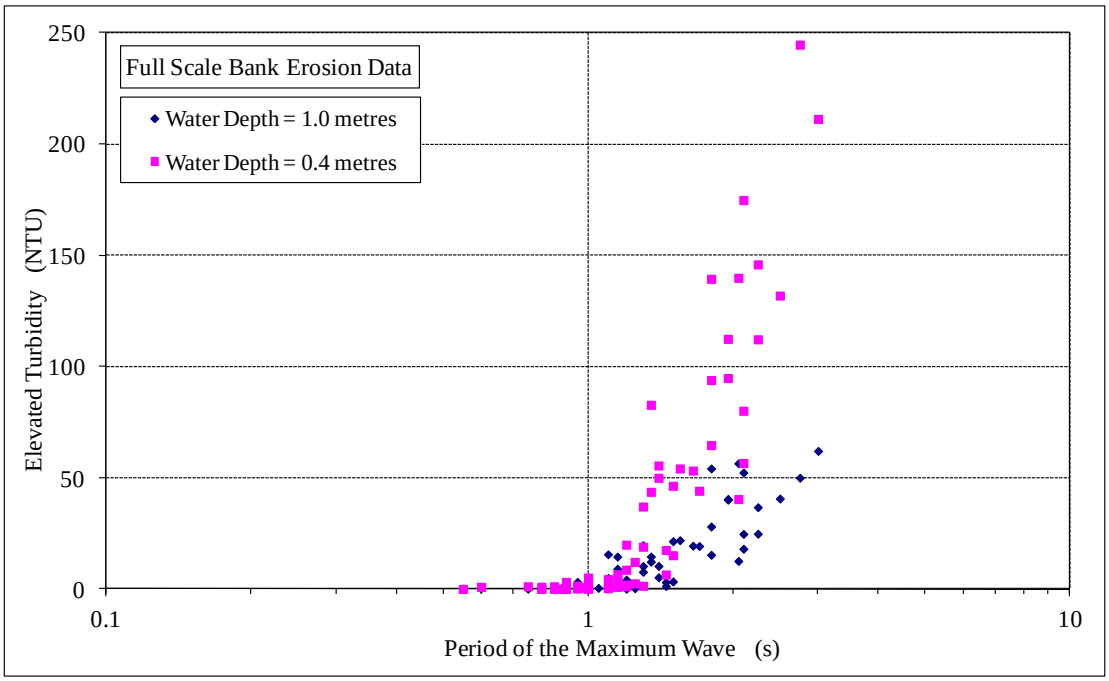

Figure 3.8 Elevated turbidity as a function of wave period (Macfarlane *et al*. 2008)

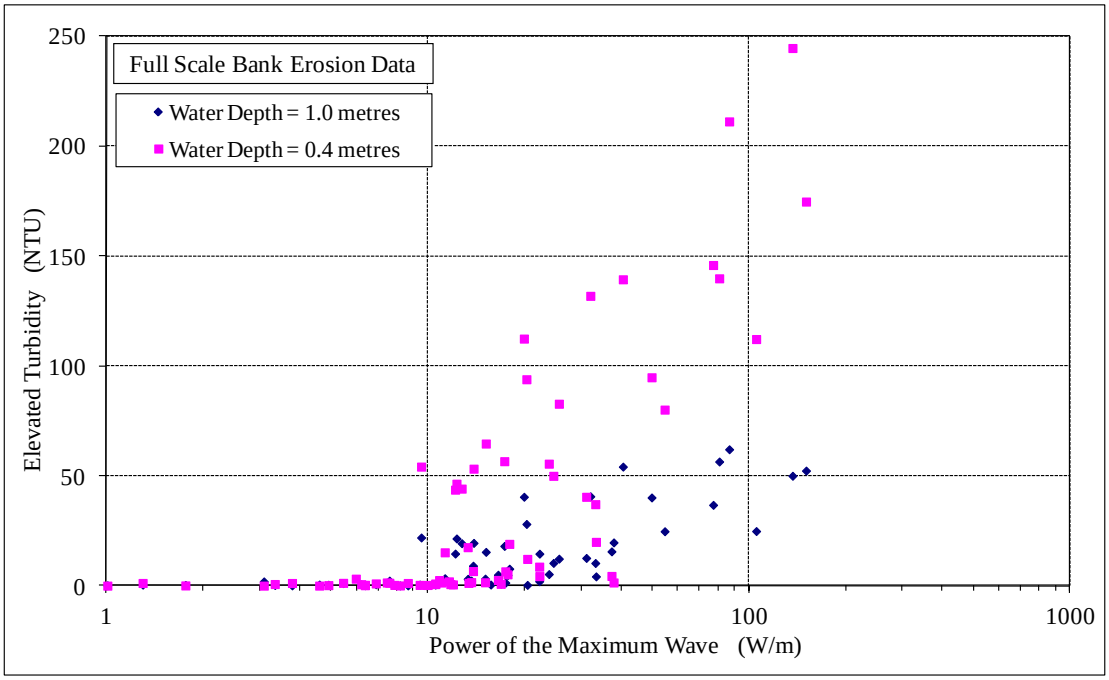

Figure 3.9 Elevated turbidity as a function of wave power (Macfarlane *et al*. 2008)

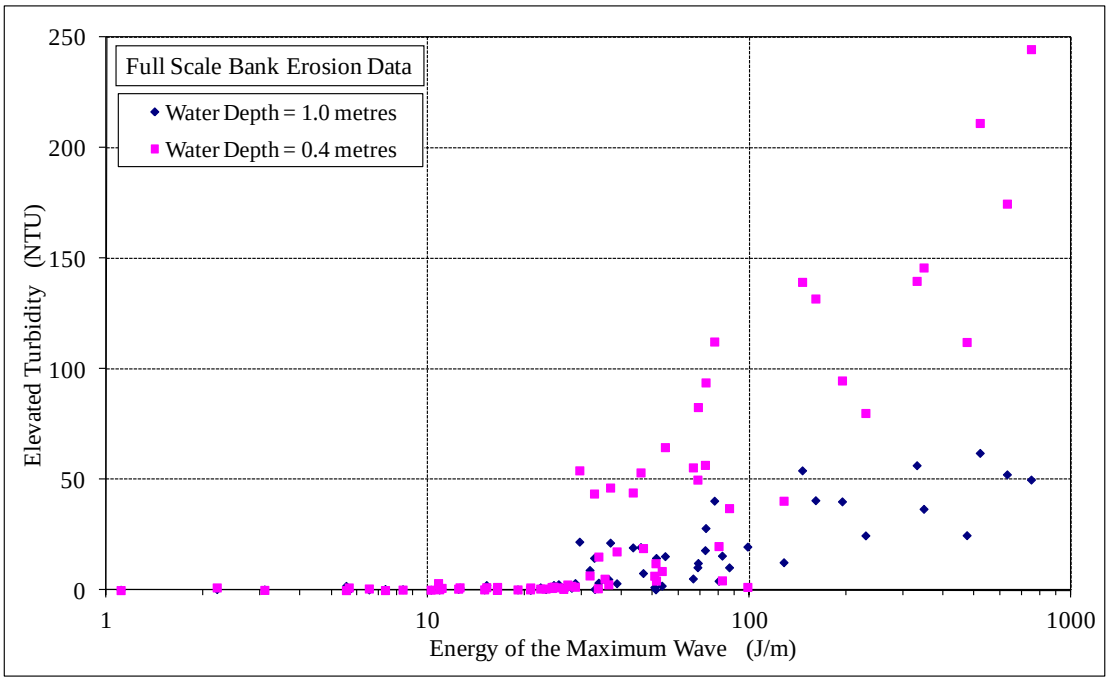

Figure 3.10 Elevated turbidity as a function of wave energy (Macfarlane *et al*. 2008)

Chapter 4

Wave Wake Prediction Techniques

4.1 Introduction

In this chapter, a review of previous work on the prediction of vessel wave wake, using both experimental and numerical techniques is undertaken. It was not intended to undertake a comprehensive review of all existing methods, or provide in-depth detail, but to provide a general background of the more common and recent methods, given that an aim of the present study was to develop a predictive tool based on experimental data.

As discussed in previous chapters, there is a demonstrated need to understand the phenomenon of vessel wave wake and to develop the means to minimise its effect through design and operation. This requires the development and validation of suitable predictive tools that quantify the characteristics of the waves generated by a wide variety of vessel hull forms under all practical operational conditions at an early stage when planning ferry and other services, including the design of vessels and waterway infrastructure.

The complex array of variables involved can make the development of wave wake prediction tools a difficult task, particularly when attempting to accurately predict the far-field wave wake from near-field measurements (Dand *et al*. 1999b; Campana *et al*. 2005). Many of the problems associated with vessel-generated waves occur in shallow and/or restricted water and, as previously discussed, the pattern of waves generated in shallow water is very different to that generated in deep water. The main factors that must be considered include the:

- characteristics of the vessel (speed, hull form, waterline length, beam, draught, displacement, etc),
- characteristics of the waterway (water depth, bathymetry, width, bank details),
- sailing line of the vessel within the waterway,
- rate of decay of the generated waves.

The development of accurate prediction tools has been significantly hampered by a lack of appropriate full scale benchmark data available in the public domain for researchers to undertake comparisons. A common opinion is that it is still necessary

to validate numerical models against experimental measurements (either/both model scale or in-situ) before they can be used for managing wave wake in a particular situation, regardless of what type of model is deemed the most appropriate (Stern *et al*. 2002; Campana *et al*. 2005; Murphy *et al*. 2006; Campana *et al*. 2008).

4.2 Literature Review

There are many references that provide background information on the topic of vessel wave wake, including a recent book authored by Lyakhovitsky (2007) which discusses in detail many hydrodynamic aspects of ship operation in shallow water, including a chapter on the environmental impacts as a result of ship generated waves. Murphy *et al.* (2006) conducted a literature review on research and current practice related to vessel wave wake to provide an overview of the findings, methodologies and mitigation strategies. The authors discuss many possible impacts that can be attributed to vessel wave wake, including: hydromorphological (erosion), ecological (aquatic plants, fish, macroinvertibrates, noise, water quality), and cultural heritage impacts.

Another general discussion paper is provided by Phillips and Hook (2006), who also provide an outline of Risk Assessment Passage Plans (RAPP) which are required in the United Kingdom for all high-speed craft or any vessel that can potentially exceed $Fr_h > 0.85$. The authors also suggest that hazards can be split into 3 groups: close to the sailing line, at a distance, at the shore.

Thomson (1887) and Havelock's (1908) theories provide reasonable estimates of the propagation angle, wavelength, period and propagation speed for just the leading wave of the finite water wave pattern. Unfortunately, neither theory can be used for estimating the height of any of the waves generated. In addition, close to the critical speed ($Fr_h = 1$) strongly non-linear waves (including solitons) are generated, which cannot be described by Havelock's theory alone.

Part of the following literature review was conducted by the author while a member of the ITTC Resistance Committee and has previously appeared within the Committee's full report to the ITTC (Campana *et al*. 2008).

4.2.1 Prediction of Wave Wake - Experimental Measurement

The prediction of ship generated waves by direct measurement through the conduct of scale model experiments may appear to be standard practice in ship hydrodynamics, however some significant problems exist. More often than not, the characteristics of the waves are required at large lateral distances from the sailing line of the vessel, making direct measurement impossible within conventional towing tanks. Tank width restrictions often result in the need to make measurements relatively close to the model; thus requiring some form of extrapolation method to obtain predictions in the medium and far-field. Such extrapolations are often based on the assumptions of uniform water depth and linear theory and far-field properties. The wave profile must be measured sufficiently far from the model to avoid local wave effects, but not so far that it is affected by reflections from the tank walls.

Macfarlane (2002) conducted a series of wave wake experiments to quantify the point at which ship model generated waves are likely to be unacceptably affected within a conventional 'narrow' towing tank. The measurements from the towing tank were directly compared to a similar series of tests conducted on the same models within a wide basin. All experiments were conducted within deep water. The results confirmed that significant limitations on probe positions relative to the tank walls were found to exist, particularly at length Froude numbers in excess of 0.7.

Possible solutions to overcome tank width issues include; towing the model off the centre of the tank; measuring a longitudinal wave cut at the tank wall, taking into account the reflections (with added complexity and potential errors); or using smaller models or wider tanks.

Since the water depth also plays an important role in most wave wake problems, it is also essential that precise scaling of the water depth be achieved. Few facilities exist internationally that are both relatively wide and have the ability to precisely model a wide range of water depths.

Special care is required when conducting scale model experiments at trans-critical speeds, particularly at and close to the critical speed. Cox (2000) presented results from a series of experiments conducted within a conventional towing tank that found that the closer the speed to critical and the shallower the water, the larger the variability of the results. It is likely that exaggerated sinkage, surge and draw down,

solitary wave formation and unsteadiness may result, but this may not occur, or occur differently, in reality. This could be partly due to the different boundary layers at model and full scale, which changes the 'effective' blockage. Several authors report that solitons (for example Jiang 2001) may be generated upstream of the vessel, whilst others (Doyle *et al*. 2001; Robbins *et al*. 2011) report unsteadiness in wave height as the model progresses down the tank or basin. The properties of solitons can change with water depth, channel width, vessel form and vessel speed (Remoissenet 1999).

The challenges associated with the prediction of wave wake based on model test data, particularly in regard to limitations in facility width when measurements in the medium to far field are of more interest, is likely to have contributed to the increasing number of studies in recent years that have included the conduct of site-specific full scale experiments, for example: Macfarlane and Cox, 2004; Soomere, 2005; Velegrakis *et al*., 2006; Varyani, 2006; Parnell *et al.*, 2007; Kumar *et al*., 2007; Balzerek and Koslowski, 2007; Parnell *et al*., 2008; Kurennoy, 2009. As with any experiments conducted within uncontrolled environments there can be many factors that adversely affect the quality (and quantity) of experimental data, although some useful guidelines to minimise problems have been provided in some of the aforementioned references and in PIANC (2003).

It is commonly argued (for example, Sorensen 1973, Renilson and Lenz 1989, Macfarlane and Renilson 2000, Molland *et al*. 2004) that the height of the maximum wave within the sub-critical wave pattern can be extrapolated from one lateral location to another in uniformly deep water using a simple exponential decay rate for a point disturbance. The decay exponent, n, for a point disturbance with distance is -1/2 within the Kelvin angle and -1/3 at the cusp locus line (along the extremities of the Kelvin wedge). Many authors thus argue that the divergent waves generated by a vessel in deep water decay with an exponent of -1/3; other authors, however, contest the validity of the application of this result to wave patterns generated by ships rather than point disturbances. For example, Doctors and Day (2001) and Doctors and Zilman (2004a) calculated from numerical predictions that decay exponents lie between -1.06 and -0.20, depending upon the speed of the vessel. Following a comprehensive series of physical model tests on a wide variety of hull forms over a large range of sub-critical speeds, Macfarlane (2002) found that the decay exponent varied between -0.45 and -0.2 from which it was concluded that the value of -1/3 represented a reasonably practical engineering representation for deep water waves. It

is generally agreed that this is certainly not valid in water of finite depth, as confirmed by Robbins *et al*. (2007) who conducted model scale experiments to show that the wave height decay coefficient can vary significantly with depth Froude number (refer Figure 2.9).

Doyle (2001) conducted both model and full scale experiments to investigate the waves generated by large high-speed ferries operating at super-critical speeds. It was observed that measurement of the maximum wave height alone is an insufficient representation of the problems associated with these shallow water waves since the decay exponent is a function of their frequency.

Macfarlane (2002) used data from model experiments to develop a tool for the prediction of the characteristics of the maximum wave generated by a wide variety of hull forms operating at sub-critical speeds in deep water. The tool provides a means of comparing the global geometrical parameters of vessel hulls with regard to their wave wake propensities. Some example results were included in Figures 3.1 and 3.2.

Chalkias and Grigoropoulos (2007) carried out a series of experiments using large scale manned models to eliminate problems due to tank wall effects and reduced magnitude of scale effects. These experiments were conducted in a sheltered waterway, where careful site selection can provide desired water depths. A real time kinematics (RTK) system was used to monitor the model track and speed with respect to the wave recording location. The authors measured dynamic trim, heel and sinkage and present results for maximum wave height and the corresponding period at several lateral locations from the sailing line for each of the two ship models investigated. This data is used to determine the wave decay rate, where it was found that the decay rate can be significantly influenced by the number of lateral wave measurements and their location, particularly if these measurements are spread over a wide range from the near to far field.

Macfarlane (2006) and (2009) investigated the correlation between model and full scale wave wake data and found generally good agreement. It is concluded that a correlation factor of unity (1.0) is appropriate when scaling model data for similar catamaran hull forms travelling within the range of speeds investigated (typically $0.16 < Fr_L < 1.0$). The author's latter work (2009) noted the generation of more than one significant wave at super-critical depth Froude numbers and the implications that this may have when assessing potential wave wake issues.

Full scale onsite experimental data has also recently been utilised to investigate the effects on riverbank erosion and to assist in the development of regulatory criteria, Macfarlane and Cox (2004) and (2007), Macfarlane *et al*. (2008).

Unfortunately, there is still a lack of good quality, well detailed full scale data in the public domain that is suitable for the validation of numerical predictions.

4.2.2 Prediction of Wave Wake - Computational Methods

The use of computational techniques to predict vessel wave wake is not a straightforward task as many only consider the near field waves and then require some form of extrapolation to the medium or far field. Stern *et al*. (2002) recommend that special care is needed to retain numerical accuracy at these larger distances.

Linear Theory

The most basic prediction methods adopt linearised theories based on Kelvin singularities, which have the advantage over most alternatives in that calculations in the far field can be achieved without the need to calculate the intervening wave pattern, provided the water depth remains constant. These methods are often based on slender body approximations, which can provide reasonably accurate predictions of the dynamic sinkage and trim effects at low length Froude numbers. However there is less reliability at higher speeds as dynamic sinkage and trim and the flow from transom sterns are all considered to have an influence on the generated waves (Campana *et al*. 2005).

Doctors *et al*. (1991) state that a simple calculation of wave resistance alone using standard wave resistance theory can provide an excellent indication of wave height and hence the probability of causing issues such as bank erosion.

Day and Doctors (2001), Molland *et al*. (2001 and 2003) and Lazauskas (2007 and 2009) contend that simple linear methods, such as Michell's thin-ship wave resistance theory (Michell 1898) can be extended and generalized to provide fast, accurate estimates of wave resistance and wave patterns, particularly for thin ships. Each have shown that linear theory can obtain satisfactory predictions of the leading part of the wave cut, provided that the ship hull or demihulls can be considered slender. A similar method was adopted by Doctors and Zilman (2004b) to predict trends in wave effects due to hull spacing or stagger for multihulls. Related theories have been used

to investigate the prediction of the waves from other surface vessels such as air cushion vehicles, planing hulls and surface effect ships, Doctors and Day (2000), Tuck *et al*. (2002) and Doctors (2004).

Tuck *et al*. (2000, 2002) and Lazauskas (2009) have explored ways in which some real fluid effects, such as the effect of eddy viscosity, can be incorporated into linear theory. They argue that the wave patterns close to the vessel sailing line are more realistic due to the inclusion of some of the fine detail that is ignored by inviscid theory.

Chalkias and Grigoropoulos (2005) investigate two methods of applying a potential flow panel method to predict the near-field waves from four high-speed monohulls operating in deep water. The first method treats the steady flow as a special case of time-harmonic flow in the frequency domain. The second method is a sister method solving the time-domain flow. The solution algorithms are based on a 3-dimensional Rankine Panel Method (RPM) where the two physical variables (i.e. the velocity potential and the free surface elevation) are represented with a higher order B-spline basis function. It is claimed that the methods are numerically stable resulting in no numerical damping and small numerical dispersion, so that there is no significant error in the free surface deformation. It is also claimed that the algorithms can handle transom sterns by applying a set of smooth detachment conditions of the flow at the transom and introducing a strip of 'wake' panels trailing the transom. The same authors also compare large scale experimental data with numerical predictions using the abovementioned linear code and nonlinear potential flow codes (SHIPFLOW^{TM}), where the nonlinear code appears to produce the more favourable comparison (Chalkias and Grigoropoulos 2007).

Nonlinear Theory

As discussed previously, several approximations are usually required when using linear theory to predict vessel generated waves. These approximations can be avoided by adopting a hybrid approach where a non-linear approach is applied in the near field and a linear approach to extrapolate to the medium and far field. For this to be valid, it has to be assumed that the waves are less steep in the far-field.

Raven (2000) presented a method that adopts a nonlinear potential flow theory to model the near field using a Rankine panel approach and extrapolate to the far-field by reconstructing the calculated wave spectrum. This was only undertaken for the

case of uniform water depth and at sub-critical speeds. Raven comments that there is little point attempting this method at trans-critical speeds due to the lack of validation of the near field solution. For super-critical speeds he suggests one possibility is to adopt a conservative assumption of no decay due to the non-dispersive nature of the outer waves.

A broadly similar approach is presented by Brizzolara and Bruzzone (2003) however, the agreement between the numerical prediction and experiments is least good for the leading wave and better for the subsequent waves, although limited results are presented. In general, this is the reverse of most other similar studies.

Soding (2006) suggests the use of nonlinear Rankine source methods to determine near-field waves followed by a constant-depth method (with the vessel either travelling in a straight course or a curved path) to model the far-field waves. The waves within an analysis rectangle behind the ship are used to extrapolate the wave field up to an arbitrarily large distance. The wave field is approximated as a superposition of regular, linear deep-water or shallow-water (Airy) waves. If the far-field waves are in a region possessing variable depth (with small variations in slope), then it is suggested that the number of dimensions can be reduced by one by substituting the time variable with a frequency variable and approximating the dependence of flow variables on the vertical coordinate by that of a regular wave of low steepness on a horizontal bottom. This is achieved for each wave frequency separately.

Soding also suggests that the predictions could reach a logical conclusion by modelling the waves breaking on (a small part of) the shore using a free-surface RANS method, however this has not been demonstrated. Results for a single test case are provided for each of the covered methods, namely: the near-field waves, far-field waves at a constant depth (for both a straight course and curved path), and far-field waves within a region of variable water depth. The author concludes the paper by stating that comparisons with experiments are planned.

Most studies appear to assume that profiles of waves generated by fast ferries can be described by classical linear wave theory, however, Soomere *et al*. (2005) suggest that this is not applicable with many of the long period waves when in shallow water and that a more appropriate model for long waves in shallow water is the Korteweg-

de Vries (KdV) equation (for cnoidal waves) which have more realistic, narrow crests and broader troughs than sine waves.

Soomere (2007) summarises the non-linear parts of a ship's wave wake, where the central topic is the generation of solitons by ship motion both in channels and in unbounded sea areas. There are 267 references cited in this review article. The optional non-linear components of ship wake such as the very narrow V-like wake components, packets of monochromatic waves, ship-generated depression areas, and supercritical bores are also discussed. A variety of different non-linear equations that have been used to study the generation of solitons are discussed, including: the Boussinesq equation, the nonlinear (cubic) Schrodinger equation and its various generalizations, the Korteweg-de Vries and the Kadomtsev-Petviashvili (KP) equations. Soomere (2006) provides further discussion on non-linear equations that have been used to study the generation of solitons, with particular emphasis on the KP equations.

Soomere and Engelbrecht (2006) investigate events where considerable increases in wave amplitudes occur due to nonlinear superposition of solitary waves in shallow water. Such interactions have recently been proposed as an explanation for the generation of freak waves. The authors suggest that a suitable model for the description of the interaction of soliton-like shallow water waves travelling under slightly different directions is the KP equation.

Unsteady RANS simulations for a Wigley hull running at high speed in deep water and running at sub-critical speed in shallow water are presented by Sakamoto *et al*. (2007). Three types of investigations are made including an uncertainty analysis, the high-speed effect and shallow water effect. The resistance, pressure variation, wave pattern, boundary layer and vortices are studied. The authors state that the work presented is the first step toward the application of the URANS method to high-speed ship study. Free surface wave patterns at different Froude numbers clearly show the typical high-speed effect that a diverging wave dominates a transverse wave as Froude number is increased.

In practice, many real-world wave wake problems are affected by local bathymetry, which may result in the waves shoaling, dispersing, refracting, reflecting and/or focussing. To address this, various studies have also adopted hybrid methods which

use Boussinesq-type models for the far-field (Kofoed-Hansen *et al*. 1999; Whittaker *et al*. 1999; Raven 2000; Jiang *et al*. 2002; Yang 2002; Madsen *et al*. 2006).

Some work focuses on the prediction of ship wave wake near the shore. Hong and Doi (2006) have developed a numerical method by using the interface capturing method and the Constrained Interpolation Profile (CIP) method. A comparison against experimental data shows the suitability of the prediction technique. The study has shown that the first wave run-up on the shore is the biggest of the first three waves, despite the height of the first wave being the lowest of the three when offshore. Erikson *et al*. (2005) describe a model to predict swash motion based on solutions to the nonlinear shallow water equations to account for interaction between up-rush and back-wash at the still water shoreline and within the swash zone. The model was tested against wave groups representing vessel generated wave trains (run in a small wave basin). Accounting for swash interaction markedly improved results with respect to the maximum run-up length for cases with gentle foreshore slopes (but no improvement for steep slopes). In addition, an equation to predict the onset and degree of swash interaction including the effects of bed friction was developed.

Torsvik *et al*. (2006) and Torsvik (2006) investigate the passage through the trans-critical speed region of a moving ship in a shallow channel using numerical simulations based on a 1-dimensional version of forced Boussinesq equations. The transition is accomplished either by accelerating the ship in a region of constant depth or by moving the ship with constant speed over a sloping bathymetry. Results show that the generation of upstream solitary waves depends on the time required for the transition, with large waves being generated for long transition times. It is also apparent that the shape of the wave pattern and the maximum amplitude of the waves differ significantly whether the Froude number increase or decrease during the transition of the trans-critical region.

To determine the hull form parameters most affecting wave wake Robbins (2004) and Robbins and Renilson (2006) created a systematic series of typical low wave wake-energy catamaran hull forms (consisting of parent hull and six variants). A contemporary panel method code (SHIPFLOW^{TM}) was used to generate free surface elevations which were then analysed using a decay method. Regression analysis of the results helped to produce a simple prediction tool which the authors developed to allow early design assessments of particular hull forms. The regression analysis

confirmed that the length on displacement ($L/\nabla^{1/3}$) and L/B ratios are the most dominant hull parameters.

Tornblom (2000) also compared wave wake predictions using the potential flow module of SHIPFLOW^{TM} against experimental results, but for three types of vessel, including a tanker, large monohull ferry and a catamaran, each travelling alongside a vertical or sloping bank. The comparison was acceptable in a limited number of sub-critical cases, but found to be poor at trans-critical and super-critical speeds.

4.3 Concluding Remarks on Prediction Techniques

This review of experimental and numerical methods commonly adopted internationally for quantifying wave wake has found that most either obtain or produce a record of the entire wave train (usually in the time domain). The aim of many CFD approaches is to produce a detailed description of the entire wave pattern.

However, in all cases known to the author the process of assessing whether these waves meet one or more specific regulatory criteria requires only a very limited amount of salient data to characterise these waves – often simply using the height alone or the height and period of just a single *maximum* wave from the entire wave pattern. With present technology, it is hard to justify the time required and additional complexities involved in adopting some CFD techniques if the assessment against such criteria is the sole purpose. In such cases it may be more advisable to use other more rapid and equally accurate and reliable methods, such as the recent advances using Michell's integral (Lazauskas 2009). In addition, the experimental uncertainties for full scale craft in the field can be so great as to often make the differences between many of these methods negligible.

Following the review of prediction techniques described in this chapter, it was concluded that there was a need for a tool that could rapidly and accurately predict the primary characteristics of the three key waves described in Section 3.3. The tool should also have the ability to readily compare the resultant predictions against suitable regulatory criteria. The tool, and the physical scale model experiments from which it was based, are described in the following chapters.

Chapter 5

Wave Wake Experiments

5.1 Introduction

A primary aim of the present study was to develop a tool that can accurately predict the wave wake characteristics of a wide variety of different hull forms operating over a wide range of vessel speeds and water depths. This tool was to be developed using data acquired through the conduct of an extensive series of physical scale model experiments. It was therefore imperative that the experiments were as well designed as possible to meet this need such that objective conclusions could be drawn from the resultant empirical model (Montgomery 2009).

The author previously conducted experiments to investigate the wave wake characteristics of a wide variety of hull forms within a wide basin, however all of these tests were conducted at a single water depth that was considered to be effectively infinite (deep) (Macfarlane 2002). A basic wave wake predictive tool was developed based on this deep water experimental data. As previously discussed, finite water depths have a very large effect on vessel generated waves, thus the need for a predictive tool with a far greater range of capabilities.

The construction at AMC of a 35 m long by 12 m wide basin with a flat concrete floor and the ability to vary water depth from zero to 0.9 m provided the opportunity to extend the existing dataset to investigate the effect that water depth has on the waves generated by the same wide range of hull forms. This facility is ideally suited for conducting hydrodynamic experiments with an emphasis on maritime operations within shallow water environments, such as harbours, estuaries and rivers. It has a winch-driven carriage for towing ship models at prescribed speeds, a multi-element wave generator and a non-contact digital video motion capture system. Further details of the facility can be found at the AMC website (2012).

The program of experiments conducted has been summarised in Table 5.1. Details of these experiments are discussed in the following sub-sections.

5.2 Test Variables

5.2.1 Ship Models

The previous wave wake experiments in deep water involved over 80 different hull forms, Macfarlane (2002). Details of these hull forms were reviewed, from which 17 were selected to cover both monohulls and catamarans, covering a wide range of $L/\nabla^{1/3}$ ratios.

Hull forms were only selected if they were considered as being typical of those types that regularly frequent sheltered waterways. Although a wide range of hull forms were covered, there was one exception in that none of these existing designs were particularly representative of typical water ski or wakeboarding boats – which are very frequently used on sheltered waterways (refer Section 2.4). Thus, a further two cases were added to the 17 selected from the original deep water study. These two vessels typically possess very low $L/\nabla^{1/3}$ (4.8 to 5.2) and L/B (2.9 to 3.1) ratios.

Also included in the study are several monohulls and catamarans that have been deliberately designed as passenger only ferries for sheltered waterway operation by minimising wave generation. These hull forms have relatively high $L/\nabla^{1/3}$ and L/B ratios (8.5 to 11.7 and over 9.0 respectively).

In summary, the test program includes scale models of 11 different monohulls and 8 different catamaran hull forms. Principal particulars of each are listed in Table 5.1 and a simplified body plan of each hull has been provided in Appendix A. The Froude law of similitude was used to satisfy geometric and inertia scaling requirements.

The ship models were towed from the projected thrust line for all tests. The ballasting and trimming of the models was conducted as per ITTC Recommended Procedure 7.5-01-01-01 (ITTC 2008).

According to ITTC Recommended Procedure 7.5-02-05-01 (ITTC 2008), boundary layer turbulence stimulation is recommended when the Reynolds number, based on hull length, is less than $5x10^6$. Given the waterline length of the models and the range of speeds of interest, Reynolds numbers below this level were unavoidable. However, turbulence stimulation is generally required when measuring the resistance of a ship model. It is assumed that turbulence stimulation would not make any measureable

difference to the characteristics of the waves generated by a ship model, as this is mainly done to affect boundary layer transition. Regardless, turbulence stimulation studs were attached to the models to induce turbulent flow, with their size and locations based on the ITTC Recommended Procedure 7.5-01-01-01 (ITTC 2008).

5.2.2 Water Depths

When dealing with ship operations in finite water depths it is common to refer to the non-dimensional parameter of water depth to draught ratio, h/d. This ratio is ideal when considering large ships operating within port environments as they often have a relatively constant draught over a large percentage of their length and underkeel clearances tend to be low, hence draught becomes a very important parameter. Typical values of h/d of interest can be as low as 1.05. However, in the case of recreational craft and small commercial vessels the draught can vary notably over their length and it can be common for the propulsion system (such as a propeller) to extend a relatively large distance below the hull draught, thus it is rare to encounter very low h/d values. Therefore, in this study water depth has been non-dimensionalised by vessel length, h/L. Both h/L and h/d are provided in Table 5.1 for each case. As can be seen, h/d ranges from 3.0 to 10.7 for all models at the shallowest water depth.

It is known that the shallower the water depth beneath a vessel (or under keel clearance) the more dramatic the effect can be on wave generation (refer Chapter 2). Therefore, simply conducting experiments at a single finite water depth would be very unlikely to provide adequate detail to describe the effect of water depth for the purposes of the intended prediction tool. This was confirmed following a review of the results from experiments conducted by Macfarlane and Hinds (2001) where wave wake measurements were obtained for a single ship model at eight different finite water depths (plus a deep water case). It was estimated that three finite water depths, plus deep water, would provide a suitable data set for the purposes of the present study.

The actual depths for the experiments were selected such that they represented real life scenarios found from a study of typical vessel operations in several key Australian sheltered waterways. Details of this study, including a list of vessels and locations, are provided in Appendix B. The findings from this study have been summarised in Figure 5.1, where the water depth-to-vessel length ratios (h/L) for each

case have been plotted as a function of $L/\nabla^{1/3}$. Note that the h/L for each case reflects the shallowest section of the vessel's route. In many cases this may not represent a large portion of the entire journey, but often will represent locations where vessel wave wake may pose the greatest risks.

In Figure 5.1, the vast majority of cases fall within the range of $0.25 < h/L < 1.5$. All three cases where the h/L is lower than 0.25 are for existing vessels that presently operate under severe speed restrictions due to the very restricted waterways in which they operate. For example, the sole catamaran with an h/L of approximately 0.1 is the 35 m long RiverCat operating in the upper reaches of the Parramatta River (Patterson Britton & Partners 1995; Bishop 2003).

This study supports the earlier statement that the majority of vessels operating on Australian waterways are small recreational craft (mostly monohulls) and small commercial vessels. Almost all of the catamarans are commercial vessels, usually passenger ferries, cruise vessels or charter vessels.

This study of existing vessels and local operations was used to design the program of scale model experiments. The lower boundary of h/L values covered for both monohulls and catamarans is shown in Figure 5.1. This range includes all but a few extreme cases of the example vessel operations shown in this figure. Given the very limited number and site specific nature of these cases, it was considered difficult to justify the significant increase in the size of the test program to include the very low water depths required to simulate such outliers. Note that the sole case with a very low $L/\nabla^{1/3}$ (approximately 3.5) is for a personal water craft (JetSki). Details of each test condition are provided in Table 5.1.

Consideration was also given to potential issues that may result from conducting model scale tests in very shallow water. As discussed in Section 2.1.7, work by Robbins *et al*. (2011) indicates that the height of the leading wave (Wave A) may be significantly unsteady over time at some trans-critical speeds. The study presents data at values of h/L of 0.08, 0.16, 0.24 and 0.32, with the greatest levels of unsteadiness found at the extreme case of $h/L = 0.08$. There is little or no evidence of any unsteadiness with the angle of the leading wave at trans-critical speeds.

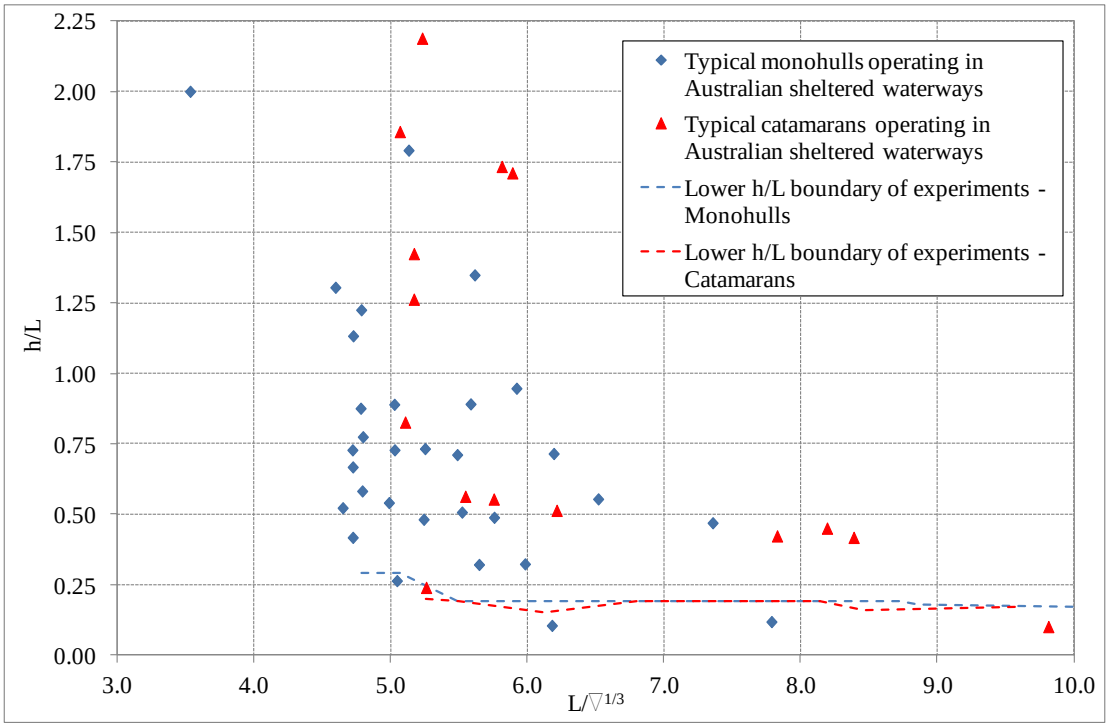

Figure 5.1 Typical vessel operations within Australian sheltered waterways

5.2.3 Vessel Speeds

The aim from the outset of the project was to consider the widest practical range of vessel speeds. For all hull forms the slowest speeds investigated were such that the waves generated were small enough as to be considered almost negligible. For each ship model, experiments were conducted up to, or close to, the maximum offered by the facility. In almost all cases, the maximum attainable towing speed of the facility was greater than what would be considered a practical maximum speed for each particular hull form. The only exception was the ski boat, as this type of craft regularly operates at relatively high length Froude numbers, particularly when involved in competitive sporting activities. To achieve these high Fr_L within the AMC facility would result in the size of the ship model being unacceptably small. Thus, the selected scale factor resulted in a model of acceptable size and the maximum speed attainable, although below the desired maximum, was high enough to cover most of the important speed region when considering wave generation. Also taken into consideration was the availability of good quality full scale experimental data for several very similar ski boats (Macfarlane and Cox 2004; Macfarlane 2010). This data covers a wide range of speeds, well in excess of the maximum achieved during

these model experiments. Correlation between the model and full scale data is investigated in Section 6.5.

Consideration was also given to the optimum increment in speed. This involved a review of previously obtained model and full scale test data in both deep and finite water depths (Macfarlane and Hinds 2001; Doyle 2001; Macfarlane 2002; Macfarlane and Cox 2004; Robbins *et al*. 2007). It was concluded that an increment of no greater than $Fr_L = 0.10$ should result in an adequately defined curve for the purpose of developing a wave wake prediction tool. For the majority of the test program the speed increment was maintained within the range of $0.05 < Fr_L < 0.07$, and at no time did the increments exceed 0.09. Thus, this has resulted in very well defined curves, particularly over the sub-critical and super-critical speed regimes.

However, it is accepted that a finer speed increment may be desirable close to the critical depth Froude number (high trans-critical speeds) if the purpose is to precisely describe behaviour in this region due to rapid changes in most of the variables of interest. Often the interest in this region is on the development of unsteady phenomena such as the generation of solitons (see for example Remoissenet 1999; Dand *et al*. 1999a; Jiang 2001; Robbins *et al*. 2011).

5.3 Experimental Equipment and Procedures

5.3.1 Equipment

There were two key items of experimental equipment that were required to undertake the experimental program: a towing system to tow the ship models, including carriage, and a test rig from which to deploy and calibrate an array of surface wave sensors. A diagram of the layout of the experimental equipment within the basin is provided in Figure 5.2.

The ship model towing system consisted of an electric winch connected to a grooved drum in which the dynamic tow cable was wound onto during operation. An advantage of this type of system over other commonly used methods is that it eliminates the possibility of slip, particularly when the towing loads are high (generally during acceleration, deceleration and/or high speeds). A digital programmable logic control system, including feedback, provided a reliable means of ensuring the models were towed at the desired steady state speed.

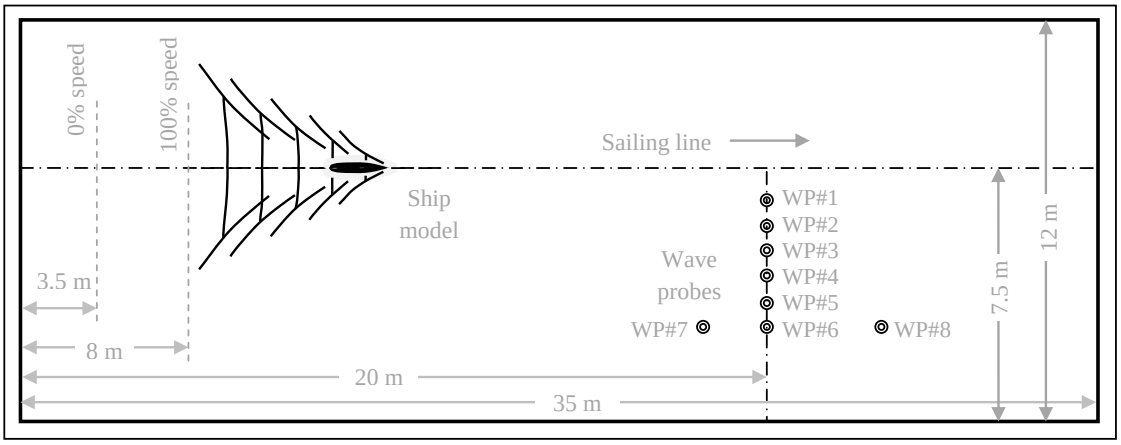

Figure 5.2 Layout of hydrodynamic test basin

The dynamic towline from the winch drum was connected to a lightweight carriage which ran upon a pair of parallel static cables that extended the full length of the 35 m long basin. The ship model was connected to the carriage through two vertical posts, each of which ran through a pair of bearings rigidly mounted to the carriage. The base of the forward post was connected to the model via a ball joint and the aft post through a combined ball joint and longitudinal slide bearing. The model was constrained in surge, sway and yaw, but had freedom in heave, pitch and roll.
The longitudinal centreline of the winch system, hence also the ship model, was not located in the transverse centre of the 12 m wide basin, but offset by 1.5 m to one side. This allowed measurement of the generated waves over a greater transverse distance.

Previous work by the author recommended that the wave wake profile be obtained at a minimum of four transverse locations between the near to medium field in order to accurately estimate the wave decay rate (Macfarlane 2002). For this study a minimum of six transverse wave probes were adopted (in some cases up to 12 were implemented). Figure 5.2 shows the general location of the ‘standard’ array of wave probes that was adopted for the majority of the test program.

The closest probe to the ship model (wave probe #1) was located at a lateral distance (y) of 1.00 m from the sailing line of the model. This was considered the closest practical distance, based on previous experience with local wave effects that can occur close to a passing ship model (Macfarlane 2002). In most cases, the first, second and third probes were spaced one metre apart (y = 1.00, 2.00 and 3.00 m respectively). Subsequent probes were more closely spaced (generally no more than 0.50 m apart). It is often the case that the more distant probes provide more reliable

wave profile data, primarily since the greater distance has allowed the waves to disperse (refer Section 2.2.1).

A test rig was developed that allowed the main transverse wave probe array to be easily swung from the test location (perpendicular to the side wall of the basin) to be close to, and parallel with, the side wall of the basin. This allowed for easy access to each wave probe for calibration and checking without disturbing the water in the basin.

For some of the experiments a longitudinal array of wave probes was also deployed with the primary aim to investigate potential unsteadiness in the waves generated, particularly close to critical depth Froude number. This topic is discussed in detail by Robbins *et al*. (2011).

5.3.2 Instrumentation

The speed of the model was determined using a pulse encoder connected to the electrically driven winch drum. This system was calibrated by measuring the time taken to traverse between two points of a known distance apart (in this case the distance was 15 m, which started approximately 13 m prior to the transverse wave probe array). The two points were identified within the data recorded as ‘spikes’, caused as the forward post on the carriage passed through two beams from low-class lasers (with the beams separated by the 15 m distance).

Each of the wave probes were of standard resistance type hard-wired to a power supply and signal conditioner supplied by Hydraulics Research Wallingford (HRW). The length of each wave probe was 300 mm and an amplifier was used to apply a suitable gain to obtain the optimum signal resolution for the expected range of wave heights/troughs (typically around 100 mm). Each probe was calibrated by using a graduated staff, with readings taken at increments of 10 mm. For each wave probe the range of calibration exceeded the range of values measured in the experiments and the calibration factors varied less than 0.75% over the entire test program. The wave probes were calibrated on a daily basis and included all items of the measurement chain, including probe, cables, signal conditioner, amplifier and analogue to digital converter.

A low-class laser beam emitter was installed in such a way as to provide a precise indication when the bow of the ship model was level with the main array of transverse wave probes. This assisted the determination of the location of the ship model relative to the recorded wave pattern.

5.3.3 Test Procedure and Data Acquisition

Initial readings of all instruments were taken prior to each run and were checked between runs to ensure that no notable drift had occurred. The carriage was accelerated to the predetermined speed and data acquisition was commenced at a designated longitudinal location in the basin to maintain consistency. The sample rate was set at 200 Hz with the number of samples recorded varying to ensure that all relevant data was acquired (the duration of data acquisition varied with the speed of the model). Sufficient time was allowed between consecutive runs to achieve calm water conditions.

5.4 Analysis Process

5.4.1 Analysis of the Time Series Data

Spectral analysis, using Fast Fourier Transforms (FFT) was considered as an alternative to the analysis process adopted (as described within this chapter). Discussion related to the use of spectral analysis in the context of the experimental data obtained in this study has been provided in Appendix C.

In this sub-section, the analysis process is explained for a single test run – which represents a single ship model, water depth and model speed. The entire model test program (summarised in Table 5.1) consists of over 950 such runs.

As outlined in Section 5.3, wave profiles were obtained at a minimum of six transverse locations. The time series data for each individual run was imported into an Excel macro workbook where they were ‘zeroed’ by subtracting the initial readings and converted from voltages into units of vertical displacement (in millimetres) by applying the relevant calibration factors for each of the wave probes. A similar process was undertaken for the measurement of the model speed, only this was converted into units of metres per second. The model speed data was plotted as a function of time and an average reading determined over the time period that the

model was at steady state (this period was manually adjusted by the user). Both the length of the ship model and the water depth for the run in question were input into the Excel spreadsheet which allowed both the depth and length Froude numbers for that specific run to be calculated.

The wave surface elevation data (in mm) was plotted as a function of time, with each wave probe presented in a separate worksheet. A set of three 'windows' were then manually positioned along the time axis to aid the identification of the three waves of interest, Waves A, B and C (as discussed and outlined in Section 3.3). Characteristics of these three waves, such as height, period and energy, are displayed. Each of the abovementioned features can be seen in the example provided in Figure 5.3.

The next worksheet within the Excel macro workbook provided a summary of the quantities obtained for Waves A, B and C for all six (or more) wave probes. This included the height and period of the wave, plus the time that the peak of the wave occurred within the run. Using this time and the measured speed of the model the distance that this peak occurs downstream of the bow of the ship model was determined. These downstream distances for Waves A, B and C at each wave probe were then plotted as a function of transverse distance from the model sailing line, as shown in the example in Figure 5.4. This plot provides an indication of the shape of each of the wave fronts and can highlight if there have been any obvious errors in the selection of the key waves at each wave probe, as the curve would be discontinuous. The angle (θ) of each of the three key waves was determined and displayed.

The next step was to determine the non-dimensional wave height constant (γ) and wave decay rate (n) for Waves A, B and C. This was achieved by plotting the non-dimensionalised wave height from each wave probe as a function of non-dimensional lateral distance from the sailing line. An example is shown in Figure 5.5 where this is plotted for Wave A. Both the wave height and lateral distance are non-dimensionalised by dividing by the length of the ship model. By adding a trendline of the power form shown in Equation 2.3 the wave height constant γ and the wave decay rate n were determined, as discussed in Section 2.1.6 and displayed in the example shown in Figure 5.5.

The wave period, T, is determined by measuring the time between consecutive peaks (or troughs) and simply obtaining the average over all wave probes at each lateral location. It is expected that the wave period should not change appreciably with

increasing lateral distance from the model sailing line, however, in practice, it is sometimes possible to find some variation at the closest wave probes to the model (wave probe #1). This probe is almost always within one ship model length from the model sailing line, which is considered to be in the near-field, thus there has been little opportunity for the waves to disperse by this stage (refer Figure 2.8). As a result, the wave period has been determined by averaging the values from all of the more distant wave probes. The wave period is normalised by dividing by the square root of the length of the ship model. An example of wave period (for Wave A) plotted as a function of lateral distance from the sailing line can be seen in the lower section of Figure 5.5.

When analysing each run, it is strongly recommended that the θ and T from each of the six (or more) wave probes be compared as this can ensure that the same wave is selected at each lateral location, as these quantities should remain relatively constant. It was also found easier to start analysis at the greatest lateral distances (for example wave probe #6) and work towards the ship model sailing line. This was because the waves further away have dispersed sufficiently thus making the 'key' waves much more identifiable than is the case with the longitudinal wave cuts close to the model (particularly with the closest wave probe).

To aid the next phase of the analysis process, all relevant quantities obtained from this single test run are summarised on a single worksheet within the Excel workbook dedicated to each specific run, as shown in the example provided in Figure 5.6.

Test Details				Model Details		Water Depth			Principal Particulars								Ratios						
Hull No.	Case No.	Test Session Cond. No.	Run Numbers	AMC Model Number	Monohull or Catamaran	h (mm)	h / L	h / d	Δ (kg)	L (m)	B monos (mm)	B_{OA} cats (mm)	Demihull B (mm)	Demihull s (mm)	d (mm)	i_E (deg)	L / B monohulls	B / d monohulls	L / B_{OA} catamarans	L / B demihull	B / d demihull	L / d	L / $\nabla^{1/3}$
1	1	D1	D455-D467	00-01H	Monohull	2200	2.11	34.9	10.550	1.042	345				63	24.5	3.020	5.476				16.5	4.79
	2	11	138-150			900	0.86	14.3	10.550	1.042	345				63	24.5	3.020	5.476				16.5	4.79
	3	33	417-430			600	0.58	9.5	10.550	1.042	345				63	24.5	3.020	5.476				16.5	4.79
	4	61	778-790			300	0.29	4.8	10.550	1.042	345				63	24.5	3.020	5.476				16.5	4.79
2	5	90	1144-1158	10-37H	Monohull	900	0.96	15.3	7.317	0.934	315				59	15.0	2.965	5.339				15.8	4.85
	6	81	1023-1036			600	0.64	10.2	7.317	0.934	315				59	15.0	2.965	5.339				15.8	4.85
	7	80	1009-1022			300	0.32	5.1	7.317	0.934	315				59	15.0	2.965	5.339				15.8	4.85
3	8	D2	D440-D452	00-01L	Monohull	2200	2.13	41.5	8.700	1.035	345				53	24.5	3.000	6.509				19.5	5.07
	9	12	151-166			900	0.87	17.0	8.700	1.035	345				53	24.5	3.000	6.509				19.5	5.07
	10	34	431-443			600	0.58	11.3	8.700	1.035	345				53	24.5	3.000	6.509				19.5	5.07
	11	62	791-803			300	0.29	5.7	8.700	1.035	345				53	24.5	3.000	6.509				19.5	5.07
4	12	89	1130-1143	10-37L	Monohull	900	0.97	16.7	6.052	0.929	315				54	15.0	2.949	5.833				17.2	5.14
	13	82	1037-1050			600	0.65	11.1	6.052	0.929	315				54	15.0	2.949	5.833				17.2	5.14
	14	79	995-1008			300	0.32	5.6	6.052	0.929	315				54	15.0	2.949	5.833				17.2	5.14
5	15	D3	D215-D227	97-02H	Monohull	2200	1.38	22.0	25.340	1.600	399				100	20.0	4.010	3.990				16.0	5.49
	16	3	33-45			900	0.56	9.0	25.340	1.600	399				100	20.0	4.010	3.990				16.0	5.49
	17	35	444-457			600	0.38	6.0	25.340	1.600	399				100	20.0	4.010	3.990				16.0	5.49
	18	65	830-842			300	0.19	3.0	25.340	1.600	399				100	20.0	4.010	3.990				16.0	5.49
6	19	D4	D200-D212	97-02L	Monohull	2200	1.38	23.9	20.340	1.595	399				92	20.0	3.997	4.337				17.3	5.89
	20	4	46-58			900	0.56	9.8	20.340	1.595	399				92	20.0	3.997	4.337				17.3	5.89
	21	36	458-471			600	0.38	6.5	20.340	1.595	399				92	20.0	3.997	4.337				17.3	5.89
	22	66	843-855			300	0.19	3.3	20.340	1.595	399				92	20.0	3.997	4.337				17.3	5.89
7	23	D5	D275-D287	97-10	Monohull	2200	1.39	36.1	12.195	1.578	305				61	12.2	5.174	5.000				25.9	6.91
	24	88	1117-1129			900	0.57	14.8	12.195	1.578	305				61	12.2	5.174	5.000				25.9	6.91
	25	84	1064-1076			600	0.38	9.8	12.195	1.578	305				61	12.2	5.174	5.000				25.9	6.91
	26	76	954-966			300	0.19	4.9	12.195	1.578	305				61	12.2	5.174	5.000				25.9	6.91
8	27	D6	D78-D90	96-08H	Monohull	2200	1.37	38.6	9.000	1.605	199				57	11.5	8.065	3.491				28.2	7.78
	28	1	2-16			900	0.56	15.8	9.000	1.605	199				57	11.5	8.065	3.491				28.2	7.78
	29	39	495-507			600	0.37	10.5	9.000	1.605	199				57	11.5	8.065	3.491				28.2	7.78
	30	63	804-816			300	0.19	5.3	9.000	1.605	199				57	11.5	8.065	3.491				28.2	7.78
9	31	D7	D63-D75	96-08L	Monohull	2200	1.38	44.0	6.320	1.600	199				50	11.5	8.040	3.980				32.0	8.73
	32	2	17-30			900	0.56	18.0	6.320	1.600	199				50	11.5	8.040	3.980				32.0	8.73
	33	40	508-520			600	0.38	12.0	6.320	1.600	199				50	11.5	8.040	3.980				32.0	8.73
	34	64	817-829			300	0.19	6.0	6.320	1.600	199				50	11.5	8.040	3.980				32.0	8.73
10	35	D8	X1-X20	97-30	Monohull	2200	1.34	52.4	6.504	1.641	238				42	14.0	6.895	5.667				39.1	8.86
	36	8	99-111			900	0.55	21.4	6.504	1.641	238				42	14.0	6.895	5.667				39.1	8.86
	37	46	578-590			600	0.37	14.3	6.504	1.641	238				42	14.0	6.895	5.667				39.1	8.86
	38	58	739-751			300	0.18	7.1	6.504	1.641	238				42	14.0	6.895	5.667				39.1	8.86
11	39	D9	W2-W14	99-17	Monohull	2200	1.20	78.6	3.902	1.827	199				28	13.5	9.181	7.107				65.3	11.70
	40	86	1091-1103			900	0.49	32.1	3.902	1.827	199				28	13.5	9.181	7.107				65.3	11.70
	41	85	1077-1090			600	0.33	21.4	3.902	1.827	199				28	13.5	9.181	7.107				65.3	11.70
	42	77	967-980			300	0.16	10.7	3.902	1.827	199				28	13.5	9.181	7.107				65.3	11.70
12	43	D10	D650-D662	00-03	Catamaran	2200	1.48	27.5	23.210	1.489		708	204	504	80	16.5			2.103	7.299	2.550	18.6	5.26
	44	10	125-137			900	0.60	11.3	23.210	1.489		708	204	504	80	16.5			2.103	7.299	2.550	18.6	5.26
	45	44	554-564			600	0.40	7.5	23.210	1.489		708	204	504	80	16.5			2.103	7.299	2.550	18.6	5.26
	46	56	715-725			300	0.20	3.8	23.210	1.489		708	204	504	80	16.5			2.103	7.299	2.550	18.6	5.26
13	47	D11	D635-D647	93-07	Catamaran	2200	1.76	34.4	13.580	1.250		429	144	212	64	15.5			2.914	8.681	2.250	19.5	5.28
	48	5	59-72			900	0.72	14.1	13.580	1.250		429	144	212	64	15.5			2.914	8.681	2.250	19.5	5.28
	49	28	349-362			600	0.48	9.4	13.580	1.250		429	144	212	64	15.5			2.914	8.681	2.250	19.5	5.28
	50	71	893-905			300	0.24	4.7	13.580	1.250		429	144	212	64	15.5			2.914	8.681	2.250	19.5	5.28
14	51	D12	Z19-Z46	99-01	Catamaran	2200	1.38	25.9	25.302	1.600		712	191	512	85	12.0			2.247	8.377	2.247	18.8	5.50
	52	22	291-302			900	0.56	10.6	25.302	1.600		712	191	512	85	12.0			2.247	8.377	2.247	18.8	5.50
	53	42	532-542			600	0.38	7.1	25.302	1.600		712	191	512	85	12.0			2.247	8.377	2.247	18.8	5.50
	54	74	930-940			300	0.19	3.5	25.302	1.600		712	191	512	85	12.0			2.247	8.377	2.247	18.8	5.50
15	55	D13	V25-V46	99-27	Catamaran	2200	1.13	28.2	32.818	1.945		692	225	500	78	8.0			2.811	8.644	2.885	24.9	6.13
	56	87	1104-1116			900	0.46	11.5	32.818	1.945		692	225	500	78	8.0			2.811	8.644	2.885	24.9	6.13
	57	83	1051-1063			600	0.31	7.7	32.818	1.945		692	225	500	78	8.0			2.811	8.644	2.885	24.9	6.13
	58	78	981-993			300	0.15	3.8	32.818	1.945		692	225	500	78	8.0			2.811	8.644	2.885	24.9	6.13
16	59	D14	D500-D512	93-03H	Catamaran	2200	1.36	30.6	13.720	1.614		471	110	361	72	8.5			3.427	14.673	1.528	22.4	6.80
	60	13	167-179			900	0.56	12.5	13.720	1.614		471	110	361	72	8.5			3.427	14.673	1.528	22.4	6.80
	61	47	591-603			600	0.37	8.3	13.720	1.614		471	110	361	72	8.5			3.427	14.673	1.528	22.4	6.80
	62	53	677-689			300	0.19	4.2	13.720	1.614		471	110	361	72	8.5			3.427	14.673	1.528	22.4	6.80
17	63	D15	D515-D527	93-03L	Catamaran	2200	1.38	35.5	7.620	1.589		471	110	361	62	8.5			3.374	14.445	1.774	25.6	8.14
	64	14	180-193			900	0.57	14.5	7.620	1.589		471	110	361	62	8.5			3.374	14.445	1.774	25.6	8.14
	65	48	604-616			600	0.38	9.7	7.620	1.589		471	110	361	62	8.5			3.374	14.445	1.774	25.6	8.14
	66	54	690-703			300	0.19	4.8	7.620	1.589		471	110	361	62	8.5			3.374	14.445	1.774	25.6	8.14
18	67	D16	Y1-Y15	98-16H	Catamaran	2200	1.21	37.3	10.250	1.822		459	82	377	59	6.5			3.969	22.220	1.390	30.9	8.46
	68	17	227-239			900	0.49	15.3	10.250	1.822		459	82	377	59	6.5			3.969	22.220	1.390	30.9	8.46
	69	30	377-389			600	0.33	10.2	10.250	1.822		459	82	377	59	6.5			3.969	22.220	1.390	30.9	8.46
	70	59	752-764			300	0.16	5.1	10.250	1.822		459	82	377	59	6.5			3.969	22.220	1.390	30.9	8.46
19	71	D17	Y25-Y39	98-16L	Catamaran	2200	1.21	41.5	6.932	1.818		459	82	377	53	6.5			3.961	22.171	1.547	34.3	9.61
	72	18	240-253			900	0.50	17.0	6.932	1.818		459	82	377	53	6.5			3.961	22.171	1.547	34.3	9.61
	73	31	390-402			600	0.33	11.3	6.932	1.818		459	82	377	53	6.5			3.961	22.171	1.547	34.3	9.61
	74	60	765-777			300	0.17	5.7	6.932	1.818		459	82	377	53	6.5			3.961	22.171	1.547	34.3	9.61

Table 5.1 Details of test program and ship model principal particulars (in descending order of L/$\nabla^{1/3}$)

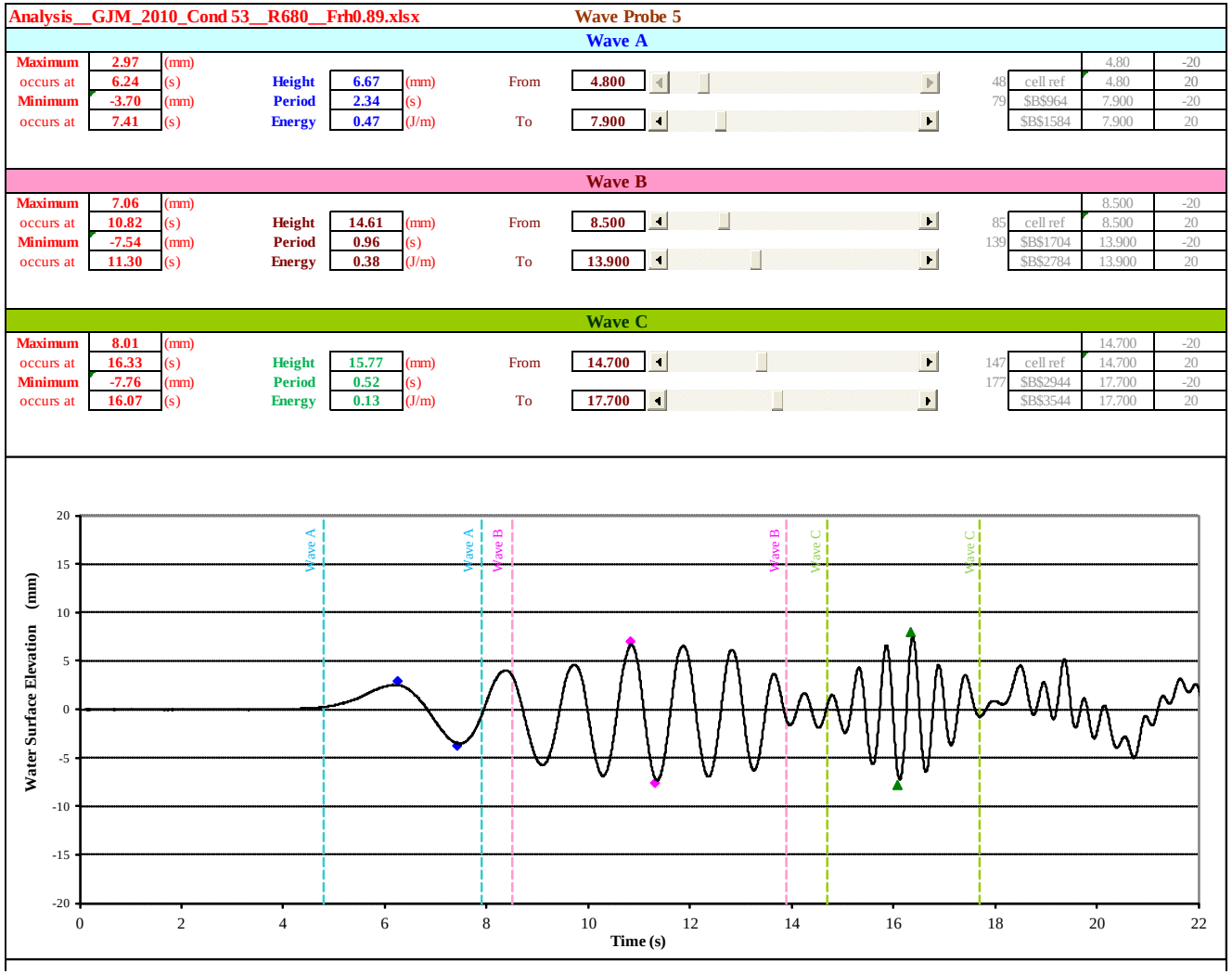

Figure 5.3 Example of analysis of a single wave elevation time series

		Analysis__GJM_2010_Cond 53__R680__Frh0.89.xlsx											
		Wave A				Wave B				Wave C			
	Speed												
	1.532	Wave Angle		82.3	degrees	Wave Angle		36.7	degrees	Wave Angle		15.7	degrees
	(m/s)												
	Offset, y	Height	Period	@ Time	Distance	Height	Period	@ Time	Distance	Height	Period	@ Time	Distance
	(m)	(mm)	(s)	(s)	(m)	(mm)	(s)	(s)	(m)	(mm)	(s)	(s)	(m)
Probe 1	1	26.3	2.14	6.07	9.29	44.4	0.81	7.89	12.08	29.5	0.59	9.00	13.78
Probe 2	2	14.0	2.40	6.00	9.18	28.6	1.14	9.16	14.02	17.1	0.54	11.12	17.03
Probe 3	3	9.4	2.43	6.12	9.37	20.7	1.00	10.53	16.13	18.9	0.53	13.73	21.03
Probe 4	3.5	7.6	2.33	6.24	9.56	18.5	1.05	10.64	16.30	18.0	0.53	14.77	22.62
Probe 5	4	6.7	2.34	6.24	9.56	14.6	0.96	10.82	16.57	15.8	0.52	16.07	24.61
Probe 6	4.5	5.8	2.21	6.38	9.76	11.1	0.96	10.96	16.78	14.9	0.57	17.11	26.20

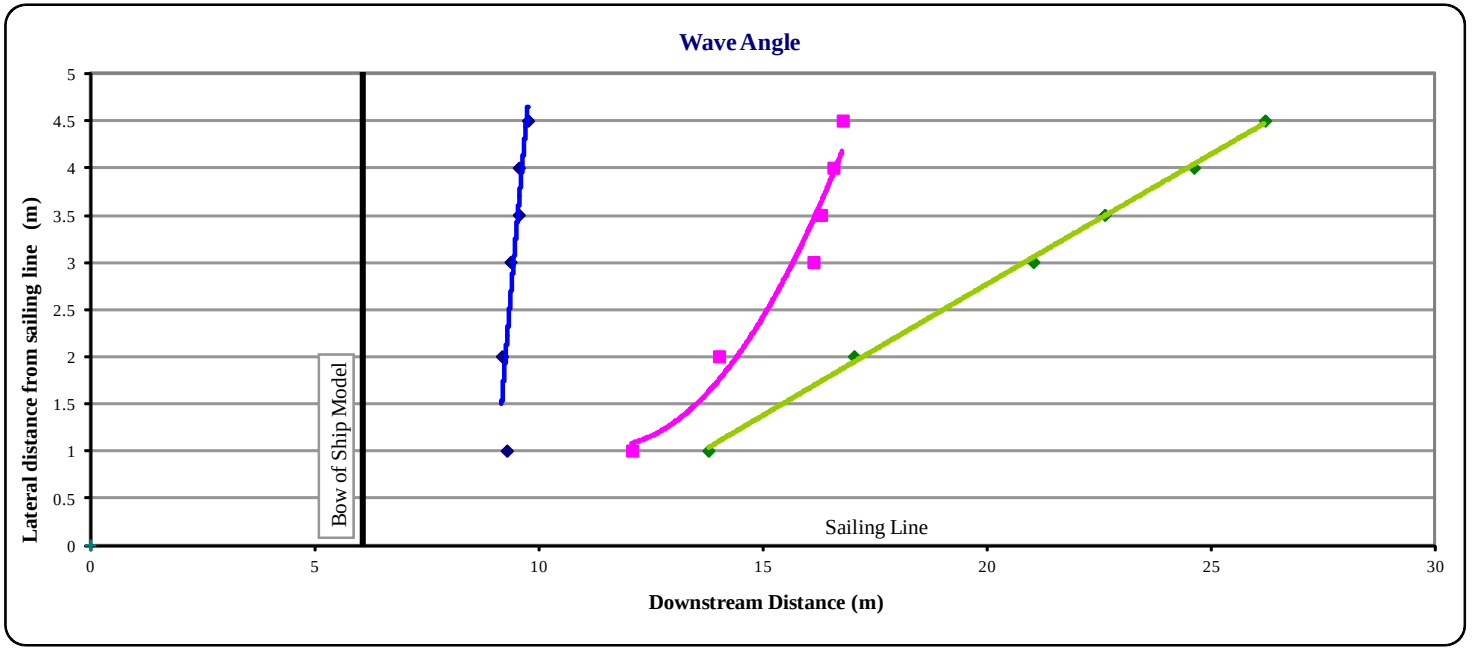

Figure 5.4 Example of wave angle analysis

Analysis__GJM_2010_Cond 53__R680__Frh0.89.xlsx											Wave A
	Model Scale			Non Dimensional		Deep Water Decay		Finite Water Decay		Period	
	Offset (y) (m)	Height (mm)	Period (s)	Offset (y/L)	H/L x 1000	γ 10.377	n - 1/3	γ	n best fit	T (s)	
Probe 1	1.0	26.34	2.140	0.62	16.322	10.377		10.377	-1.004	2.342	
Probe 2	2.0	14.00	2.400	1.24	8.674	8.236					
Probe 3	3.0	9.35	2.430	1.86	5.793	7.195					
Probe 4	3.5	7.62	2.330	2.17	4.723	6.835					
Probe 5	4.0	6.67	2.340	2.48	4.131	6.537					
Probe 6	4.5	5.82	2.210	2.79	3.606	6.285					

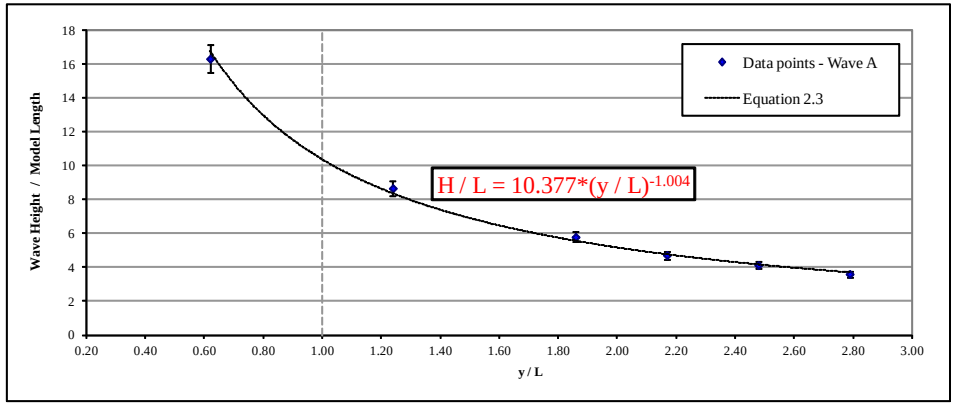

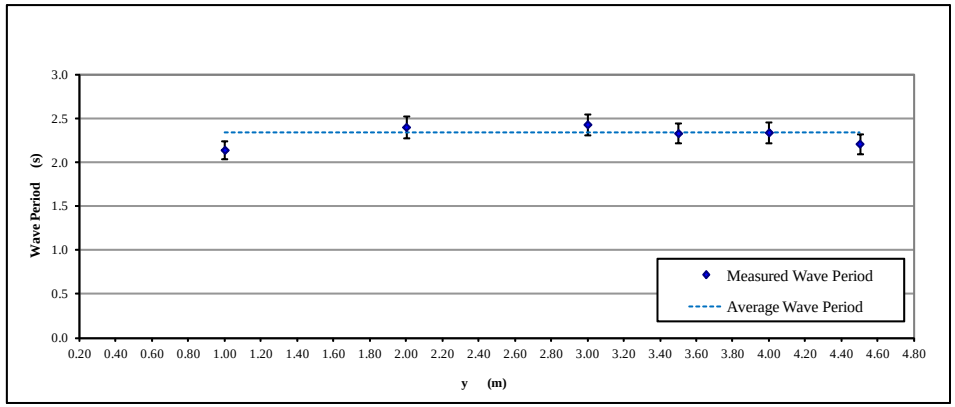

Figure 5.5 Example of analysis of wave height constant, wave decay and wave period (for Wave A)

							Wave A				Wave B				Wave C			
AMC Model Number	**h** (m)	**L** (m)	**Δ** (kg)	**u** (m/s)	**Fr_h**	**Fr_L**	**γ_A**	**T_A** (seconds)	**n_A**	**θ_A** (degrees)	**γ_B**	**T_B** (seconds)	**n_B**	**θ_B** (degrees)	**γ_C**	**T_C** (seconds)	**n_C**	**θ_C** (degrees)
93-03	0.300	1.614	13.720	1.532	0.893	0.385	10.377	2.342	-1.004	82.3	19.800	0.99	-0.853	36.7	14.600	0.54	-0.421	15.7

Figure 5.6 Example of output file from analysis spreadsheet

5.4.2 Analysis of Data for Each Ship Model

Approximately 13 to 15 different speeds (runs) were investigated for each ship model at each water depth. The output (as described in the previous sub-section), from each run for this ship model at the same water depth was then imported into a worksheet within a new Excel workbook. A similar process was conducted for the results for this ship model from tests at each of the other water depths (such that all results for this ship model are within the same workbook). Each of the measured quantities could then be plotted and compared. Examples of this data are presented and discussed in Section 5.5.

A complete re-analysis of all previously existing experiments conducted in deep water was done in order to maintain consistency in analysis procedure and to extract values for all three key waves (A, B and C), plus the determination of wave angle, which had previously not been undertaken (refer Macfarlane, 2002).

The process of combining the results from all nineteen ship models is covered in detail within Chapter 6, which deals with the development of the wave wake prediction tool.

5.5 Effect of Vessel Speed and Water Depth

It was deemed essential to have a good understanding of the results for each of the measured quantities and how these varied with changes in water depth and vessel speed in order to determine which techniques were best suited for the development of the wave wake prediction tool. To investigate this, the results from the experiments on all nineteen ship models at each of the four water depths were generated and studied. It was considered impractical and unnecessary to present the results from all ship models, which constitute at least 456 individual graphs (comprising 24 graphs for each of the 19 ship models). Thus, a complete set of results for just a single ship model have been presented in this sub-section. Significant trends and dependencies were identified and discussed.

Initially, each of the four key measured variables (γ, T, n, θ) are covered separately, but some features that appear common between these variables are also discussed. In all of the figures in this sub-section each variable is plotted as a function of speed, in

terms of both depth and length Froude number, as it is shown that both of these non-dimensional forms of speed can be very influential. A total of 24 figures are presented and discussed in this sub-section, comprising: four variables (γ, T, n, θ), three waves (A, B, C) and two variants of speed (Fr_h, Fr_L).

It was not considered important which of the nineteen different hull forms were selected for the purposes of this example, as the primary focus is to gain an understanding of the effect of vessel speed and water depth, not hull form. The hull selected for the example is monohull 97-02L, as it represents the mid-range of slenderness ratios investigated, i.e. it has the sixth largest (and sixth smallest) $L/\nabla^{1/3}$ of all eleven monohulls in the test program with a value of 5.89 (refer Table 5.1 for the principal particulars of this hull).

The effect of hull form is investigated in Section 6.4, following the description of how the wave wake prediction tool was developed.

5.5.1 Wave Height Constant, γ

Wave A – the wave height constant for Wave A, γ_A, is shown as a function of depth Froude number, Fr_h, in Figure 5.7 and as a function of length Froude number, Fr_L, in Figure 5.8. A total of four data series are shown in each figure, representing the three different finite water depths and the deep water case, shown as ratios of water depth to model length, h/L.

In Figure 5.7 it is clear that there is a significant change in γ_A for each of the finite water depth cases around the onset of the trans-critical depth Froude numbers (Fr_h ~0.75). From Figure 5.8, it can be seen that the curves for all four water depths are effectively the same (i.e. a function of Fr_L and not water depth) for all sub-critical depth Froude numbers – that is, once the ship hull reaches the onset of the trans-critical range (Fr_h ~0.75) the wave height constant, γ_A, varies significantly from the deep water case. To aid discussion, the point at which the trans-critical region commences, nominally taken as Fr_h = 0.75, has been indicated in Figure 5.8 for each of the three finite water depth cases (by the dashed vertical lines).

As an example, for an h/L of 0.19 (the shallowest water depth) the wave height constant γ_A at a Fr_L of 0.32 is the same as the deep water case (as are the other two larger h/L cases), but at the next highest Fr_L (0.39) there is a significant increase –

this corresponds to a Fr_h of 0.89, which is well within the trans-critical region where it is expected that depth will affect γ_A.

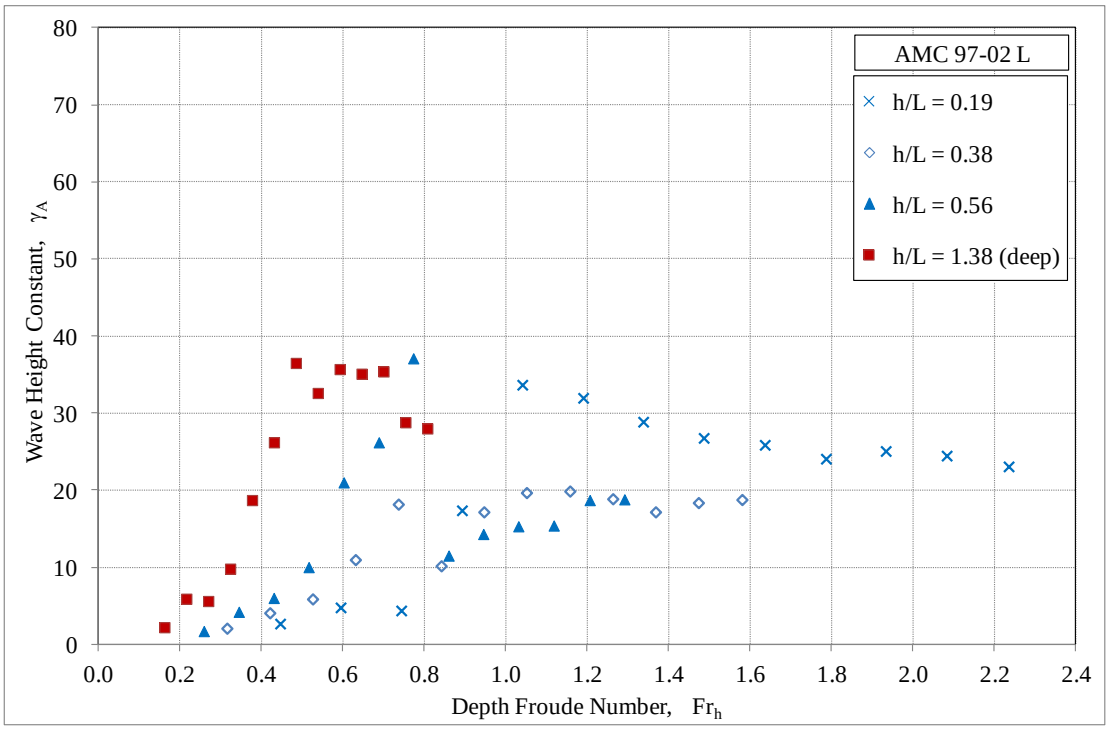

Figure 5.7 Wave height constant for Wave A, γ_A, as a function of Fr_h

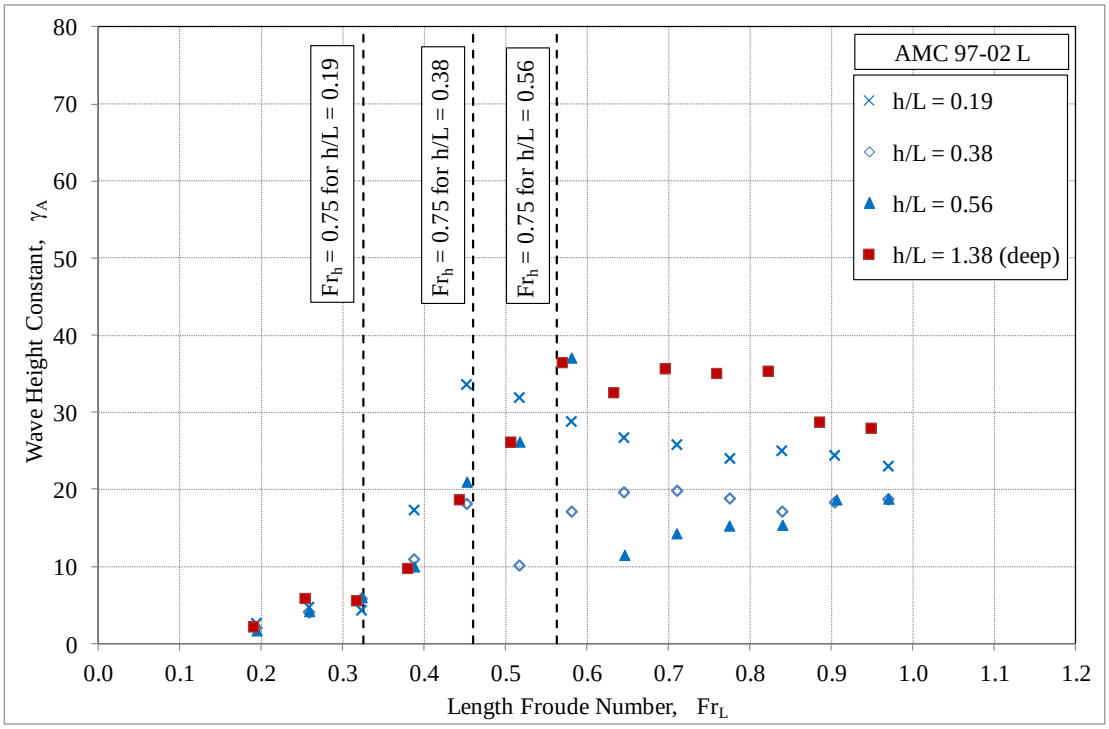

Figure 5.8 Wave height constant for Wave A, γ_A, as a function of Fr_L

Similarly, for an h/L of 0.56 (the deepest of the finite water depths) the wave height constant γ_A at a Fr_L of 0.58 is the same as the deep water case (36.5), but at the next highest Fr_L (0.65) there is a significant change, although in this case there is a notable reduction – this corresponds to a Fr_h of 0.86.

As Fr_h increases to super-critical speeds (Fr_h in excess of 1.0, Figure 5.7) the values for γ_A remain relatively steady as speed is further increased, however there is a gradual decrease for the shallowest case, h/L = 0.19. It is feasible that each of the curves for the finite water depths may have converged around a γ_A value of approximately 20 had it been possible to conduct much higher depth Froude numbers at the greater finite water depths.

The point at which the trans-critical speed region commences is a topic of discussion in itself (refer Chapter 2 and Robbins *et al*. 2011). In Section 2.1.7, the rapid increase in the angle of the leading wave, θ_A, was noted, as was the increase in crest length at these speeds (Figure 2.7). When analysing this experimental data it was observed that special care had to be taken while attempting to identify the leading wave, Wave A, at trans-critical speeds. This has led to some dramatic, rather than gradual, changes (either an increase or decrease) in values for γ_A during the transition from sub-critical to trans-critical speeds, as can be seen in the example shown in Figure 5.7 (between $0.75 < Fr_h < 0.85$). The reason for this dramatic change is, in part, due to transformation in the wave pattern at trans-critical speeds, particularly with the angle of the leading wave, and the manner in which the experimental data has been interpreted. To assist in describing what is occurring, two examples are discussed in more detail.

Firstly, for the deepest of the three finite water cases, h/L = 0.56, the two speeds between which this transition occurs are Fr_h = 0.77 and 0.86 (Figure 5.7). Due to this being a relatively ‘deep’ finite water depth, these Fr_h correspond to relatively high length Froude numbers (Fr_L ~0.58 and 0.65), refer Figure 5.8. A closer investigation of the results for these two speeds at this value of h/L is provided in Figure 5.9, where the non-dimensionalised wave height (H/L) (which relate to γ_A) is plotted as a function of non-dimensionalised lateral distance (y/L), similar to the example provided in Figure 5.5. The value of γ_A at Fr_h = 0.77 and h/L = 0.56 is high at 37.1, but the result is very different at the next highest Fr_h = 0.86 where γ_A is less than a third of this value at just 11.5 (the values of γ_A are the constants in the power equations displayed).

In Figure 5.9 it can be seen that at $Fr_h = 0.77$ the data points 'oscillate' about the curve of best fit of power form (Equation 2.3), whereas at $Fr_h = 0.86$, the data points fall very much in line with the power curve. The reason for the oscillations at the slower of the two speeds is that there are multiple wave crests occurring within the lateral distance covered by the array of wave probes (as discussed in Section 2.1.7), thus the wave elevation will fluctuate when transiting from one wave crest to the next as lateral distance increases. At the higher speed, where the wave angle has increased enough that all probes observe the same single leading wave crest, there is a gradual decrease in the height of this sole wave with increasing y.

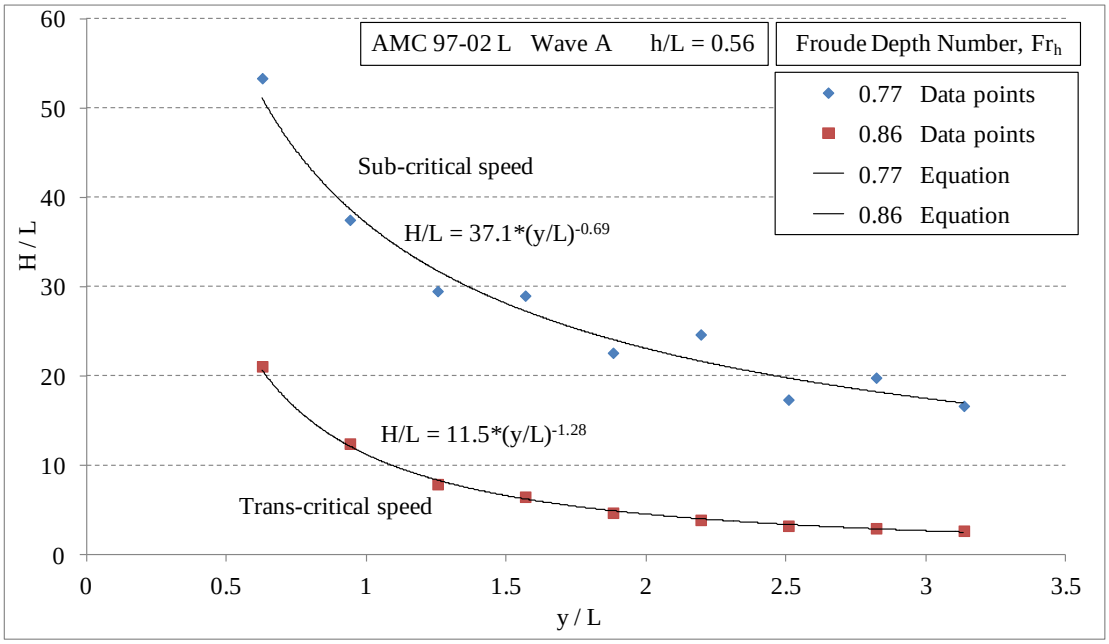

Figure 5.9 H/L as a function of y/L: Wave A, h/L = 0.56

An "aerial view" of the crests of the leading waves is shown in Figure 5.10 using model scale experimental data for the abovementioned two runs at $Fr_h = 0.77$ and $Fr_h = 0.86$. This figure is similar to the example provided in Figure 2.7. At $Fr_h = 0.77$, there are clearly several wave crests. For example, the first crest (about 1.8 m downstream) extends laterally between the wave probes at y = 1.5 to 2.5 m. Several other wave crests occur further downstream. These results confirm that the cause of the oscillations seen in Figure 5.9 are due to the presence of multiple wave crests within the lateral distance covered by the array of wave probes.

Although the Fr_h is very similar between the two examples shown in Figure 2.7 ($Fr_h = 0.78$) and Figure 5.10 ($Fr_h = 0.77$), it should be noted that the number, angle and

lengths of the wave crests vary, which is to be expected as the h/L (and Fr_L) vary between these two examples.

As expected, only a single long wave crest is present at the higher speed of Fr_h = 0.86 (Figure 5.10). This accounts for the good fit between the data points and the power curve of best fit shown in Figure 5.9.

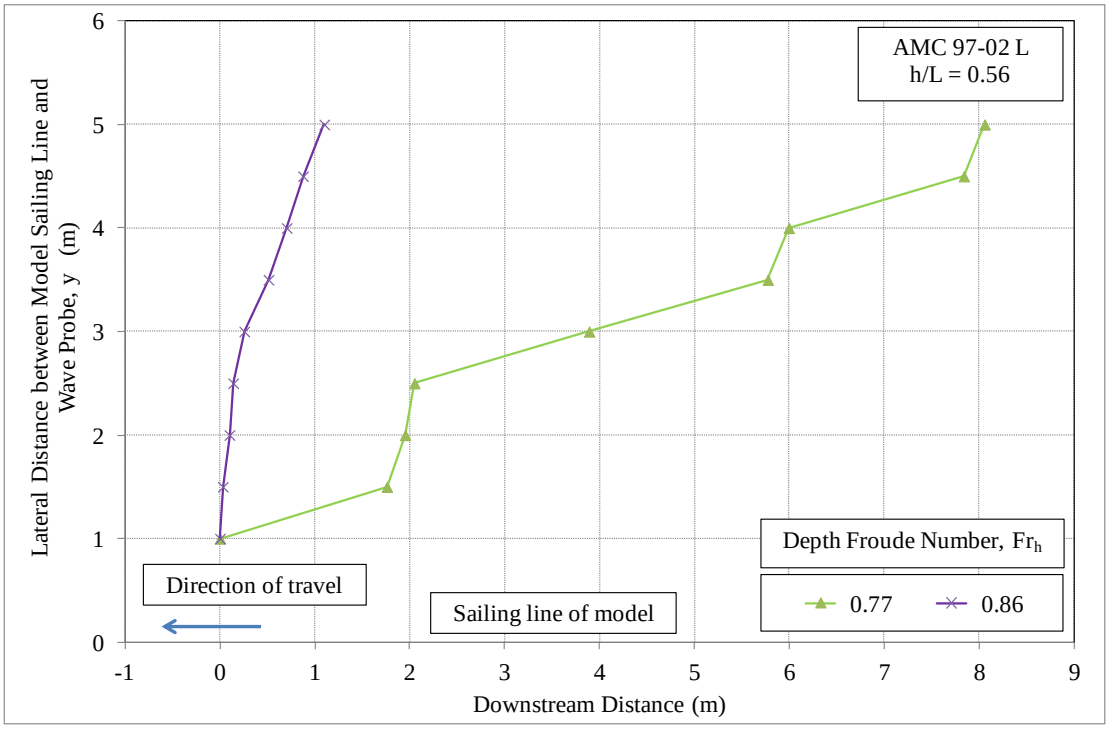

Figure 5.10 Crest angles of Wave A, y as a function of downstream distance

There is a similar situation in the second example which involves the shallowest finite water case, h/L = 0.19, but in this instance the apparent onset of trans-critical speeds occurs at the relatively low Fr_L (~0.32 to 0.39), refer Figure 5.8. The value of γ_A is also low at 4.3 at Fr_h = 0.75 but then increases four-fold to 17.3 by Fr_h = 0.89. There is also a further dramatic increase up to the peak value of 33.6 at the next highest speed. For this example, the values for H/L are plotted as functions of y/L for Fr_h of 0.75 and 0.89 in Figure 5.11. The data points for the slower speed still oscillate about the power curve of best fit, however these oscillations are not as obvious due to the relatively low values. At the next highest speed, where it was possible to identify a single wave crest across all wave probes, the data points fell very much in line with the power curve.

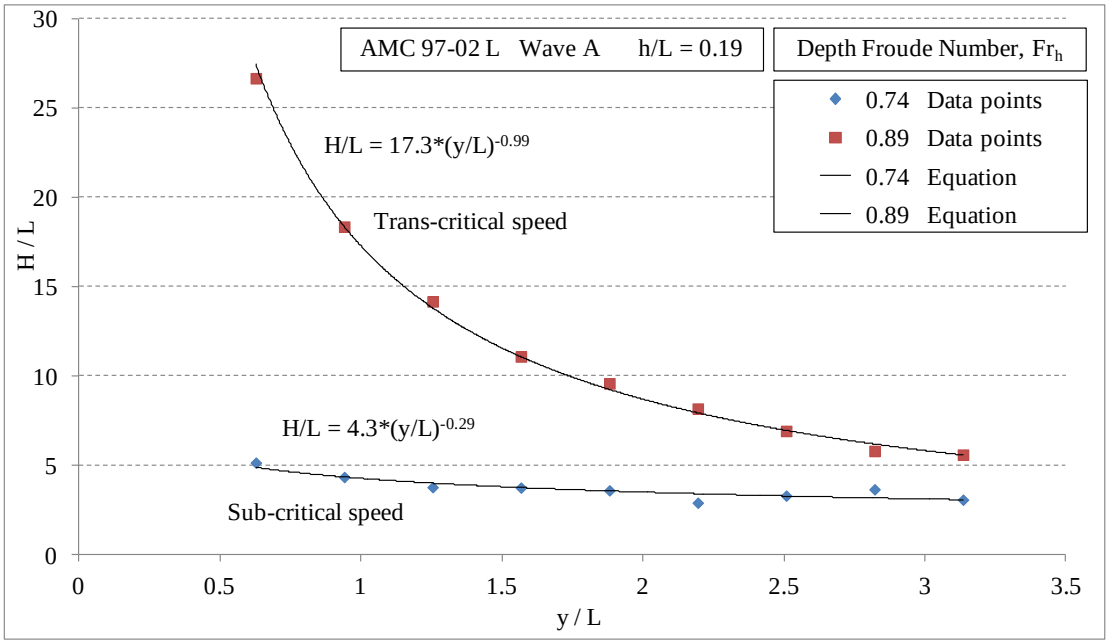

Figure 5.11 H/L as a function of y/L: Wave A, h/L = 0.19

For almost all cases within the present study (including all 19 different ship models), the slowest speed where it was possible to clearly identify this single leading wave crest across all lateral wave probes occurred between $0.8 < Fr_h < 0.9$. There were only a few instances where this was not the case, on each occasion it involved a ship model that possessed a very low $L/\nabla^{1/3}$ ratio. It is believed that this was because these models generated much higher waves, making it an easier task to identify this wave, particularly at the wave probes furthest away where the wave height will have decayed the most.

The discussion above describes some of the observations around the onset of trans-critical speeds, including changes in wave angle and the number of wave crests involved, however it does not explain why there were such notable changes in γ_A at these specific speeds. As will be outlined later in this sub-section, not only are there significant changes in wave angle occurring, but also in wave period and the decay rate, all of which are interrelated. It has been observed that the height of the leading trans-critical wave is generally relatively high close to the ship model but decays very rapidly with increasing y, hence resulting in relatively large values of wave decay exponent, as can be seen in the examples presented in Figures 5.9 and 5.11.

In Figure 5.9 (where h/L = 0.56), the value for γ_A observed at the slower (sub-critical) speed ($Fr_h = 0.77$) was high ($\gamma_A = 37.1$), but then decreased rapidly at the next highest (trans-critical) speed of $Fr_h = 0.86$ ($\gamma_A = 11.5$). It is noted that at this water depth, Fr_h

= 0.77 corresponds to a relatively high length Froude number (close to $Fr_L = 0.75$), such that γ_A is at or close to its peak when the transition into trans-critical speeds occurs, as is evident in Figure 5.8 (by comparing against the results for the deep water case, h/L = 1.38).

From Figure 5.8, where γ_A can be compared for all four h/L cases at corresponding Fr_L, it can be seen that the maximum γ_A is almost always generated in the deep water case (h/L = 1.38). The only exception is at the shallowest finite water case (h/L = 0.19) where γ_A is notably greater than the deep water case in the range of $0.35 < Fr_L < 0.52$.

Wave B – the wave height constant for Wave B, γ_B, is shown as a function of Fr_h in Figure 5.12 and as a function of Fr_L in Figure 5.13. As for Wave A, all four h/L cases are plotted in these figures.

There are some similarities between γ_A and γ_B, in that water depth has influenced the results, but to a much lesser degree for γ_B. In Figure 5.13 it can be seen that the influence is almost negligible at the deepest finite water depth (h/L = 0.56) as the results are generally very similar to the deep water case (h/L = 1.38). As h/L decreases, the greater the effect that water depth appears to have on γ_B. There is clearly a significant change in γ_B at the shallowest depth (h/L = 0.19), particularly at trans-critical Fr_h where γ_B is greater than the deep water case at corresponding Fr_L. The results for speeds above $Fr_L = 0.65$ at all four water depths converge (towards a value of approximately 35) as Fr_L increases.

Wave C – the wave height constant for Wave C, γ_C, is shown as a function of Fr_h in Figure 5.14 and as a function of Fr_L in Figure 5.15.

It is clear from Figure 5.15 that water depth has an almost negligible effect on this wave as the results for all finite water depths are very similar to the deep water case (h/L = 1.38) over the entire range of speeds investigated.

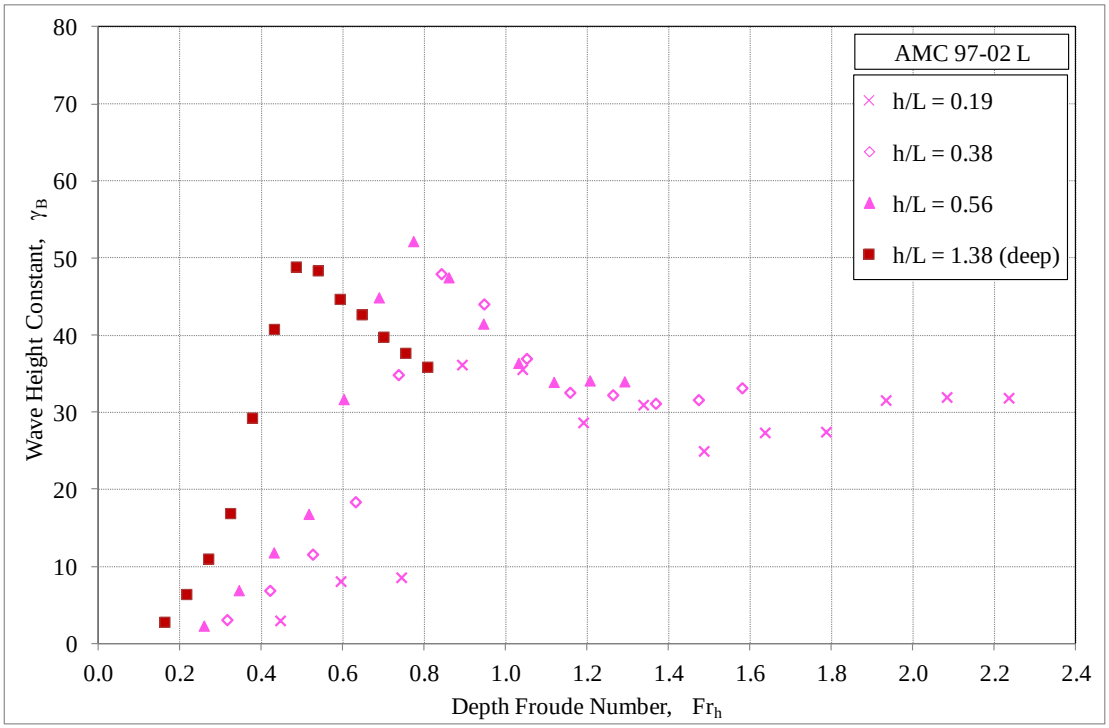

Figure 5.12 Wave height constant for Wave B, γ_B, as a function of Fr_h

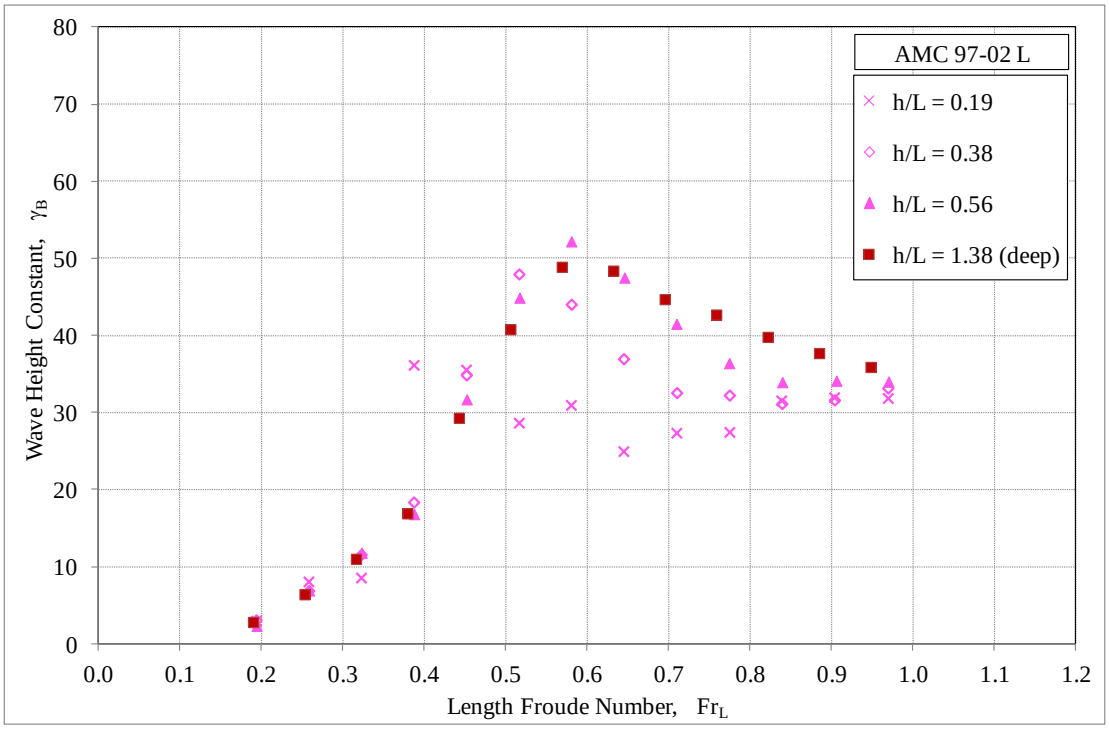

Figure 5.13 Wave height constant for Wave B, γ_B, as a function of Fr_L

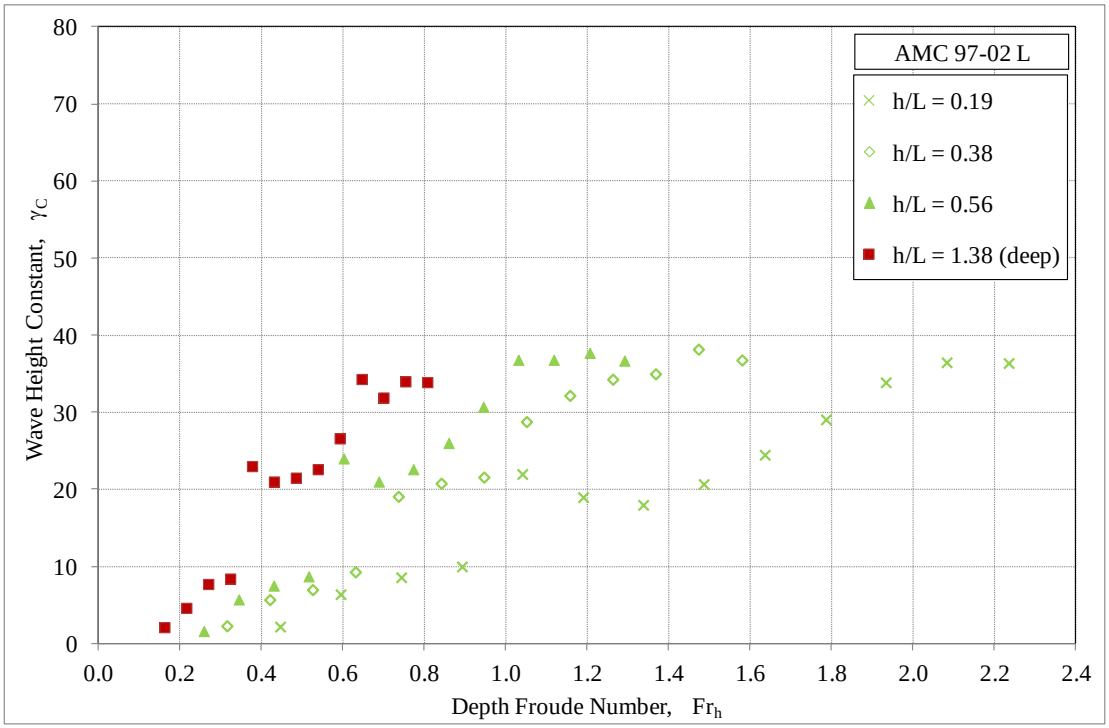

Figure 5.14 Wave height constant for Wave C, γ_C, as a function of Fr_h

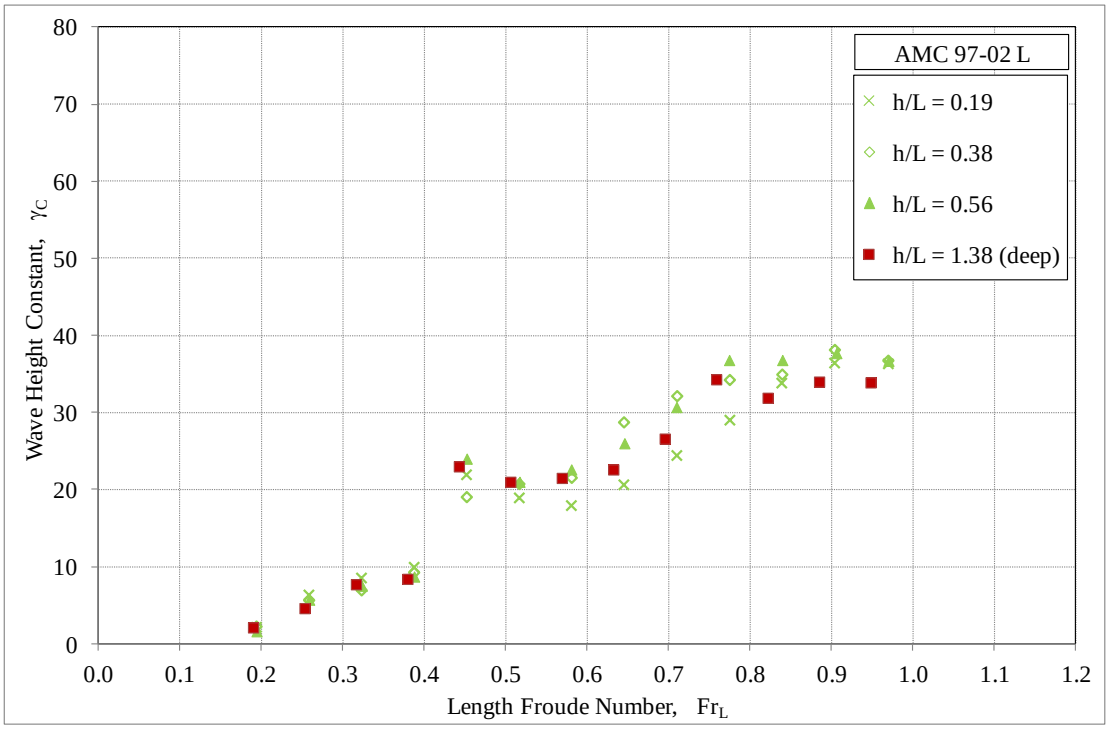

Figure 5.15 Wave height constant for Wave C, γ_C, as a function of Fr_L

Summary for Wave Constant,γ (Waves A, B and C) – The wave height constant for Wave A is clearly affected by water depth to a significant degree, whereas depth appears to have a lesser effect on Wave B and almost negligible effect on Wave C.

Of the three waves, it is Wave B that possesses the highest peak values for γ (found from comparing Figures 5.8, 5.13 and 5.15). These occur at the deeper water depths and at around Fr_L of 0.6. In general, it was the deep water case that had the greatest (or equal greatest) values for γ at all length Fr investigated. There were only a few exceptions to this, which occurred at trans-critical speeds for the shallowest case, h/L = 0.19, where γ for Wave A (see Figure 5.8) and Wave B (see Figure 5.13) notably exceeded those for the deep water case (around $Fr_L = 0.4$). This finding is noteworthy as operating in such conditions would likely generate very damaging waves.

5.5.2 Normalised Wave Period, T'

Wave A – the normalised wave period for Wave A, T_A', is shown as a function of Fr_h in Figure 5.16 and as a function of Fr_L in Figure 5.17. In Figure 5.16 it can be seen that wave period for the deep water case (h/L = 1.38) gradually increases with increasing Fr_h, right up to the maximum speed available (approximately $Fr_h = 0.78$). For the three finite water depth cases wave period rapidly increases to a peak with the onset of trans-critical speeds (around $0.75 < Fr_h < 0.85$), then the period gradually decreases as Fr_h is further increased. It is clear from this figure that the curves for all three finite water depths are effectively the same for all speeds within both the trans-critical and super-critical zones (from about $Fr_h = 0.75$ and greater).

By referring to Figure 5.17, where T_A' is plotted as a function of Fr_L, it can be seen that each of the finite water depth curves closely match that of the deep water case (h/L = 1.38) for all sub-critical speeds up until a depth Froude number of about 0.75 (the onset of trans-critical speed). This point is different for each of the three finite water cases, so to aid discussion, the point at which $Fr_h = 0.75$ has been indicated in this figure for each finite water depth case (by the dashed vertical lines).

Very similar results to those described above were found for all nineteen of the ship models tested (as listed in Table 5.1), not just in the form of the curves but the values of the peak around $Fr_h = 0.9$ were similar in all cases (this is discussed in more detail in Chapter 6).

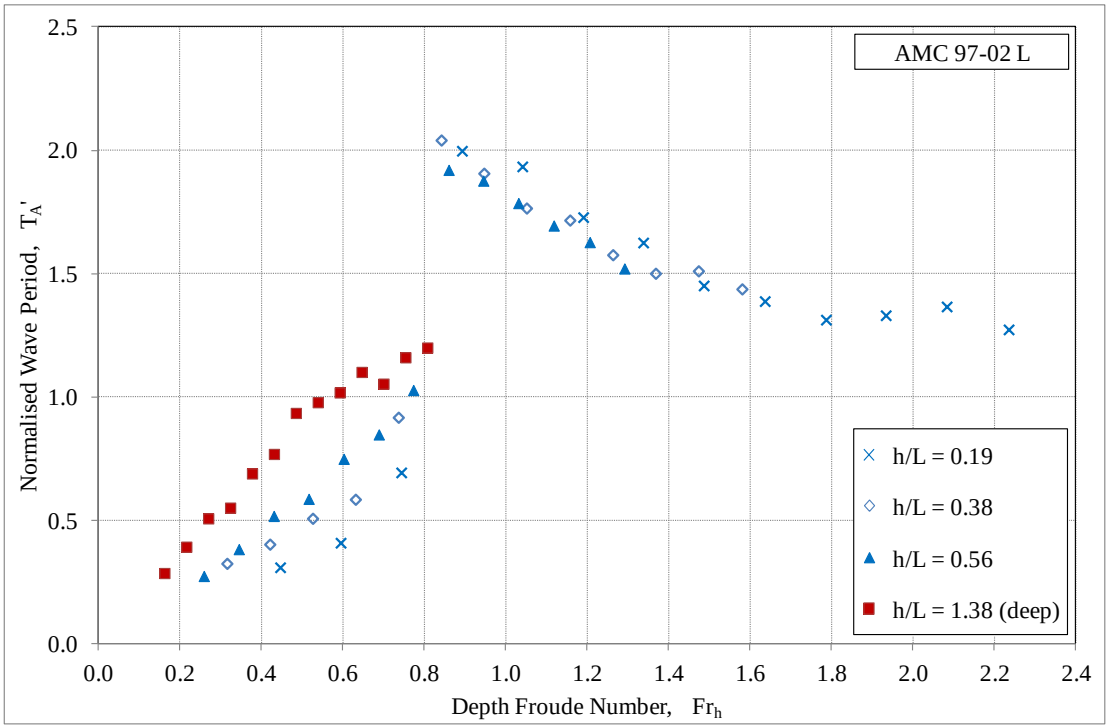

Figure 5.16 Normalised wave period for Wave A, T_A', as a function of Fr_h

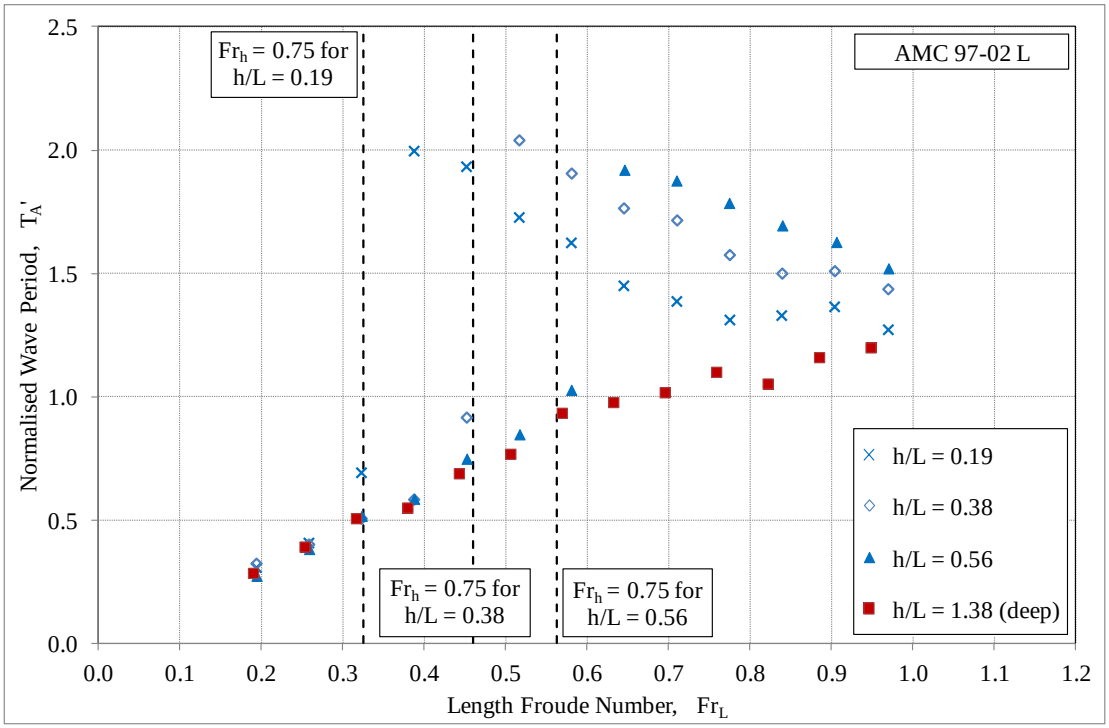

Figure 5.17 Normalised wave period for Wave A, T_A', as a function of Fr_L

From these results it can be concluded that the period of the leading wave, T_A', is very significantly altered by finite water depth and that there is a rapid increase in wave period in the trans-critical zone. This increase in period is associated with the rapid increase in wave angle within the trans-critical zone as discussed in Section 2.1.7. It can also be concluded that, for all trans-critical and supercritical speeds, for a given Fr_h the period of this wave will be the same for any combination of vessel speed and water depth. As expected, the results for all the finite water cases at sub-critical speeds closely match the deep water case.

Wave B – the normalised wave period for Wave B, T_B' is shown as a function of Fr_h in Figure 5.18 and as a function of Fr_L in Figure 5.19. As for Wave A, there is a relationship between T_B' and Fr_L for all sub-critical speeds as the curves all correspond to the deep water case within this speed range (refer Figure 5.19). T_B' is notably greater at trans-critical speeds for all the finite water depth cases than for the deep water case.

For the deep water case, T_B' rises sharply up to Fr_L around 0.45, after which it very gradually rises until Fr_L of 0.7, beyond which T_B' is effectively constant. In contrast, at the higher Fr_L the periods for each of the three finite water cases (at super-critical speeds) appear to gradually reduce from their peaks that occurred within their respective trans-critical speed zones. The curves for each of the finite water depths (h/L= 0.19, 0.38 and 0.56) have all converged with the deep water curve (refer Figure 5.19).

Wave C – the normalised wave period for Wave C, T_C' is shown as a function of Fr_h in Figure 5.20 and as a function of Fr_L in Figure 5.21. As was the case for the wave height constant, γ_C, water depth does not have any notable effect on the period of Wave C, as is evident in Figure 5.21, where all four curves are relatively similar.

Summary for Wave Period, T *(Waves A, B and C)* – The wave period for the leading wave, Wave A, is clearly affected by water depth to a significant degree, whereas water depth has little or no effect on Wave C, because of its shorter wavelength. The period of all three waves are unaffected by water depth at all sub-critical speeds (Fr_h < 0.75).

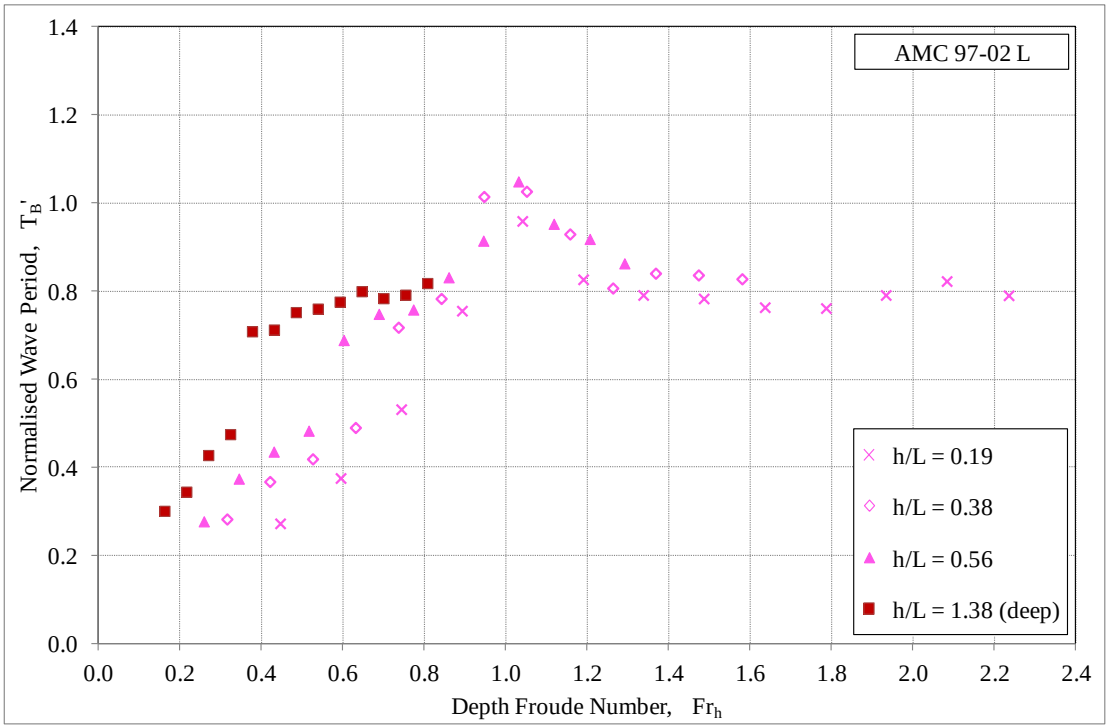

Figure 5.18 Normalised wave period for Wave B, T_B', as a function of Fr_h

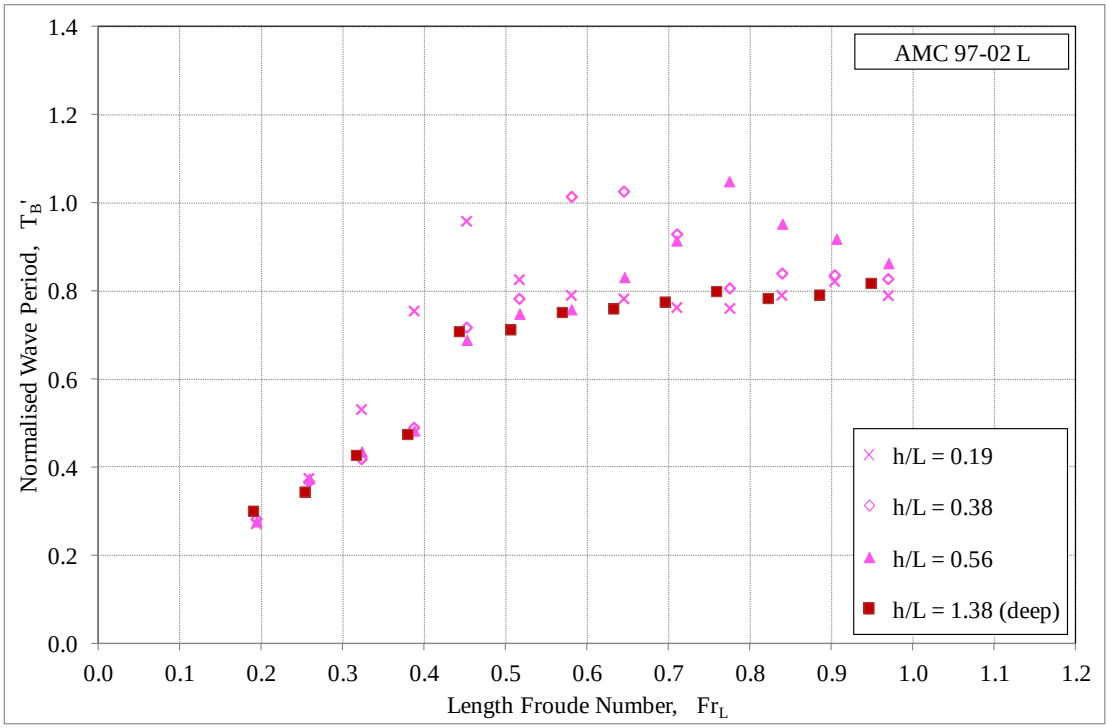

Figure 5.19 Normalised wave period for Wave B, T_B', as a function of Fr_L

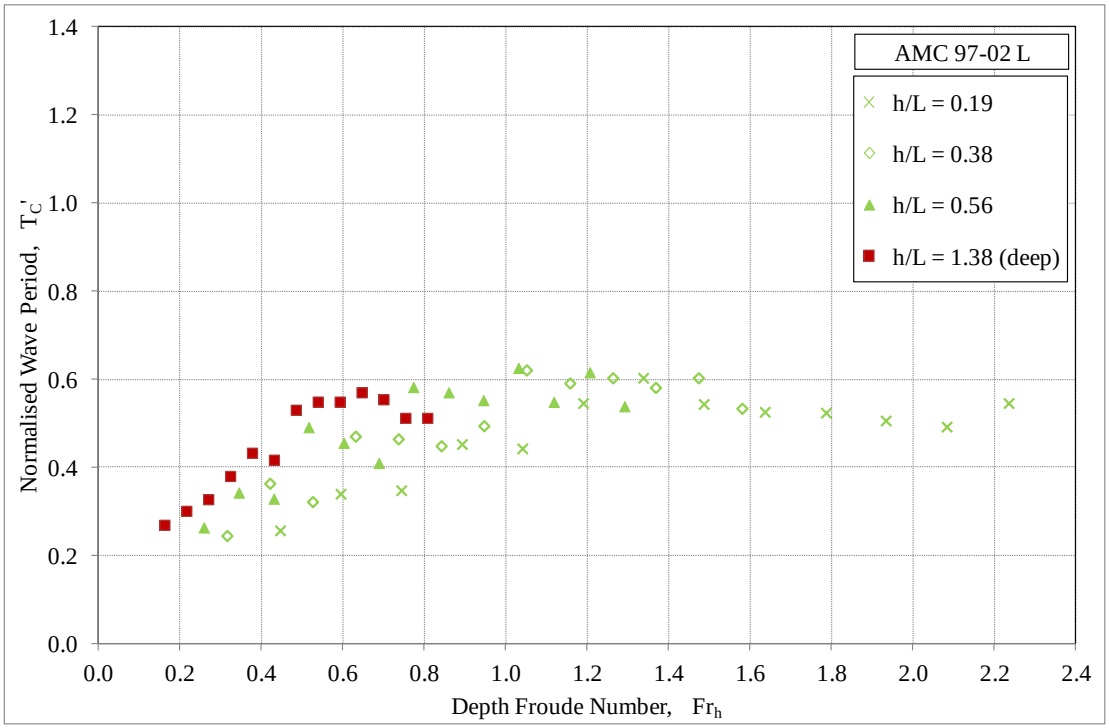

Figure 5.20 Normalised wave period for Wave C, T_C', as a function of Fr_h

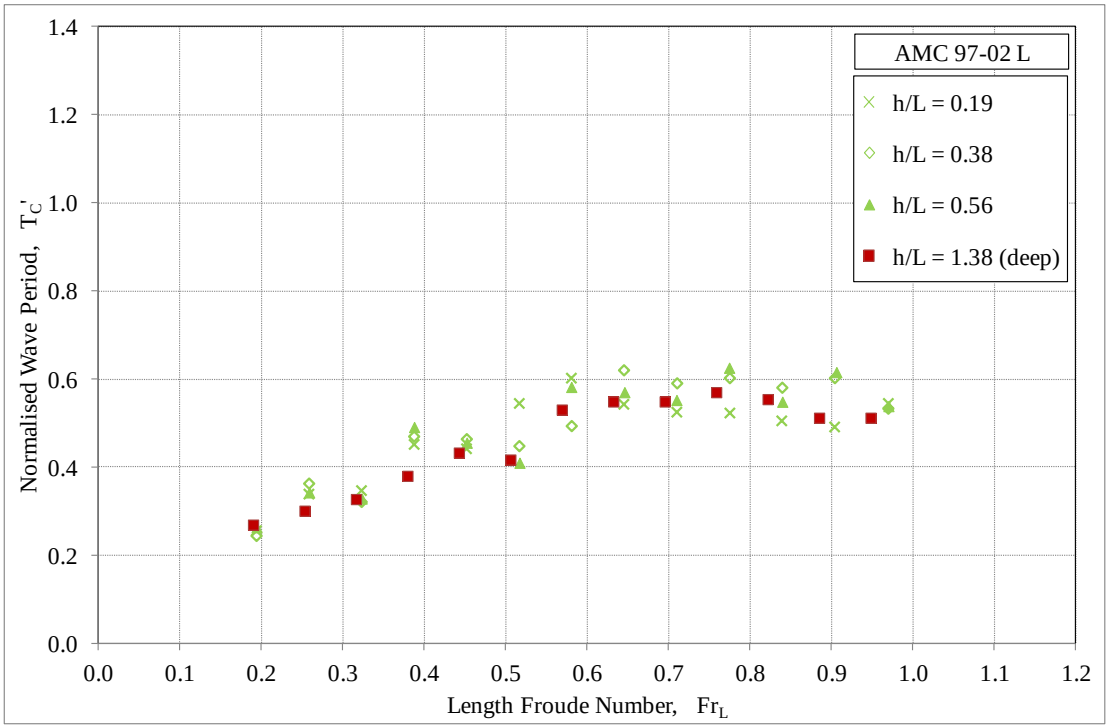

Figure 5.21 Normalised wave period for Wave C, T_C', as a function of Fr_L

The period of Wave A, T_A', rapidly increases with an increase in speed within the trans-critical zone. At supercritical speeds, the period of this wave will be approximately the same for any combination of vessel speed and water depth (Fr_h).

For Wave B, it was found that periods for all the finite water depth cases within the trans-critical speeds exceed the deep water values, which causes an increased likelihood of generating damaging waves in such conditions. In addition, at super-critical speeds T_B' converges towards the relatively constant values found at high speed in deep water.

As Wave A is defined as being the longest wave, it will always possess the longest wave periods, followed by Waves B and C (refer to the definitions provided in Section 3.3). But, the degree of difference is significant, with maximum values of T' for Wave A (~2.0) typically being approximately double that of Wave B (~1.0). The maximum for Wave C was approximately 0.64. As previously discussed, the period is of utmost importance when considering waves generated within sheltered waterways that possess sensitive shorelines, so it is extremely useful to quantify and understand the vast differences between these three waves.

5.5.3 Wave Decay Rate, n

Wave A – the wave decay rate for Wave A, n_A, is shown as a function of Fr_h in Figure 5.22 and as a function of Fr_L in Figure 5.23. The first observation is that water depth clearly has a major influence on the decay rate of Wave A, particularly for trans-critical speeds where there are very high decay rates (approximately -1.3). Such values indicate a very rapid decay in height as the wave propagates away from the ship model, as seen in the example in Figure 5.5.

As expected, wave decay rates for all sub-critical speeds (up to approximately Fr_h = 0.7) fall within the range of -0.2 to -0.45, as previously found by Cox (2000) and Macfarlane (2002). There does not appear to be any clear trends between each of the four water depth cases at super-critical speeds. This topic is investigated further in Chapter 6 where the results for all 19 ship models are compared.

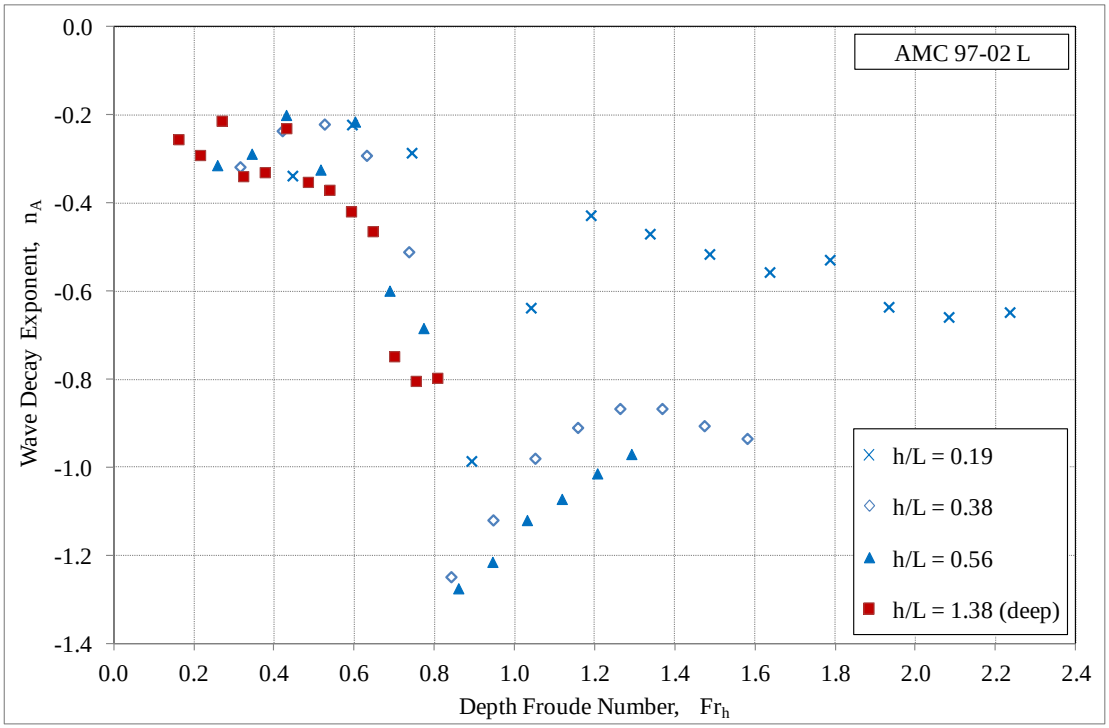

Figure 5.22 Wave decay exponent for Wave A, n_A, as a function of Fr_h

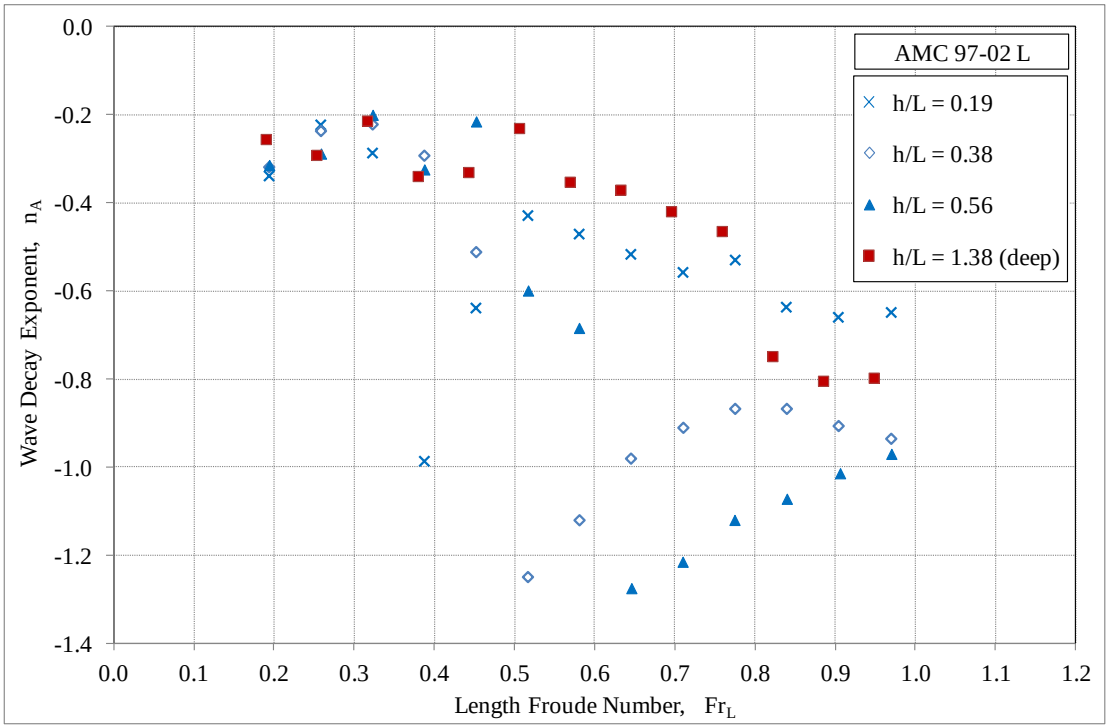

Figure 5.23 Wave decay exponent for Wave A, n_A, as a function of Fr_L

Wave B – the wave decay rate for Wave B, n_B, is shown as a function of Fr_h in Figure 5.24 and as a function of Fr_L in Figure 5.25. The significant drop in wave decay rate found for Wave A around trans-critical speeds are generally not observed for Wave B, although a minor drop is present for the shallowest finite water depth (h/L = 0.19). As was found for the decay rate of Wave A, n_A, there are no clear trends between each of the four water depth cases at super-critical speeds. However, there is generally an increase in the decay rate for Wave B as speed is increased above Fr_L = 0.6.

Wave C – the wave decay rate for Wave C, n_C, is shown as a function of Fr_h in Figure 5.26 and as a function of Fr_L in Figure 5.27. For this wave, there appears to be no notable variation that can be attributed to water depth. As can be seen in Figure 5.27, there is a relatively small range of wave decay rates and these correspond relatively closely to the range found for sub-critical speeds by Macfarlane (2002).

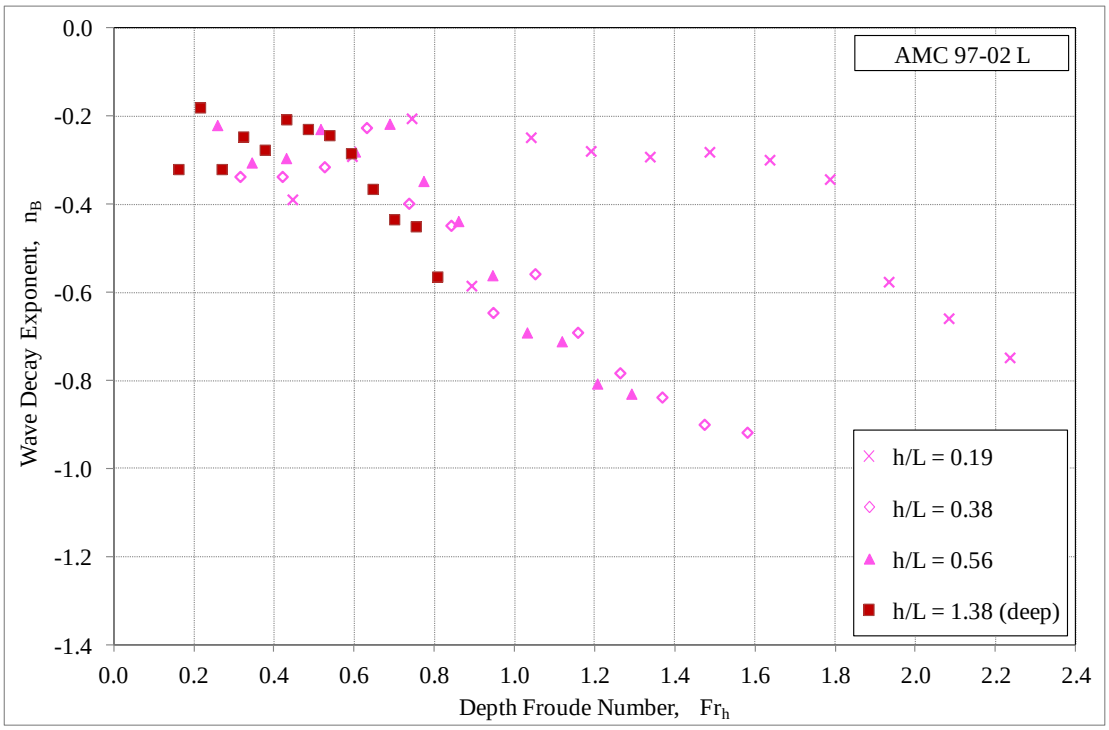

Figure 5.24 Wave decay exponent for Wave B, n_B, as a function of Fr_h

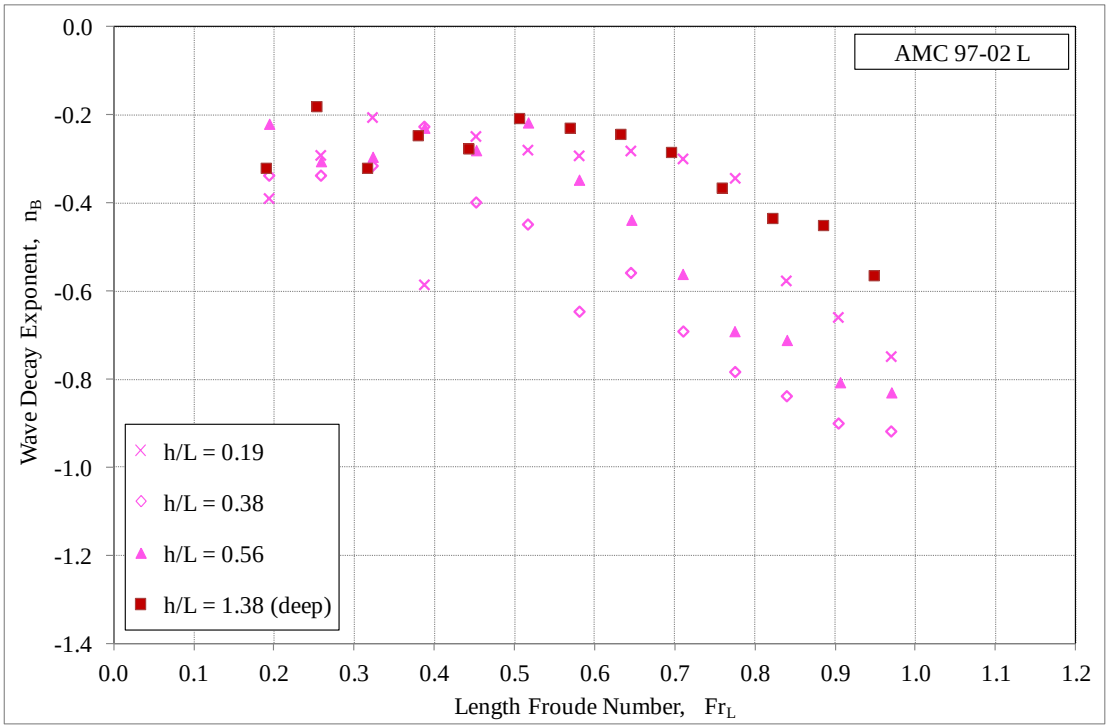

Figure 5.25 Wave decay exponent for Wave B, n_B, as a function of Fr_L

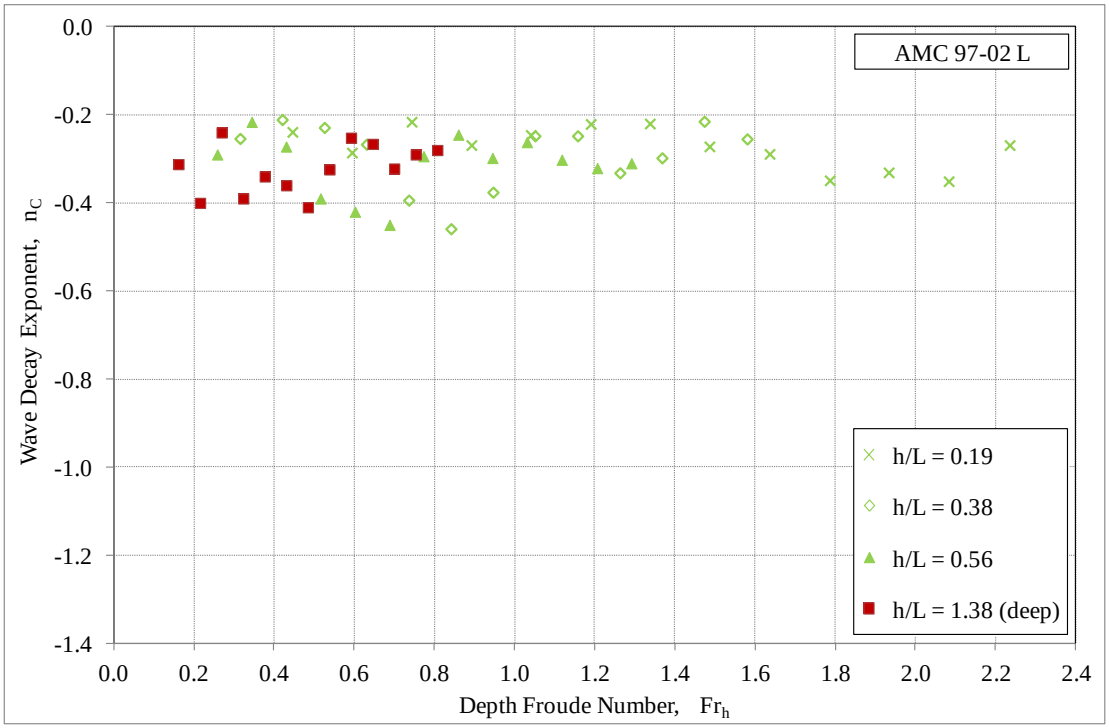

Figure 5.26 Wave decay exponent for Wave C, n_C, as a function of Fr_h

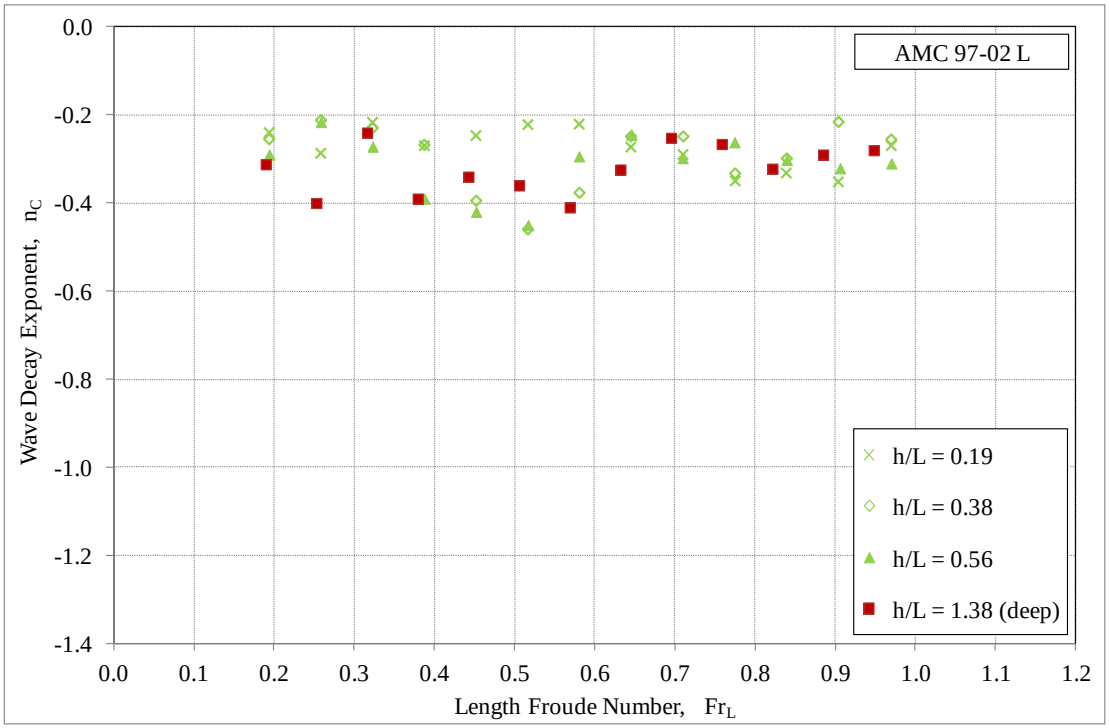

Figure 5.27 Wave decay exponent for Wave C, n_C, as a function of Fr_L

Summary for Wave Decay, n *(Waves A, B and C)* – Water depth has a major influence on the decay rate of Waves A and B which generally results in an increased rate of decay, at both trans-critical and super-critical speeds. This concurs with the work of Doctors and Day (2001) and Robbins *et al*. (2007).

This also supports previous work investigating wave decay rates at sub-critical speeds by the author (Macfarlane 2002). The focus of the previous study was solely on the wave with the maximum height at sub-critical speeds, which corresponds with Wave B for the above example in the present study.

There is very little published data on the decay rate of the leading waves at super-critical speeds, particularly when it comes to measured values beyond the medium field. Doyle (2001) conducted wave wake experiments in a wide shallow basin using models of similar size to the present study, but in Doyle's case the model was towed very close to one side of the basin to allow wave measurements at much greater lateral distances.

To investigate if this increased lateral distance has an influence on the wave decay of the leading wave beyond the medium field, a comparison against some of Doyle's data is provided in Figure 5.28. In this figure, the non-dimensional wave height

values (H/L) are plotted as functions of non-dimensional lateral distance (y/L) for the catamaran model from the present study that provided the closest match in $L/\nabla^{1/3}$ to Doyle's data (also a catamaran). The values for h/L and Fr_h are similar for each case (as documented in Figure 5.28). There is a range of y/L where data exists for both Doyle's and the present study ($0.5 < y/L < 2.8$) and the H/L values compare well in this range.

The super-critical waves from the present study decay at a very similar rate to those of Doyle, noting that the decay exponent is calculated (using Equation 2.3) over quite different lateral distances (up to 2.8 ship lengths for the present study, compared to 5.5 ship lengths in the case of Doyle). This indicates that the decay rates determined from the present study may also be applicable over a lateral distance greater than 2.8L, however, it is recommended that care be taken in making this assumption as further work is required to confirm if this is generally the case.

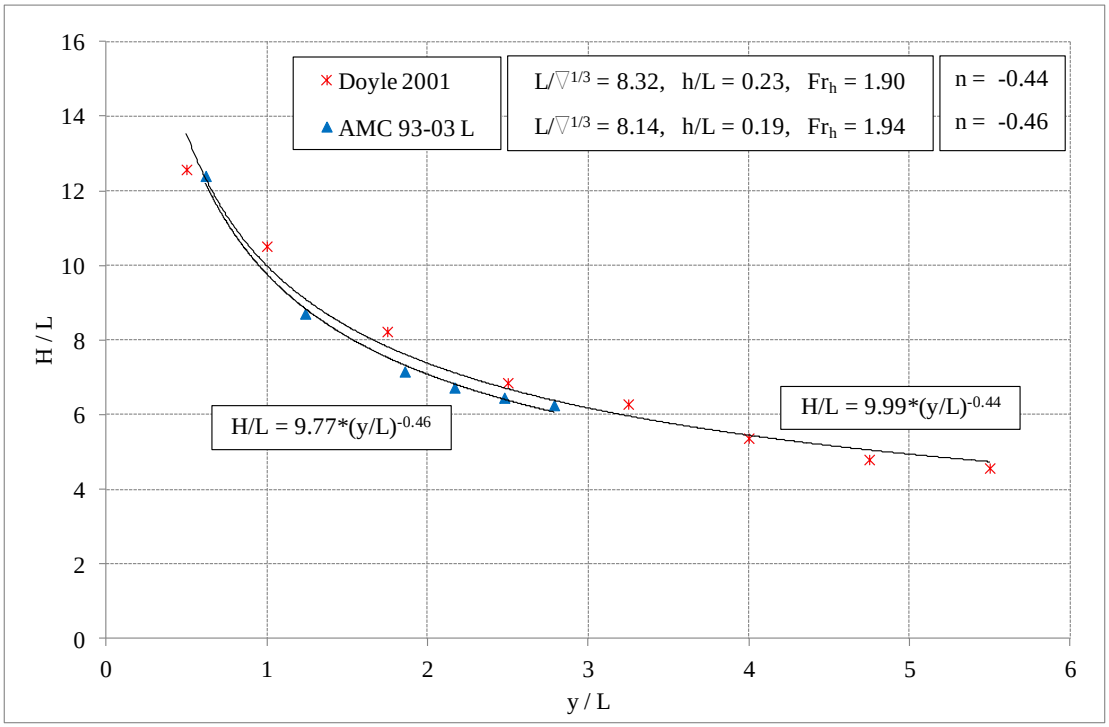

Figure 5.28 H/L as a function of y/L: Wave A, comparison with Doyle (2001)

5.5.4 Wave Angle, θ

Wave A – the wave angle for Wave A, θ_A, is shown as a function of Fr_h in Figure 5.29 and as a function of Fr_L in Figure 5.30. It is very clear in Figure 5.29 that the curves

for all four water depth cases are similar and that the form of the curves are in agreement with that originally proposed by Havelock (1908), as shown in Figure 2.4. As expected, the wave angle for sub-critical speeds (up to approximately $Fr_h = 0.75$) for all h/L cases is close to the theoretical value of $19^o28'$ as predicted by Thomson (1887). The characteristic rapid rise in angle within the trans-critical zone, followed by the gradual decrease within the super-critical zone, is clearly evident. Similar results have been found for the leading wave by other authors, such as Weggel and Sorensen (1986) and Robbins *et al*. (2009).

Wave B – the wave angle for Wave B, θ_B, is shown as a function of Fr_h in Figure 5.31 and as a function of Fr_L in Figure 5.32. The effect of water depth on θ_B is notably less than that found for θ_A. It is evident that the effect of depth clearly reduces as h/L increases, particularly around the critical speed.

Wave C – the wave angle for Wave C, θ_C, is shown as a function of Fr_h in Figure 5.33 and as a function of Fr_L in Figure 5.34. As was the case with the wave period and wave height constant, water depth does not appear to have any notable effect on the angle of Wave C, as is evident in Figure 5.34, where all four curves are very similar.

Summary for Wave Angle, θ (Waves A, B and C) – As expected, water depth has a major influence on the angle of Wave A, seen as a rapid increase within the trans-critical speed range. The results presented here closely match those from previous studies of the leading wave. This concurs with the results for wave period of Wave A, where there was also a rapid increase with the onset of trans-critical speeds (refer Figures 5.16 and 5.17). The angle of Wave C was found to be unaffected by water depth, whereas Wave B was affected, particularly close to critical speed, but to a much lesser degree than found for Wave A.

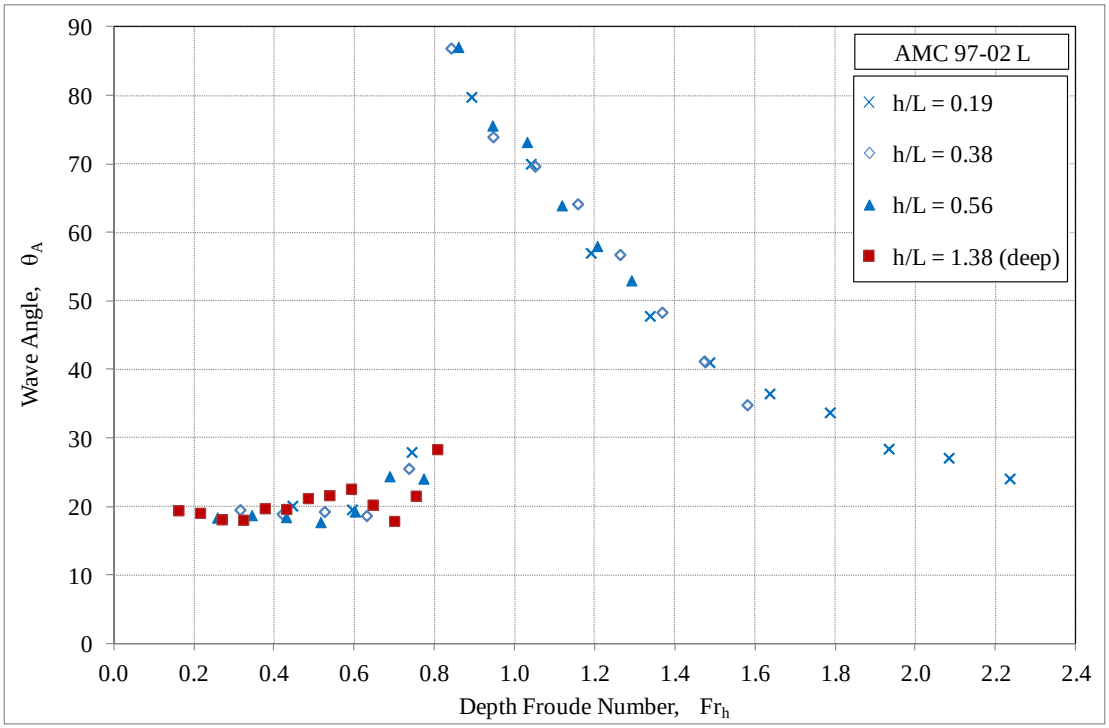

Figure 5.29 Wave angle for Wave A, θ_A, as a function of Fr_h

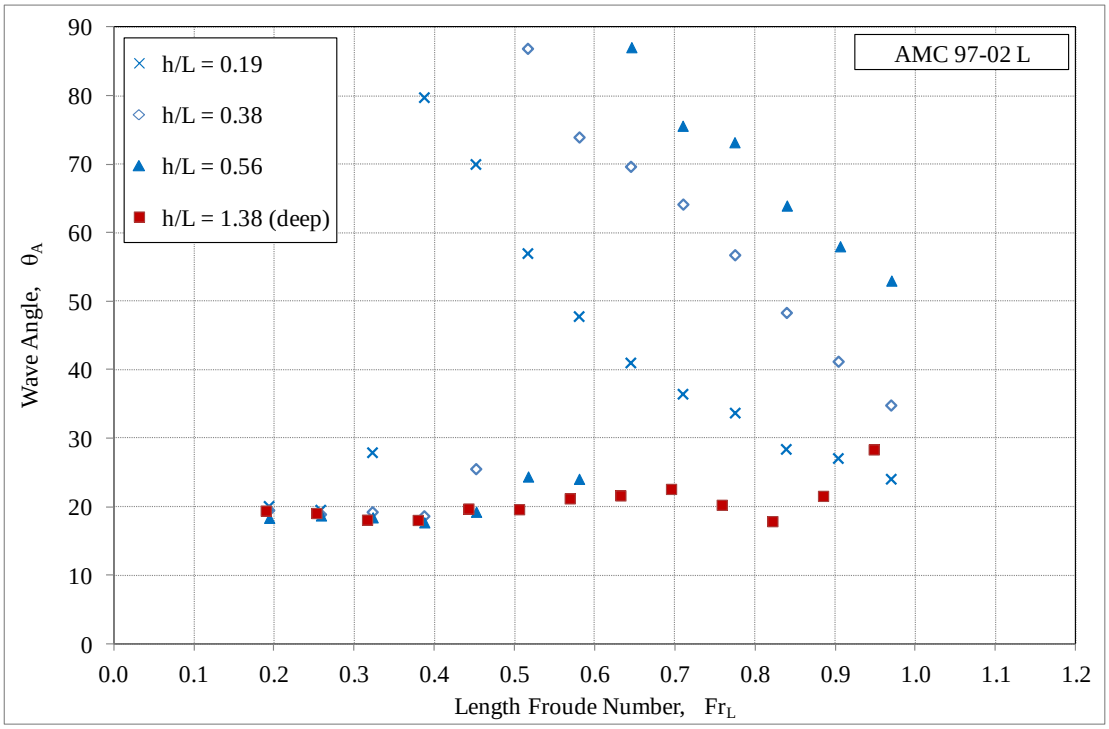

Figure 5.30 Wave angle for Wave A, θ_A, as a function of Fr_L

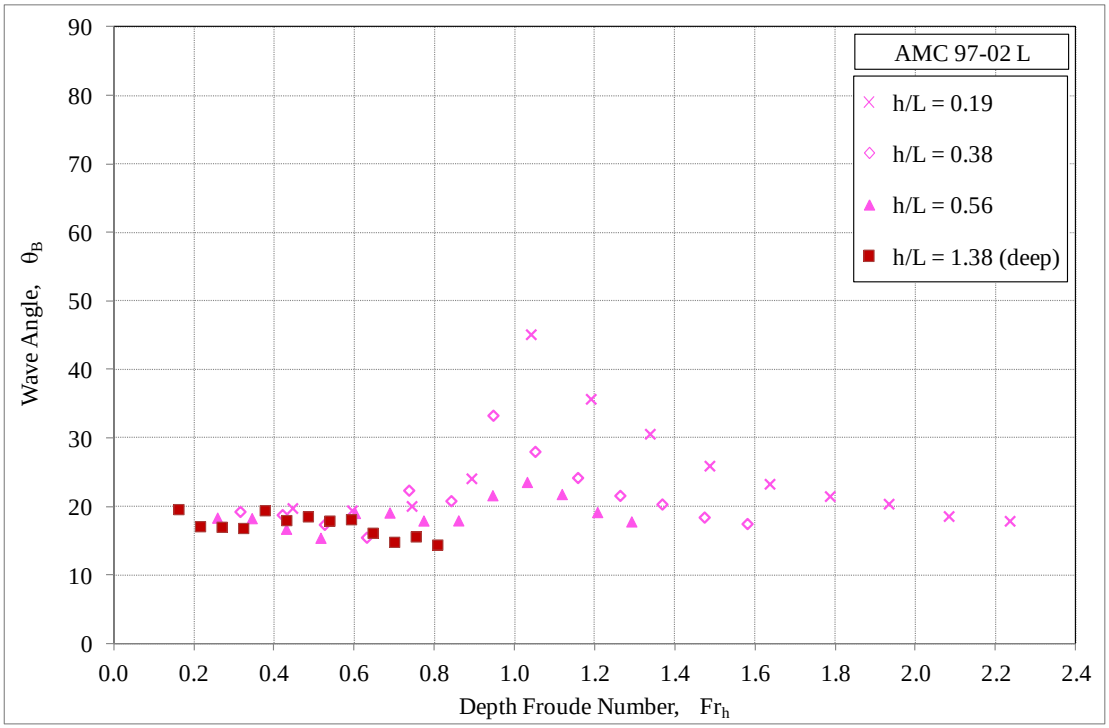

Figure 5.31 Wave angle for Wave B, θ_B, as a function of Fr_h

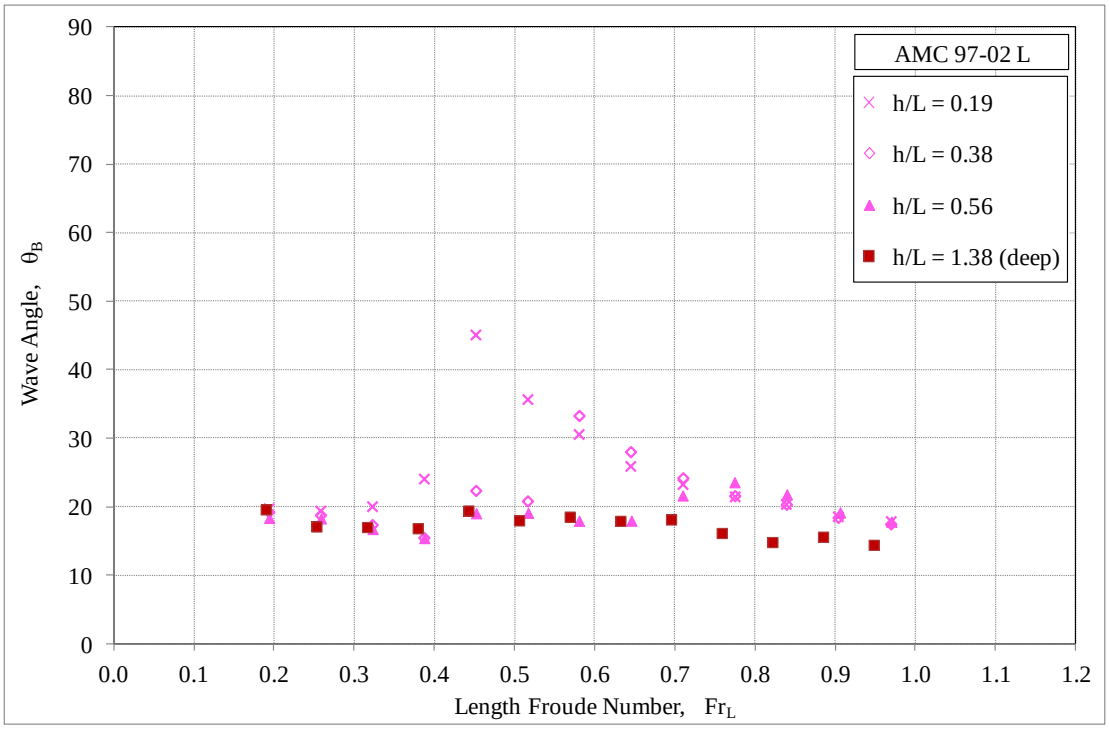

Figure 5.32 Wave angle for Wave B, θ_B, as a function of Fr_L

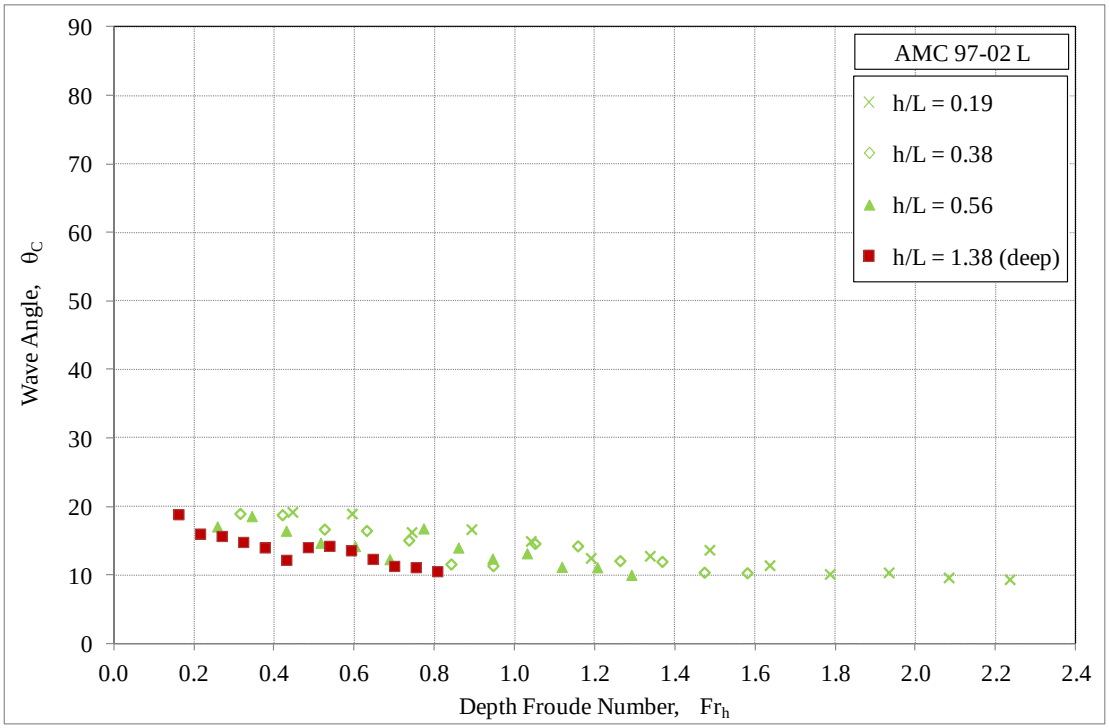

Figure 5.33 Wave angle for Wave C, θ_C, as a function of Fr_h

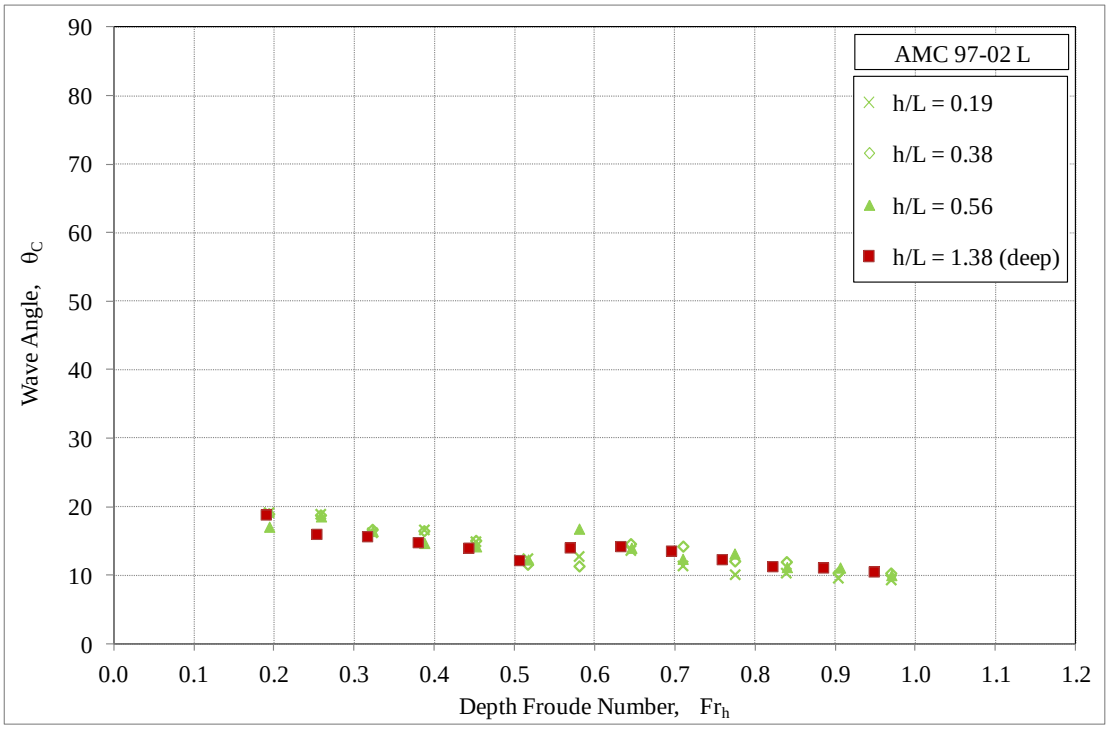

Figure 5.34 Wave angle for Wave C, θ_C, as a function of Fr_L

Chapter 6

Wave Wake Prediction Tool

6.1 Introduction

This chapter outlines the development of a tool for predicting the relevant wave wake characteristics generated by a wide range of recreational and small commercial vessels operating at sub-critical, trans-critical and super-critical speeds.

One of the key factors in the development of a successful predictive tool is the selection of appropriate input parameters (or independent variables), and to only include those parameters that have a significant influence on the predicted result (Couser *et al*. 2004).

In the previous chapter details were provided of a comprehensive series of scale model experiments to investigate vessel wave wake, where the results were presented and discussed to investigate the effect of vessel speed and water depth (where the results for just a single hull form were presented). As outlined in Section 1.2, an aim of the present study was to investigate and discuss the effect of vessel hull form, particularly for operation at trans-critical and super-critical speeds (i.e. finite water depths). The experimental test program obtained a similar data set for a total of 19 different hull forms: 11 of which were monohulls and 8 catamarans, each covering a wide range of slenderness ratios. Results for one of these hull forms were presented and discussed in Section 5.5.

The next task was to develop a method to accurately and effectively compare the results from all 19 hull forms, taking into consideration the variation in model size (refer Table 5.1). It was desired that the chosen method be capable of identifying significant trends between hull form and water depth, and to also be able to provide accurate predictions for a specific type and size of vessel operating at a specified speed(s) and water depth(s). Determination of the wave decay rate makes it also possible to predict wave characteristics at any lateral distance from the vessel sailing line.

Several methods were considered, including: multiple regression analysis, neural networks, and a series of look-up tables. For statistical regression methods to provide

acceptable results an appropriate non-linear function must first be found, StatSoft (1994). The use of multiple regression analysis was ruled out after encountering difficulties establishing a relationship between dependent and independent parameters, particularly when faced with highly non-linear relationships, occasionally including discontinuities, between Froude number (both length and depth) and wave period, wave decay rate and wave angle. Examples of where such nonlinearities occurred can be seen in Figures 5.16 (period), 5.22 (decay) and 5.29 (angle). In such cases, an attempt was made to describe the data using two or more formulae, however this posed further issues as the point at which the discontinuities occur vary between hull forms (and also water depths), resulting in a complex process to meld the regression equations for each variable into a cohesive package.

Initial investigations into the application of artificial neural networks to the comprehensive set of experimental data provided indications that a workable solution could be obtained, as one of their key advantages is their ability to model complex non-linear functions relatively quickly and accurately (Sarle 1994). Couser *et al*. (2004) used artificial neural networks to predict ship hull resistance, based upon post-processed (smoothed) tank test data. Further work by the same authors, Mason *et al*. (2005), indicate that neural networks can also be directly fitted to the raw (un-smoothed) experimental data, as it is felt that the additional smoothing step may introduce errors.

When an artificial neural network is applied to any data set, it is important to select a sufficient number of neurons to provide a good fit with respect to the independent variable. For the present study, where many highly non-linear relationships exist with respect to Froude number, this required a relatively large number of neurons, which resulted in significant over-fitting with respect to other key input parameters such as $L/\nabla^{1/3}$ and particularly h/L (where there was a maximum of only four points). In artificial neural network problems, over-fitting may result in the accurate prediction of the training data, but new input data is often poorly predicted. This was found to be the case with the data in the present study.

As part of this trial using neural networks, all the experimental data was systematically tabulated in a logical form that could be readily compiled within a single Excel Workbook. Having the data stored in this manner presented the opportunity to further the development of a predictive tool based upon a semi-automated series of look-up tables. As this would result in a tool that met the intended

goals of being able to readily investigate trends in the results and provide the desired predictions, further efforts concentrated on developing and validating this particular method. The operation of this tool is described in detail in the next sub-section.

6.2 Development of the Prediction Tool

6.2.1 Method of Operation

The predictive tool was based upon the model scale experimental data presented in the preceding chapters. Its purpose is to predict the four key variables of wave height (via the constant, γ), wave period (T), wave decay rate (n) and wave angle (θ) for each of the three waves of interest (A, B and C), as described in Section 3.3. The analysis process that was consistently applied to all experimental data has been described in Chapter 5.

The results for each of the nineteen hulls have been compiled within a single Excel Workbook, with the results of each hull contained within a separate Worksheet. Each of these Worksheets contains the principal particulars of the hull, as listed in Table 6.1. Each Worksheet contains four blocks of experimental results, one for each of the water depths investigated. Each of these blocks contains values for each of the variables listed in Table 6.2 for each of the model speeds tested (of which there were approximately 13 to 15 per water depth). Also listed for each speed (run) are the hull identification number, test condition number and the run number. Each Worksheet typically consists of 52 rows of data (for a typical case consisting of 13 model speeds and four water depths).

Primary Particular	**Symbol**	**Units**
Monohull or Catamaran		
Length (waterline)	L	metres
Beam (waterline)	B	metres
Draught (maximum)	d	metres
Half angle of entry	i_E	degrees
Displacement	Δ	tonnes

Table 6.1 Principal particulars

The input data from which any desired comparison or prediction is based is provided in a separate Worksheet. The required inputs are listed in Table 6.3. A picture of the Input Worksheet for the tool, named the *Wave Wake Predictor*, is provided in Figure 6.1. Data is input within the bright yellow coloured cells only.

Variable	**Symbol**	**Units**
Model speed	u	metres/second
Water depth	h	metres
Wave A – Wave height constant	γ_A	
Wave A – Wave period	T_A	seconds
Wave A – Wave decay rate	n_A	
Wave A – Wave angle	θ_A	degrees
Wave B – Wave height constant	γ_B	
Wave B – Wave period	T_B	seconds
Wave B – Wave decay rate	n_B	
Wave B – Wave angle	θ_B	degrees
Wave C – Wave height constant	γ_C	
Wave C – Wave period	T_C	seconds
Wave C – Wave decay rate	n_C	
Wave C – Wave angle	θ_C	degrees

Table 6.2 List of variables for each model speed

Vessel Details	**Symbol**	**Units**
• Monohull or Catamaran		
• Length	L	metres
• Displacement	Δ	tonnes
• Speed	u	knots
Environment Details		
• Water depth	h	metres
• Water density	ρ	kilograms/metre^3
• Lateral distance from vessel sailing line to point of interest	y	metres

Table 6.3 List of desired input variables for comparison or prediction

From the inputs listed in Table 6.3, the following parameters and ratios are calculated for the desired case: Fr_h, Fr_L, h/L, ∇, $L/\nabla^{1/3}$. Each of the following steps are performed within each of the nineteen Worksheets (representing the different hulls). Firstly, the scale factor, *R*, that is required to allow the model scale data to correspond to the desired (input) full scale case is calculated by dividing the desired (input) L by the L of each ship model (according to Froude scaling laws).

The desired full scale ship speed is converted from knots into metres/second (by multiplying by the conversion factor of 0.5144) and the corresponding desired model scale speed, for each hull, is calculated using Equation 6.1.

$$u_m = \frac{u_s}{\sqrt{R}} \tag{6.1}$$

The look-up process involves two primary linear interpolations, firstly between the two model scale speeds that are closest to the desired (input) value. This task is undertaken for four sub-sets of data, one for each of the four water depths. This will result in four sets of interpolated data that correspond to the desired Fr_L, but each of the four sets will be for a different Fr_h.

A second linear interpolation is performed on the two sets of data that have an h/L value closest to that calculated using the desired (input) values for L and h (appropriately selected using a look-up process). The resultant data set will now correspond to the desired values for Fr_h and Fr_L.

The dimensional values of wave height are calculated using the resultant values for γ and n using Equation 6.2, for each of the three waves of interest.

$$H = \gamma \left(\frac{y}{L}\right)^n \tag{6.2}$$

The full scale wave height is calculated by multiplying the model H by the scale, *R*, and the wave period by multiplying T by the square root of *R*. No scaling is required for both the wave decay rate and angle.

At this point the *Wave Wake Predictor* provides several means to compare the resultant data for all nineteen hulls to investigate trends (refer Section 6.3), or a third and final look-up and interpolation can be performed to obtain predictions that are specific for a desired (input) slenderness ratio, $L/\nabla^{1/3}$, for either a monohull or

catamaran (based on input values of L and Δ). The output results are provided in tabular format, as shown in Figure 6.2. Examples of this output in graphical format have been provided and discussed in Section 6.4.

6.2.2 Limitations and Assumptions

As with any predictive tool, there are limits of applicability that should be applied when using the *Wave Wake Predictor*. To avoid misunderstanding of the results, many of the physical limits within the available data have been built into the Input Worksheet through the use of checks and warnings. Each of these are described in this sub-section. Examples of how they appear in the prediction tool are visible in Figures 6.1 and 6.2. The range of parameters of the *Wave Wake Predictor* have been summarised in Table 6.4.

	Monohulls		Catamarans	
	Minimum	Maximum	Minimum	Maximum
$L / \nabla^{1/3}$	4.79	11.70	5.26	9.61
Fr_h	0.16	2.36	0.16	2.24
Fr_L	0.18	1.34	0.17	1.10
h / L	0.16	2.13*	0.15	1.76*
h / d	3.00	78.60*	3.50	41.50*

* considered infinite (deep) water

Table 6.4 *Wave Wake Predictor*: range of parameters

Vessel Speed

There are two stages to this checking process. In the first, the desired (input) speed is converted to a model scale speed (in m/s) and checked against the available data for each ship model. One of three possible outcomes will be displayed: (a) Desired speed is within the available range, (b) Desired speed is below the minimum available, or (c) Desired speed is above the maximum available.

Wave Wake Predictor

Input Data

Water depth	h	6	metres	
Vessel waterline length	L	17	metres	
Vessel speed	u_s	16	knots	
Lateral distance from vessel sailing line to measurement point	y	20	metres	Measurement point is within the near to medium field.
Depth Froude number	Fr_h	1.07		Super-Critical depth Froude number - care should be taken while passing through trans-critical speed range
Length Froude number	Fr_L	0.64		
Water depth to vessel length ratio	h/L	0.35		
Lateral distance to vessel length ratio	y/L	1.18		
Monohull or catamaran	Mono/Cat	mono		
Vessel displacement	Δ	12	tonnes	
Fresh or salt water	Fresh/Salt	salt		
Water density	ρ	1025	kilograms/metre^3	
Displaced volume	∇	11.71	metres^3	Slenderness ratio is within available range for monohulls (range available = 4.79 up to 11.70)
Slenderness ratio	$L/\nabla^{1/3}$	7.49		
Wave Wake Rule Benchmark wave height	H_b	450	millimetres	
Benchmark wave height	T_b	2.5	seconds	

Checks and Warnings for Individual Data Sets

Hull No.	Model	Mono / Cat	Speed Range	Finite or Deep Water	Water Depth
1	00-01 H	Monohull	Speed is within available range	Using Finite Water Data	Depth is within available range
2	10-37 H	Monohull	Speed is within available range	Using Finite Water Data	Depth is within available range
3	00-01 L	Monohull	Speed is within available range	Using Finite Water Data	Depth is within available range
4	10-37 L	Monohull	Speed is within available range	Using Finite Water Data	Depth is within available range
5	97-02 H	Monohull	Speed is within available range	Using Finite Water Data	Depth is within available range
6	97-02 L	Monohull	Speed is within available range	Using Finite Water Data	Depth is within available range
7	97-10	Monohull	Speed is within available range	Using Finite Water Data	Depth is within available range
8	96-08 H	Monohull	Speed is within available range	Using Finite Water Data	Depth is within available range
9	96-08 L	Monohull	Speed is within available range	Using Finite Water Data	Depth is within available range
10	97-30	Monohull	Speed is within available range	Using Finite Water Data	Depth is within available range
11	99-17	Monohull	Speed is within available range	Using Finite Water Data	Depth is within available range
12	00-03	Catamaran	Speed is within available range	Using Finite Water Data	Depth is within available range
13	93-07	Catamaran	Speed is within available range	Using Finite Water Data	Depth is within available range
14	99-01	Catamaran	Speed is within available range	Using Finite Water Data	Depth is within available range
15	99-27	Catamaran	Speed is within available range	Using Finite Water Data	Depth is within available range
16	93-03 H	Catamaran	Speed is within available range	Using Finite Water Data	Depth is within available range
17	93-03 L	Catamaran	Speed is within available range	Using Finite Water Data	Depth is within available range
18	98-16 H	Catamaran	Speed is within available range	Using Finite Water Data	Depth is within available range
19	98-16 L	Catamaran	Speed is within available range	Using Finite Water Data	Depth is within available range

Figure 6.1 Prediction tool *Input Worksheet*

Wave Wake Predictor

Input Summary

Water depth	h	6	metres	
Vessel waterline length	L	17	metres	
Vessel speed	u_s	16	knots	
Lateral distance from vessel sailing line to measurement point	y	20	metres	Measurement point is within the near to medium field.
Depth Froude number	Fr_h	1.07		Super-Critical depth Froude number - care should be taken while passing through trans-critical speed range
Length Froude number	Fr_L	0.64		
Water depth to vessel length ratio	h/L	0.35		
Monohull or catamaran	Mono/Cat	mono		
Vessel displacement	Δ	12	tonnes	
Fresh or salt water	Fresh/Salt	salt		
Water density	ρ	1025	kilograms/metre^3	
Displaced volume	∇	11.71	metres^3	Slenderness ratio is within available range for monohulls (range available = 4.79 up to 11.70)
Slenderness ratio	$L/\nabla^{1/3}$	7.49		

Results Summary

γ_A	H_A model	H_A ship	T_A model	T_A ship	T_A'	n_A	θ_A	γ_B	H_B model	H_B ship	T_B model	T_B ship	T_B'	n_B	θ_B	γ_C	H_C model	H_C ship	T_C model	T_C ship	T_C'	n_C	θ_C
	(mm)	(mm)	(s)	(s)			(deg)		(mm)	(mm)	(s)	(s)			(deg)		(mm)	(mm)	(s)	(s)			(deg)
9.4	13.1	140	2.17	7.1	1.71	-0.82	69	16.8	24.6	263	1.28	4.2	1.01	-0.49	30	15.0	22.8	244	0.73	2.4	0.58	-0.27	12

Figure 6.2 Prediction tool *Output Worksheet*

In general, the range of model scale speeds investigated is consistent for all ship models, however, there are a small number of exceptions (for example, the ski boat models were tested to a higher maximum speed than all other models). The variation in model size will result in the scale factor required to make all ship models correspond to the desired full scale vessel being different, hence a similar story for the model scale speed. Therefore, it is possible for the desired (input) vessel speed to be within the available range for some ship models, and outside this range for others.

In such circumstances, and when predictions are sought for a specific desired (input) slenderness ratio (based on input L and Δ), a further check is made to ensure that the desired speed is within the available range for the two hulls that are closest to this $L/\nabla^{1/3}$. If this is not the case, the user will be informed as such.

Water Depth

The desired (input) values for water depth and vessel length are used to determine the desired h/L ratio and checked against the available data for each ship model (recalling that experiments were conducted at three finite water depths and one that was effectively deep water). If the desired h/L is within the available range then the user is informed of this.

Should the desired h/L be lower than the lowest available for any of the ship models, predictions are still computed but the user is alerted to the fact that they are based solely on the data for the lowest available h/L, and that these predictions may not be valid.

There is no such problem in cases where the desired h/L is equal to or greater than the maximum available, as these experiments were conducted at a water depth that is effectively infinite, i.e. all speeds are considered to be sub-critical. The deep water experimental data is therefore used in these cases, and the user is informed of this fact. The actual value of h/L is displayed for all scenarios.

Trans-Critical Speeds

As discussed in Chapter 5, a highly non-linear relationship was found to exist between Froude number and the wave measures of interest (γ, T, n and θ) as a vessel approaches critical speed (particularly at low values of h/L). It was recognised that a more comprehensive test program (larger number of runs and smaller increment of speed) may have been required in the high trans-critical region to provide more

accurate predictions and identify the presence of any unsteady phenomena (such as the generation of solitons).

It was strongly recommended that vessel operations at or close to critical speed be avoided (were possible), due to the excessively high and long period waves that can be generated in this region. As a result, it is argued that there is little practical reason to provide any more accurate predictions than presently available. However, it is acknowledged that a vessel operator, or user of the prediction tool, be fully aware when the combination of vessel speed and water depth puts them in this region of concern. Therefore, a suitable warning has been built into the Input Worksheet of the *Wave Wake Predictor* when this occurs.

The warning consists of a text message, indicating that the desired combination of speed and water depth has resulted in a trans-critical speed, and a colouring of the appropriate cells. For low trans-critical speeds (starting at $Fr_h = 0.75$) the cells change from white to a light red. This red becomes more vibrant as Fr_h approaches unity.

A text message is also provided to indicate when operation is either sub-critical or super-critical. In the case of super-critical speeds the appropriate cells are coloured light green, to distinguish this from the other two regimes (as can be seen in the example shown in Figure 6.1).

6.2.3 Verification

In this context, *verification* is defined as the check that the computer coding within the prediction tool is a correct representation of the intended operations and procedures necessary to complete the required tasks. Whereas, *validation* of the prediction tool is the proof of its applicability. The verification of operation of the *Wave Wake Predictor* is covered in this sub-section and the validation is covered, through comparison with full scale trials data, in Section 6.5.

The correctness of the many calculations conducted within the tool was verified at several stages during its development. The first stage followed the completion of the Worksheet for first hull, where each of the look-up operations, interpolations and calculations were manually checked and compared against an independently worked solution.

The second stage was conducted once the data for all nineteen hulls had each been imported into their own individual Worksheets (which were based on the original, verified Worksheet). As the format and layout of the original Worksheet was deliberately undertaken in a very logical and systematic manner, it was assumed that the vast majority of operations should still be correct, provided the experimental data for each of the 'new' hulls was imported in the correct locations and sequence. Thus, this verification check concentrated upon this specific undertaking for each of the remaining 18 hulls. In addition, a manual check similar to the first stage of verification was conducted on a random selection of hulls to provide confidence that no unforeseen errors were made. At this point, various plots were also generated in order to investigate significant trends between hull principal particulars. The formation of these plots also proved to be a useful double-check of some of the tool's operations.

The third stage of verification concentrated on the specific component of the tool associated with the predictions for a specific hull, which required a further series of look-up operations, interpolations and calculations using just the resultant values from each of the 19 hulls.

The fourth and final stage of verification focussed on the operations specific to the many inbuilt warnings and checks related to the limitations of applicability (as outlined in the previous sub-section). This task also involved some changes to the user interface with the tool to improve user friendliness.

Upon completion, each Worksheet was protected to avoid any accidental alteration of data or formulae. Only those few cells requiring the user to provide details into the Input Worksheet can be altered.

6.3 Effect of Hull Form

In Section 5.5 the experimental results for just a single ship model were presented and the influence that vessel speed and water depth has on the wave wake generated was discussed. The development of the *Wave Wake Predictor*, based upon experimental data for nineteen different ship models, has provided a means to investigate the effect that hull form, as well as vessel speed and water depth, has on wave wake. In this Section, examples of the output from the tool have been used to achieve this goal.

In the first set of examples, all four wave measures (γ, T, n and θ) have been plotted as functions of $L/\nabla^{1/3}$ for each of the three key waves (A, B and C) in Figures 6.3 to 6.6. In each of these figures all results are valid for constant input values of h = 6 m, L = 17 m and u_s = 16 knots. From Figure 6.3 it is clear that hull form has a significant influence on the height of the waves generated, with γ generally decreasing with an increase in $L/\nabla^{1/3}$ for all three waves. A similar result was found by Macfarlane *et al.* (2008) where the height of the maximum wave was plotted as a function of $L/\nabla^{1/3}$ (see Figure 3.1). These results confirm that wave height can be significantly reduced through the use of relatively long and light vessels.

It is also possible to use the results presented in Figure 6.3 to compare the relative merits of monohulls and catamarans. In general, catamarans are found to possess a lower wave height constant than a monohull at the same $L/\nabla^{1/3}$. However, this may not be a truly practical comparison given that the relative carrying capacities of a monohull and catamaran of equal $L/\nabla^{1/3}$ are not likely to be comparable.

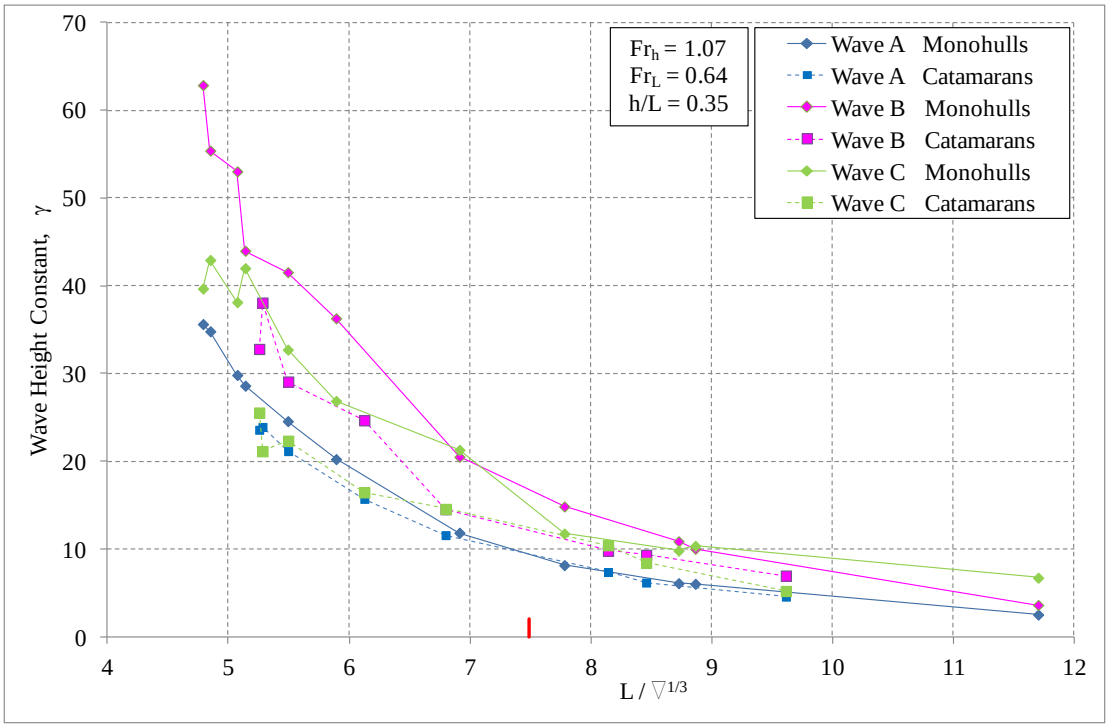

Figure 6.3 Example of prediction tool output: γ as a function of $L/\nabla^{1/3}$

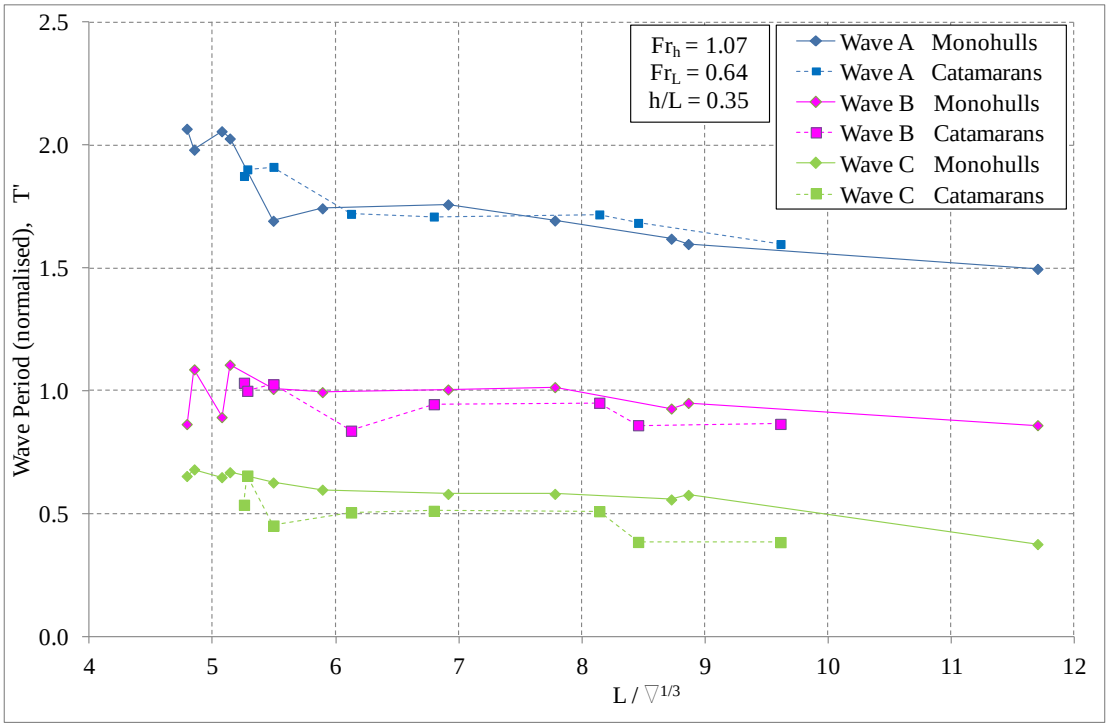

Figure 6.4 Example of prediction tool output: T' as a function of $L/\nabla^{1/3}$

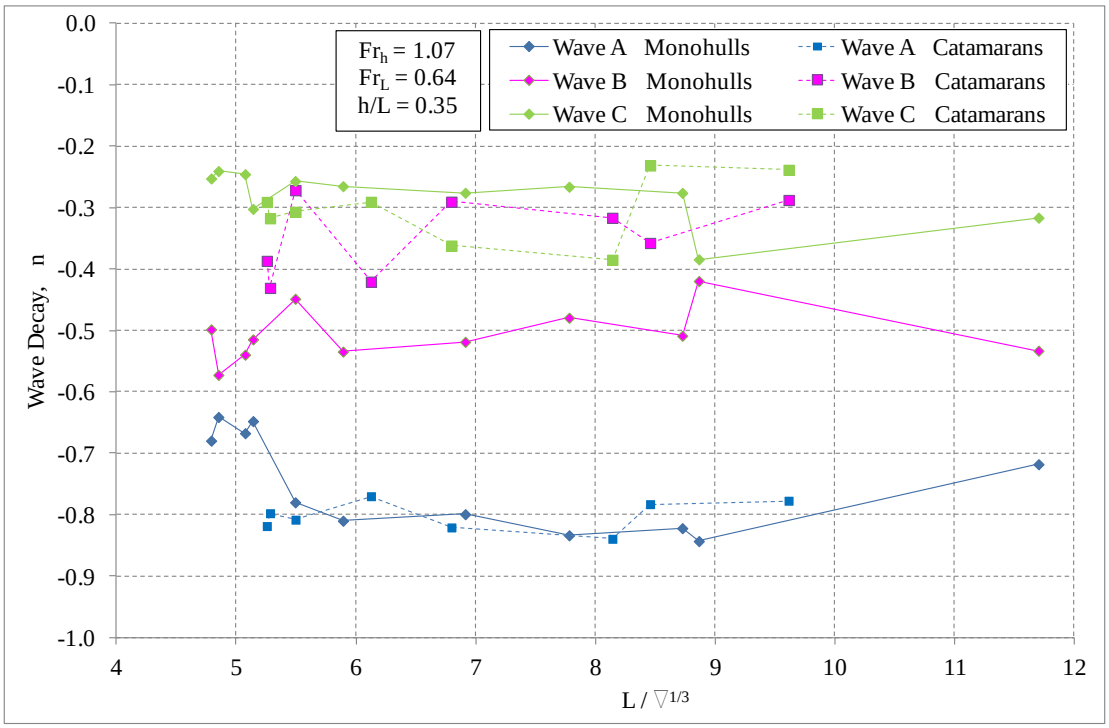

Figure 6.5 Example of prediction tool output: n as a function of $L/\nabla^{1/3}$

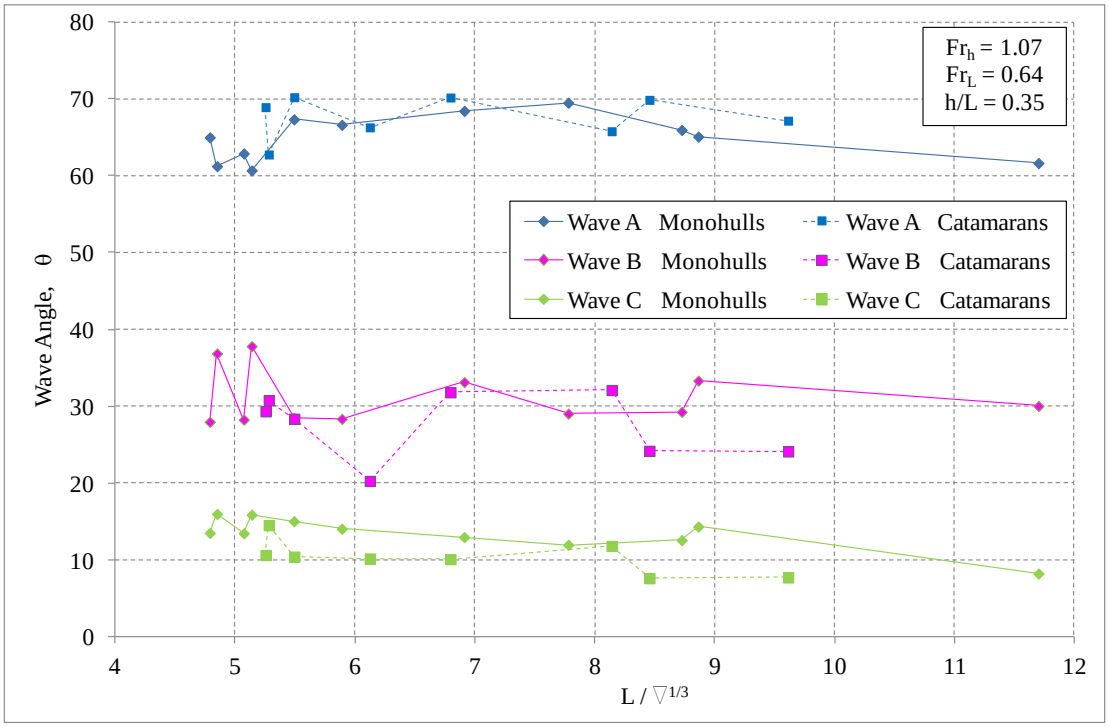

Figure 6.6 Example of prediction tool output: θ as a function of $L/\nabla^{1/3}$

Hull form has a much lesser influence on the period of the three waves, as can be seen in Figure 6.4, where there is generally only a marginal reduction in period with increasing $L/\nabla^{1/3}$. There is also less difference between the period of the waves generated by monohulls and catamarans, particularly with the two longer waves, A and B. For this example, and combination of water depth, vessel length and speed, there is a marked difference in the periods of Waves A, B and C. In the vast majority of published cases, where wave wake analyses have only considered the single highest wave, the longest period waves (Wave A) have been ignored, despite the likelihood that they may potentially be the most damaging waves generated, as discussed in Chapter 3.

The decay rate exponents for each of Waves A, B and C are plotted as functions of $L/\nabla^{1/3}$ in Figure 6.5. Although more scatter is present than was the case for wave period, the wave decay rate is also generally not strongly affected by hull form. For this combination of water depth, vessel length and vessel speed the longer the wave period, the greater the rate of decay. Figure 6.6 shows that wave angle also does not alter to any notable degree with a change in $L/\nabla^{1/3}$.

As mentioned, the results presented in Figures 6.3 to 6.6 are all for specific values of water depth, vessel length and vessel speed. It is a very simple task to obtain results

for other values of each of these variables and this was undertaken in a systematic manner with the general trends identified for this example found to be typical for most combinations (within the limits of the prediction tool, as outlined in Sections 5.2 and 6.2).

The effect that basic hull form parameters, other than $L/\nabla^{1/3}$, have on these measures (particularly γ) were also investigated. This included L/B, L/d, B/d and i_E, of which examples are provided in Figures 6.7, 6.8, 6.9 and 6.10 respectively. Only L/B and L/d show any predictable relationship with γ. The general trend indicates that an increase in either L/B or L/d will result in a decrease in wave height, although, the results shown in Figures 6.7 and 6.8 represent some of the better examples found to support this deduction – there were many cases where the trend was less obvious. Note that demihull beam, not overall beam, has been used to define L/B for each catamaran in the example provided in Figure 6.7.

It is concluded that wave height is the only one of the four measures that is significantly influenced by hull form, with only a marginal or negligible effect on wave period, decay and angle. It has also been confirmed that the single most important hull form parameter was the length-displacement ratio ($L/\nabla^{1/3}$). As previously shown, all four measures are very dependent upon the water depth and vessel speed and hence all these factors are very important when attempting to quantify vessel wave wake.

In coastal engineering terms, energy states tend to jump in orders of magnitude, not in incremental percentages. In many respects the push by designers to improve the wave wake characteristics of their vessels by a nominal modest percentage is likely to be somewhat inconsequential in erosion terms. Generally, a vessel design either will or will not work – small changes to design parameters such as waterline beam, draught and angle of entrance are unlikely to turn a design that causes excessive erosion into an acceptable one.

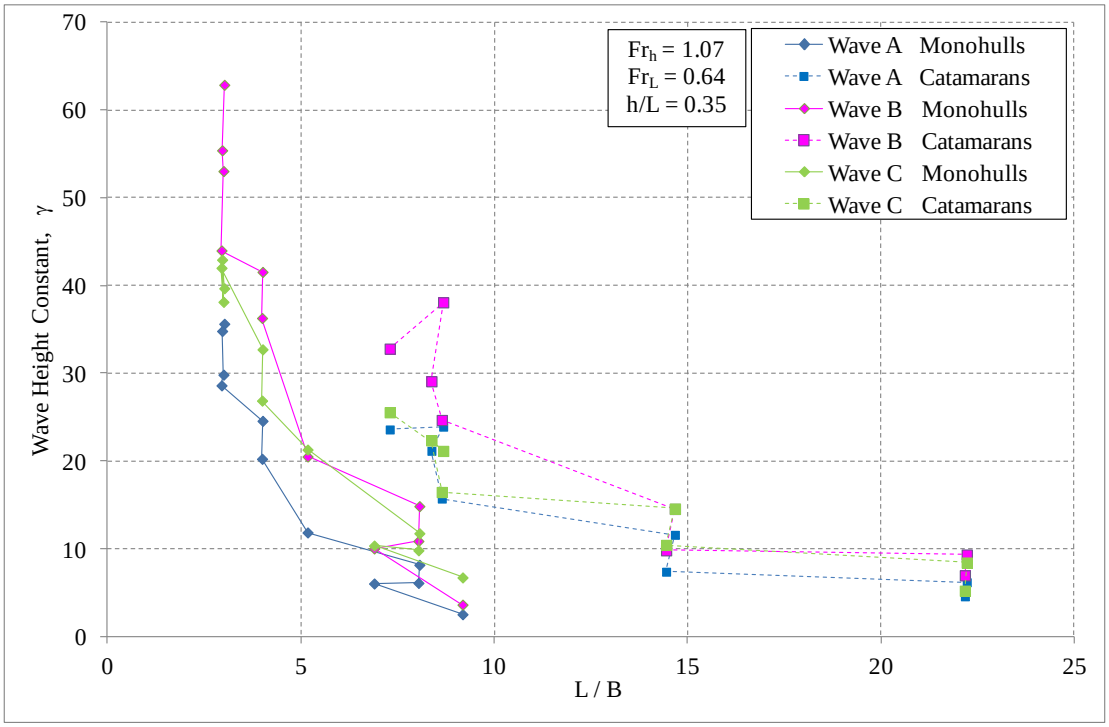

Figure 6.7 Example of prediction tool output: γ as a function of L/B

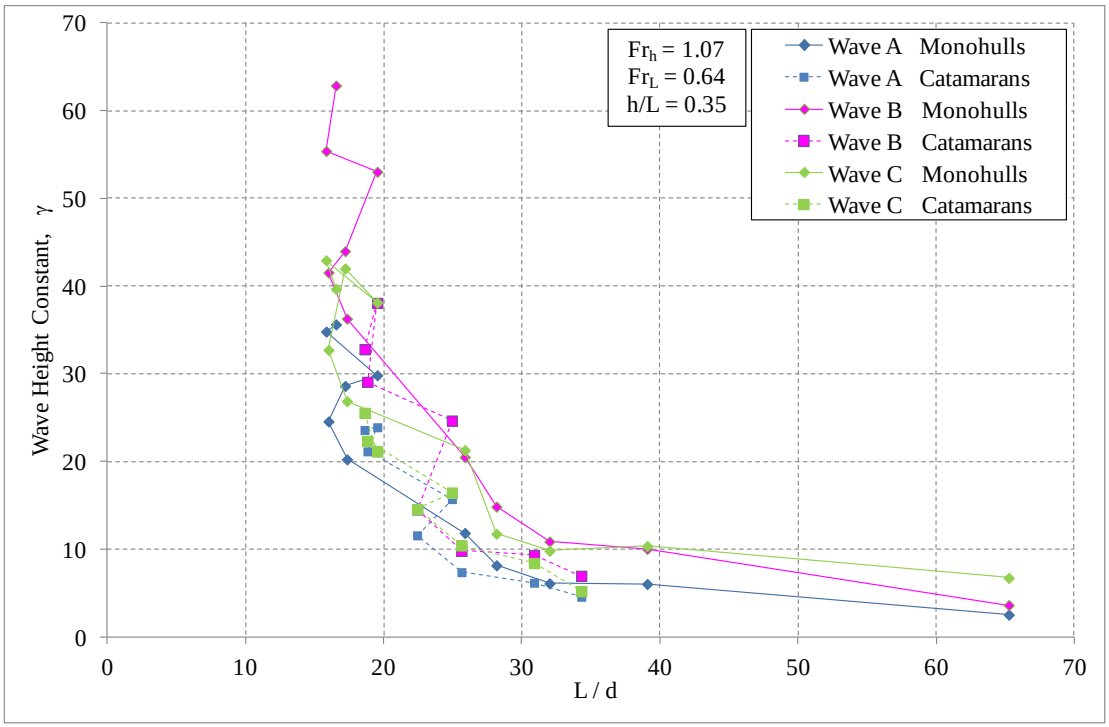

Figure 6.8 Example of prediction tool output: γ as a function of L/d

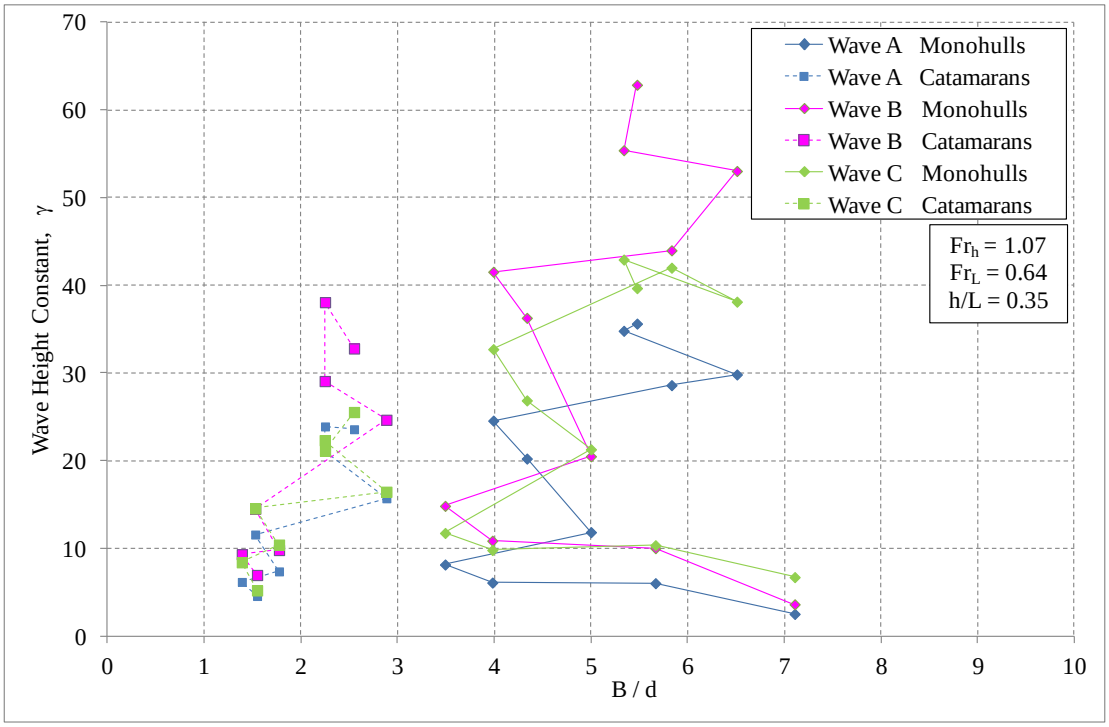

Figure 6.9 Example of prediction tool output: γ as a function of B/d

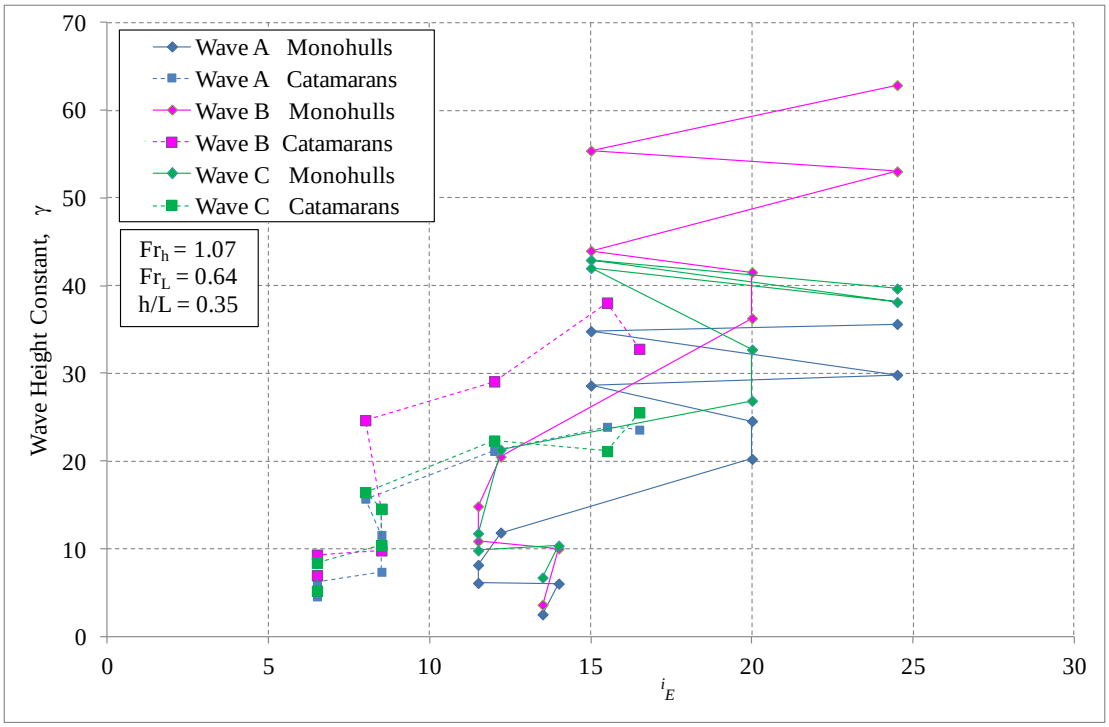

Figure 6.10 Example of prediction tool output: γ as a function of i_E

6.4 Application of the *Wave Wake Predictor*

Predictions of the wave wake characteristics of a specific vessel (either monohull or catamaran) can be provided simply by inputting the desired vessel length and displacement, in addition to the water depth and vessel speed for the proposed operation. Predictions are made by conducting another look-up and interpolation within the *Wave Wake Predictor*, this time using the desired vessel length and displacement to calculate the resultant $L/\nabla^{1/3}$.

The data presented in Figure 6.3 can be used to demonstrate this process. If the length and displacement of a proposed monohull are 17 m and 12 t respectively, the resultant $L/\nabla^{1/3}$ will be 7.5, indicated in Figure 6.3 as a small red tick along the x-axis. An interpolation is conducted between the data for the monohull models just below and above this value of $L/\nabla^{1/3}$(6.91 and 7.78 in this example) for Waves A, B and C. A similar routine is conducted to obtain predictions for the other wave measures of T, n and θ, although as shown previously, these measures do not vary as much with changes in $L/\nabla^{1/3}$. The resultant predictions for this single speed example are provided in tabular form under 'Results Summary' in Figure 6.2.

It is often useful to obtain predictions at many different vessel speeds, or water depths, hence a means of obtaining such data has been incorporated into the prediction tool. For example, the resultant wave height for a monohull of L = 17 m and $\triangle$ = 12 t operating in h = 6 m water depth at y = 20 m is plotted as a function of speed for the approximate range of $0.35 < Fr_h < 1.60$ in Figure 6.11. Plots of wave period, decay and angle as functions of the same conditions are shown in Figures 6.12, 6.13 and 6.14 respectively. Similar plots are readily provided for other forms of speed measurement, including: Fr_L, Fr_∇ and full scale speed (knots).

In Figure 6.12, it is clear that the period of Waves B and C remain relatively constant at higher speeds (in this case at speeds where $Fr_h > 1.2$). This concurs with the results from full scale experiments presented in Figure 3.3. The period of Wave A, however, continues to reduce at these higher speeds.

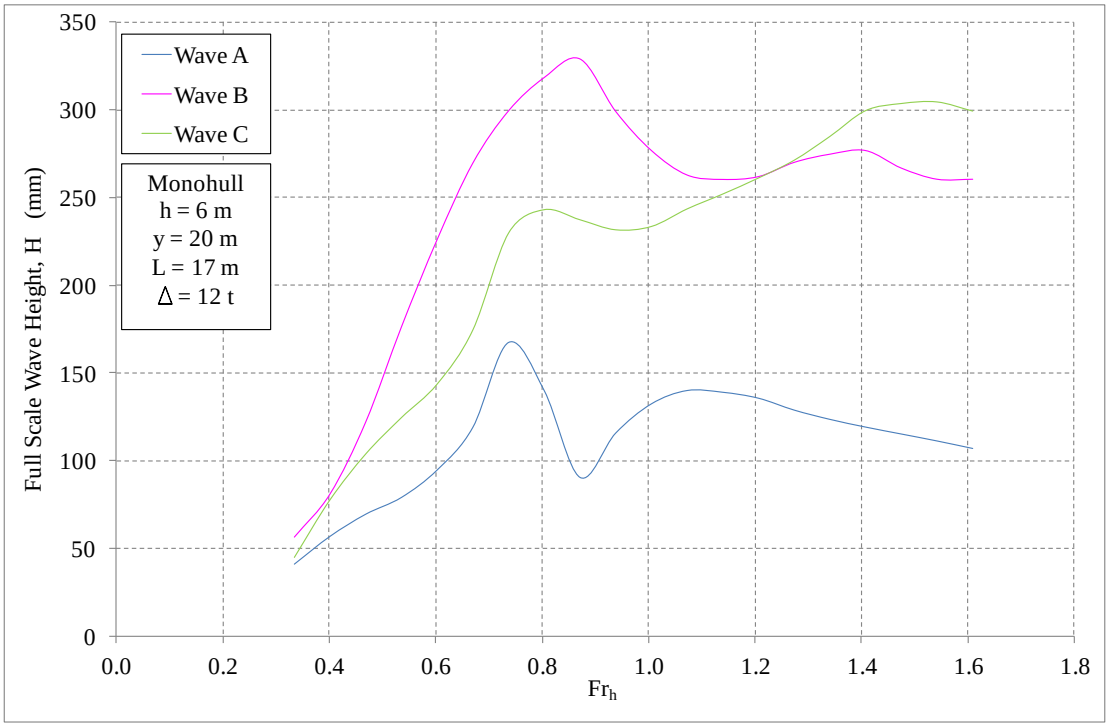

Figure 6.11 Example of prediction tool output: H as a function of Fr_h

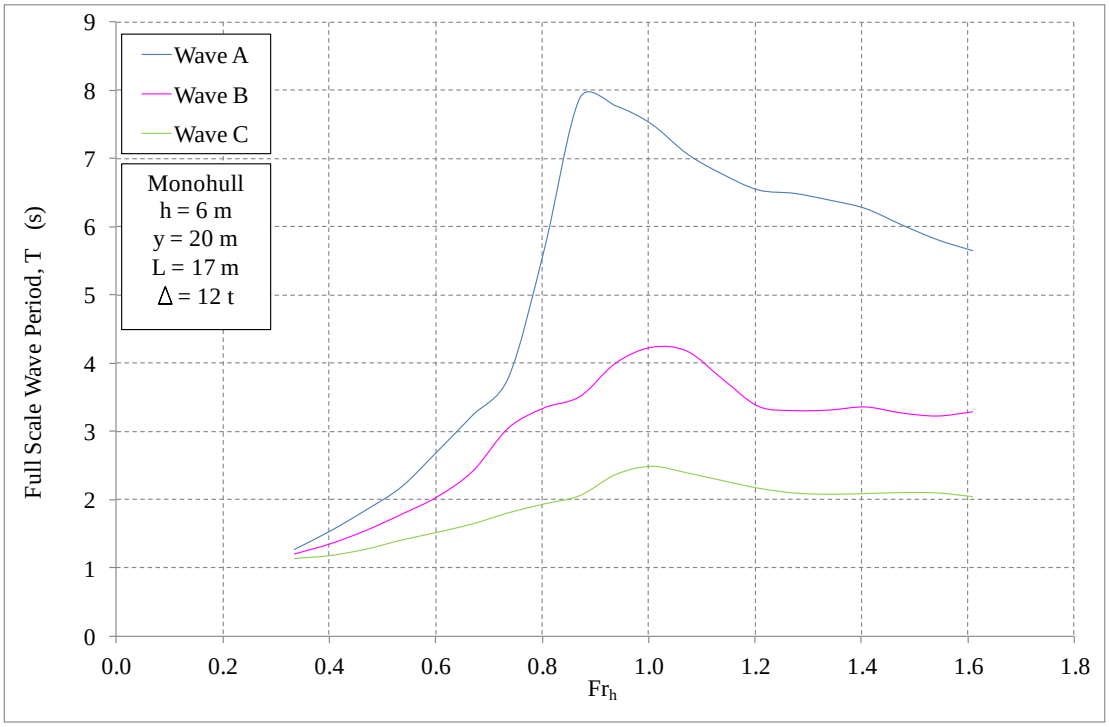

Figure 6.12 Example of prediction tool output: T as a function of Fr_h

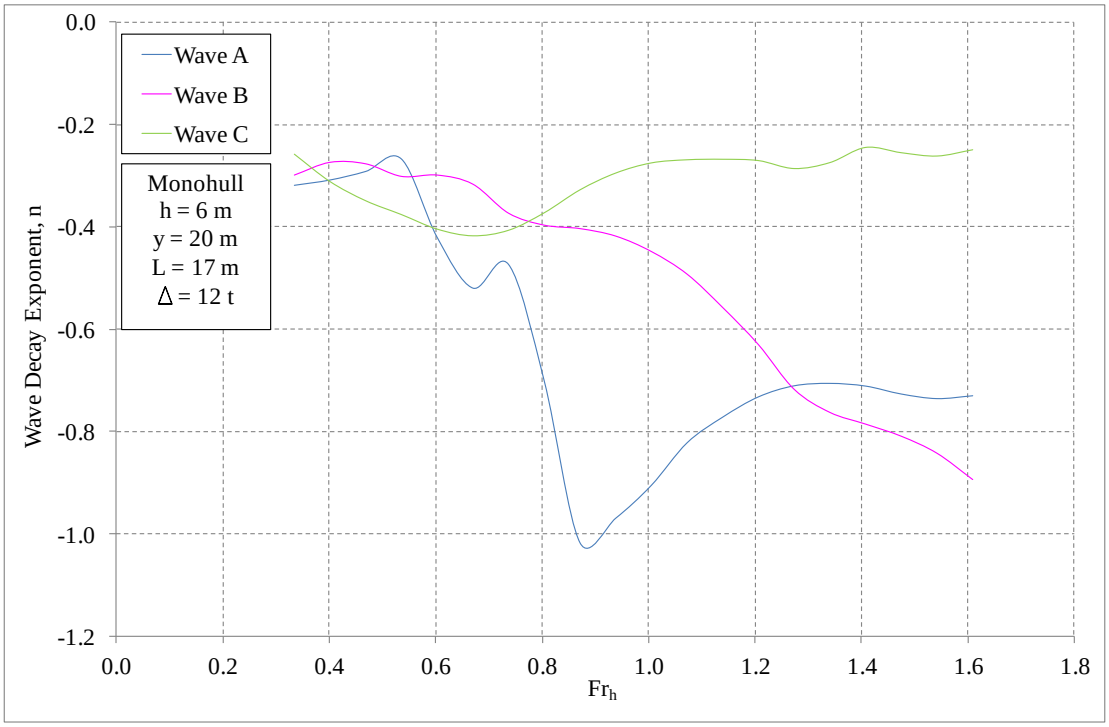

Figure 6.13 Example of prediction tool output: n as a function of Fr_h

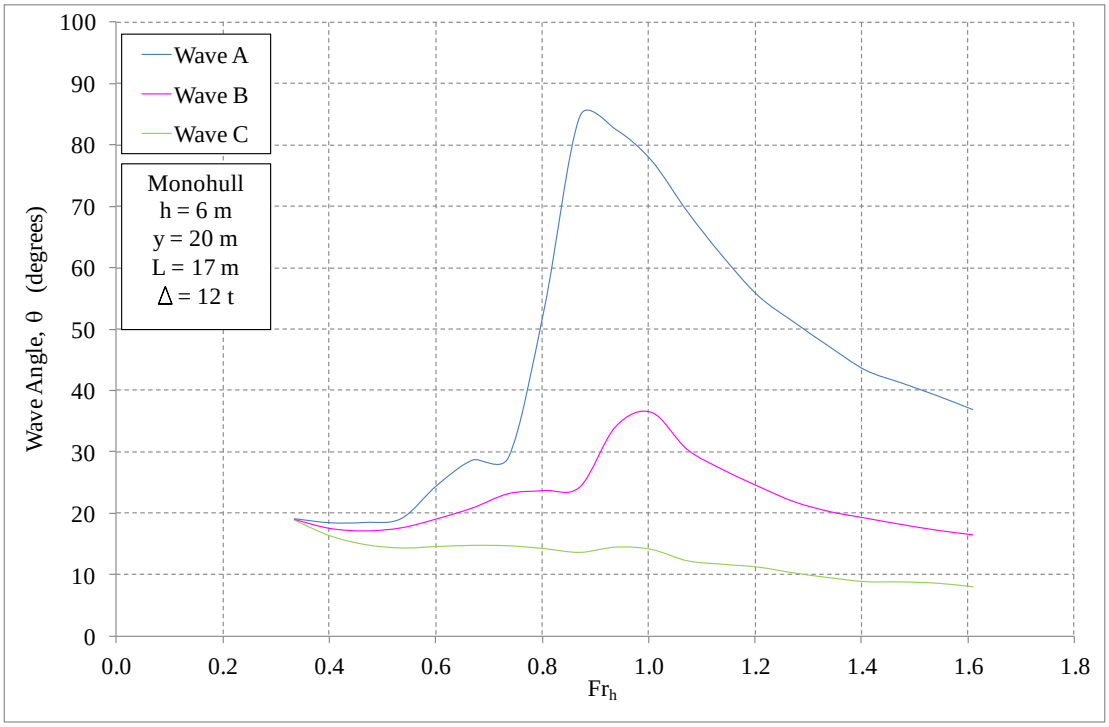

Figure 6.14 Example of prediction tool output: θ as a function of Fr_h

By keeping the vessel speed constant and only varying water depth it is possible to use the tool to generate graphs that highlights the effect that changes in water depth have on the characteristics of the generated waves. As an example, the resultant wave

height for a monohull of L = 17 m and △ = 12 t operating at a constant speed of 15 knots at y = 20 m is plotted as a function of water depth in Figure 6.15. Similarly, plots of wave period, decay and angle as functions of the same conditions are shown in Figures 6.16, 6.17 and 6.18 respectively.

In all four of these plots it is clear that 'deep' water occurs around h = 24 m, as all curves remain constant at greater depths. Figure 6.15 highlights that it is possible to reduce wave height by operating at a 'favourable' finite water depth, however, Figure 6.16 confirms that this is very likely to come at the expense of generating very long period waves, which may well be a worse scenario with respect to shoreline erosion. The data presented in Figures 6.17 and 6.18 provide further evidence to that presented and discussed in Section 5.5 that water depth has a significant influence on the characteristics of Wave A, a relatively minor effect on Wave B, but little or no effect on Wave C.

In Figure 3.2 it was shown that the height of the maximum wave varies approximately linearly with vessel displacement for deep water conditions (Macfarlane *et al*. 2008). The *Wave Wake Predictor* has been used to confirm that this is the case for Waves A, B and C at super-critical speeds, as can be seen in the example provided in Figure 6.19.

Similar processes used to obtain the predictions presented in this sub-section have also been adopted during the validation of the prediction tool in Section 6.5.

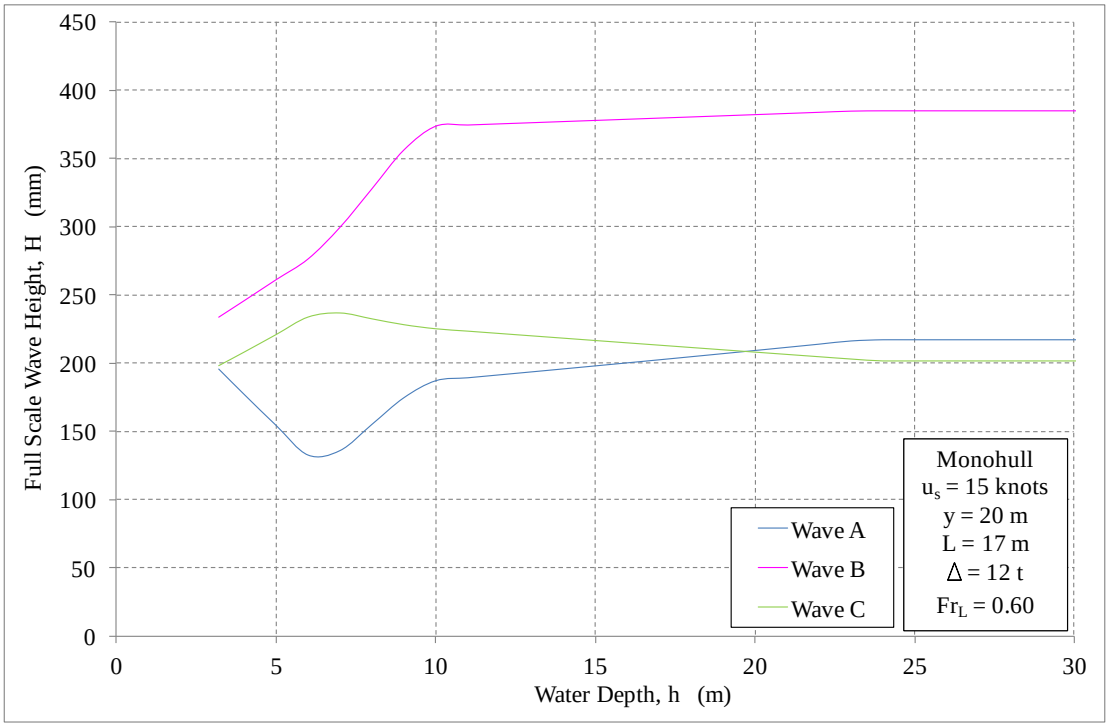

Figure 6.15 Example of prediction tool output: H as a function of h

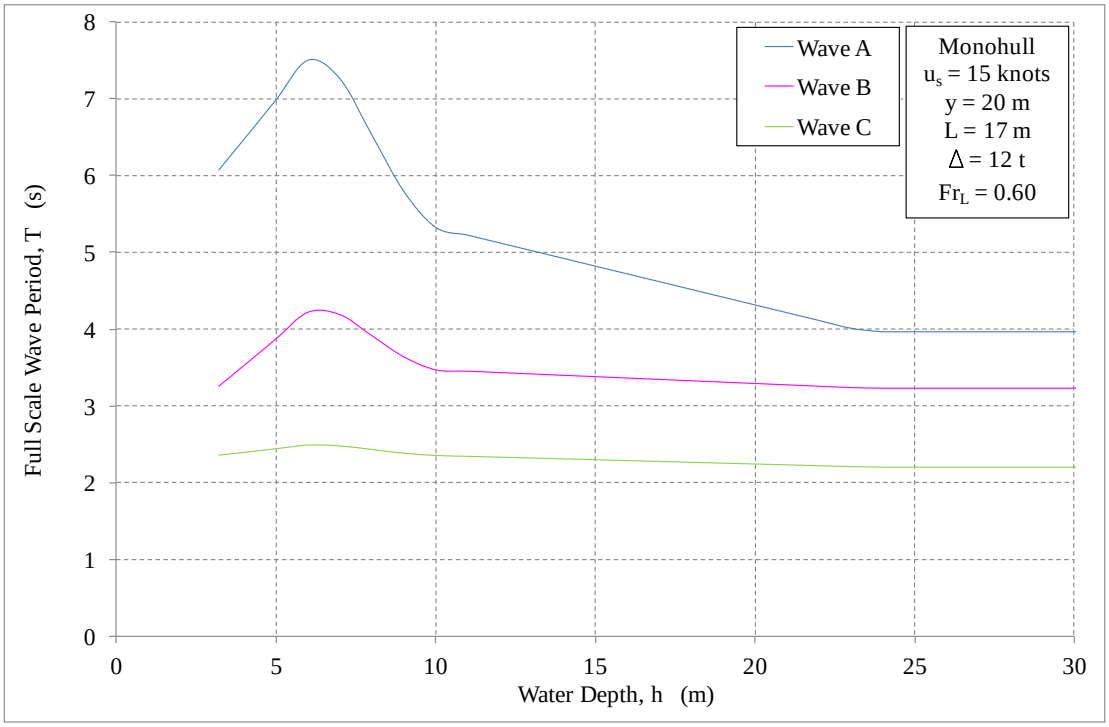

Figure 6.16 Example of prediction tool output: T as a function of h

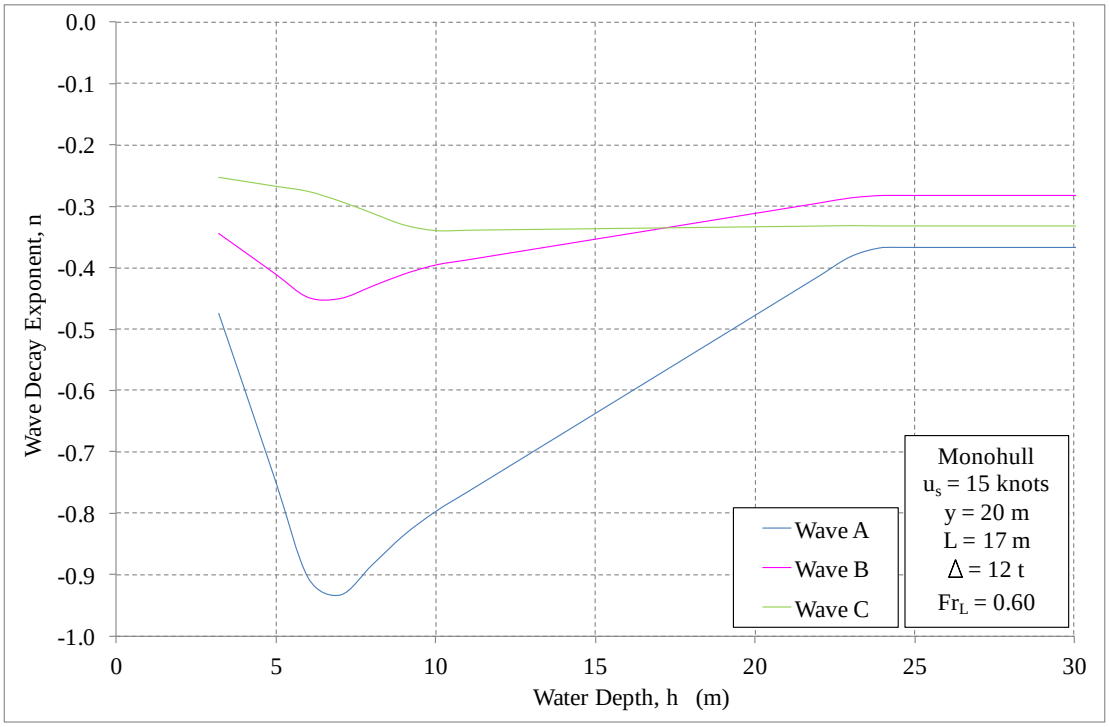

Figure 6.17 Example of prediction tool output: n as a function of h

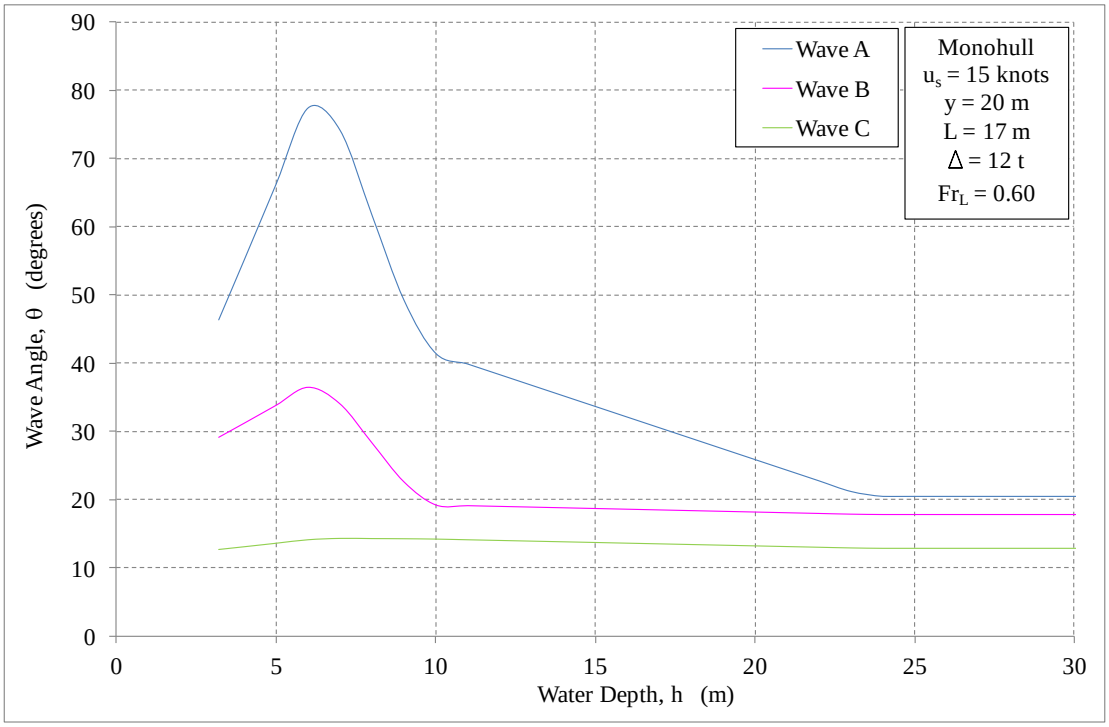

Figure 6.18 Example of prediction tool output: θ as a function of h

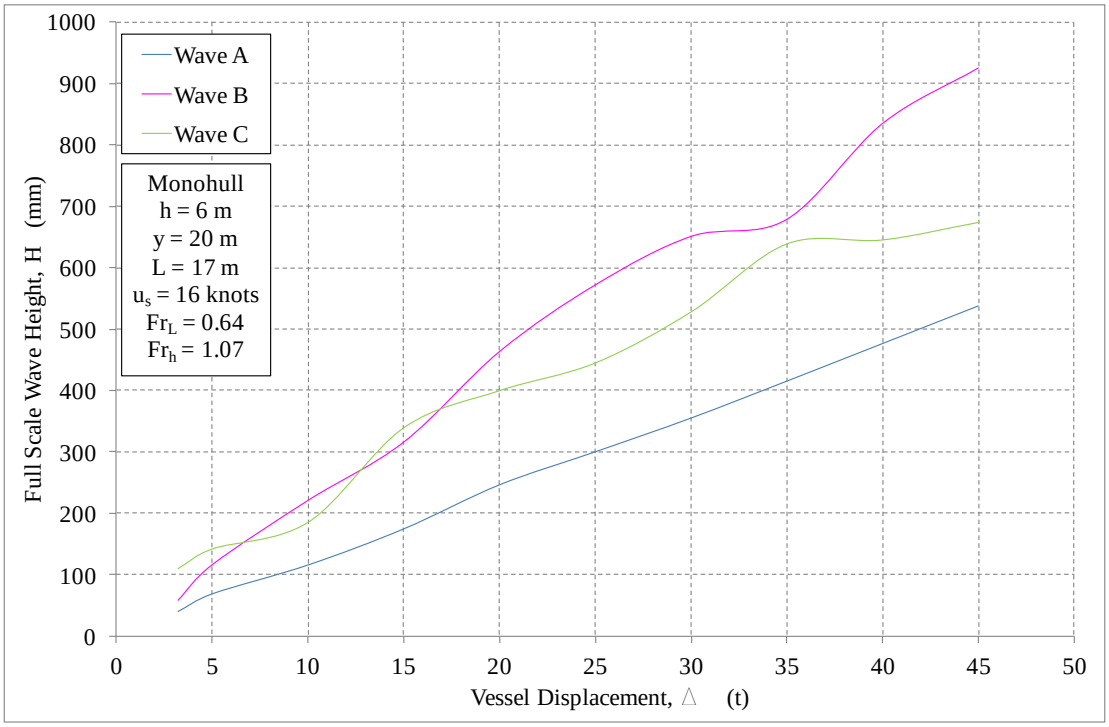

Figure 6.19 Example of prediction tool output: H as a function of Δ

6.5 Validation of the *Wave Wake Predictor*

6.5.1 Introduction

Proof of the applicability, or validation, of the *Wave Wake Predictor* has been investigated through the comparison of its predictions against wave wake data collected from several series of full scale trials conducted on various different types of hull form on several different sheltered waterways. This sub-section outlines general details of the conduct of these full scale trials, presents comparisons between measurements and predictions and discusses the correlation between the two.

6.5.2 Conduct of Full Scale Wave Wake Trials

The success of field trials is highly dependent on having rigorous and time-proven testing methodology, instrumentation and analysis procedures. Vessel wave wake is not a steady-state phenomenon (from a fixed reference frame) and its assessment is reliant on consistency.

The testing methodology adopted for this study ensured that the results were not site-specific and can be transposed with other results from other sites. Full-scale experiments are often subjected to many natural and procedural influences that affect the accuracy of the results. Quite besides complications such as wind waves, currents, and variable water depths, other influences must be tempered to improve accuracy and repeatability. The most important issues are discussed below, including some comments relating to experimental data utilised in the present study, as summarised in Table 6.5.

Water Depth at Vessel Sailing Line

In the present study, tests were conducted in both deep and finite water (at several different water depths) to provide adequate data to validate predictions for vessels operating at sub-critical, trans-critical and super-critical speeds. The water depth for each test site is reported in Table 6.5 and in each case this depth remained relatively constant along the vessel sailing line.

Water Depth at Measurement Point

Besides the need for relatively constant water depth along the sailing line, there must also be adequate depth at the measurement point to minimise wave shoaling, as this will clearly influence wave elevation. It is also advisable that the bathymetry between the vessel sailing line and measurement point be recorded. Both of these factors were addressed during the conduct of the experiments for the present study.

Vessel Sailing Line

The sailing line must be straight and vessels must adhere to that straight course during the approach to the measurement point. It is recommended that marker buoys (a minimum of two) be deployed to act as a guide to the sailing line, taking into consideration the required lateral distance between the centreline of the vessel's track path and the location of the measurement point(s). This was done for all experiments in the present study. In addition, in some cases the test vessel's track, speed and heading were obtained using recordable Global Positioning Systems (GPS) units.

Constant Vessel Speed

As indicated earlier, the wave wake field generated by any vessel will vary with vessel speed. The test vessel must be travelling at a steady-state speed for a considerable distance before reaching the measurement point, and maintain this over the test course, for the wave field to also be considered steady. This distance will

depend on the vessel speeds and lateral distance(s) to the measurement point(s) of interest. This factor probably remains one of the single greatest causes of variation in field experiments on small craft. Particular attention was paid to this issue during the conduct of the experiments for the present study and several repeat runs were conducted to minimise experimental uncertainty.

Wave Probe Position

The wave probe(s) must be positioned such that they are beyond any localised refraction caused by shallow water, or diffraction due to solid obstacles or irregular shoreline shape. Also, if an existing structure onto which the probes can be attached is not available, the water depth should not be so deep as to create practical set-up problems. Each of these factors were considered during the conduct of the experiments for the present study which is believed to have minimised any negative influences on the data collected.

Wave Probe Mounting Structure

Wave probes should be mounted on a sufficiently rigid structure such that it does not move when experiencing passing waves. If a wave probe is capable of moving laterally during field experiments, the resulting wave periods will be contaminated. Similarly, any vertical movement will result in variations in wave height. Alternatively, sea-bed mounted instrumentation, such as pressure sensors, can be adopted. Adequately rigid structures were adopted for all cases in the present study.

Shoreline Types

The test methodology was arranged to make it independent of the shoreline type, allowing direct comparison between results from other test programs. The tests at each of the selected sites were conducted well away from the shoreline, so can be regarded as being independent of the shoreline type.

Bank Reflectivity

The wave wake of a passing vessel may take many seconds to pass completely by the measurement point. This is particularly so for high-speed, deep water wakes. If the probe is set too close to the bank, reflected waves may contaminate the traces. Gently sloping (beach-type) banks are less reflective than steeper forms. For the present study, wave probes were located well away from the shore, except in one scenario when this was unavoidable, the probes were located alongside a gently sloping bank.

Interference

Minimisation of the ambient wave background is another critical issue. Ideally, the test location must not be open to wind waves, uncontrolled incidental vessel wave wake and excessive currents or water turbulence. Extra care was taken to provide adequate opportunities such that all tests were conducted during calm conditions. No tests were conducted when the average height of ambient wind waves exceeded approximately 10% of the vessel waves of interest. Ambient conditions were monitored constantly during the conduct of all experiments.

Current

The general effect of current on test results can be predicted, but it becomes very complicated when testing in shallow water where the vessel operates close to the depth-critical speed. Generally, for a given speed over the ground (not through the water), wave heights increase when travelling up-current and wave periods become longer. For the vessel travelling up-current to achieve the same speed over the ground, it must travel at a faster speed through the water to counter the opposing current flow. The result is the equivalent to travelling at that higher speed through the water with no current present.

The increase in period when travelling up-current is due to two effects. Firstly, the period may increase due to the higher speed through the water, as it would if the vessel travelled faster in still water. Secondly, the propagation speed of the waves (relative to the earth fixed wave probe) has a current component, so the waves travel across the probe slower, creating an apparent increase in period. For the divergent waves, which propagate obliquely, the current effect on period is less than the transverse waves, which propagate parallel to the sailing line. This is further complicated if the vessel is travelling obliquely to the current itself, which is unlikely in a river environment. It should also be noted that current velocity is likely to vary at different positions within a river, and over time.

As an example, a vessel travelling at 4 knots over the ground into a 2 knot current is travelling at 6 knots through the water, so the wave parameters are representative of the 6-knot speed. If the vessel turns and travels at 4 knots over the ground with the 2-knot current, it effectively is travelling at 2 knots through the water and produces waves as such.

When the current speed is a substantial fraction of the vessel speed, the wave results will be influenced. Similarly, when the current velocity is a small fraction of the vessel speed, as is the case at high speeds, the resulting wave data scatter is small.

With the advent of low-cost GPS units it is now often more cost-effective to carry a GPS unit than to fit a speed log. The GPS will give vessel speed over the ground, whereas the speed log will give speed through the water. Technically, speed through the water is the most applicable measurement when a speed limit is applied to a waterway, as it correctly accounts for current (provided shallow water effects are not present). However, it is likely that GPS units will be more prevalent and so speed limitations must reflect the worst-case condition, travelling up-current.

In most cases for the present study the ambient current was negligible. In the cases where current may have made a measureable difference a flow meter was implemented (close to the sailing line of the test vessel). However, the effect from the current has been assumed to be minimal given that the measured flow speeds were relatively low (average of approximately 0.05 m/s, maximum of 0.15 m/s). These measurements were taken into consideration as part of the uncertainty analysis (refer Appendix D).

Instrumentation

The correct use and calibration of appropriate instrumentation is of utmost importance to any experimental program. It is essential that instrumentation such as wave probes be calibrated and checked regularly as variations in conditions (such as water density, temperature and salinity and air temperature) can drastically alter the accuracy of measured data (PIANC 2003).

It is recommended that all wave probes be calibrated within the laboratory prior to and following each test session. It is often difficult to conduct comprehensive and accurate calibrations during on-site experiments, however, it is recommended that on-site checks at least be made at the start and on completion of each test session. The above procedure was adopted during the present study with good repeatability between the on-site and laboratory calibration factors (less than 1.5% variation). The only notable difference between the calibrations was a zero shift, which was to be expected due to minor variations in water level during the course of each test session.

Recording of the water surface elevation was commenced well prior to the arrival of the test vessel so as to provide a baseline noise measurement before the arrival of the wake waves at each of the wave probes.

There are a number of technical factors related to the instrumentation and data acquisition that should also be addressed to ensure good quality data is obtained. These include wave probe resolution, analogue to digital conversion resolution and sample rate. For the present study the wave probes had a resolution of approximately 1.0 mm, analogue to digital conversion resolution was 12-bit and a sample rate of at least 100 Hz was adopted for all on-site experiments. The sample rate should be sufficiently high so as to allow clear definition of all waves of interest (both vessel and wind generated).

Lateral Distance Between Measurement Point and Vessel Sailing Line
Dispersion can create difficulties when assessing wave traces obtained through the conduct of physical experiments (refer Section 2.2.1). Where a wave trace is taken close to a vessel (within, say, half a boat length), the trace may appear to consist of only a few waves, when in fact these waves represent many more waves of differing wavelength superimposed. It takes approximately 1-2 boat lengths for waves to disperse sufficiently such that the period of individual waves can be measured with certainty. Wave height is affected to a lesser degree.

Similarly, an overly large lateral distance between measurement point(s) and vessel sailing line (say, more than five boat lengths) can allow time for natural elements, such as wind and current, to influence the vessel generated waves. However, if a primary aim of the experiments is to investigate wave attenuation over distance then even larger lateral distances (for example, ten boat lengths), may be required.

The lateral distances for each test case in the present study are provided in Table 6.5. For trials conducted on rivers, a minimum distance from the sailing line to the shore of one-quarter of the river width is recommended since vessels operating on rivers, particularly at speed, are most likely to navigate the mid-half of the river.

Number of Test Runs
Due to many of the issues discussed above, it is recommended that multiple runs be conducted at each nominal vessel speed increment to ensure a sufficiently robust statistical database is acquired. For the present study, at least two repeat runs were

conducted at each nominal vessel speed (in some cases many more runs were undertaken).

6.5.3 Results: 24 m Catamaran

Full scale trials were conducted on a 24 m L_{OA} Catamaran over a range of sub-critical, trans-critical and super-critical speeds, as outlined in Table 6.5. Further details on these full scale trials and corresponding model scale tests are provided in Macfarlane (2009). The full scale heights of Wave A for this vessel are presented as functions of Fr_L in Figure 6.20. Three sets of data are presented in this figure, including the full scale trials data, predictions from model scale test results and predictions from the *Wave Wake Predictor*. The model scale tests on the 24 m Catamaran (model AMC 98-08) were conducted and analysed independently from those used to develop the prediction tool, so, like the full scale trials data, are also suitable for validation purposes.

Similar plots are provided in Figures 6.21 and 6.22 for the heights of Waves B and C respectively, and in Figures 6.23, 6.24 and 6.25 for the periods of Waves A, B and C. Uncertainty analysis has been conducted on both the model and full scale measurements to determine if the variation in results was within the predicted accuracy. The uncertainty limits have been presented using error bars in Figures 6.20 to 6.25. Details concerning the uncertainty analysis are given in Appendix D.

As would be expected for tests in an uncontrolled environment, there is a reasonable degree of scatter in the full scale trials data. However, there is good correlation in all cases as the predictions from the *Wave Wake Predictor* generally fall within the estimated limits of uncertainty for both the full scale data and the independent predictions from model scale experiments, as illustrated in Figures 6.20 – 6.25.

In addition, the acceptable level of agreement between the predictions based on the independently conducted model scale tests and the full scale trials data confirm that a correlation factor of close to unity be applied when using model scale experimental data to predict full scale wave heights and periods for similar vessels operating within the range of depth and length Froude numbers.

The full scale trials results presented here (Figures 6.20 to 6.25) originate from the same raw data as those presented in Macfarlane (2009), but the data has been

reanalysed to obtain the wave heights and periods for all three waves of interest (A, B and C). As discussed in Section 3.3, it is not uncommon to find more than one significant wave in a wave pattern that should be identified and assessed, particularly for vessels operating at super-critical speeds (examples were provided in Figures 3.5 and 3.6). Results presented by Macfarlane (2009) identified two distinct packets of waves, each packet with quite differing wave periods, but with the short-period wave being the highest (see the time series plot in Figure 3.6).

For the higher speeds, around $0.8 < Fr_L < 1.0$ (where the Fr_h are super-critical), Macfarlane (2009) found that the periods of the groups of long and short waves were approximately 4.0 s and 2.0 s respectively. The relevant figure from Macfarlane (2009) has been reproduced here in Figure 6.26 (note that this figure shows more full scale data than that visible in Figures 6.20 to 6.25 - only 50% of the full scale runs were reanalysed in the present study as this was deemed to be more than adequate for comparative purposes). It can be seen that the period of 4.0 s corresponds with the data for Wave B in the present analysis (Figure 6.24) and the period of 2.0 s corresponds with Wave C (Figure 6.25). Importantly, at each of the speeds in this range the highest wave was consistently Wave C. This highlights a major flaw in the commonly adopted criteria that only assesses the highest wave generated, as in these cases Waves A and B would have been ignored, but both are much more damaging to sensitive shorelines due to their much higher periods. The implications of this are investigated further in Chapter 7 when considering regulatory criteria.

In Section 2.1.9 the potential contribution of a vessel's propulsion system to the wave wake was discussed. Based upon the limited investigations and details presently available, it has been estimated that the height of some of the waves generated may increase by up to 10% due to the presence of the propulsors. All full scale trials data presented within this thesis, such as that presented in Figures 6.20 to 6.25, will naturally include the contribution from the vessel's propulsion system, whereas the model scale test data and output from the *Wave Wake Predictor* do not.

Location of Full Scale Trials	Vessel Description	Water Depth	Length Overall	Length Waterline	Vessel Disp.	Lateral Distance	Non-dimensional Coefficients			Speed Range	
		h (m)	L_{OA} (m)	L (m)	Δ (kg)	y (m)	$L/\nabla^{1/3}$	h/L	y/L	Fr_L	Fr_h
Macquarie Harbour, Tasmania	24 m Catamaran	12.0	24.0	21.71	55,000	30	5.76	0.55	1.38	0.28 - 1.00	0.38 - 1.35
Lower Gordon River, Tasmania	29 m Catamaran	12.0	29.0	25.36	69,600	50	6.22	0.47	1.97	0.16 - 0.28	0.23 - 0.41
Lower Maroochy River, Queensland	Skiboat #1	4.1	5.4	4.50	1,220	23	4.25	0.91	5.11	0.64 - 2.18	0.67 - 2.29
Lower Maroochy River, Queensland	Skiboat #2	4.1	6.3	5.50	1,340	23	5.03	0.75	4.18	0.87 - 1.73	1.01 - 2.00
Lower Maroochy River, Queensland	Skiboat #3	4.1	6.3	5.50	1,550	23	4.79	0.75	4.18	0.81 - 1.58	0.93 - 1.83
Upper Maroochy River, Queensland	Skiboat #4	2.5	5.4	4.60	1,520	23	4.03	0.54	5.00	0.70 - 2.05	0.96 - 2.78
Upper Maroochy River, Queensland	Skiboat #5	2.5	5.4	4.50	1,100	23	4.40	0.56	5.11	0.93 - 1.87	1.25 - 2.50
Noosa River, Queensland	Water Bus	6.2	8.2	8.20	3,900	23	5.25	0.76	2.80	0.42 - 1.53	0.49 - 1.76
Brisbane River, Queensland	Aluminium Runabout	6.1	7.75	6.75	2,480	23	5.03	0.90	3.41	0.42 - 2.09	0.44 - 2.20

Table 6.5 Details of full scale trials data used for validation

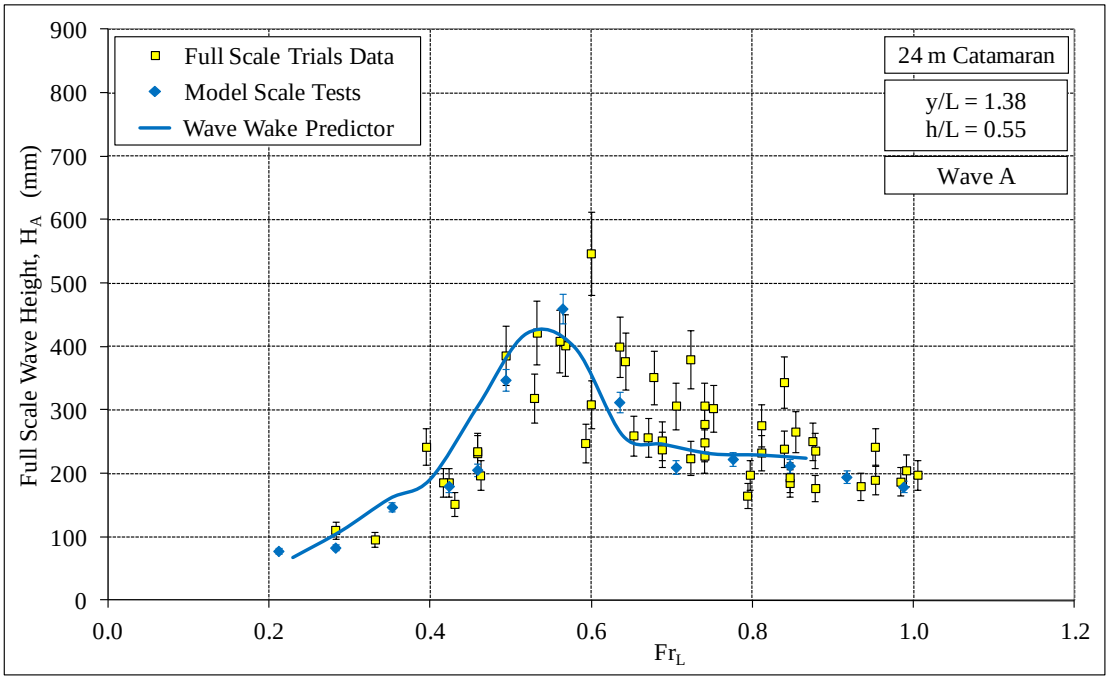

Figure 6.20 Validation: 24 m catamaran, Wave A, H_A as a function of Fr_L

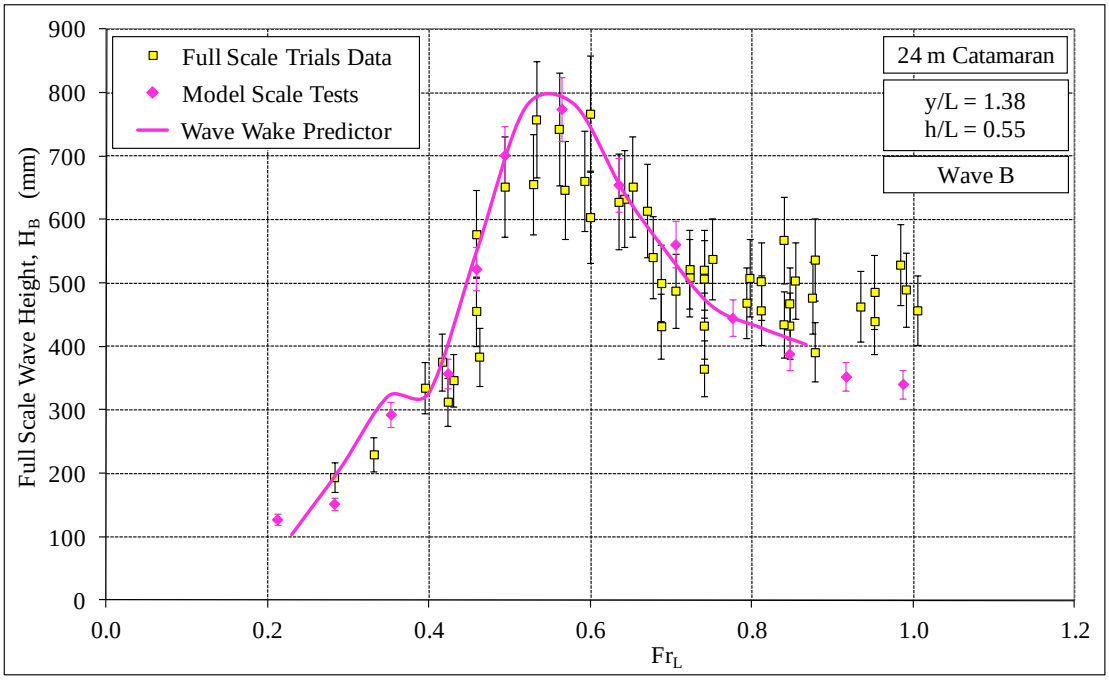

Figure 6.21 Validation: 24 m catamaran, Wave B, H_B as a function of Fr_L

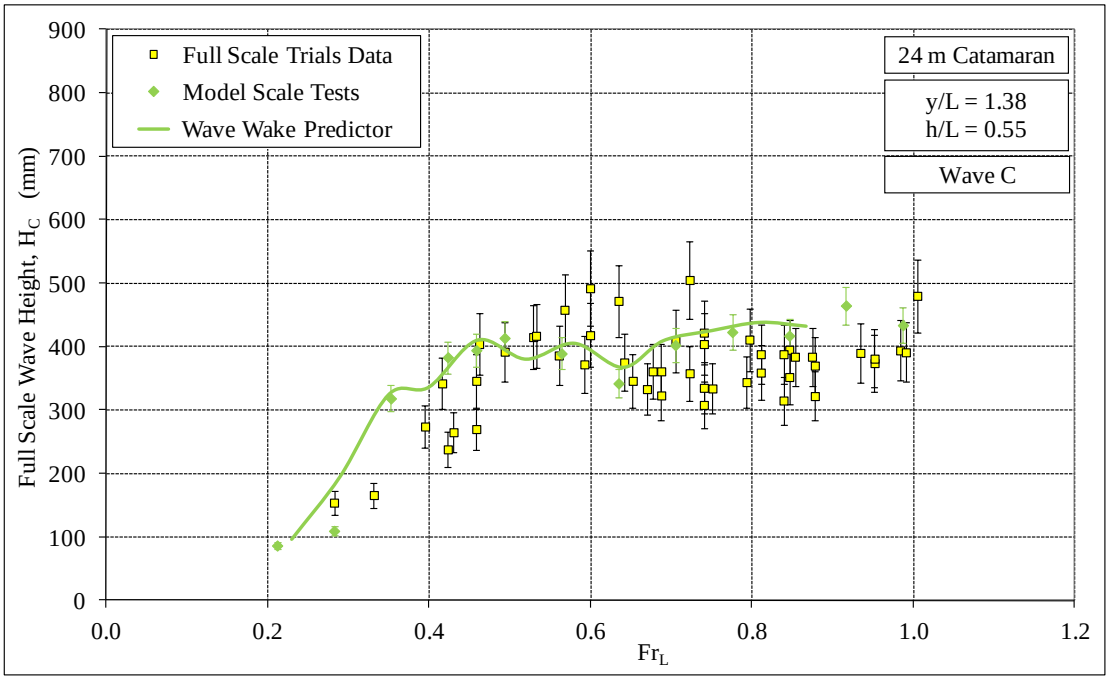

Figure 6.22 Validation: 24 m catamaran, Wave C, H_C as a function of Fr_L

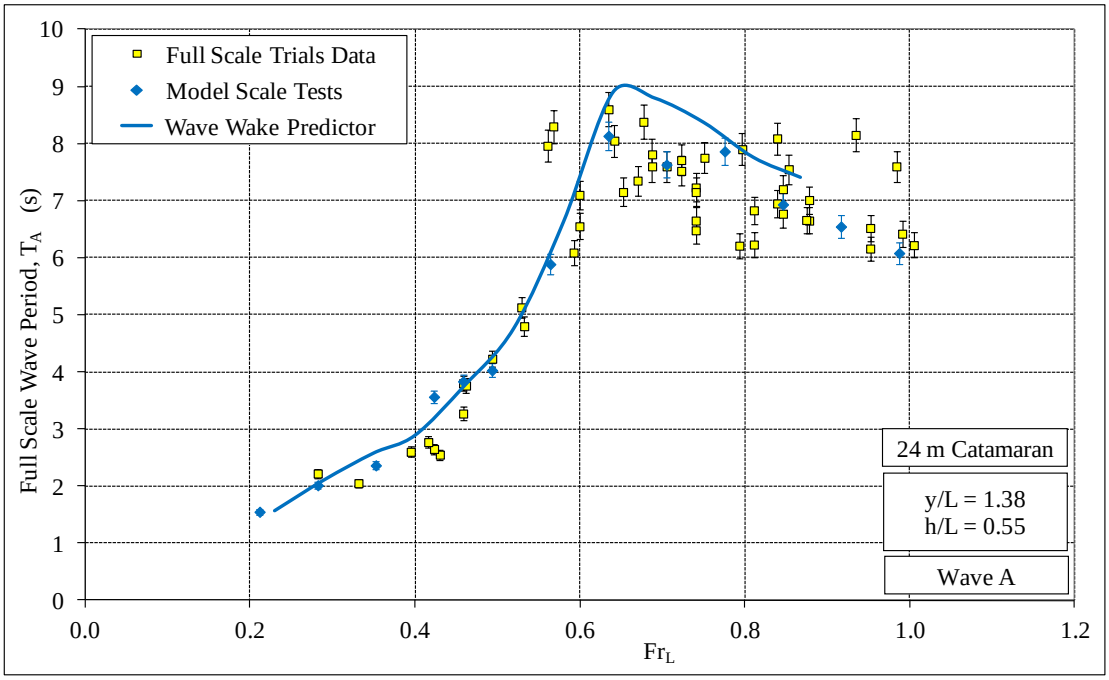

Figure 6.23 Validation: 24 m catamaran, Wave A, T_A as a function of Fr_L

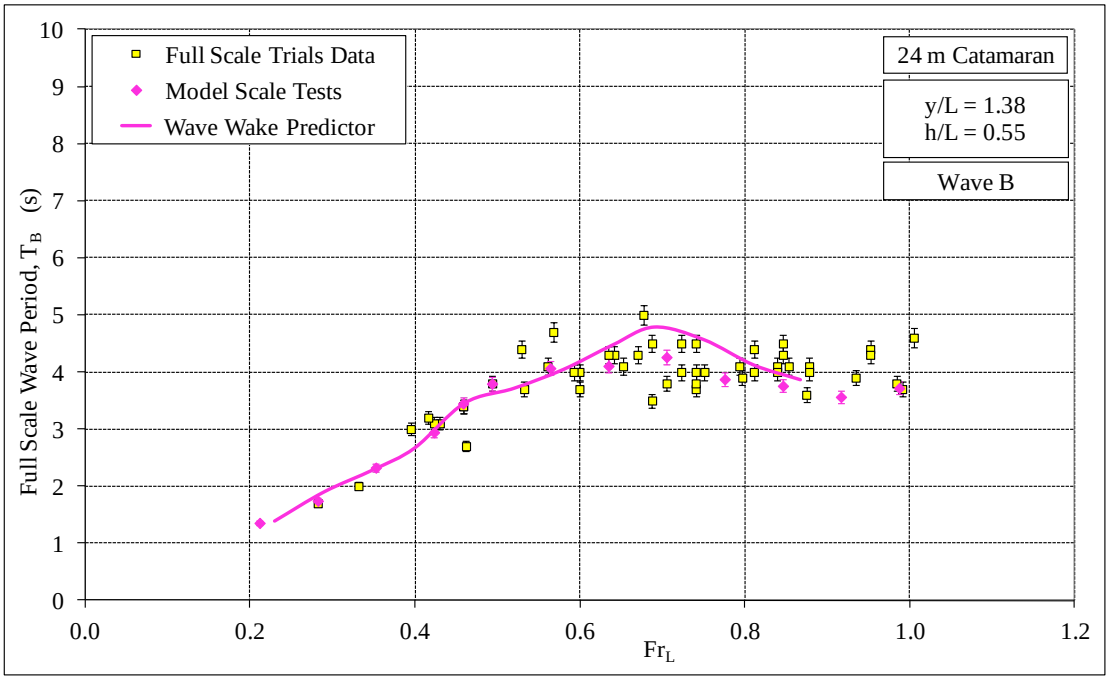

Figure 6.24 Validation: 24 m catamaran, Wave B, T_B as a function of Fr_L

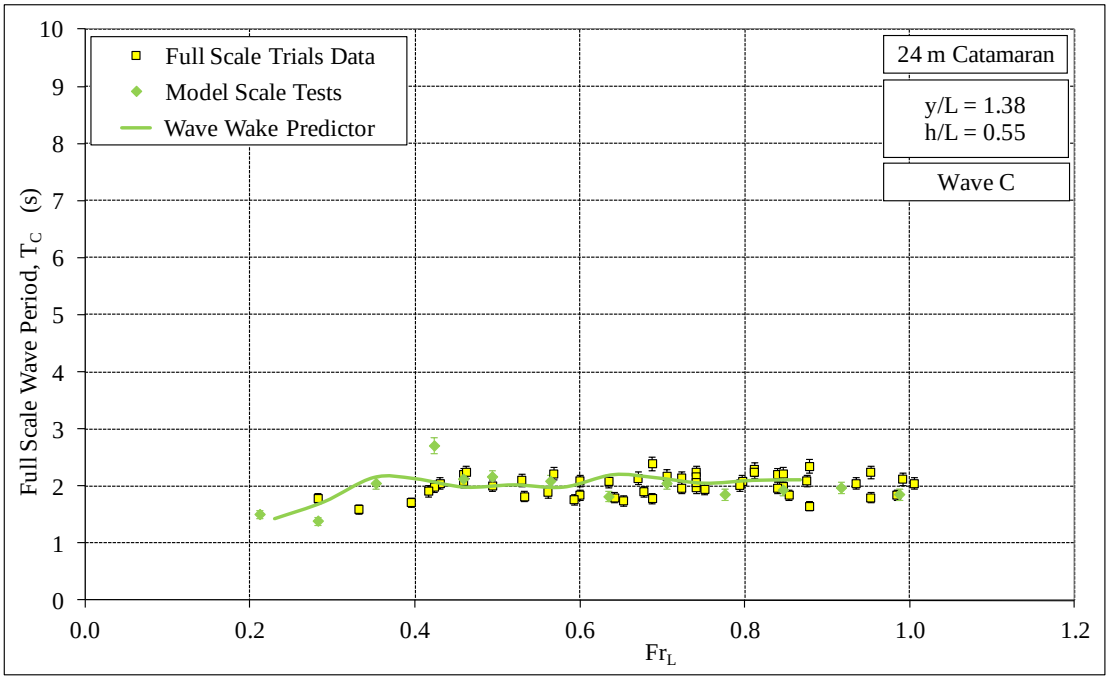

Figure 6.25 Validation: 24 m catamaran, Wave C, T_C as a function of Fr_L

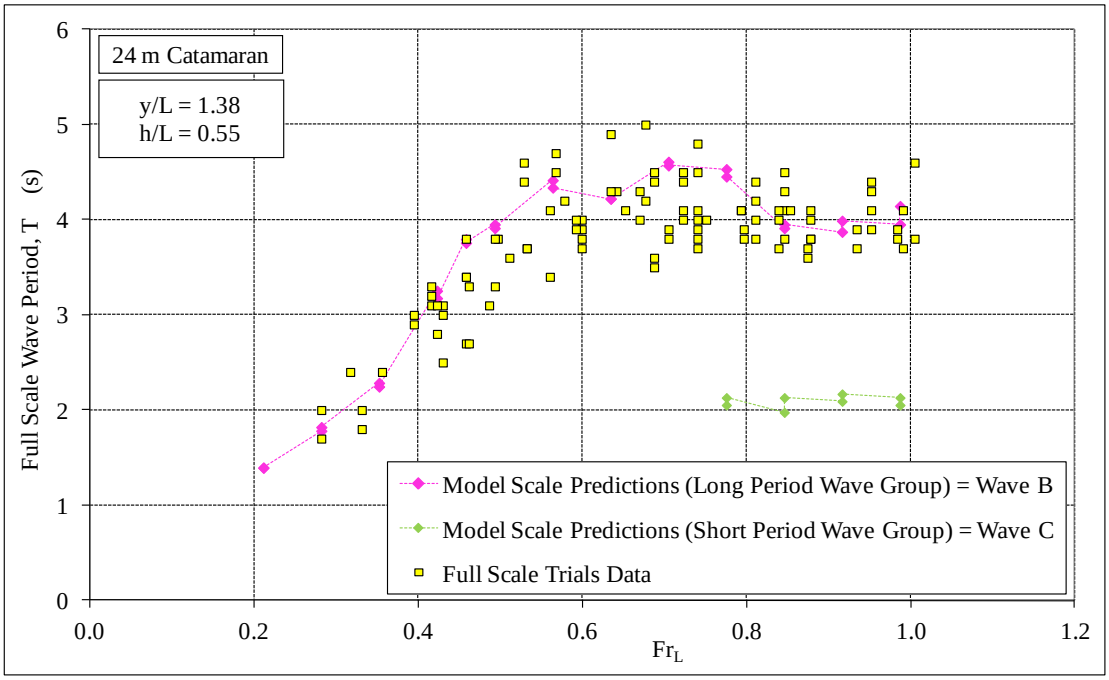

Figure 6.26 24 m catamaran, T as a function of Fr_L (from Macfarlane 2009)

6.5.4 Results: 29 m Catamaran

Full scale trials were conducted on a 29 m L_{OA} Catamaran over a small range of low sub-critical speeds, typical of the allowable speeds for commercial vessels on the lower Gordon River, as outlined in Table 6.5. The full scale trials results presented here originate from the same raw data as those presented in Macfarlane (2006), but the data has been reanalysed to obtain the wave heights and periods for Waves A, B and C. The full scale heights of all three of these waves as measured from the full scale trials and predicted by the *Wave Wake Predictor* for this vessel are presented as functions of Fr_L in Figures 6.27, 6.28 and 6.29 for Waves A, B and C respectively. Similar plots are provided in Figures 6.30, 6.31 and 6.32 for the periods of these three waves. As can be seen, in all cases there is good correlation as the predictions from the *Wave Wake Predictor* generally fall within the estimated limits of uncertainty for the full scale data.

It is clear from these six figures that the difference between the three waves, in height and period, is relatively minor, which is to be expected for these slow sub-critical speeds. In such circumstances, the identification and assessment of just the single highest wave, and its corresponding period, may be justified, but the examples shown in Figures 6.27 to 6.32 indicate that *Wave Wake Predictor* has the ability to distinguish between each wave.

Macfarlane (2006) compared model scale test data against the full scale trials data presented here, which displayed excellent agreement. This confirms that a correlation factor of close to unity be applied when using model scale data to predict full scale wave heights and periods for similar vessels operating within the range $0.1 < Fr_L < 0.3$.

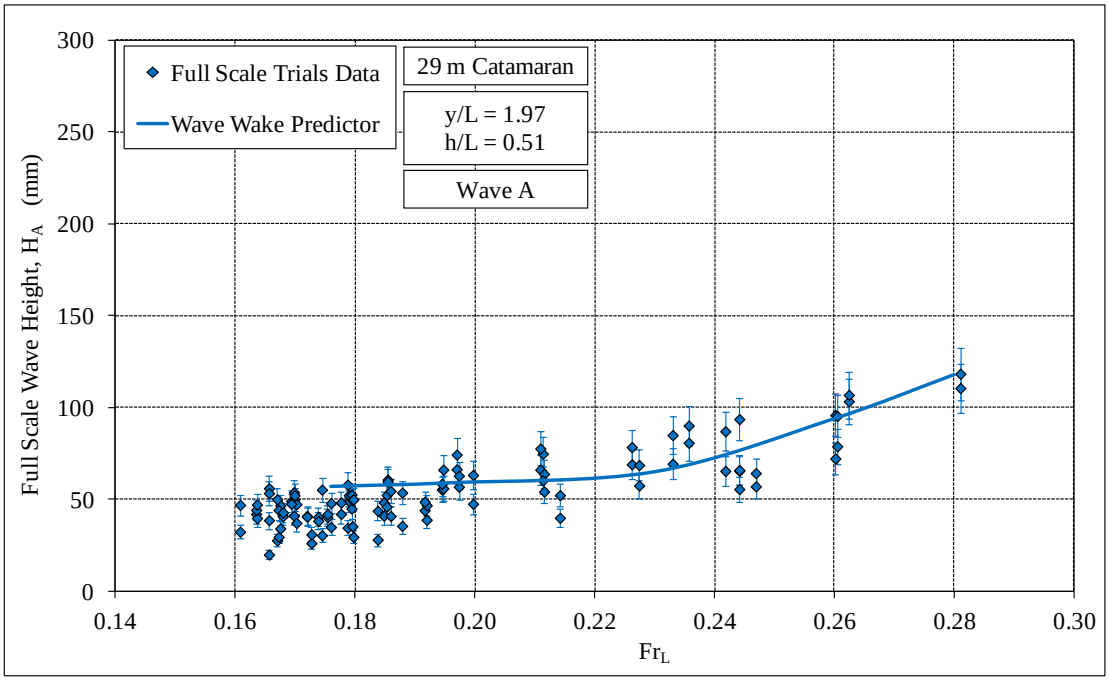

Figure 6.27 Validation: 29 m catamaran, Wave A, H_A as a function of Fr_L

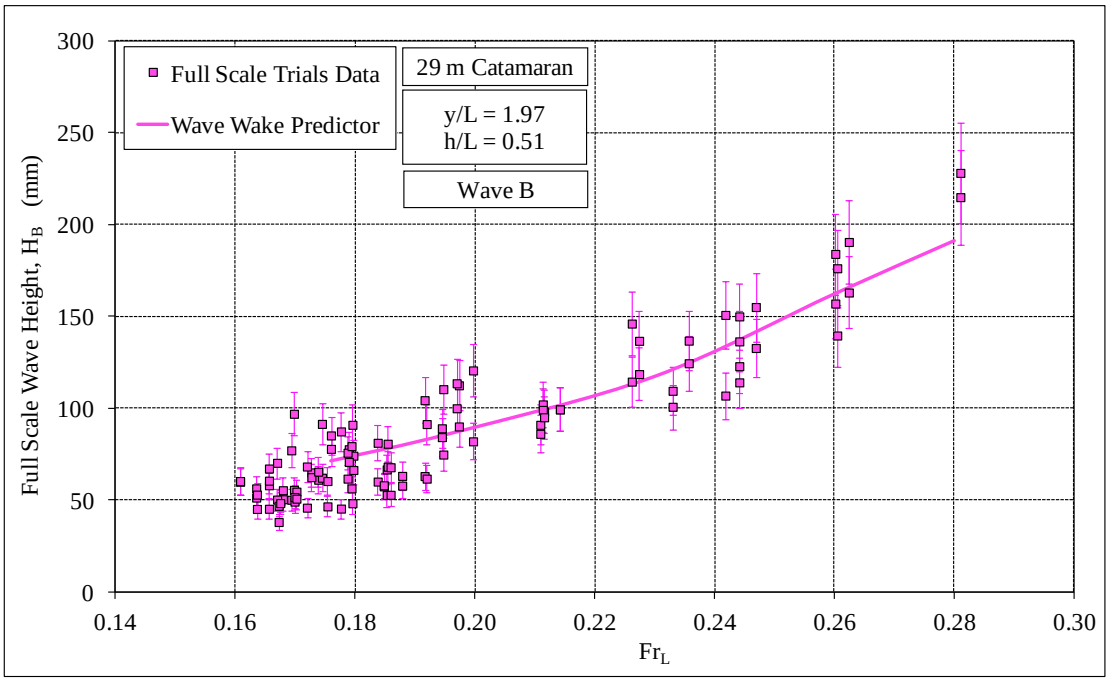

Figure 6.28 Validation: 29 m catamaran, Wave B, H_B as a function of Fr_L

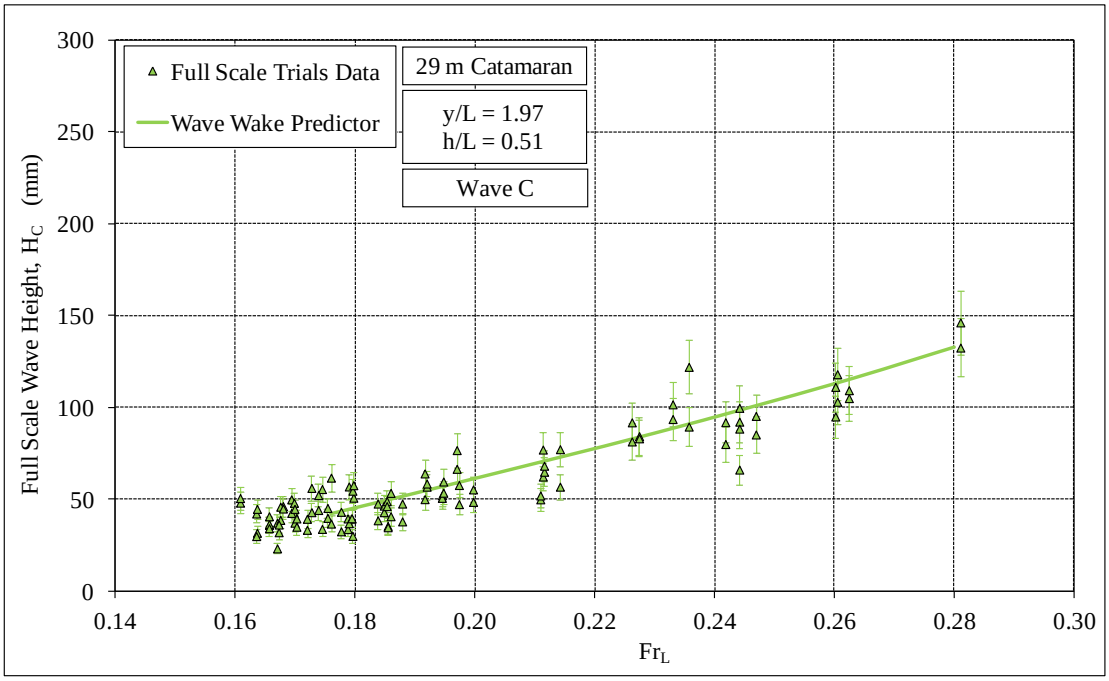

Figure 6.29 Validation: 29 m catamaran, Wave C, H_C as a function of Fr_L

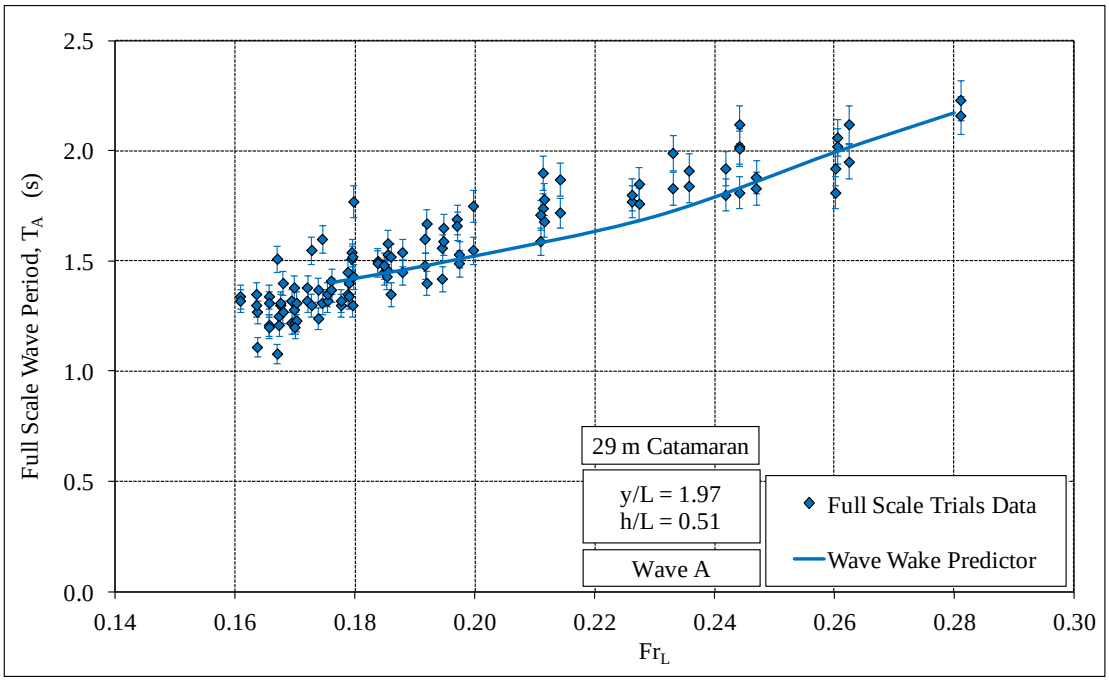

Figure 6.30 Validation: 29 m catamaran, Wave A, T_A as a function of Fr_L

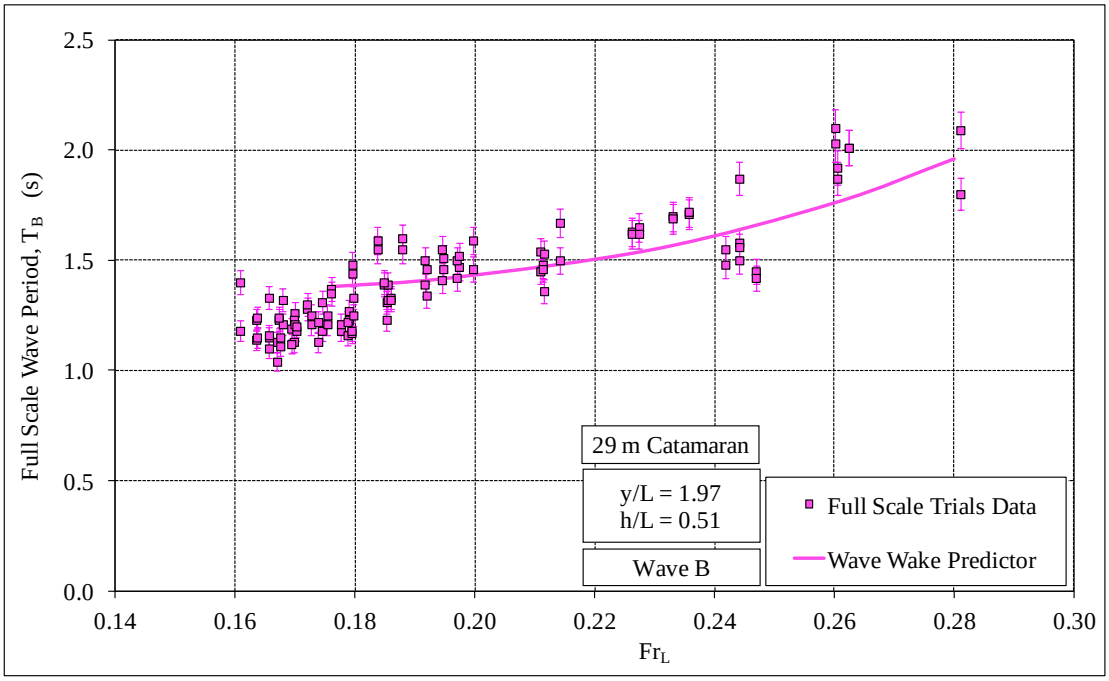

Figure 6.31 Validation: 29 m catamaran, Wave B, T_B as a function of Fr_L

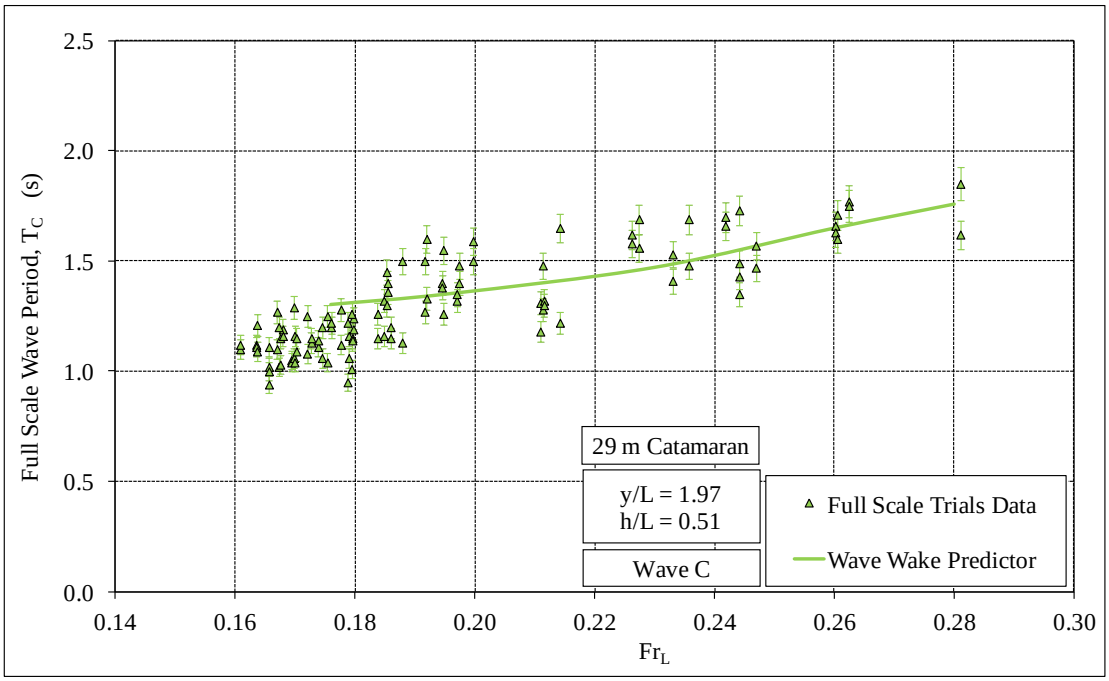

Figure 6.32 Validation: 29 m catamaran, Wave C, T_C as a function of Fr_L

6.5.5 Results: Ski Boats

Full scale trials were conducted on five different ski boats over a range of sub-critical, trans-critical and super-critical speeds, typical of those speeds regularly used by proponents of water-skiing and wakeboarding, as outlined in Table 6.5. The full scale trials results presented here originate from the raw data previously presented in Macfarlane and Cox (2003 and 2005), but the data has been reanalysed to obtain the wave heights and periods for Waves A, B and C. The measured heights of Wave A for these five ski boats are presented as functions of Fr_L in Figure 6.33. Also shown in this figure are the predicted heights from the *Wave Wake Predictor*. There are some small differences in the waterlines lengths and displacements of each of the five ski boats (refer Table 6.5), with the predictions presented in these figures based on the specific particulars for ski boat #3. Similar plots are provided in Figures 6.34 and 6.35 for the heights of Waves B and C respectively, and in Figures 6.36, 6.37 and 6.38 for the periods of Waves A, B and C. As can be seen, there is good correlation as the predictions from the *Wave Wake Predictor* generally fall within the estimated limits of uncertainty for the full scale data.

The original analysis of the full scale data as presented in Macfarlane and Cox (2003 and 2005) only considered the single highest wave. For all cases where the speed was greater than approximately $Fr_L = 0.9$ the highest wave was Wave C, meaning that all these 'maximum' waves also possess the shortest periods, thus they may not be the most significant when considering erosion of the shoreline.

The maximum available speed for predictions is limited by the maximum speed attainable within the test facility where the model scale experiments were performed (approximately $Fr_L = 1.35$ for the size of models for this type of hull form). Further investigation may be undertaken to allow the prediction tool to extrapolate beyond this limit in cases where reliable full scale data is available. This should be possible in the case of typical ski boats given that the correlation is good and the full scale data indicates that the wave height and periods at higher speeds is relatively steady.

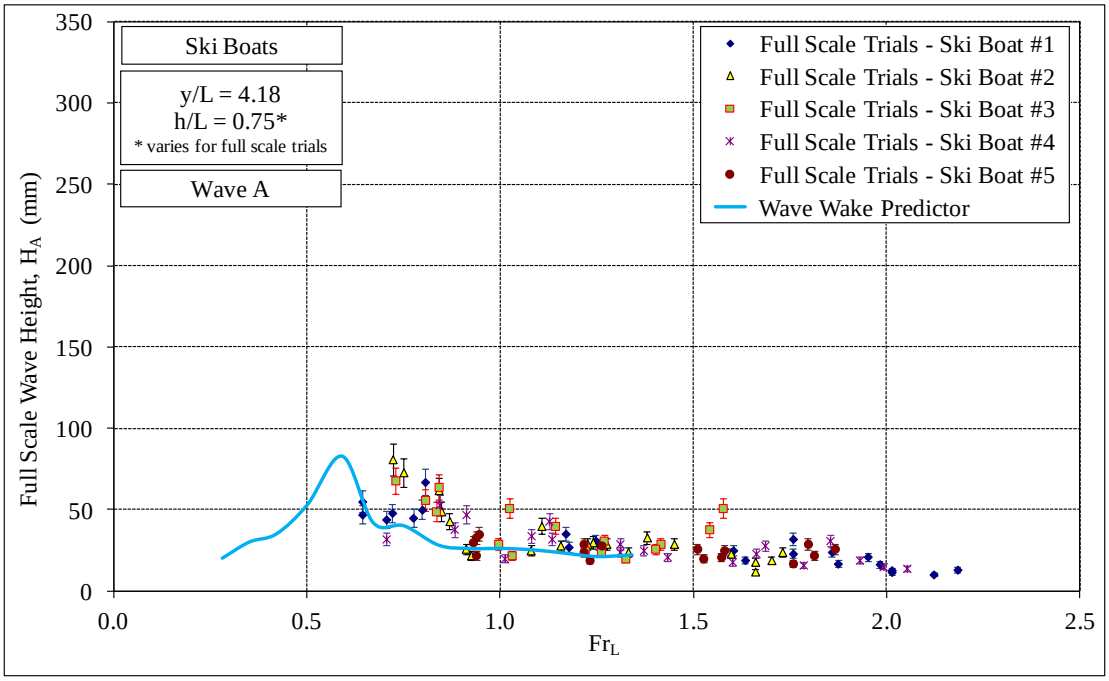

Figure 6.33 Validation: Ski boats, Wave A, H_A as a function of Fr_L

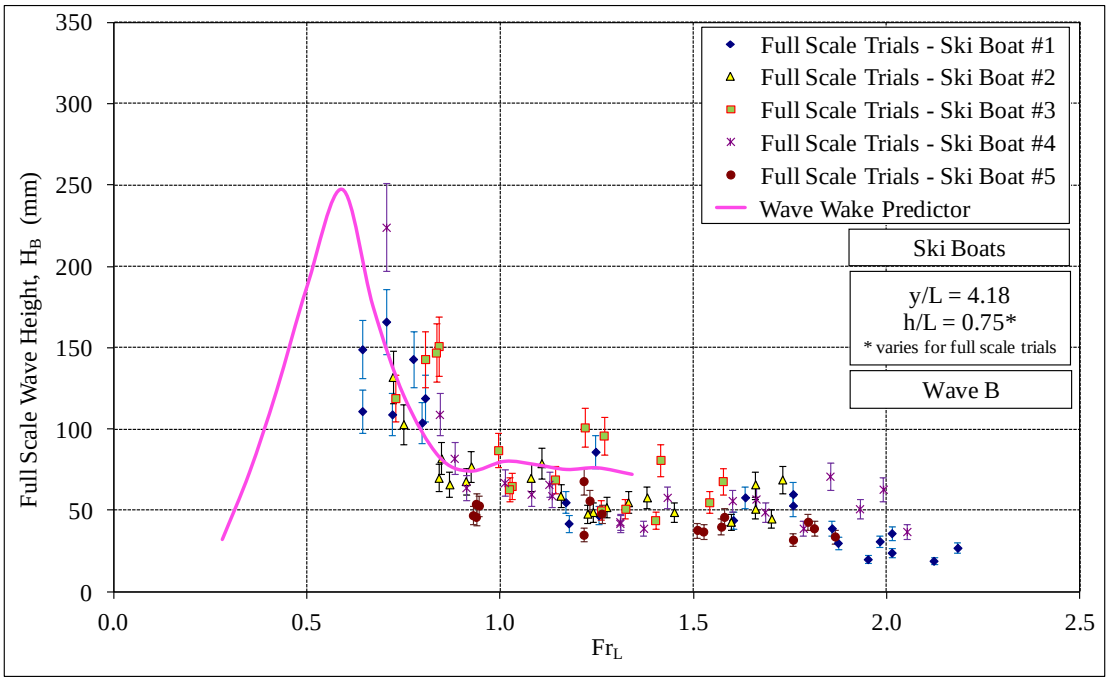

Figure 6.34 Validation: Ski boats, Wave B, H_B as a function of Fr_L

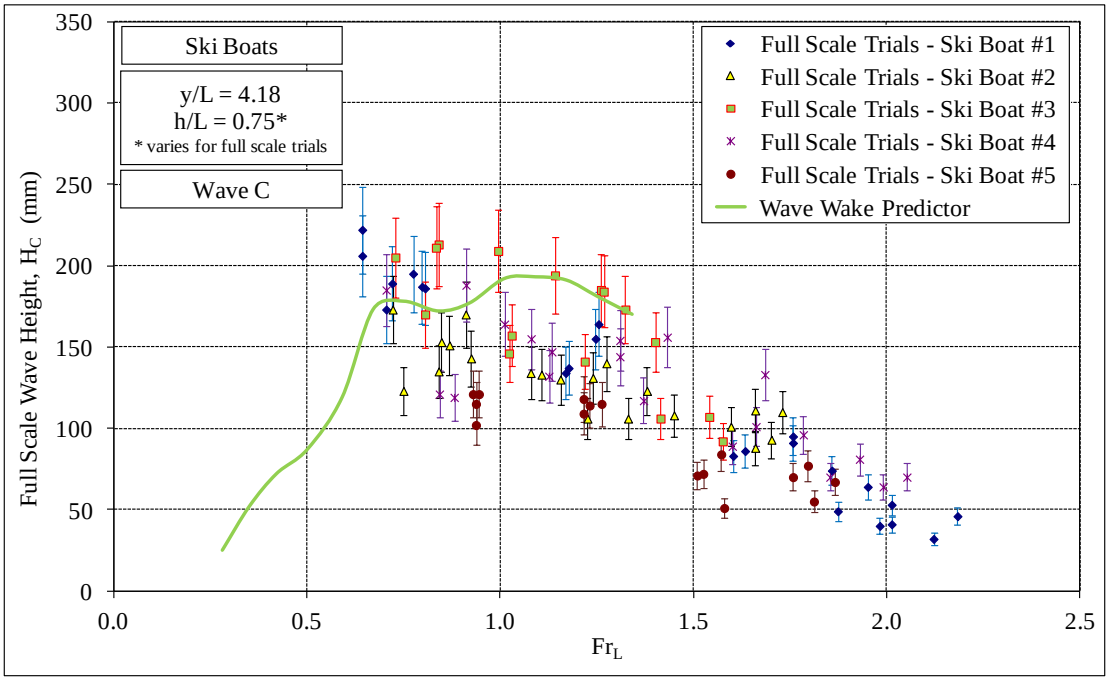

Figure 6.35 Validation: Ski boats, Wave C, H_C as a function of Fr_L

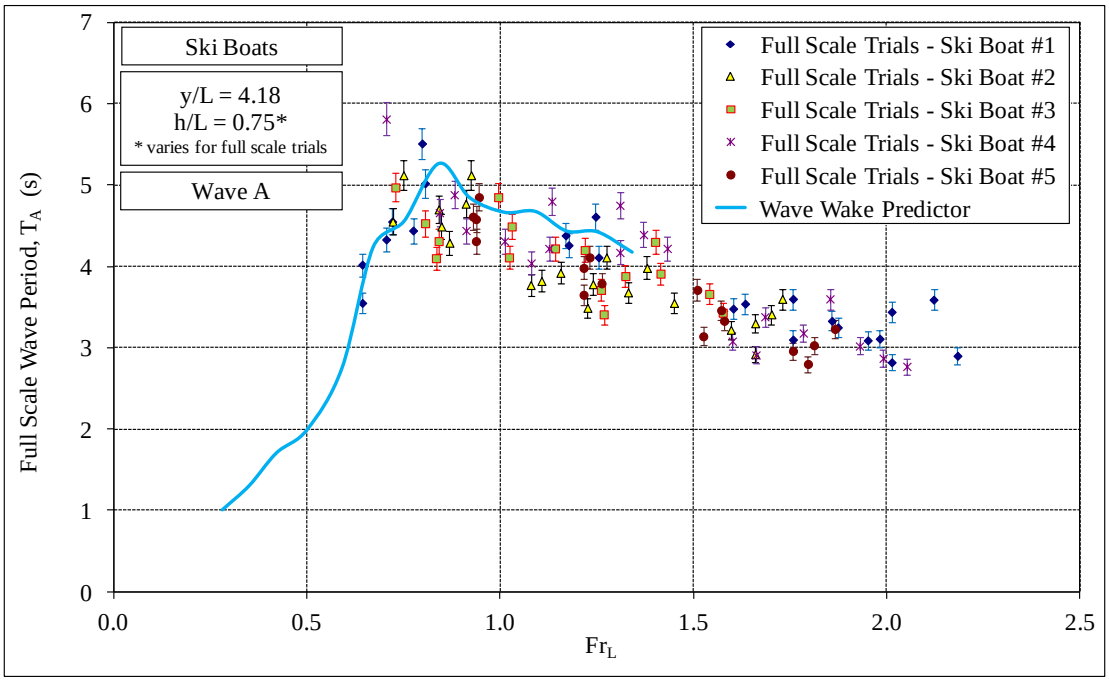

Figure 6.36 Validation: Ski boats, Wave A, T_A as a function of Fr_L

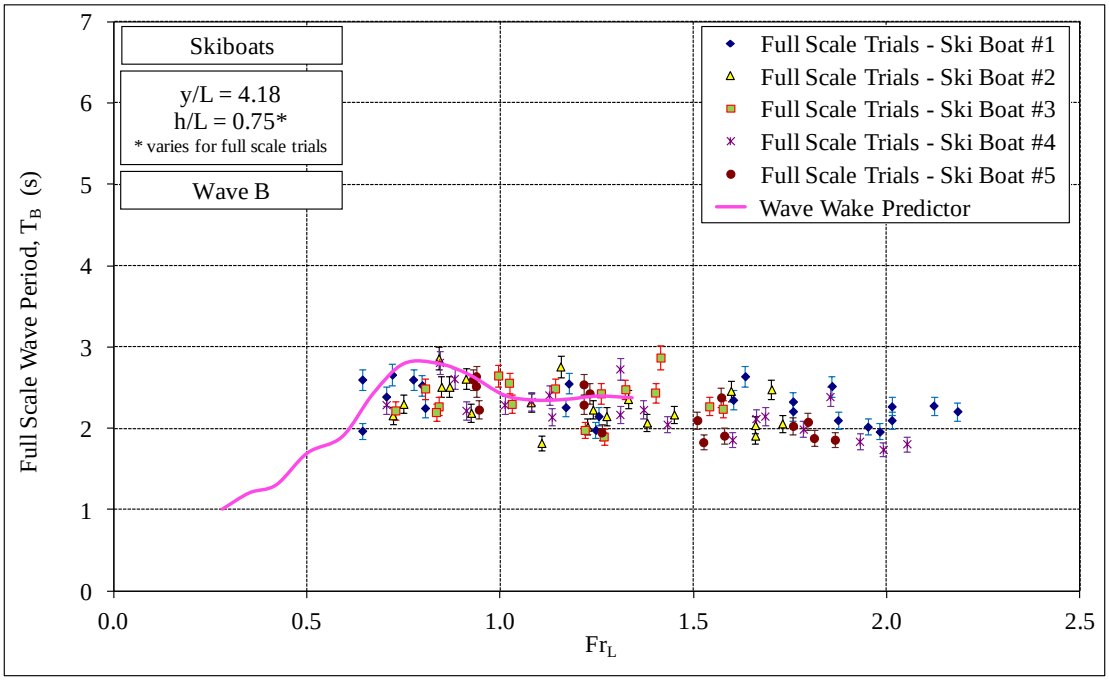

Figure 6.37 Validation: Ski boats, Wave B, T_B as a function of Fr_L

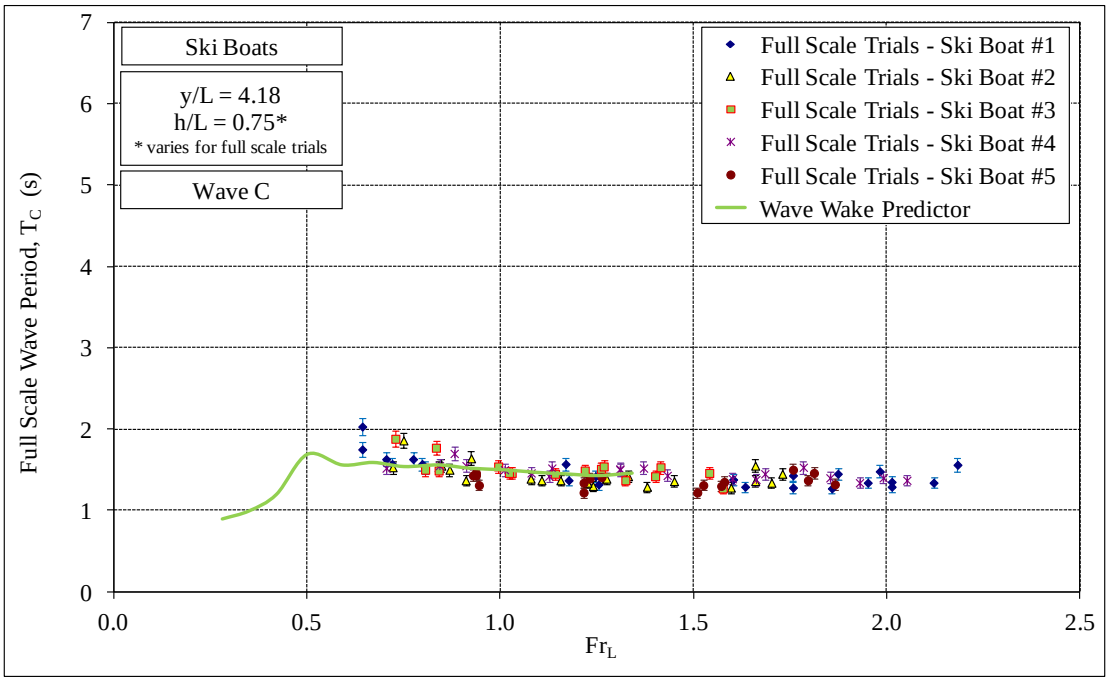

Figure 6.38 Validation: Ski boats, Wave C, T_C as a function of Fr_L

6.5.6 Results: Additional Vessels

A limited number of full scale trials were conducted on a further two small craft that are typical of those that regularly operate on Australian sheltered waterways, one an 8.2 m L_{OA} commercial passenger vessel (water bus) and the other a 7.75 m L_{OA} centre console aluminium runabout. Trials were conducted on both vessels over a range of sub-critical, trans-critical and super-critical speeds, as outlined in Table 6.5. The full scale trials results presented here were reanalysed to obtain the wave heights and periods for Waves A, B and C from data originally presented in Macfarlane and Cox (2003).

The full scale heights of all three of these waves as measured from the full scale trials and predicted by the *Wave Wake Predictor* for the water bus are presented as functions of Fr_L in Figure 6.39. A plot is provided in Figures 6.40 for the periods of these three waves. Similarly, a comparison between measured and predicted values of height and period for the aluminium runabout are presented in Figures 6.41 and 6.42 respectively. Although limited full scale data is available for both these cases there is still good correlation with the predictions from the *Wave Wake Predictor*. As was the case for the ski boats (Figures 6.33 – 6.38), it is the shortest period wave (Wave C) that has the greatest height at high speed (in excess of $Fr_L = 0.8$) for both of the small craft presented in Figures 6.39 (water bus) and 6.41 (aluminium runabout).

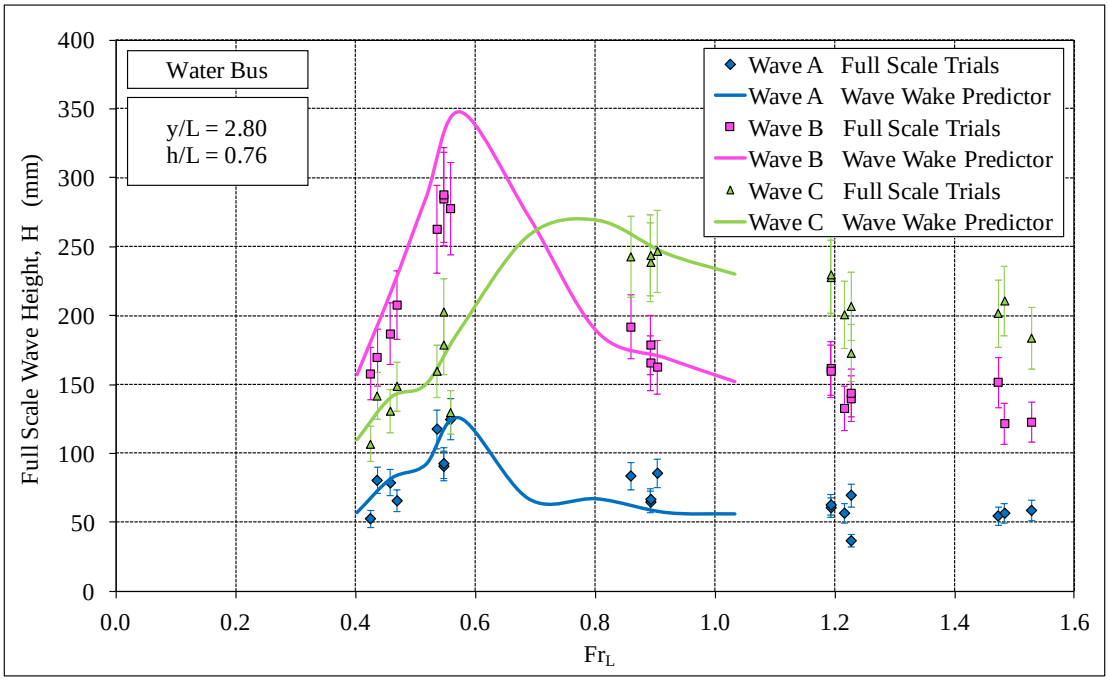

Figure 6.39 Validation: Water bus, H as a function of Fr_L

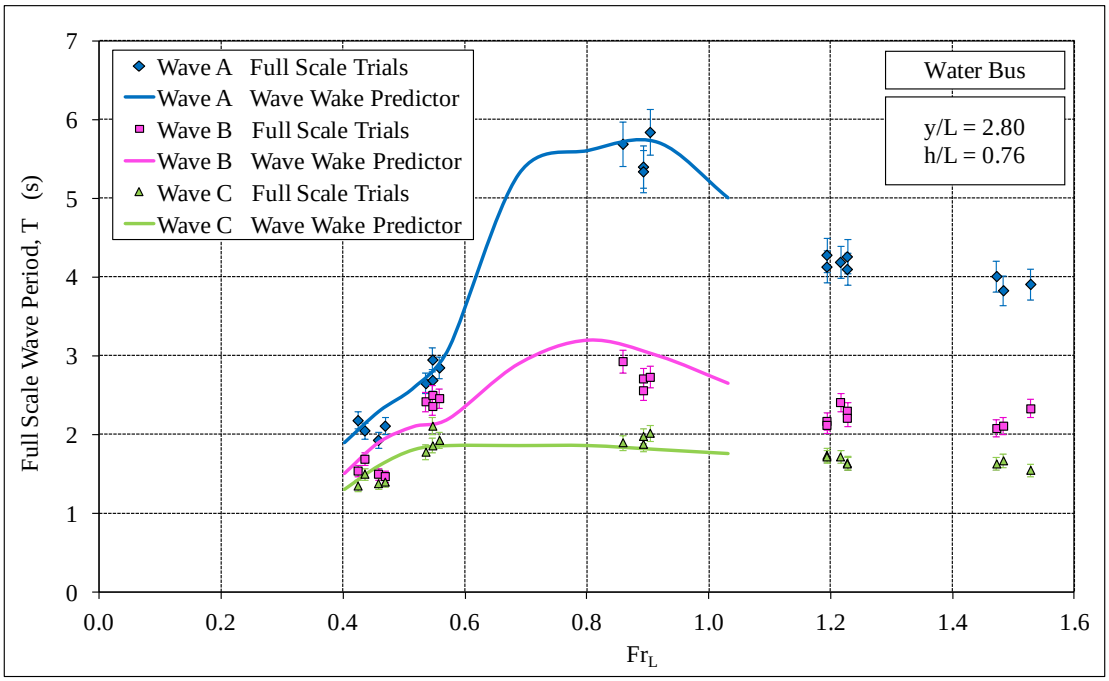

Figure 6.40 Validation: Water bus, T as a function of Fr_L

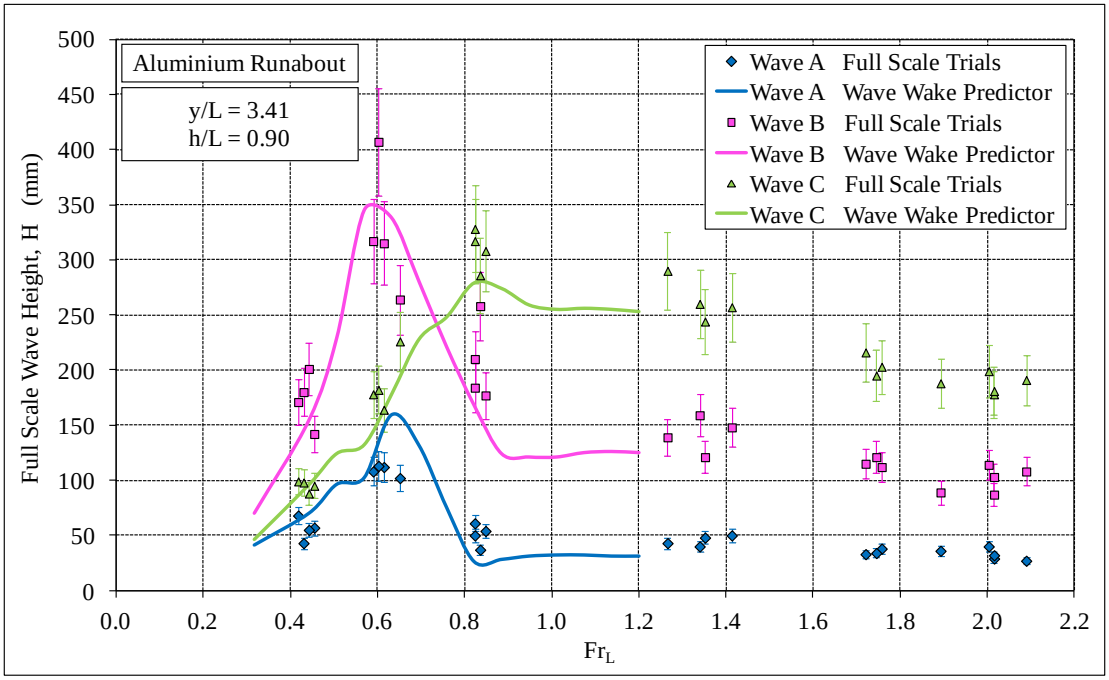

Figure 6.41 Validation: Aluminium runabout, H as a function of Fr_L

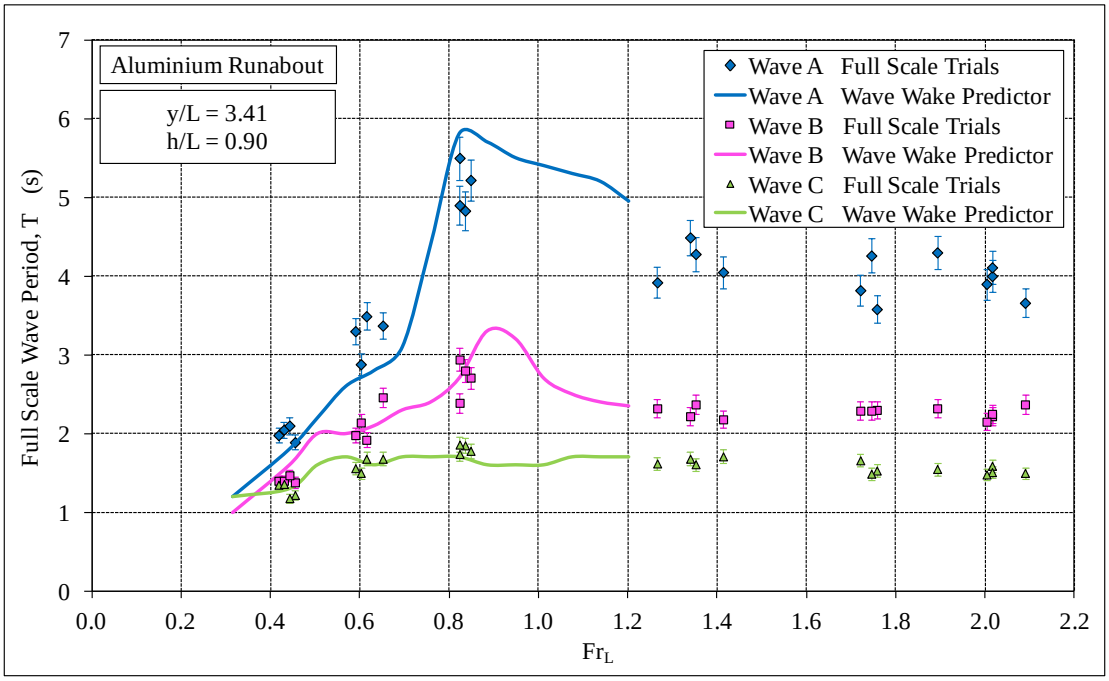

Figure 6.42 Validation: Aluminium runabout, T as a function of Fr_L

6.5.7 Concluding Remarks on Validation

Validation of the applicability of the *Wave Wake Predictor* has been achieved through the comparison of predictions against wave wake data collected from full scale trials conducted on two catamarans (L_{OA} of 24 and 29 m), five ski boats (L_{OA} ranging between 5.4 to 6.3 m), an 8.2 m L_{OA} commercial passenger vessel (water bus) and a 7.75 m L_{OA} centre console aluminium runabout. This ensured that validation of the predictive tool was investigated for a range of different vessel types operating at sub-critical, trans-critical and super-critical speeds. In all cases there was good correlation with predictions from the *Wave Wake Predictor* generally falling within the estimated limits of uncertainty for the full scale data.

There is a reasonable degree of scatter in the full scale trials data, but this is not unusual for tests in an uncontrolled environment. However, it is very clear from all the trials data at trans-critical and super-critical speeds that there are significant differences in the height and period between Waves A, B and C. This is particularly evident for the period of these three waves, for example, in most cases the period of Wave A was at least double, and up to four times, that of Wave C. It was also discussed how previous analysis of the raw data from the full scale trials concentrated just upon the quantification of the single highest wave, which was often found to be

Wave C – the wave possessing the shortest period. This was particularly the case for the smaller craft at Fr_L in excess of 0.8. This has led to the potentially most damaging waves (A and B), with considerably higher periods, being inadvertently ignored in previous environmental impact assessments.

The *Wave Wake Predictor* was found to provide reliable predictions when compared against results from model scale experiments that were not used within the development of the prediction tool.

By comparing predictions to independently measured values (both model and full scale) it can be seen that the *Wave Wake Predictor* provides a means to approximate the wave wake characteristics of marine vessels operating in either deep or shallow water. This provides a new method for estimating when damaging waves will be generated and provide guidance on key hull form parameters for minimising bank erosion and other wave wake issues.

Finally, agreement between the predictions based on both the independently conducted model scale tests and the *Wave Wake Predictor* against the full scale trials data confirm that a correlation factor of close to unity be applied when using model scale experimental data to predict full scale wave heights and periods for similar vessels.

Additional full scale data is available for many of the vessels listed in Table B.1 in Appendix B should further validation of the *Wave Wake Predictor* be necessary. The author has conducted preliminary comparisons between predictions and some of this data with all results adding further support to the abovementioned conclusions.

Chapter 7

Wave Wake Regulatory Criteria

7.1 Introduction

This chapter commences with background information on the need for wave wake criteria and a brief review of current practice. As outlined in Section 1.2, an aim of this study was to identify suitable criteria for assessing and regulating small commercial vessels and recreational craft when operating on sheltered waterways and the implementation of this criterion within the *Wave Wake Predictor*. This has provided a system that predicts all potentially damaging waves generated and assesses if each will meet or exceed suitable limits to minimise or eliminate wave wake related problems, such as shoreline erosion.

7.1.1 The Need for Wave Wake Criteria

The imposition of operating regimes to reduce the consequences of vessel wave wake is a relatively new phenomenon worldwide. Some long-standing vessel operating limits can be found, but are almost always based on blanket speed restrictions as opposed to other more scientific measures.

Before starting up any new commercial vessel operation it is important and often a requirement that a tolerance assessment be undertaken, consisting of a social impact, environmental impact and wave wake risk assessment (Feldtmann 2000). For example, in the United Kingdom it is a requirement that a Risk Assessment Passage Plan be prepared for all high-speed craft or any vessel that can potentially exceed $Fr_h > 0.85$ (Phillips and Hook 2006).

There are several reasons for introducing operating restrictions. Several of the more common reasons that have been associated with vessel operations on sheltered waterways include:

- *Reducing foreshore erosion.* As previously discussed, erosion is one of the most common concerns for protected waterways where the vessel wave wake regime has grown in magnitude well beyond the natural wave climate. In many cases, erosion can be readily attributed to increased vessel traffic. In other cases, wave wake may simply be an easily recognisable component of a

much broader range of problems, some of which may require solutions beyond what is politically palatable. It is occasionally the case that the erosion problem may not have manifested itself if the foreshore had not been altered in the first instance. A prime example is that of canal housing estates, where maximisation of land area is paramount to the financial return (Cox 2000). The branching canals are often deep and narrow to accommodate large recreational craft, but are unstable over a long term. Several years after the estate has been developed the erosion begins, but long after the developer has moved on.

- *Limiting the effects of wave wake on moored vessels*. The residential development of waterfront land has led to a proliferation of private marinas and jetties. This has become particularly so in cities where disused harbourside industrial land has been gentrified and replaced with medium density housing, complete with private vessel berthing facilities. The negative effects of constant vessel traffic on moored vessels quickly leads to confrontation.
- *Limiting the effects on maritime structures such as marinas (and their moored vessels) and seawalls*. This can be divided into three sub-sections. Firstly, commercial maritime structures such as seawalls are usually designed by qualified engineers using proven design methods. They rely on an assessment of the expected wave climate, which can be upset if a new type of vessel, such as a high-speed ferry, is introduced onto the waterway. Secondly, private seawalls often require no local council design assessment beyond the submission of a development application (and payment of the commensurate fee). Such seawalls may be designed and built with little regard to the wave climate and the fact that even stable foreshores are not static but in a state of dynamic equilibrium. There is the assumption that a seawall will last a lifetime, completely ignoring the fact that it exists in a dynamic environment and therefore may deteriorate at an ever-increasing rate if not properly designed. Thirdly, the effect of vessel wave wake on commercial activities such as marinas can have a financial consequence beyond just the infrastructure.
- *Ensuring that other waterway users are not adversely affected by vessel waves*. Vessel wave wake, notably the steep divergent waves, can prove dangerous for other waterway users, particularly rowers and junior sailors. The natural roll period of small craft often coincides with the period of these steep waves, placing these vessels in an uncomfortable or dangerous position.

- *Reducing the impact of shoaling waves on foreshore users*. The long-period waves created by high speed ferries operating at super-critical speeds in shallow water can grow in height substantially as they move into very shallow water. Instances have been reported in Europe and the United Kingdom where swimmers on beaches and people walking on seaside promenades have been caught unawares by waves that appear to come from nowhere, often long after the ferry has passed (Fresco 1999).
- *Using speed restrictions as an indirect means of addressing other issues, such as safety of navigation, noise and even unsociable behaviour*. This is common in built-up waterways surrounded by residential developments. Although the waterways are public spaces and open to public recreation, control is occasionally skewed away from public usage and somewhat towards protecting the amenity of waterfront residents. This is sometimes justifiably so, but it is also used as an easy, low-cost means of circumventing proper (and expensive) environmental policing, such as the control of engine noise.

The majority of the wave wake-limiting criteria implemented over the past two decades are targeted at either large, high-speed ferries on coastal routes or have been formulated to specific vessels on specific routes. Few are aimed at a broad range of vessel types, where a blanket speed limit is often viewed as the simplest method to define, implement and police.

7.1.2 Criteria Requirements

The development of wave wake criteria has gradually built with the growing interest in vessel wave wake issues. Nowhere in the world does there exist a comprehensive methodology for assessing wave wake-related impacts and introducing vessel operating regimes, without resorting to lengthy and expensive field studies.

Marine regulatory authorities have been overwhelmed by the complexity of the issues, which extend well beyond their traditional maritime roles. The knowledge base from which to draw is both limited in size and depth. This is a relatively new science and one that is a long way from developing conclusive answers.

In an effort to quantify vessel-generated waves, Macfarlane and Renilson (1999) suggested that the measure or measures used to form the basis of any wave wake criteria meet the requirements outlined in Table 2.1 (Section 2.1.6).

In addition to the requirements listed in Table 2.1, Macfarlane and Cox (2007) suggest that wave wake criteria must also have the following attributes:

- The number of variables must be limited if the criteria are to be applied without resorting to individual vessel testing;
- The criteria and their variable inputs should not be over-simplified to the point where their effectiveness is diluted;
- The degree of subjectivity in deriving the value of the variables must be reduced, otherwise the criteria will become open to manipulation and abuse; and,
- Any empirical equations derived must have a proper mathematical basis and obey the laws of similitude (i.e., must have certain properties that retain their mathematical integrity with varying input data so as not to be specific only to the data from which they were derived).

It is considered highly unlikely that any Government agency or commercial entity would be willing to commit funds towards a full wave wake testing program on every waterway with existing or potential wave wake problems. The aim of wave wake research should be to define wave wake characteristics that are independent of any given site and are formulated in a manner such that they can be transferred between sites with confidence.

The ultimate aim of the regulatory authorities would be to have a set of criteria that can be applied over a variety of waterway types without the need to resort to the testing of individual vessels on specific routes, though this will always remain the best option for sensitive areas where a high degree of certainty is required.

7.1.3 Review of Recent Developments

Several reviews of wave wake-limiting criteria implemented over the past two decades have been conducted (for example, Macfarlane 2002; Glamore *et al*. 2005; Murphy *et al*. 2006; Macfarlane and Cox 2007).

Possibly the most universally applied criterion is the *blanket speed limit*, where all vessels using the waterway are limited to a fixed maximum speed. This form of criterion is easy to both implement and police. However, there are two main drawbacks of the approach. Firstly, it can unfairly penalise certain vessels that may produce much ‘less’ wave wake than others, which is of concern for commercial

vessel operations and does not encourage operators/designers to optimise their designs for minimal wave wake.

The second point stems from the first, in that it single-handedly ignores the fundamental principles of ship hydrodynamics. The point at which a vessel begins to produce a significant wave wake is dependent not only on its speed, but also its waterline length. As described in Chapter 2, wave generation is a length Froude number dependent relationship and blanket speed limits ignore this fact. It is quite possibly the case that a proposed speed limit may have the correct intent for some vessels, but may allow others to operate at speeds greater than they should.

The introduction of high speed craft in the 1980s saw the establishment of more selective operating criteria, with the simplest form a limit on the maximum height of wave that any craft could generate. The intention was to reduce vessel speed in order to eliminate the generation of 'large' waves, but this only considered the height of the waves, not the period. This criterion has since been demonstrated to be at best unreliable and at worst incorrect. For example, a criterion of wave height was adopted for vessel operations on Sydney Harbour during the 1990s yet there have been reports of significant foreshore damage (Kogoy 1998). To further complicate matters, the lateral distance between the vessel's sailing line and the measurement point was often not specified, when this has clearly been shown to have a strong influence on wave height. Nor was a precise definition for wave height often provided. A review of published data in this field was undertaken by Macfarlane (2002) with the results highlighting that there are many varied forms and definitions for wave height, all of which can have considerable influence on the value derived. Fortunately, this overly simplistic criteria is no longer in common use.

Of the more advanced measures, wave power and energy (per wavelength and unit width of wave crest), as depicted in Equations 2.13 and 2.10 respectively, have gained the greatest acceptance in the profession. These are certainly the most widely quoted potential wave wake indicators.

In the late 1990s an energy-based criterion was adopted by Washington State Ferries for Rich Passage in Puget Sound. This criterion states that the energy (calculated using Equation 2.10) of the "highest significant wave of the wave train as measured 300 m from the centreline of vessel travel in deep water" must be less than 2,450 J/m (Stumbo *et al*. 1999). The value of 2,450 J/m was determined from a study on

specific sites in Rich Passage involving coastal engineers measuring beach erosion, marine biologists measuring the effect on marine organisms and naval architects measuring the vessel wave wake.

These criteria are now known as the Washington State Ferries (WSF) criteria and appear to have become a de facto standard for other regions in the United States, such as the San Francisco Bay area and Mobile Bay, Alabama (Austin 1999). The application of this criterion with its explicit energy limit (2,450 J/m) and lateral distance (300 m) to other regions is questionable. Strictly speaking, it is only applicable to the specific conditions in Rich Passage (such as bank slope, water depth, marine environment and tidal range). However, lacking any other yardstick, these criteria have been adopted and their use is spreading (Macfarlane and Cox 2007).

As with many European countries, Denmark has adopted high-speed coastal ferries as a viable means of passenger and car transportation. These vessels are typically large (in excess of 80 m) catamarans, though high-speed monohulls are becoming just as common (Kofoed-Hansen and Mikkelsen 1997). When entering and leaving port and along some near-coast sections of the routes, these high-speed ferries can create long-period waves that shoal in height as they move into shallow water. Inshore fishermen in small boats and swimmers on beaches have been caught by such waves, some being estimated at 3 m in height.

Kofoed-Hansen and Mikkelsen (1997) outlined the initial criteria proposed by the Danish Maritime Authority in response to the operation of high-speed car ferries in Danish waters. These limits are 0.35 m wave height measured in 3 m water depth with a corresponding wave period of 9 s. The energy of such waves remains substantial due to the wave period, but the intention of the height restriction is to limit wave shoaling. The shorelines in question are in partially exposed locations and cannot be considered as sheltered waters.

The methodology used to develop these criteria was fairly simple. Conventional ferries have been operating on the same routes for years with far fewer wave wake problems, producing waves that are regarded as acceptable. The high-speed ferry criteria result in a wave at the shoreline at least similar in height to that of a conventional ferry, even though the period may be longer.

These simple criteria were later re-worked into an equation, applicable in 3 m water depth, Kofoed-Hansen *et al*. (2000):

$$H_{HSC} \leq H_c \sqrt{\frac{T_c}{T_{HSC}}} \qquad (7.1)$$

Where H_c and T_c are the acceptable wave height and wave period of conventional craft, respectively. Standard values of H_c = 0.5 m and T_c = 4.5 s were determined from on-site measurements (Kofoed-Hansen and Mikkelsen, 1997).

Equation 7.1 is effectively a constant wave power criterion. Allowing this variable relationship between height and period goes some way towards a criterion that recognises the relative influence of different wave parameters, but this specific criterion was designed to limit wave height in near shore areas, not necessarily as a means of erosion mitigation.

Criteria similar to the above were also adopted in Sweden in 1999, where all operators must apply for, and obtain, an approval to operate from the Swedish Maritime Administration (Strom and Ziegler 1998; Allenström *et al*. 2003).

Similarly, the Marlborough District Council in New Zealand has adopted a bylaw to limit the speed of vessels operating in Tory Channel and Queen Charlotte Sound (Parnell and Kofoed-Hansen 2001; Croad and Morris 2003). Under these regulations, operators may apply for an exemption from the speed limits if they can demonstrate that, at a higher speed, the ship characteristics will comply with a variant of the Danish criteria. In this case, Equation 7.1 is applied wave-by-wave over the whole wave record, not just the long-period waves, and H_{HSC} and T_{HSC} are based on the clear definitions outlined in IAHR (1989). These two minor modifications have been implemented to avoid potential issues from the subjectiveness of identifying the single most significant wave in a wave train. At least one application submitted to the Council to increase the maximum allowable speed for a high-speed vessel is known to have been rejected on grounds that it would create damaging wave wake.

The Permanent International Association of Navigation Congresses coordinated a working group to develop guidelines for the effective management of wave wake from large high-speed vessels operating in coastal regions (PIANC 2003). It was concluded that experience to date confirmed that the effective management of large high-speed vessel wave wake is a multi-faceted problem that defies a simple “one

size fits all" solution. Waterway managers and high-speed vessel operators are encouraged to follow the guidelines for conducting a route assessment and developing management measures.

7.1.4 Wave Energy or Power?

As discussed, the vast majority of wave wake regulatory criteria used today are now based upon both the wave height and period of a characteristic wave. Many of these criteria use wave power or energy, but both of these are derived from the two basic measures of wave height and period.

Both wave power and wave energy were shown in Section 3.4 to be useful indicators of erosion potential, however, there is some conjecture as to which may be the more relevant. Power is a measure of the wave energy expended over a given time whereas energy is a simple measure of the energy content of a particular wave.

Wave power is a parameter commonly used in coastal engineering where coastal processes occur over long periods and therefore may be better characterised by a time-based parameter such as power.

However, wave energy is often used when assessing the wave wake from a passing vessel as this can define a discrete event that has a definite start and finish, compared to naturally occurring waves such as wind waves that are often better analysed over time. Similarly, tidal events are often used as an argument against energy-based criteria, as tides are both long in period and can be high in range, yet may cause little erosion relative to their "energy". It is reasonable to argue that tidal shorelines already have features to resist tidal impacts (tides are cyclical and not incidental), and tidal flows do not have a wave-like structure.

In this context, wave power can sometimes be a misleading measure. For instance the values of different characteristic parameters of several deep-water waves are shown in Table 7.1. The values of wave power and energy are relative only, having been referred back to their base parameters of H^2T and H^2T^2 respectively (from Equations 2.13 and 2.10 respectively).

In this example, the energy of the single most significant wave from all three wave 'generators' (wind, small cruise boat and high speed river ferry) are equivalent (i.e.

the values in the last column are all the same). If wave height was used as the determinant of erosion potential, the values in Table 7.1 would suggest that the wind waves generated in high wind conditions would be more damaging than any of the boat waves. A similar result is found for wave power, H^2T. It must be noted that the relative erosion is not a linear function of any wave parameter, as the doubling of any wave parameter does not necessarily lead to a doubling of erosion levels.

Example	**Type**	**Height, H** (m)	**Period, T** (s)	**Power, P** $\mathbf{H^2T}$ (W/m)	**Energy, E** $\mathbf{H^2T^2}$ (J/m)
1	Large wind wave	0.30	1.33	0.12	0.16
2	Small cruiser	0.23	1.75	0.09	0.16
3	High-speed river ferry	0.08	5.00	0.03	0.16

Table 7.1 Wave parameters for typical sheltered waterway waves
(note that wave power and energy are per unit crest width and wavelength)

However, as previously discussed, experience gained worldwide over the past decade has demonstrated that the most potent damage has been caused by the operation of vessels that generate longer wave periods when operating in confined waterways. Wave energy is therefore regarded as a more reliable measure of the erosion potential of vessel wave wake within such regions due to the equal weighting of both wave height and period. Thus, a wave energy-based approach has been adopted within the present study in the development of suitable regulatory criteria for the operation of small craft on sheltered waterways.

7.2 Proposed Regulatory Criteria

7.2.1 The *Wave Wake Rule*

It is recommended that wave wake criteria appropriate for regulating vessel operations on sheltered waterways be based upon a variant of the concept originally formulated for operation of large high speed craft operating in Danish coastal waters (Equation 7.1). As previously covered, there is a constant wave power relationship in

this equation, whereas in the present study, it is proposed that it is wave energy that remains constant, as indicated in Equation 7.2:

$$H = H_b \frac{T_b}{T} \qquad (7.2)$$

where both H_b and T_b are benchmark values (constants) and appropriate values should be determined to suit the site-specific conditions. This topic is discussed further in the following sub-section.

The constant-energy approach (as shown in Equation 7.2) is referred to as the *Wave Wake Rule*.

7.2.2 Benchmark Values of Wave Height and Period

The benchmark values for wave height and period in Equation 7.2, H_b and T_b, can be determined through one of several methods, with the primary aim to identify the threshold below which the impact of vessel wave wake no longer presents an issue for the region of concern.

An ideal example to illustrate one method is from the original application of the Danish constant-power criteria, where Kofoed-Hansen and Mikkelsen (1997) measured the 'acceptable' waves of the conventional ferries already operating on the route of interest. The benchmark values in this case were $H_c = H_b = 0.5$ m and $T_c = T_b = 4.5$ s.

An example of another suitable method for determining appropriate benchmark values is through the conduct of on-site measurements of the rate of erosion, such as the experiments described in Section 3.4.3 where the turbidity resulting from vessel wave wake was measured. In the case of the results presented in Section 3.4.3, the benchmark values where bank erosion was found to be minimal or negligible for Zones 1 and 2 on the lower Gordon River were determined to be $H_b = 70$ mm (Figure 3.7) and $T_b = 1.0$ s (Figure 3.8).

These elevated turbidity results are plotted, along with the *Wave Wake Rule* using these benchmark values in Figure 7.1, where wave height is plotted as a function of wave period. The curve for the *Wave Wake Rule* indicates a line of constant energy equal to that of the benchmark values. The intention is that the height and period of

each of the three significant waves (A, B and C) generated by a vessel (at a specific speed and lateral distance) must lie below the *Wave Wake Rule* to indicate that minimal or no erosion (turbidity) will occur.

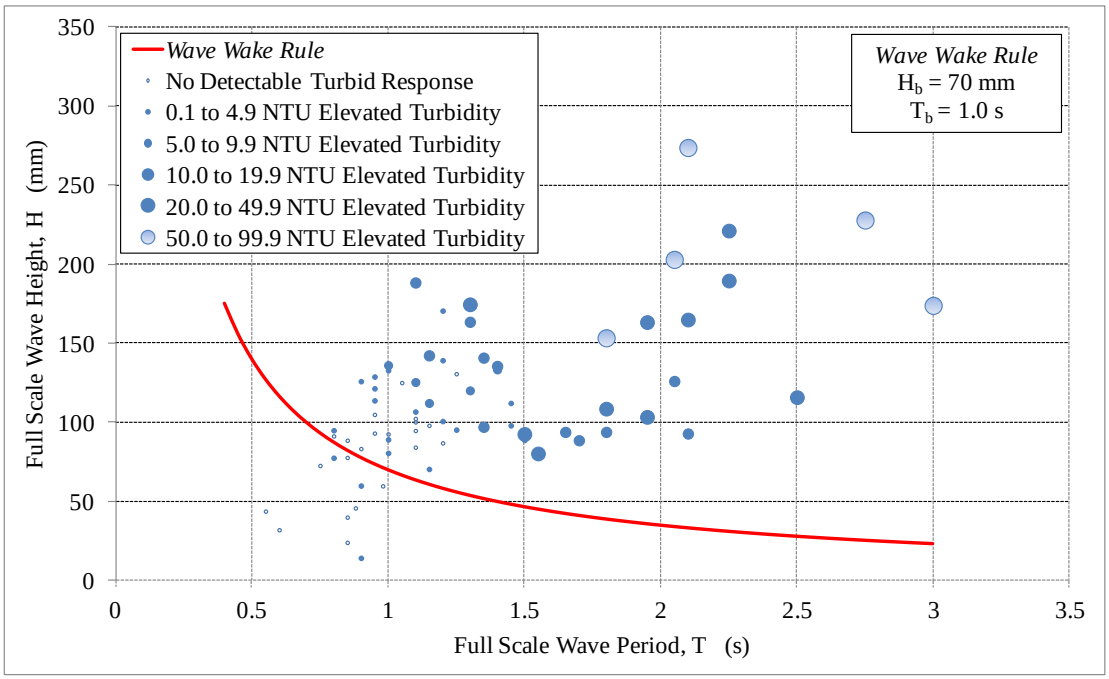

Figure 7.1 Measured turbidity used to define *Wave Wake Rule* constants (experimental data from Macfarlane *et al*. 2008)

A further example of an alternative method for determining appropriate benchmark values is through the comparison with the natural wind wave climate. As covered in Section 2.5.4, sheltered shorelines in a wind wave environment are often dynamically stable and beach areas adjust in response to the prevailing wave climate and sediment budget. As a result, several studies have attempted to assess vessel generated waves by comparing their energy against those of the local wind waves (Pattiaratchi and Hegge 1990; Soomere and Rannat 2003; Glamore 2008; Macfarlane and Gourlay 2009; Kelpsaite 2009; Kelpsaite *et al*. 2009; Houser 2010).

As an example, both Pattiaratchi and Hegge (1990) and Macfarlane and Gourlay (2009) used hindcasting techniques (USACERC 1977 and 1984, refer Section 2.5.4) to estimate the height and period of the naturally occurring wind waves at several sites on the Swan River in Perth, Western Australia, and compare these against vessel wave wake. Typical results for several sites on the river are provided in Table 7.2, where values for the following three cases are provided: maximum, 1% exceedence and 10% exceedence. The exceedence values indicate the percentage of wind waves

that exceed the given values over a given period of time, such as an annual basis. The expected wind wave heights and periods vary throughout the river due to changing fetch lengths from the meandering nature of the river and varying widths and wind conditions.

Further consideration of the frequency of vessel traffic and shoreline erosion thresholds may be required to determine which of these levels would be the most appropriate as benchmark values for use in the *Wave Wake Rule*, but it is unlikely to be the maximum values if the vessel is to make regular transits of this section of river and erosion is to be avoided.

Wind Waves Level	Site #1		Site #2		Site #3	
	H (mm)	T (s)	H (mm)	T (s)	H (mm)	T (s)
Maximum	180	1.1	220	1.4	410	1.8
1% exceedence	90	0.8	120	1.1	240	1.5
10% exceedence	40	0.6	70	0.8	140	1.3

Table 7.2 Example wind wave heights and periods on Swan River (Pattiaratchi and Hegge 1990; Macfarlane and Gourlay 2009)

In summary, three specific examples of very different methods that can and have been used to determine appropriate benchmark values for application with the proposed *Wave Wake Rule* have been provided, including (a) the characteristics of waves generated by vessels that have proven through successful operation that they generate an acceptable wave wake, (b) direct measurement of erosion caused by passing vessels, and (c) comparing against the characteristics of wind-generated waves that naturally occur in the region (either through hind-casting or measurement). Other possible methods may also exist.

7.3 Use of the *Wave Wake Predictor* with the *Wave Wake Rule*

One of the research questions posed in Section 1.2 relates to the development of a wave wake prediction tool that could be combined with suitable regulatory criteria to readily and accurately assess the wave wake of marine vessels, particularly when operating in confined waterways with shallow water depths. A significant advance in the assessment of wave wake offered by the proposed method is the combination of the predictions of all three key waves from the *Wave Wake Predictor* (Waves A, B and C) with the constant energy-based regulatory criteria provided by the *Wave Wake*

Rule. By considering each of these waves it is assured that all potentially damaging waves will be assessed, which was not possible with many of the assessment processes currently in use that consider just a single significant wave.

For instance, some high-speed vessels, particularly those that claim to possess "wave wake reducing characteristics" (which are more strictly often only wave *height* reducing characteristics by way of high length-displacement ratio) have the potential to satisfy an apparently reasonable energy criterion but still cause erosion. Prime examples of this are the various "low-wave wake" catamaran ferries operating on the Parramatta and Brisbane Rivers. Such vessels have been found capable of generating wave periods considerably in excess of the existing waterway wave climate (up to 4-5 times longer), but with low accompanying height when travelling at high speed. It is likely that these low but long-period waves would not have been assessed in any scenario that only assesses a single maximum wave.

An example of this is illustrated graphically in Figure 7.2 where the *Wave Wake Rule* is plotted along with the predictions from the *Wave Wake Predictor* for the 24 m Catamaran discussed in Section 6.5.3 (and Macfarlane 2009) where full scale trials data for this vessel was used as part of the validation process. In Figure 7.2 wave height is plotted as a function of wave period and the curve for the *Wave Wake Rule* indicates a line of constant energy equal to that of the benchmark values (in this example H_b = 450 mm and T_b = 2.5 s). The three significant waves (A, B and C), generated by the 24 m Catamaran at the supercritical speed of Fr_h = 1.11, as predicted by the *Wave Wake Predictor* are shown. In this example the Fr_L = 0.83, h/L = 0.55 and y/L = 1.38.

The significant feature of Figure 7.2 is that Wave C – the highest wave – lies below the *Wave Wake Rule*, indicating that it meets the criteria, however both Waves A and B clearly exceed the same constant-energy criteria. This example confirms that current wave wake assessment methods based on a single maximum wave cannot ensure that all waves within a wave train will meet any constant-energy (or similar) criteria. Subsequently, it is possible for vessels assessed using such techniques to pass the criteria, but may still cause the various wave wake related problems previously discussed.

The identification of the three significant waves, including the longest, highest and maximum energy waves, combined with the use of a constant-energy wave wake

criteria (with benchmark values appropriate for the region of interest) will ensure that these problems are avoided or minimised.

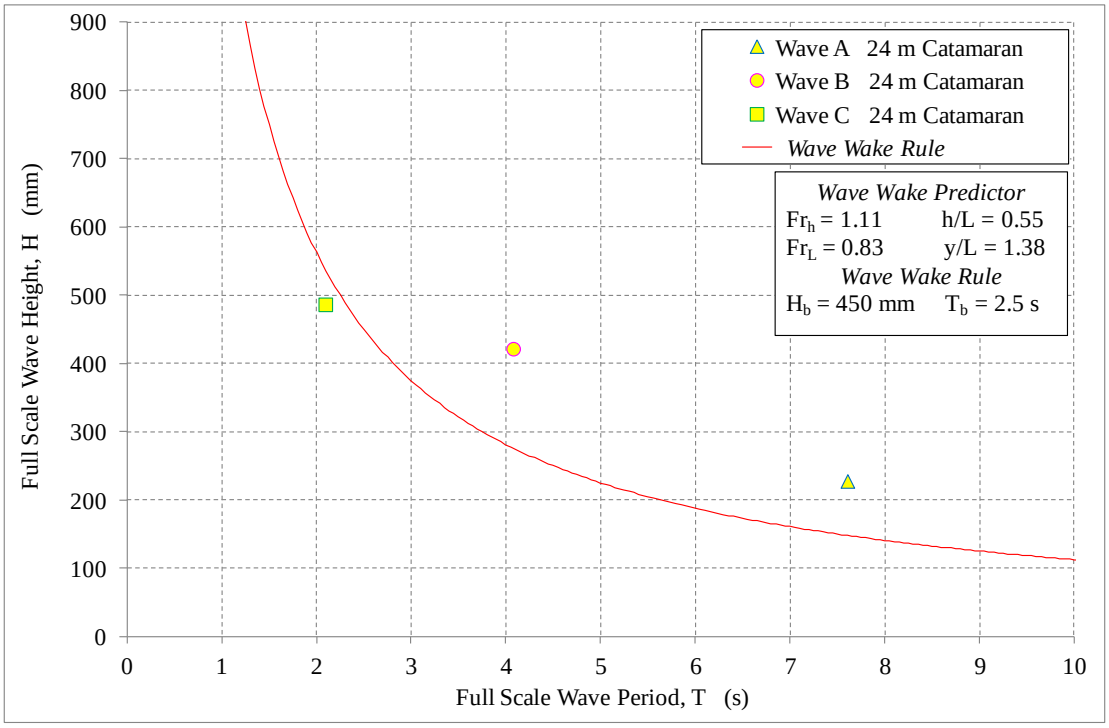

Figure 7.2 *Wave Wake Rule* and *Wave Wake Predictor*: 24 m Catamaran

The data presented in Figure 7.2 has been replicated in Figure 7.3, but in this case the predictions for other monohulls and catamarans of varying $L/\nabla^{1/3}$ from the *Wave Wake Predictor* have been added (all having the same L as the 24 m Catamaran and travelling at the same speed and lateral distance and in the same depth of water). This illustrates that there are many hull forms that can meet this same criteria under similar circumstances, as well as many that fail by an even greater extent. It should be noted that this does not necessarily mean that the vessels of alternative $L/\nabla^{1/3}$ can meet the desired load carrying capacity.

Another example where the combined application of the *Wave Wake Predictor* and *Wave Wake Rule* can assist in a scientific assessment of the likely impacts is with the issue of recreational activities such as water skiing and wakeboarding being conducted in regions with sensitive shorelines. As covered in Chapter 2, this is a commonly occurring issue within Australia (and overseas), particularly within rivers and estuaries close to population centres, for example: Lesleighter 1964; Scholer 1974; Macfarlane and Cox 2003; Todd 2004; Watkins 2004; Howden 2004;

Macfarlane and Cox 2005; GHD 2006; Cameron and Hill 2008; O'Reilly 2009; Macfarlane 2010; Worley Parsons 2010; Glamore 2011.

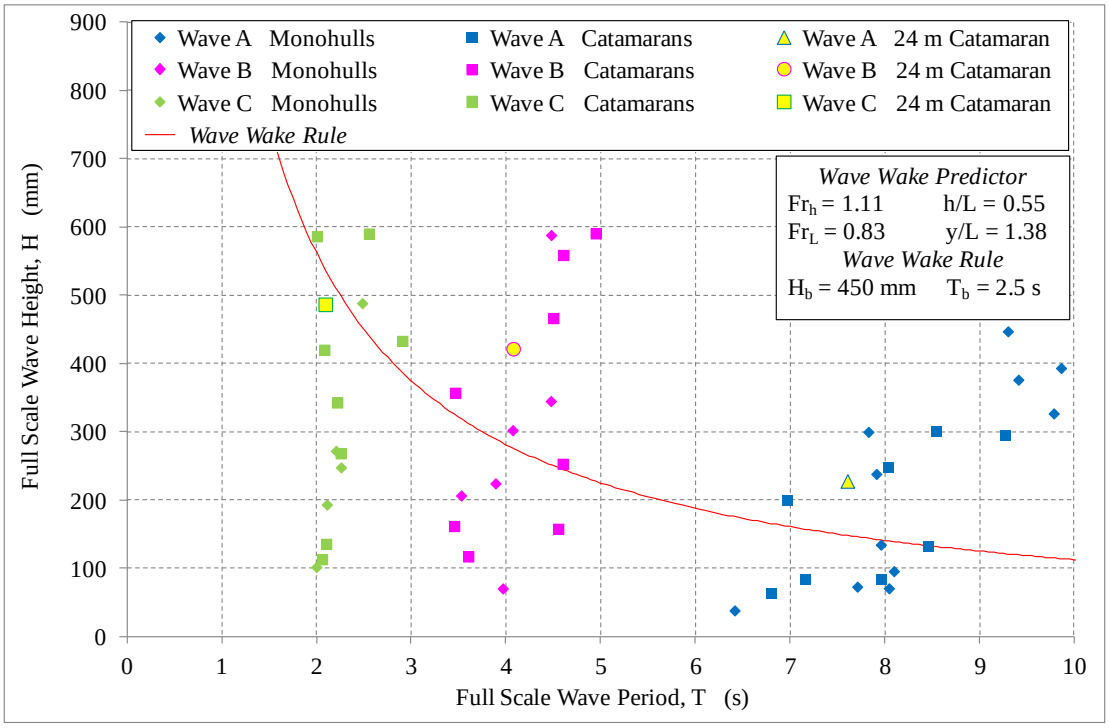

Figure 7.3 *Wave Wake Rule* and *Wave Wake Predictor*: 24 m Catamaran and other hull forms

All of the studies listed above involve locations where the fetch is very limited so they can all be considered as low energy environments, but their shorelines would be expected to be dynamically stable and accustomed to the naturally occurring wind wave environment. In order to illustrate how the fetch can affect the characteristics of the wind waves, the benchmark values for the curves of constant energy from the *Wave Wake Rule* for three different scenarios are plotted in Figure 7.4. The values for H_b and T_b for fetch distances of 100, 500 and 1,000 m and constant wind velocity of 10 m/s have been obtained from the hindcast wind wave data provided in Table 2.2. As expected, as the fetch reduces so does the wind wave height and period, hence also the constant-energy curves from the *Wave Wake Rule*.

Also shown in Figure 7.4 are the predictions of Waves A, B and C for a typical ski boat having the particulars provided in Table 6.5 for Ski Boat #3. Data is provided for the four vessel speeds of 12, 17, 22 and 30 knots, with each of these being representative of typical speeds for certain activities. For example, 17 knots is commonly adopted by wakeboarders, 22 knots is a typical speed for water-skiing

(particularly using two skis), 30 knots is more common for slalom skiing (single ski), barefoot skiing and jump skiing, while 12 knots is sometimes used for slow speed trick skiing (Solomon 1997; Bostian 2010).

It can be seen that when the speed of the ski boat is increased the period of the longest wave, Wave A, decreases significantly and its height gradually reduces. In contrast, the period of Waves B and C only reduces very marginally, or not at all, but the heights of these waves reduce significantly as speed is increased. This concurs with the full scale periods presented in Figure 3.3 and predictions from the *Wave Wake Predictor* given in Figure 6.12.

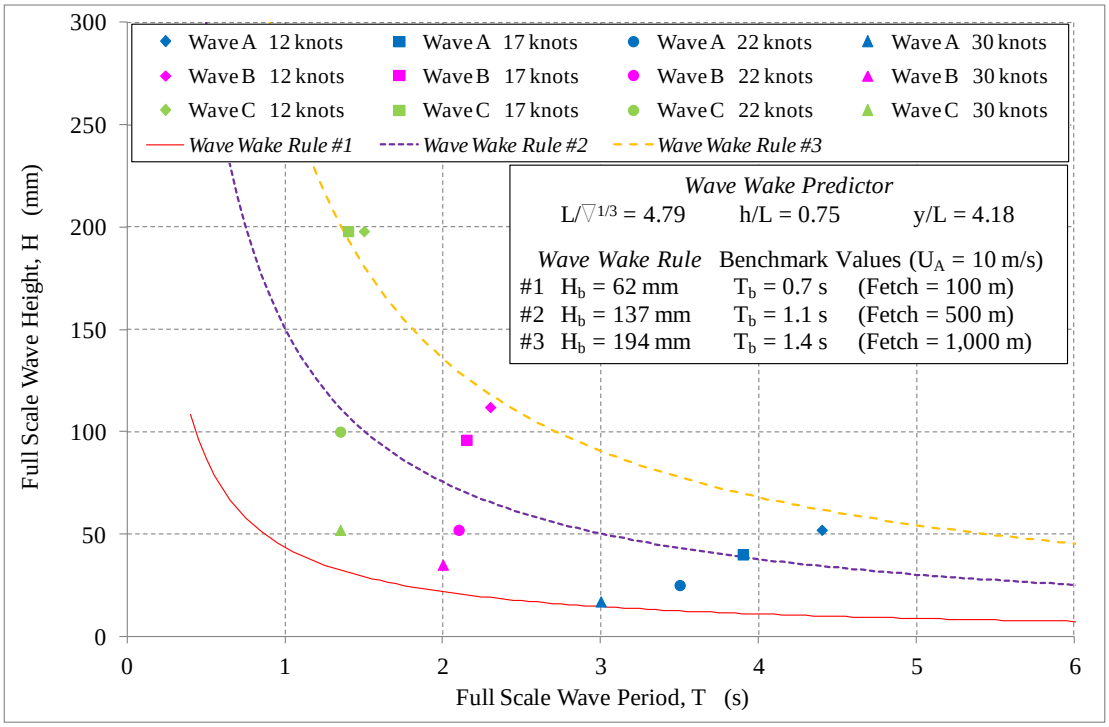

Figure 7.4 *Wave Wake Rule* and *Wave Wake Predictor*: Ski Boat

By comparing the predicted waves with the three different criteria curves, each representing the different fetch distances, it is clear that the activities conducted at the slower speeds, such as wakeboarding, should only be conducted in regions of relatively long fetch (in the order of 1,000 m) if shoreline erosion is to be avoided, or the activities should be conducted at greater distances from sensitive shorelines (which may not be possible in narrow rivers). Ski boat operation at the higher speeds (22 and 30 knots) is less likely to generate damaging waves and thus can be undertaken in more fetch-limited regions.

Another important factor that should be taken into consideration is that the ski boat data provided in Figure 7.4 relates to constant speed in a straight line, but it is common for such water sports to involve regular stopping, starting and turning (refer Section 2.1.8). As any boat accelerates through the various speed regimes it will obviously pass through those zones when larger, more damaging waves will be created.

Chapter 8

Conclusions, Recommendations and Further Work

8.1 Conclusions and Recommendations

The quantification of wave wake generated by marine vessels operating in sheltered waterways has been investigated in an attempt to provide an accurate and rapid method to determine, at design and planning stages, whether damaging or dangerous waves will result. Many published studies have shown that vessel generated waves can result in damage to the surrounding shoreline, moored vessels or other marine structures, and can endanger people working or enjoying activities in small craft or close to the shore.

A review of experimental and numerical methods commonly adopted internationally for quantifying wave wake has indicated that most either obtain or produce a record of the entire wave train (usually in the time domain). However, when these waves are assessed for their potential to be damaging or dangerous, only a very limited amount of salient data is used – often simply by the height alone or the height and period of the highest wave (or some other *maximum* wave).

Many CFD methods generate very detailed 3-dimensional wave pattern information, only for this data to be reduced to a much more manageable size when being assessed against regulatory criteria, such as the height and period of just the highest wave at a single lateral distance from the vessel. This raises the question as to why very slow and complicated CFD methods should be favoured, particularly when other more rapid and equally accurate and reliable methods exist. In addition, the experimental uncertainties associated with the measurement of the wave wake of full scale craft in the field can be so great as to often make the differences between various prediction methods negligible.

In this work it has been demonstrated that the identification and quantification of just a single wave for finite water conditions, which has generally been accepted practice in recent decades, is inadequate at identifying all potentially damaging waves within a vessel generated wave train. It is recommended that at least three waves be considered (termed Waves A, B and C). Wave A is defined as the leading divergent wave, which is the wave that will possess the longest period. Wave B is defined as

the most significant wave following the leading wave. The period of this wave will be shorter than the leading wave, but often not by a large margin, whereas the height is very often greater than the leading wave. This wave often possesses the greatest wave energy, but may not necessarily be either the longest or the highest wave in the wave train. It is also common for a group of short period divergent waves to be generated and Wave C is defined as being the highest wave within this group. This wave always follows Waves A and B, hence will possess the shortest wave period of the three key waves, but there are occasions, particularly at super-critical speeds, where this wave is the highest generated. However, because of its significantly shorter period, it is very likely that this wave will not be the most significant wave when considering sheltered waterways, as the period may be similar to the local naturally occurring wind wave environment.

Previous analysis of full scale wave wake trials data of small commercial vessels and recreational craft concentrated upon the quantification of just the single highest wave. A reassessment of this data, where all three key waves were identified, found that the highest wave was often Wave C (with the shortest period), particularly for speeds in excess of approximately $Fr_L = 0.85$. This was the case for all seven small craft investigated in this study (with $L_{OA} < 8.5$ m). This has led to the potentially most damaging waves (A and B), with considerably higher periods, being inadvertently ignored in previous environmental impact assessments.

Experimental data has been analysed to determine the four primary parameters of wave height constant, wave period, wave decay exponent and wave angle for each of the three significant waves. This analysis has confirmed that finite water depth can affect these three waves very differently: the leading waves (Wave A), which possess the longest period, are significantly altered, with large changes occurring to all four wave parameters between sub-critical, trans-critical and super-critical speeds. In general, most of the extreme values occur within the trans-critical speed regime, particularly as the vessel approaches critical speed ($Fr_h = 1.0$). A much lesser effect was found for Wave B, whereas there is almost negligible finite water depth effect on the shortest waves (Wave C), because the period of these waves is generally too short for the limited depth to have any noticeable effect. As expected, the characteristics of all three waves were confirmed as being very dependent upon vessel speed.

A *Wave Wake Predictor* has been developed that can predict the primary vessel wave wake characteristics for vessel operations at sub-critical, trans-critical and super-

critical vessel speeds. This tool has been specifically developed to deal with typical vessels that operate in sheltered waterways where bank erosion is a potential issue.

The *Wave Wake Predictor* was developed using a series of semi-automated computer-based look-up tables based on the results from an extensive series of model scale experiments conducted on nineteen different ship hulls. Experiments were conducted on each hull at four different water depths (three finite and one 'deep' water case) and over a wide range of vessel speeds. Predictions of wave height, period, decay rate and angle are provided for each of the three key waves (Waves A, B and C) based on principal vessel and environment details by conducting several look-up and interpolation steps. The required vessel details include: monohull or catamaran, length, displacement and speed. Required details of the environment include: water depth, water density and the lateral distance from vessel sailing line to point of interest.

The accuracy and reliability of the *Wave Wake Predictor* has been proven through a validation process that involved the comparison of predictions against full scale data from several different hull forms operating at various water depths and vessel speeds. The benefits of identifying and quantifying the three key waves were highlighted during this validation process, as previous analysis of this full scale trials data (by the author) concentrated only on the single highest (maximum) wave, but this was found not to be the most damaging wave under certain conditions.

The prediction tool can be used to highlight vessel speeds where the most damaging waves are generated and provide guidance on key hull form parameters for minimising bank erosion and other wave wake issues. Thus, potential wave wake issues can be identified very early on in the vessel design and route planning process. For example, it was used to investigate the influence that various hull form parameters have on the characteristics of the key waves which confirmed that the single most important parameter was the length-displacement ratio ($L/\nabla^{1/3}$). Wave height was the only wave characteristic to vary significantly, with the height of all three key waves decreasing with an increase in $L/\nabla^{1/3}$, supporting the adage that it is best to make a vessel as long and as light as practical. The length-displacement ratio had a much less pronounced influence on the period of the three waves, with only a very marginal reduction in period with increasing $L/\nabla^{1/3}$. The wave decay rate and wave angle were found to be essentially unaffected by changes in $L/\nabla^{1/3}$ or any other hull form parameter.

Attempts by vessel designers to improve the wave wake characteristics of their vessels by a nominal modest percentage is likely to be somewhat inconsequential in terms of reducing bank erosion. Generally, a vessel design either will or will not work – small changes to design parameters such as waterline beam, draught and angle of entrance are unlikely to turn a design that causes excessive erosion into an acceptable one.

A regulatory criterion that is considered appropriate for the operation of typical recreational craft and small commercial vessels operating in sheltered waterways has been proposed. The *Wave Wake Rule* is based on a simple formula that adopts a constant-energy approach. It has been shown that wave energy is a more reliable measure than wave power when assessing the erosion potential of vessel wave wake in regions possessing sensitive shorelines due to the equal weighting of both wave height and wave period. The formula describes a curve that determines the allowable wave height and period, based on benchmark values that represent waves that are deemed acceptable for the region in question.

Benchmark values can be determined through one of several methods, with the primary aim to identify the threshold below which the impact of vessel wave wake no longer presents an issue for the region of concern. For example, in regions with highly sensitive shorelines the conduct of experiments to quantify the turbidity (sediment movement) can identify threshold limits of wave height and wave period for input into the *Wave Wake Rule* for regulating vessel operations to avoid, or minimise, bank erosion. Alternatively, suitable benchmark values can be determined by quantifying the waves generated by a vessel that has proven (through successful operation over time) that the waves are acceptable for the region of concern, or by comparing against the naturally occurring wind-generated waves.

This *Wave Wake Rule* can be used with the *Wave Wake Predictor* to determine appropriate guidelines for acceptable vessel operations and assess the potential reduction in bank erosion directly related to vessel wave wake. For example, a case study was undertaken to assess the likely impacts of recreational activities such as water skiing and wakeboarding in fetch-limited regions where low-energy shorelines exist. Predictions of the waves generated by typical ski boats for a range of speeds were compared against three different *Wave Wake Rule* curves, each representing different fetch distances. It was demonstrated that activities conducted at the slower speeds, such as wakeboarding, should only be conducted in regions of relatively long

fetch (in the order of 1,000 m) if shoreline erosion is to be avoided, or the activities should be conducted at greater distances from the shore (which may not be possible in narrow rivers). Ski boat operation at higher speeds (22 and 30 knots) is less likely to generate damaging waves and thus can be undertaken in more fetch-limited regions.

The wave wake predictions relate to constant speed in a straight line, but it is common for water sports such as skiing to involve regular stopping, starting and turning. Therefore, consideration should be given to the larger, more damaging waves that may be created as any boat accelerates from the sub-critical speed regimes through trans-critical and onto super-critical speeds.

In summary, a predictive tool suitable for vessel wave wake within both deep and finite water depths has been developed and validated against several series of full scale data. Sufficient information is very rapidly provided by this tool to assess, using the proposed *Wave Wake Rule*, whether potentially damaging or dangerous waves will be generated. If remedial action is required, then this tool can be used to determine safe operating conditions (vessel speed and/or lateral distance) or to provide an indication of how much the principal particulars of the vessel design would have to change in order to minimise or eliminate the generation of damaging waves.

To assess the wave wake of marine vessels in restricted waterways it is recommended that:

1. More than one individual wave be quantified, ensuring that (at the very least) the wave with the greatest energy and the longest and highest waves are identified and quantified.
2. The *Wave Wake Predictor* is used to estimate the characteristics of the three key waves for any given vessel length, displacement and speed at any specified water depth and lateral distance.
3. The height and period of these three waves be assessed against suitable regulatory criteria, such as the proposed *Wave Wake Rule*. The benchmark conditions used within this rule should be appropriate for the intended location, which may require an assessment of local site conditions and experience in this field.

8.2 Further Work

Whilst new methods have been developed to predict the wave wake of marine vessels, further work may be conducted to extend knowledge in the area and improve the proposed techniques. Several potential topics are briefly discussed:

The wave decay rates determined in this thesis are derived from model scale physical experiments where the wave profiles were measured within the near to medium field (up to about four boat lengths from the vessel sailing line). Although these lateral distances are generally suitable when considering sheltered waterways due to their limited widths, it would be advantageous to confirm the applicability of these decay rates for predicting the characteristics of all three key waves in the far field. A preliminary investigation was made between limited results from the present study with those from an independent set of model scale tests where wave profiles were obtained further afield (refer Figure 5.28). Results were promising, with the super-critical waves from the present study found to decay at a very similar rate to those of Doyle (2001), suggesting that the decay rates determined from the present study may also be applicable over larger lateral distances. A more in-depth investigation would require the acquisition of wave data at several much greater lateral distances, which is problematic for controlled environments due to the limited width of most hydrodynamic test basins. This may require the conduct of tests within a semi-controlled environment, but should provide greater confidence when predicting the characteristics of the three key waves in the far field.

The predicted wave wake characteristics assume that the water depth remains constant between the sailing line of the vessel and the lateral location of interest. Further investigation into cases where the bathymetry varies could be conducted to include the effects of refraction and shoaling due to varying depth. It should be possible to utilise the empirical-based wave decay relationships determined in the present study. It may also be possible to include the effects of ambient current using the approach proposed by Holthuijsen *et al*. (1989).

The operation of the newly developed *Wave Wake Predictor* could be enhanced in several ways. For example, the limits of applicability could be increased by obtaining data for a wider range of hull forms, finite water depths and/or vessel speeds. In Section 6.5.5 it was noted that it should be feasible to predict wave characteristics well beyond the present speed limit for ski boats by extrapolation, given the good

correlation with full scale data that exists for much greater speeds. In addition, predictions close to critical speed (around $Fr_h = 1.0$) may be improved by obtaining data at smaller speed increments.

The application of the constant-energy *Wave Wake Rule* relies upon the adoption of benchmark values of wave height and period that are generally site specific. Several different methods for determining suitable values, including some examples, were discussed in Chapter 7.2. It should be possible to develop a matrix of nominal benchmark values for a selection of generic sites with known conditions such as fetch and bank type (refer Section 2.5.2). This could provide a starting point where no more applicable data or information is readily available. In circumstances where such nominal values are adopted it is recommended that their effectiveness be monitored and reviewed.

References

Albright, C.J., 2000, 'Wake up call: using the Washington shoreline management act to protect the shorelines of Puget Sound from high speed wake wash', *Washington Law Review*, vol. 75, pp. 519-547.

Allenström, B., Bergdahl, L., Erikson, L., Eskilsson, C., Forsman, B., Hanson, H., Johansson, J. Johansson, L. and Svensson, U., 2003, 'The interaction of large and high-speed vessels with the environment in archipelagos - final report', Project Report VINNOVA, SSPA Research Report no. 122, Goteborg, Sweden.

American Institute of Aeronautics and Astronautics (AIAA), 1999, 'Assessment of experimental uncertainty with application to wind tunnel testing', AIAA S-071A-1999, Washington, D.C., USA.

American Society of Mechanical Engineers (ASME), 1998, 'Test uncertainty: instruments and apparatus', PTC 19.1-1998.

Australian Maritime College (AMC) website, Maritime engineering facilities, accessed 23 February 2012. www.amc.edu.au/maritime-engineering-and-hydrodynamics/facilities

Anderson, F.E., 1974, 'The effect of boat waves on the sedimentary processes of a New England tidal flat', *University of New Hampshire*, TR No. 1, Jackson Estuarine Laboratory.

Anderson, F.E., 1975, 'The short term variation in suspended sediment concentration caused by the passage of a boat wave over a tidal flat environment', *University of New Hampshire*, TR No. 2, Jackson Estuarine Laboratory.

Anderson, F.E., 1976, 'Rapid settling rates observed in sediments resuspended by boat waves over a tidal flat', *Netherlands Journal of Sea Research*, vol. 10, pp. 44-58.

Atlar, M., Wang, D. and Glover, E.J., 2006, 'Experimental investigation into the impact of slipstream wash of a podded propulsor on the marine environment', Proc. of IMechE, vol. 221, part M, *Journal of Engineering for the Maritime Environment*, pp.67-79.

Austin, I., 1999, 'High-speed vessels and their impacts on wetlands and habitat: a case study from San Francisco', *Proc. High Speed Craft Conference*, Victoria, British Columbia, Canada.

Balzerek, H. and Koslowski, J., 2007, 'Ship-induced riverbank and harbour damage', *Hydro International*, September, vol. 11, no. 8.

Barlow, J.B., Rae, W.H. and Pope, A., 1999, *Low speed wind tunnel testing*, 3rd edn, John Wiley & Sons, New York.

Bauer, B.O., Lorang, M.S., and Sherman, D.J., 2002, 'Estimating boat-wake-induced levee erosion using sediment suspension measurements', *Journal of Waterway, Port, Coastal and Ocean Engineering*, ASCE, vol. 128, pp. 152-162.

Bhowmik, N.G. and Demissie, M., 1982, 'Waves generated by river traffic', *Proc. Conf. Applying Research to Hydraulics Practice*, ASCE, Hydraulics Division, pp. 179-188.

Bhowmik, N.G. and Demissie, M., 1983, 'Bank erosion by waves', *Proc. Conf. Frontiers in Hydraulic Engineering*, ASCE Hydraulics Division, pp. 195-200.

Bishop, M.J., 2003, Making waves: the effects of boat-wash on macrobenthic assemblages of estuaries, Doctor of Philosophy thesis, University of Sydney, Australia.

Bonham, A.J., 1980, 'Bank protection using emergent plants against boat wash in rivers and canals', *HR Wallingford*, Report IT 206.

Bonham, A.J., 1983, 'The management of wave-spending vegetation as bank protection against boat wash', *Landscape Planning*, vol. 10, pp. 15-30.

Bouwmeester, J., 1977, 'Calculation return flow and water level depressions: new method', *Proc. 24th International Navigation Congress*, PIANC, Leningrad, SI-3, pp. 148-151.

Bostian, J., 2010, 'How to determine your boat speed when waterskiing, wakeboarding - boat speeds for different boat-towed sports', accessed 5 December 2011. http://waterski.about.com/od/driverscorne1/a/boat_speed.htm

Bradbury, J., 2005a, 'Revised wave wake criteria for vessel operation on the lower Gordon River'. *Nature Conservation Branch* report, DPIPWE, accessed 5 December 2011. http://www.dpiw.tas.gov.au/inter.nsf/Attachments/LJEM-6J26ZY?open

Bradbury, J., 2005b, 'Lower Gordon River turbidity monitoring, April 2003 – December 2004', *Nature Conservation Branch* report, DPIPWE, accessed 5 December 2011. http://www.dpiw.tas.gov.au/inter.nsf/WebPages/LJEM-6J289T?open

Bradbury, J., 2007, 'Lower Gordon River erosion – history and lessons learned', *Nature Conservation Branch* report, DPIPWE, accessed 5 December 2011. http://www.dpiw.tas.gov.au/inter.nsf/WebPages/LJEM-6J289T?open

Bradbury, J., 2010, 'Specification of acceptable vessel wave wake characteristics for operation on zone three levee bank reaches of the lower Gordon River', unpublished report for the Tasmanian Parks and Wildlife Service.

Bradbury, J., Cullen, P., Dixon, G. and Pemberton, M., 1995, 'Monitoring and management of streambank erosion and natural revegetation of the lower Gordon River, Tasmanian Wilderness World Heritage Area, Australia', *Environmental Management*, vol. 19, no. 2, pp. 259-272.

British Columbia Ferry Corporation (BC Ferries), 2000, 'Fast ferry program – wake and wash report'. Unpublished report.

Brizzolara, S. and Bruzzone, D., 2003, 'Near and distant waves of fast ships in unlimited and limited depths', *Proc. 7th Intl. Conf. on Fast Sea Transportation (FAST 2003)*, Ischia, Italy, vol. 3.

Cameron, T. and Hill, P., 2008, 'Assessing the impact of wakeboarding in the Williams Estuary, NSW, Australia – challenges for estuarine health', *Proc. 11th Intl. Riversymposium*, Brisbane, Australia.

Camfield, F.E., Ray, R.E.L. and Eckert, J.W., 1980, 'The possible impact of vessel waves on bank erosion', *U.S. Department of Transportation*, United States Coast Guard, Office of Research & Development, Washington, Report no. CG-W-1-80.

Campana, E.F., Kodama, Y., Bull, P., Day, A.H., Gorski, J., Kusaka, Y., Lee, S.H., Schweighofer, J. and Valle, J., 2005, 'Final report of the Resistance Committee', *Proc. 24th Intl. Towing Tank Conf.*, vol. 1, pp. 17-71.

Campana, E.F., Gorski, J., Chun, H.H., Day, A, Huang, D.B, Macfarlane, G.J., Mikkola, T., Tahara, Y. and Valle, J., 2008, 'Final report of the Resistance Committee', *Proc. 25th Intl. Towing Tank Conf.*, vol. 1, pp. 21-81.

Cartwright, R.A., Wilson, P.A., Molland, A.F. and Taunton, D.J., 2008, 'A low wash design for a river patrol craft with minimal environmental impact', *Intl. Journal of Maritime Engineering*, vol. 150, part A2, 37-56.

Chalkias, D.S. and Grigoropoulos, G.J., 2005, 'Wash effects of high-speed monohulls', *Proc. 8th Intl. Conf. on Fast Sea Transportation (FAST 2005)*, St. Petersburg, Russia.

Chalkias, D.S. and Grigoropoulos, G.J., 2007, 'Experimental investigations of the waves generated by high-speed ferries', *Proc. 9th Intl. Conf. on Fast Sea Transportation (FAST 2007)*, Shanghai, China.

Couser, P.R., Mason, A.P., Mason, G., Smith, C.R. and von Konsky, B.R., 2004, 'Artificial neural networks for hull resistance prediction', *Proc. 3rd Intl. Conf. on Computer and IT Applications in the Maritime Industries (COMPIT 2004)*, Siguenza, Spain.

Cox, G., 2000, 'Sex, lies and wave wake', *Proc. RINA Intl. Conf. on the Hydrodynamics of High Speed Craft – Wake Wash and Motions Control*, London, UK.

Croad, R.N. and Morris, N.A., 2003, 'Managing ship wave effects in the Marlborough Sounds', *Proc. 16th Australasian Coastal and Ocean Engineering Conference and 9th Australasian Port and Harbour Conference (Coasts and Ports 2003)*, Auckland, New Zealand.

Croad, R.N. and Parnell, K.E., 2002, 'Proposed controls on shipping activity in the Marlborough Sounds', Report to the Marlborough District Council, Opus International Consultants Limited and Auckland UniServices Limited.

Dand, I.W., Dinham-Peren, T.A. and King, L., 1999a, 'Hydrodynamic aspects of a fast catamaran operating in shallow water', *Proc. RINA Intl. Conf. on the Hydrodynamics of High Speed Craft*, London, UK.

Dand, I.W., Keuning, J.A., Chun, H.H., Doctors, L.J., Grigoropoulos, G.J., Grzybowski, P., Takaki, M. and Vogt Andersen, S., 1999b, 'Final report of the Specialist Committee on safety of high speed marine vehicles', *Proc. 22nd Intl. Towing Tank Conf.*, vol. 2, pp. 615-650.

Day, A.H. and Doctors, L.J., 2001, 'Rapid estimation of near- and far-field wave wake from ships and application to hull form design and optimization', *Journal of Ship Research*, vol. 45, no. 1.

Doctors, L.J., 2004, 'A comparison of the environmental wave generation of hovercraft and other high-speed vessels', *Proc. 5th Air-Cushion Technology Conf. and Exhib.*, Hovercraft Museum, Lee-on-Solent, UK.

Doctors, L.J. and Day, A.H., 2000, 'Wave-free river-based air cushion vehicles', *Proc. RINA Intl. Conf. on the Hydrodynamics of High Speed Craft – Wake Wash and Motions Control*, London, UK.

Doctors, J.J. and Day, A.H., 2001, 'The generation and decay of waves behind high-speed vessels', *Proc. 16th Intl. Workshop on Water Waves and Floating Bodies (IWWWFB 2001)*, Hiroshima, Japan.

Doctors, L.J., Renilson, M.R., Parker, G., Hornsby, N., 1991 'Waves and wave resistance of a high-speed river catamaran', *Proc. 1st Intl. Conf. on Fast Sea Transportation (FAST 1991)*, Trondheim, Norway.

Doctors L.J. and Zilman, G., 2004a, 'Environmental wave generation of high-speed marine vessels', *Proc. 25th Symposium on Naval Hydrodynamics*, St John's, Newfoundland and Labrador, Canada.

Doctors L.J. and Zilman, G., 2004b, 'The influence of surface tension and viscosity on the wavemaking of a model catamaran', *Proc. 19th Intl. Workshop on Water Waves and Floating Bodies (IWWWFB 2004)*, Cortona, Italy.

Dorava, J.M. and Moore, G.W., 1997, 'Effects of boat wakes on streambank erosion, Kenai River, Alaska', *United States Geological Survey*, Anchorage: Water-Resources Investigations Report 97-4105.

Downing, J.P., Sternberg, R.W. and Lister, C.R.B., 1981, 'New instrumentation for the investigation of sediment suspension processes in the shallow marine environment', *Marine Geology*, vol. 42, pp.19-34.

Doyle, R., 2001, An investigation into the wake wash of high-speed ferries in shallow water, Doctor of Philosophy thesis, Queen's University of Belfast, Ireland.

Doyle, R., Whittaker, T.J.T. and Elsaesser, B., 2001, 'A study of fast ferry wash in shallow water', *Proc. 6th Intl. Conf. on Fast Sea Transportation (FAST 2001)*, Southampton, UK.

Duffy, J.T., 2008, Modelling of ship-bank interaction and ship squat for ship-handling simulation, Doctor of Philosophy thesis, Australian Maritime College, University of Tasmania, Australia.

Ellis, J.T, Sherman, D.J., Bauer, B.O. and Hart, J., 2002, 'Assessing the impact of an organic restoration structure on boat wake energy', *Journal of Coastal Research*, Special Issue 36.

Erikson, L.H., Larson, M. and Hanson, H., 2005, 'Prediction of swash motion and run up including the effects of swash interaction', *Coastal Engineering*, vol. 52.

Erm, A. and Soomere, T., 2006, 'The impact of fast ferry traffic on underwater optics and sediment re-suspension', *Oceanologia*, vol. 48.

Feldtmann, M., 2000, 'In the wake of wash restrictions', *Proc. RINA Intl. Conf. on the Hydrodynamics of High Speed Craft – Wake Wash and Motions Control*, London, UK.

Ferguson, A., Seren, D. and McGregor, R., 1983, 'The prediction and practical measurement of ship squat in shallow water', *Proc. Marine Safety Conference 1983*, University of Glasgow, UK, Paper 12, pp. 12/1 – 12/19.

Fissel, D., Billenness, D., Lemon, D. and Readshaw, J., 2001, 'Measurement of the wave wash generated by fast ferries with upward looking sonar instrumentation', *Proc. Fast Ferries 2001 Conf.*, New Orleans, USA.

Fox, K., Gornstein, R. and Stumbo, S., 1993, 'Wake wash: issues and answers', *SNAME Pacific Northwest Section*.

Fresco, A., 1999, 'Fisherman killed by giant ferry wave', *The Times*, 21 July 1999, England, UK.

Gadd, G.E., 1994, 'The wash of boats on recreational waterways', *RINA Transactions*.

Garrard, P.N. and Hey, R.D., 1987, 'Boat traffic, sediment resuspension and turbidity in a Broadland river', *Journal of Hydrology*, vol. 95, pp. 289-297.

GHD, 2006, 'Williams River bank erosion study', Report prepared for the Port Stephens Council.

Gippel, C.J., 1995, 'Potential of turbidity monitoring for measuring the transport of suspended sediment in streams', *Hydrological Processes*, vol. 9, pp. 83-97.

Glamore, W.C., 2008, 'A decision support tool for assessing the impact of boat wakes on inland water', On-Course, PIANC, October, pp. 5-18.

Glamore, W.C., 2011, 'The myth of wakeboarding vessels and riverbank erosion', *Proc. 20th Australasian Coastal and Ocean Engineering Conf.* (Coasts & Ports 2011), Perth, Australia.

Glamore, W.C., Hudson, R. and Cox, R.J., 2005, 'Measurement and analysis of boat wake waves: management implications', *Proc. 17th Australasian Coastal and Ocean Engineering Conf. (Coasts & Ports 2005)*, Adelaide, Australia.

Gourlay, T., 2010, 'Full-scale boat wake and wind wave trials on the Swan River', CMST Report 2010-06, prepared for the Swan River Trust, accessed 8 December 2011. www.swanrivertrust.wa.gov.au

Gross, A. and Watanabe, K., 1972, 'On blockage correction', *Proc. 13th Intl. Towing Tank Conf.*

Haggerty, D.J., Sharifounnasab, M. and Spoor, M.F., 1983, 'Riverbank erosion: a case study', *Bulletin of the Assoc. of Engineering Geologists*, vol. 20, pp. 411-437.

Hamer, M., 1999. 'Solitary killers', *New Scientist*, vol.163, pp.18-19.

Havelock, T.H., 1908, 'The propagation of groups of waves in dispersive media, with application to waves produced by a travelling disturbance', *Proc. Royal Society of London*, England, Series A, pp.398-430.

Hilton, J. and Phillips, G.L., 1982, 'The effect of boat activity on turbidity in a shallow broadland river', *Journal of Applied Ecology*, vol. 19, pp.143-150.

Holthuijsen, L.H., Booij, N. and Herbers, T.H.C., 1989, 'A prediction model for stationary, short-crested waves in shallow water with ambient currents', *Coastal Engineering*, vol. 13, pp 23-54.

Hong C.B. and Doi, Y., 2006, 'Numerical and experimental study on ship wash including wave-breaking on shore', *Journal of Waterway, Port, Coastal and Ocean Engineering*, ASCE, Sept/Oct.

Houser, C., 2010, 'Relative importance of vessel-generated and wind waves to saltmarsh erosion in a restricted fetch environment', *Journal of Coastal Research*, vol. 26, no. 2, pp 230-240.

Houser, C., 2011. 'Sediment resuspension by vessel-generated waves along the Savannah River, Georgia', *Journal of Waterway, Port, Coastal, and Ocean Engineering*, ASCE, Sept/Oct.

Howden, J.T.D., 2004, Wave generation of wakeboard vessels, Bachelor of Engineering (Nav. Arch.) thesis, University of New South Wales, Australia.

Hughes, Z.J., FitzGerald, D.M., Howes, N.C. and Rosen, P.S., 2007, 'The impact of natural waves and ferry wakes on bluff erosion and beach morphology in Boston Harbor, USA', *Journal of Coastal Research*, Special Issue 50.

International Association for Hydro-Environment Engineering and Research (IAHR), 1989, 'List of sea-state parameters', *Journal of Waterway, Port, Coastal and Ocean Engineering*, ASCE, vol. 115 (6), pp. 793-808.

International Towing Tank Conference (ITTC), 2008, 'Recommended procedures and guidelines', accessed 8 December 2011. www.sname.ittc

Jiang, T., 2001, 'Ship waves in shallow water', *Frotschritt-Berichte VDI*, Series 12, No. 466.

Johnson, J.W., 1958, 'Ship waves in navigation channels', *Proc. 6th Conf. on Coastal Engineering*, Chapter 40.

Kelpsaite, L., 2009, Changing properties of wind waves and vessel wakes on the eastern coast of the Baltic Sea, Doctor of Philosophy thesis, Tallinn University of Technology, Estonia.

Kelpsaite, L., Parnell, K.E. and Soomere, T., 2009, 'Energy pollution: the relative influence of wind-wave and vessel-wake energy in Tallinn Bay, the Baltic Sea', *Journal of Coastal Research*, Special Issue 56.

Kim, Y.C. (Ed.), 2010, *Handbook of coastal and ocean engineering*, World Scientific Publishing, Singapore.

Kirk, R.M. and Single, M.B., 2000, 'Coastal impacts of new forms of transport; the case of the interisland ferries', *Environmental Planning and Management in New Zealand*. Eds. Memon, P.A. and Perkins, H., Palmerston North, New Zealand, Dunmore Press.

Kirkegaard, J., Hojtved, N. and Kristensen, H.O.H., 1998, 'Fast ferry operation in Danish waters, *Proc. 29th Intl. Navigation Congress*, International Navigation Association.

Kobayashi, N., Raichle, A.W. and Asano, T., 1993, 'Wave attenuation by vegetation', *Journal of Waterway, Port, Coastal and Ocean Engineering*, vol. 119, pp 30-48.

Kofoed-Hansen, H., 1996, 'Technical investigation of wake wash from fast ferries', *Danish Hydraulic Institute*.

Kofoed-Hansen, H., Jensen, T., Kirkegaard, J. and Fuchs, J., 1999, 'Prediction of wake wash from high-speed craft in coastal areas', *Proc. RINA Intl. Conf. on the Hydrodynamics of High Speed Craft*, London, UK.

Kofoed-Hansen, H., Jensen, T., Sørensen, O.R. and Fuchs, J., 2000, 'Wake wash risk assessment of high speed ferry routes – a case study and suggestions for model improvements', *Proc. RINA Intl. Conf. on the Hydrodynamics of High Speed Craft: Wake Wash and Motions Control*, London, UK.

Kofoed-Hansen, H. and Mikkelsen, A.C., 1997, 'Wake wash from fast ferries in Denmark', *Proc. 4th Intl. Conf. on Fast Sea Transportation (FAST 1997)*, Sydney, Australia, pp. 471-478.

Kogoy, P., 1998, 'Tidal wave of protest', *Sun-Herald*, 20th September, Sydney, Australia.

Kumar, S.A., Heimann, J., Hutchison, B.L. and Fenical, S.W., 2007, 'Ferry wake wash analysis in San Francisco Bay', *Proc. Ports 2007 Conf.*, ASCE, San Diego, USA.

Kuo, C. Y., 1983, 'Navigation and shore erosion in coastal waterways', *Proc. Frontiers in Hydraulic Engineering Conf.*, Shen, H. T. (Ed.), ASCE, Hydraulics Division, pp. 207-211.

Kurennoy, D. , 2009, Analysis of the properties of fast ferry wakes in the context of coastal management, Doctor of Philosophy thesis, Tallinn University of Technology, Estonia.

Lawler, D.M., 1993, 'The measurement of riverbank erosion and lateral channel change: a review'. *Earth Surface Processes and Landforms*, vol. 18, pp. 777-821.

Lazauskas, L.V., 2007, 'The hydrodynamic resistance, wave wakes and bottom pressure signatures of a 5900t displacement air warfare destroyer', accessed 8 December 2011. http://www.cyberiad.net/wakepredict.htm

Lazauskas, L.V., 2009, Resistance, wave-making and wave-decay of thin ships, with emphasis on the effects of viscosity, Doctor of Philosophy thesis, University of Adelaide, Australia.

Leer-Andersen, M. and Lundgren, J., 2001, 'Model testing in ocean basin', FLOWMART – D2.1.1a, Report 2000 0155-1, SSPA Sweden AB.

Lesleighter, E.J., 1964, 'Hawkesbury River – the effect of speedboat activities on bank erosion', *Department of Public Works NSW*, Report No. 106, Australia.

Lewis, E.V. (ed.), 1988, *Principles of naval architecture – Vol. II: resistance, propulsion and vibration*, SNAME, Jersey City, USA.

Lewis, W.H., 1956, 'The foreshore erosion problem in the lower reaches of the Mississippi river', *Shore and Beach*, vol. 24, no. 1, pp. 13-15.

Lighthill, J., 1978, *Waves in fluids*, Cambridge University Press.

Longo, J. and Stern, F., 2005, 'Uncertainty assessment for towing tank tests with example for surface combatant DTMB model 5415', *Journal of Ship Research*, vol. 49, pp. 55-68.

Lyakhovitsky, A., 2007, *Shallow water and supercritical ships*, Backbone Publishing Company, USA.

Macfarlane, G.J., 2002, The measurement and assessment of sub-critical vessel generated waves, Master of Philosophy thesis, Australian Maritime College, Australia.

Macfarlane, G.J., 2006, 'Correlation of prototype and model wave wake characteristics at low Froude numbers', RINA Transactions, *Intl. Journal of Maritime Engineering*, part A2.

Macfarlane, G.J., 2009, 'Correlation of prototype and model scale wave wake characteristics of a catamaran', *Marine Technology*, SNAME, vol. 46, no. 1.

Macfarlane, G.J., 2010, 'Investigation into the effect of wash of boats and wind waves on the Swan River – ski boat data', Report prepared for the Swan River Trust, AMC Search Ltd report 10/G/09.

Macfarlane, G.J. and Cox, G., 2003, 'Vessel wash impacts on bank erosion - Noosa River (between Lakes Cootharaba and Cooroibah) and Brisbane River (Kookaburra Park to the Bremer River junction)', Refereed report for the *Moreton Bay Waterways and Catchments Partnership*, AMC Search Ltd report 01/G/18.

Macfarlane, G.J. and Cox, G., 2004, 'The development of vessel wave wake criteria for the Noosa and Brisbane Rivers in Southeast Queensland', *Proc. 5th Intl. Conf. on Coastal Environment*, WIT Press, Alicante, Spain.

Macfarlane, G.J. and Cox, G., 2005, 'Vessel wash impacts on bank erosion - Maroochy River', Refereed report for the *Moreton Bay Waterways and Catchments Partnership*, AMC Search Ltd report 04/G/18.

Macfarlane, G.J. and Cox, G., 2007, 'An introduction to the development of rational criteria for assessing vessel wash within sheltered waterways', IMarEST *Journal of Marine Design and Operations*, part BII.

Macfarlane, G.J., Cox, G. and Bradbury, J., 2008, 'Bank erosion from small craft wave wake in sheltered waterways', RINA Transactions, *Intl. Journal of Small Craft Technology*, part B.

Macfarlane, G.J. and Gourlay, T., 2009, 'Investigation into the effect of wash of boats and wind waves on the Swan River', Report prepared for the Swan River Trust, AMC Search Ltd Report No. 09/G/17, accessed 8 December 2011. www.swanrivertrust.wa.gov.au.

Macfarlane, G.J. and Hinds, P., 2001, 'A preliminary investigation into shallow water wave wake', unpublished AMC report, Launceston, Australia.

Macfarlane, G.J. and Renilson, M.R., 1999, 'Wave wake – a rational method for assessment', *Proc. RINA Intl. Conf. on Coastal Ships and Inland Waterways*, London, UK.

Macfarlane, G.J. and Renilson, M.R., 2000, 'When is low wash low wash - an investigation using a wave wake database', *Proc. RINA Intl. Conf. on the Hydrodynamics of High Speed Craft: Wake Wash and Motions Control*, London, UK.

Madsen, P.A., Fuhrman, D.R. and Wang, B., 2006, 'A Boussinesq-type method for fully non-linear waves interacting with a rapidly varying bathymetry', *Coastal Engineering*, vol. 53, pp. 487-504.

Marine Accident Investigation Branch (MAIB), 2000, 'Report on the investigation of the man overboard fatality from the angling boat "Purdy" at Shipwash Bank, off Harwich on 17 July 1999', *MAIB Report* 1/10/194, 23pp.

Maritime and Coastguard Agency (MCA), 1998, 'Research Project 420 – Investigation of high speed craft on routes near to land or enclosed estuaries', *Maritime and Coastguard Agency*.

Mason, A.P., Couser, P.R., Mason, G., Smith, C.R., and von Konsky, B.R., 2005, 'Optimisation of vessel resistance using genetic algorithms and artificial neural networks', *Proc. 4th Intl. Conf. on Computer and IT Applications in the Maritime Industries (COMPIT 2005)*, Hamburg, Germany.

McConchie, J.A. and Toleman, I.E.J., 2003, 'Boat wakes as a cause of riverbank erosion: a case study from the Waikato River, New Zealand', *Journal of Hydrology*, vol. 42, pp. 163-179.

Michell, J.H., 1898, 'The wave resistance of a ship', Philosophical Magazine, series 5, vol. 45, pp. 106-123.

Miller, J.K. and Dean, R.G., 2004, 'A simple new shoreline change model', *Coastal Engineering*, vol. 51, pp. 531-556.

Millward, A., 1983, 'Shallow water and channel effects on ship wave resistance at high sub-critical and super-critical speeds, *Trans RINA*, London, UK, vol. 125, pp. 163-169.

Molland, A.F., Wilson, P.A., Turnock, S.R., Taunton, D.J.S. and Chandraprabha, S., 2001, 'The prediction of the characteristics of ship generated near field wash waves'. *Proc. 6th Intl. Conf. on Fast Sea Transportation (FAST 2001)*, Southampton, UK.

Molland A.F, Wilson P.A., Taunton D.J., Chandraprabha S. and Ghani P.A., 2003, 'Numerical estimation of ship wash waves in deep and shallow water', *Proc. 7th Intl. Conf. on Fast Sea Transportation (FAST 2003)*, Ischia, Italy.

Molland A.F, Wilson P.A., Taunton D.J., Chandraprabha S. and Ghani P.A., 2004, 'Resistance and wash wave measurements on a series of high speed displacement monohull and catamaran forms in shallow water', RINA Transactions, *Intl. Journal of Maritime Engineering*, part A2.

Montgomery, D.C., 2009, *Design and analysis of experiments*, Arizona State University, John Wiley & Sons, 7th Edition.

Murphy, J., Morgan, G. and Power, O., 2006, 'Literature review on the impacts of boat wash on the heritage of Irelands inland waterways', University College Cork, Hydraulics and Maritime Research Centre, Aquatic Services Unit and Moore Marine Services Ltd.

Nanson, G.C., von Krusenstierna, A., Bryant, E.A. and Renilson, M.R., 1994, 'Experimental measurements of river bank erosion caused by boat-generated waves on the Gordon River, Tasmania', *Regulated Rivers, Research and Management*, vol. 9, pp. 1-14.

Newman, J.N., 1977, *Marine Hydrodynamics*, MIT Press.

O'Reilly, T., 2009, 'The impact of recreational boat use on the lowermost reach of Wandandian Creek', Bachelor of Environmental Science Honours thesis, School of Earth and Environmental Sciences, University of Wollongong, Australia.

Osborne, P.D. and Boak, E.H., 1999, 'Sediment suspension and morphological response under vessel generated wave groups: Torpedo Bay, Auckland, New Zealand', *Journal of Coastal Research*, vol. 15, pp. 388-398.

Osborne, P.D., Cote, J.M., MacDonald, N. and de Waal, N., 2009, 'Impact studies and criteria for high-speed operations with foil assisted catamarans in a wake sensitive area', *Proc. 10th Intl. Conf. on Fast Sea Transportation (FAST 2009)*, Athens, Greece.

Parnell, K.E. and Kofoed-Hansen, H., 2001, 'Wakes from large high-speed ferries in confined coastal waters: management approaches with examples from New Zealand and Denmark', *Journal of Coastal Management*, vol. 29, pp 217-237.

Parnell, K.E., McDonald, S.C. and Burke, A., 2007, 'Shoreline effects of vessel wakes', *Journal of Coastal Research*, Special Issue 50.

Parnell, K.E., Delpeche, N., Didenkulova, I., Dolphin, T., Erm, A., Kask, A., Kelpsaite, L., Kurennoy, D., Quak, E., Raamet, A., Soomere, T., Terentjeva, A., Torsvik, T. and Zaitseva-Parnaste, I., 2008, 'Far-field vessel wakes in Tallinn Bay', *Estonian Journal of Engineering*, vol. 14, no.4.

Patterson Britton & Partners, 1995, 'Effects of marine traffic on the shoreline of the Parramatta River, Gladesville to Parramatta', Report to the NSW Department of Transport.

Patterson Britton & Partners, 2001, 'Parramatta River long-term shoreline monitoring study', Report prepared for the Waterways Authority of New South Wales.

Pattiaratchi, C. and Hegge, B., 1990, Impact of ferry and large vessel traffic on Swan River foreshore erosion', Centre for Water Research Report WP 452 CP, Department of Environmental Engineering, University of Western Australia.

Permanent International Association of Navigation Congresses (PIANC), 2003, 'Guidelines for managing wake wash from high-speed vessels', Report of Working Group 41, Maritime Navigation Commission, Brussels.

Phillips, S. and Hook, D., 2006, 'Wash from ships as they approach the coast', *Proc. RINA Intl. Conf. on Coastal Ships and Inland Waterways*, London, UK.

Pickrill, R.A., 1978, 'Effects of boat wakes on the shoreline of Lake Manapouri', *New Zealand Engineering*, vol. 33, pp. 194-198.

Pinkster, J.A., 2009, 'Suction, seiche and wash effects of passing ships', *Proc. Annual SNAME meeting*.

Pinkster and Naaijen, 2003, 'Predicting the effect of passing ships', *Proc. 18th International Workshop on Water Waves and Floating Bodies*, Le Croisic, France.

Queensland Environmental Protection Agency, 2002, 'Noosa riverbank erosion investigation stage 1: analysis of bank erosion' internal report.

Rapaglia, J., Zaggia, L., Ricklefs, K., Gelinas, M. and Bokuniewicz, H., 2011. 'Characteristics of ships' depression waves and associated sediment resuspension in Venice Lagoon, Italy', *Journal of Marine Systems*, vol. 85, pp. 45−56.

Raven, H.C., 2000, 'Numerical wash prediction using a free-surface panel code', *Proc. RINA Intl. Conf. on the Hydrodynamics of High Speed Craft: Wake Wash and Motions Control*, London, UK.

Remoissenet, M., 1999, '*Waves called solitons*', 3rd edition, Springer.

Renilson, M. R. and Lenz, S., 1989, 'An investigation into the effect of hull form on the wake wave generated by low speed vessels', *Proc. 22nd American Towing Tank Conference*, pp. 424 – 429.

Robbins, A.W., 2004, A tool for the prediction of wave wake for high speed catamarans in deep water, Master of Philosophy Thesis, Australian Maritime College, Australia.

Robbins, A. and Renilson, M.R., 2006, 'A tool for the prediction of wave wake', RINA Transactions, *International Journal of Maritime Engineering*, part A1.

Robbins, A., Thomas, G., Macfarlane, G.J., Renilson, M.R. and Dand, I., 2007, 'The decay of catamaran wave wake in shallow water, *Proc. 9th Intl. Conf. on Fast Sea Transportation (FAST 2007)*, Shanghai, China.

Robbins, A., Thomas, G., Renilson, M.R., Macfarlane, G.J. and Dand, I., 2009, 'Vessel trans-critical wave wake, divergent wave angle and decay', RINA Transactions. *International Journal of Maritime Engineering*. vol. 151, part A2.

Robbins, A., Thomas, G.A., Renilson, M.R., Macfarlane, G.J. and Dand, I., 2011, 'Subcritical wave wake unsteadiness', RINA Transactions, *International Journal of Maritime Engineering*, vol. 153, part A3.

Sakamoto, N., Stern, F. and Wilson, R.V., 2007, 'Reynolds-averaged Navier-Stokes simulations for high speed Wigley hull in deep and shallow water, *Journal of Ship Research*, vol. 51, no. 3, September, pp. 187-203.

Sarle, W.S., 1994, 'Neural networks and statistical models', *Proc. 19th Annual SAS Users Group Intl. Conf.*, Dallas, USA.

Savitsky, D., 1985, 'Planing craft', *Naval Engineers Journal*, Chapter 4, pp 113-141.

Schmied, S.A., Binns, J.R., Renilson, M.R., Thomas, G., Macfarlane, G.J. and Huijsmans, R., 2011, 'A novel method for generating continuously surfable waves – comparison of predictions with experimental results', *Proc. Offshore Mechanics and Arctic Engineering Conference (OMAE 2011)*, Rotterdam, Netherlands.

Scholer, H.A., 1974, 'Hawkesbury River; the effects of speedboat activities on river banks, Appendix 3, Hawkesbury River report on effects of water skiing', Public Works Department of New South Wales, Sydney, Australia.

Scott, J.R., 1970, 'On blockage correction and extrapolation to smooth ship resistance', *SNAME Transactions*, vol. 78, pp. 288-326.

Sharp, B.B. and Fenton, J.D., 1968, 'Report of investigation of a proposed dock at Yarraville', *University of Melbourne*.

Smith, D., 1990, 'Environmental impact statement for the extension of ferry services on the Parramatta River, west of Silverwater Bridge', New South Wales Department of Transport, Australia.

Soding, H., 2006, 'Far field ship waves', *Ship Technology Research*, vol. 53, no. 3.

Solomon, M., 1997, 'Waterskiing getting off the ground', Boston, Aquatics Unlimited.

Soomere, T., 2005, 'Fast ferry traffic as a qualitatively new forcing factor of environmental processes in non-tidal sea areas: a case study in Tallinn Bay, Baltic Sea', *Environmental Fluid Mechanics*, vol. 5.

Soomere, T., 2006, 'Nonlinear ship wake waves as a model of rogue waves and a source of danger to the coastal environment: a review', *Oceanologia*, vol. 48.

Soomere, T., 2007, 'Nonlinear components of ship wake waves', *ASME Transactions*, vol. 60.

Soomere, T. and Engelbrecht, J., 2006, 'Weakly two-dimensional interaction of solitons in shallow water', *European Journal of Mechanics*, part B/Fluids, vol. 25.

Soomere, T. Parnell, K.E. and Didenkulova, I., 2009, 'Implications of fast-ferry wakes for semi-sheltered beaches: a case study at Aegna Island, Baltic Sea', *Journal of Coastal Research*, Special Issue 56.

Soomere, T., Poder, R., Rannat, K. and Kask, K., 2005, 'Profiles of waves from high-speed ferries in the coastal area', *Proc. Estonian Acad. Sci. Eng*., vol. 11.

Soomere, T. and Rannat, K. 2003, 'An experimental study of wind waves and ship wakes in Tallinn Bay', *Proc. Estonian Acad. Sci. Eng*., 2003, vol. 9, pp. 157-184.

Sorensen, R.M., 1967, 'Investigation of ship generated waves', *Journal of the Waterways and Harbours Division*, ASCE, vol. 93, no. WW1, pp. 85–99.

Sorensen, R.M., 1969, 'Waves generated by model ship hull', Journal of the Waterways, Harbours Division, ASCE, vol. 95, no. WW4, pp. 513–538.

Sorensen, R.M., 1973, 'Water waves produced by ships', *Journal of the Waterways Harbours and Coastal Engineering Division*, ASCE, vol. 99. no. WW2, pp.245-256.

StatSoft™, 1994, *STATISTICA™* for Windows (vol.1): general conventions and statistics I, Software manuals, StatSoft.

Stern, F., Campana, E.F., Bugalski, T., Huang, D.B., Kodama, Y., Kusaka, Y., Lee, S.H, Perez-Rojas, L. and Raven, H.C., 2002, 'Final Report of the Resistance Committee', *Proc. 23rd Intl. Towing Tank Conf.*, vol. 1, pp. 17-87.

Strom, K. and Ziegler, F., 1998. 'Environmental impacts of wake wash from high speed ferries in the Archipelago of Goteborg', Environmental Office, Goteborg (in Swedish).

Stumbo, S., Fox, K., Dvorak, F., and Elliot, L., 1999, 'The prediction, measurement and analysis of wake wash from marine vessels', *Marine Technology*, SNAME, Winter.

Swan River Trust, 2009, 'Boating management strategy for the Swan Canning Riverpark', Perth, Ausralia.

Taato, S.H., Aage, C. and Arnskov, M.M., 1998, 'Waves from propulsion systems of fast ferries', *Proc. 14th Fast Ferry Intl. Conf.*, Copenhagen, Denmark, 24-25 February 1998.

Tasmanian Parks and Wildlife Service, 1998, Lower Gordon River Recreation Zone Plan, Tasmanian DPIPWE, Hobart.

Ten Brinke, W.B.M., Schulze, F.H. and Van Der Veer, P., 2004, 'Sand exchange between groyne-field beaches and the navigation channel of the Dutch Rhine: the impact of navigation versus river flow', *River Research and Applications*, vol. 20, pp. 899-928.

Thomson, W. (Lord Kelvin), 1887, 'On ship waves', *Proc. of the Institute of Mechanical Engineers*, pp. 409 – 433.

Todd, A., 2004, 'Maroochy River erosion study: analysis of bank erosion', Report to the *Moreton Bay Waterways and Catchments Partnership*.

Tornblom, O., 2000, Calculation of bank effects and wash waves with SHIPFLOW™, Master of Science thesis, Department of Mechanical Engineering, Lulea University of Technology, Sweden.

Torsvik, T., 2006, Long wave models with application to high-speed vessels in shallow water, Doctor of Philosophy thesis, University of Bergen, Norway.

Torsvik, T., Dysthe, K. and Pedersen, G., 2006, 'Influence of variable Froude number on waves generated by ships in shallow water', *Physics of Fluids*, vol. 18.

Tuck, E.O., 1967, 'Sinkage and trim in shallow water of finite width', *Schiffstechinick*, vol. 14, pp.92-94.

Tuck, E.O., Scullen, D.C. and Lazauskas, L.V., 2000, 'Ship-wave patterns in the spirit of Michell', *Proc. Int'l Union of Theoretical and Applied Mechanics (IUTAM) Symposium on Free-Surface Flows*, Birmingham, UK.

Tuck, E.O., Scullen, D.C. and Lazauskas, L.V., 2002, 'Wave patterns and minimum wave resistance for high-speed vessels', *Proc. 24th Symposium on Naval Hydrodynamics*, Fukuoka, Japan.

University of Nottingham, 1996, 'A procedure for assessing river bank erosion', National Rivers Authority, R&D Report 28, University of Nottingham.

U.S. Army Coastal Engineering Research Center (USACERC), 1977, *Shore protection manual*, vol. I and II, U.S. Government Printing Office, Washington, DC.

U.S. Army Coastal Engineering Research Center (USACERC), 1984, *Shore protection manual*, vol. I and II, U.S. Government Printing Office, Washington, DC.

US Army Corps of Engineers, 2008, *Coastal engineering manual*, parts 1 to 5, accessed 8 December 2011. http://publications.usace.army.mil/publications/eng-manuals/

Varyani, K.S., 2006, 'Full scale study of the wash of high speed craft', *Ocean Engineering*, vol. 33.

Velegrakis, A.F., Vousdoukas, A.M, Vagenas, A.M, Karambas, T., Dimou, K. and Zarkadas, T., 2006, 'Field observations of waves generated by passing ships: a note', *Coastal Engineering*, vol. 54.

von Krusenstierna, A., 1990, River bank erosion by boat-generated waves on the lower Gordon River, Tasmania, Master of Science thesis, Department of Geography, University of Wollongong, Australia.

Wang, D., Atlar, M. and Mesbahi, E., 2002, 'Experimental investigation on propeller wash using laser Doppler anemometry', *Proc. 3rd Intl. Conf. on High Performance Vehicles (HIPER'02)*, Bergen, Norway, 14-17 September, pp. 422-436.

Watkins, M., 2004, 'The issue of erosion', *Boarder Magazine - Wakeboarding Culture*, vol. 5, issue 2.

Weggel, J.R., and Sorensen, R.M., 1986, 'Ship wave prediction for port and channel design', *Proc. Specialist Conf. on Innovations in Port Engineering and Development in the 1990's*, ASCE Coastal and Ocean Division, pp. 797-814.

Wehausen, J.V. and Laitone, E.V., 1960, 'Surface waves', *Encyclopedia of Physics: Fluid Dynamics* III, Ed. Flugge, S., Springer-Verlag, Berlin, vol. 9, pp 445-814.

Werenskiold, P. and Stansberg, C.T., 2001, 'Wake model tests – 31m catamaran', FLOWMART Work Package 2 – Task 2.1, Marintek, report no. 603527.

Whittaker, T.J.T., Bell, A.K., Shaw, M.R., and Patterson, K., 1999, 'An investigation of fast ferry wash in confined waters', *Proc. RINA Intl. Conf. on the Hydrodynamics of High Speed Craft*, London, UK.

Whittaker, T.J.T., Bell, A.K., Shaw, M.R., and Patterson, K., 2000a, 'An investigation of fast ferry wash in confined waters', *Proc. 16th Intl. Fast Ferry Conf.*, Acropolis, Nice, France.

Whittaker, T.J.T., Doyle, R. and Elsaesser, B., 2000b, 'A study of leading long period waves in fast ferry wash', *Proc. RINA Intl. Conf. on the Hydrodynamics of High Speed Craft: Wake Wash and Motions Control*, London, UK.

Wikipedia, 2010, 'Fast ferry scandal' accessed 8 December 2011. http://en.wikipedia.org/wiki/Fast_Ferry_Scandal

Worboys, G., Lockwood, M. and De Lacy, T. (eds.), 2005, *Protected area management: principles and practice*, Oxford University Press

Worley Parsons, 2010, 'Williams River: riverbank erosion study', Report prepared for the Port Stephens Council.

Yang, Q., Faltinsen, O.M. and Zhao, R., 2001, 'Wash of ships in finite water depth', *Proc. 6th Intl. Conf. on Fast Sea Transportation (FAST 2001)*, Southampton, UK.

Appendix A

Ship Model Body Plans

This appendix contains a simplified body plan of each hull included in the series of physical scale model experiments outlined in Table 5.1. For catamarans, the body plan for a single demihull is shown. Refer to Table 5.1 for further details of each hull, including centreline-to-centreline spacing of demihulls. Drawings are not to scale.

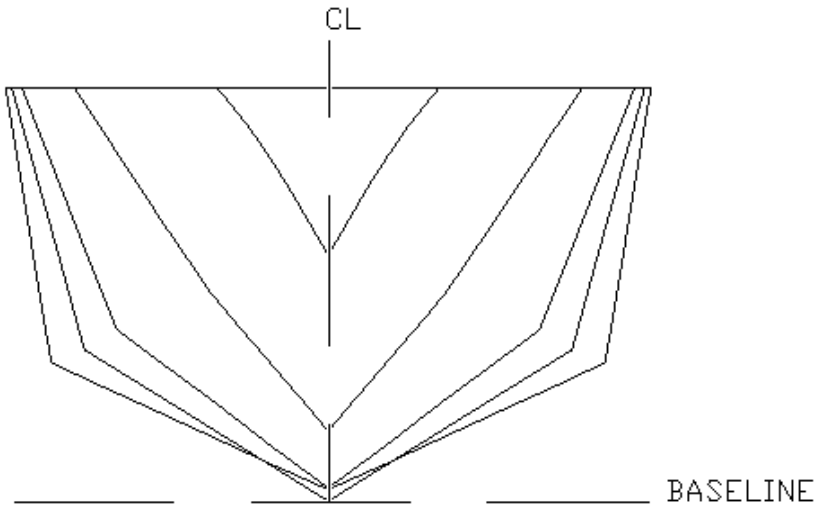

Figure A.1 Model AMC 00-01, Monohull, Hull #1, #3

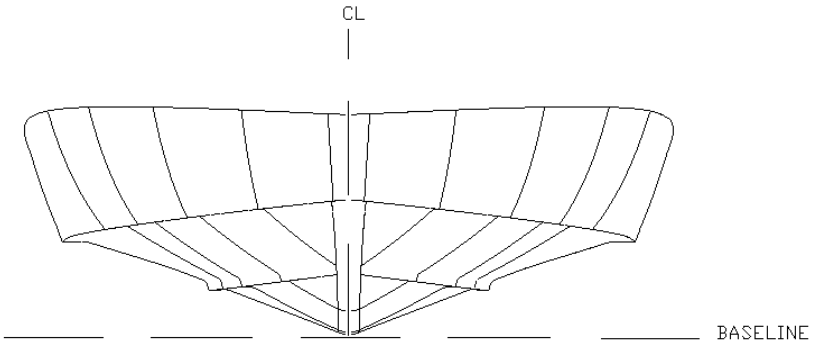

Figure A.2 Model AMC 10-37, Monohull, Hull #2, #4

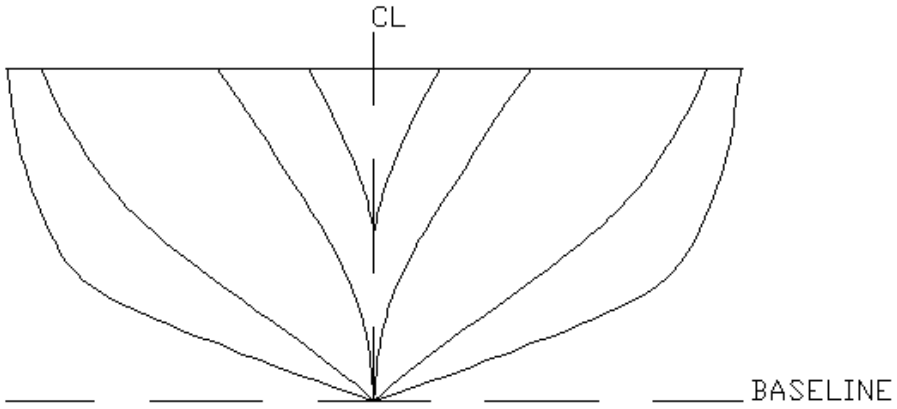

Figure A.3 Model AMC 97-02, Monohull, Hull #5, #6

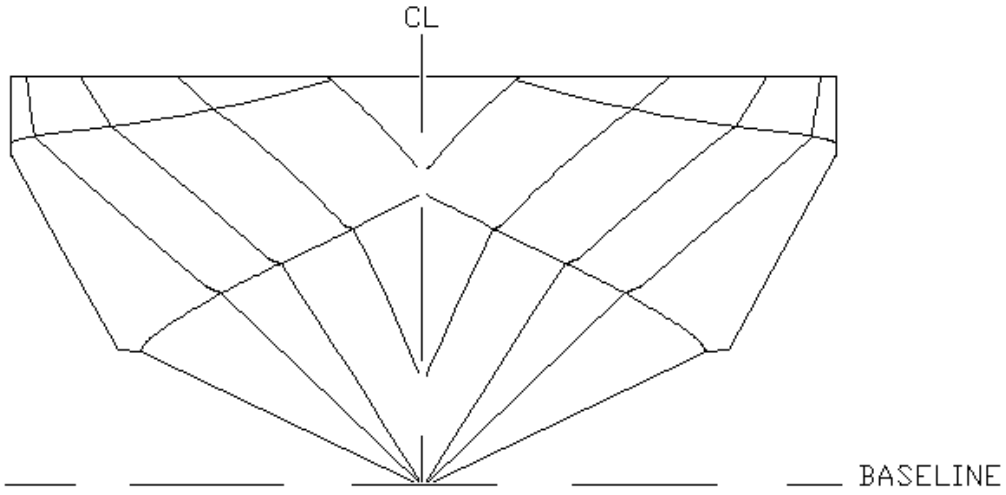

Figure A.4 Model AMC 97-10, Monohull, Hull #7

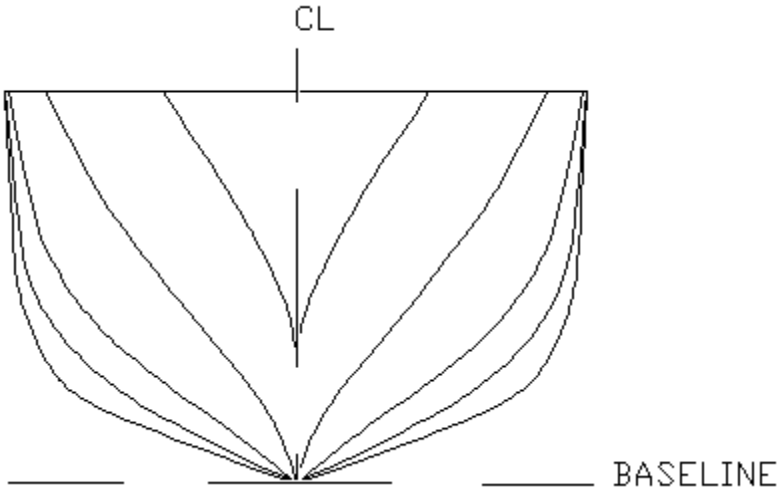

Figure A.5 Model AMC 96-08, Monohull, Hull #8, #9

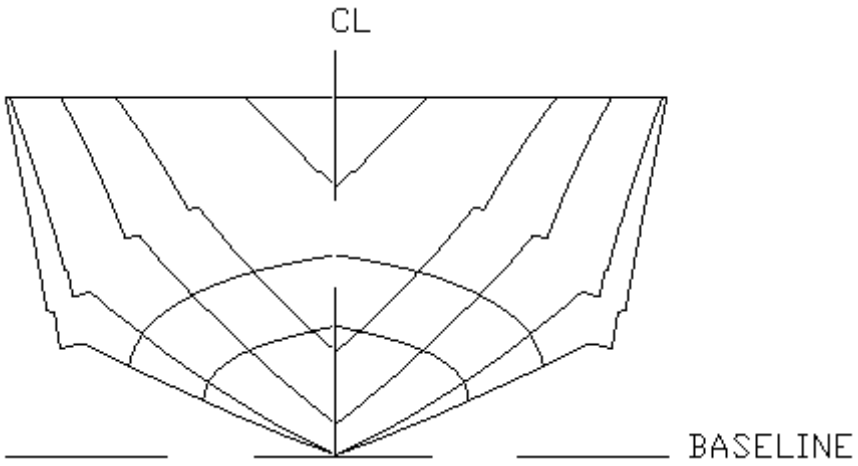

Figure A.6 Model AMC 97-30, Monohull, Hull #10

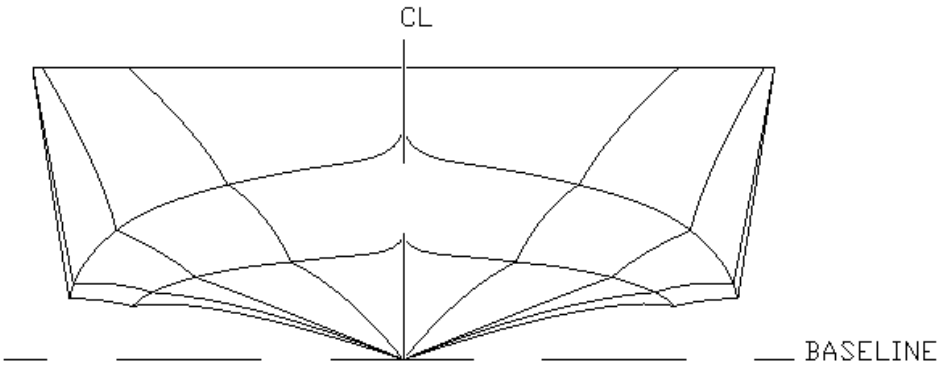

Figure A.7 Model 99-17, Monohull, Hull #11

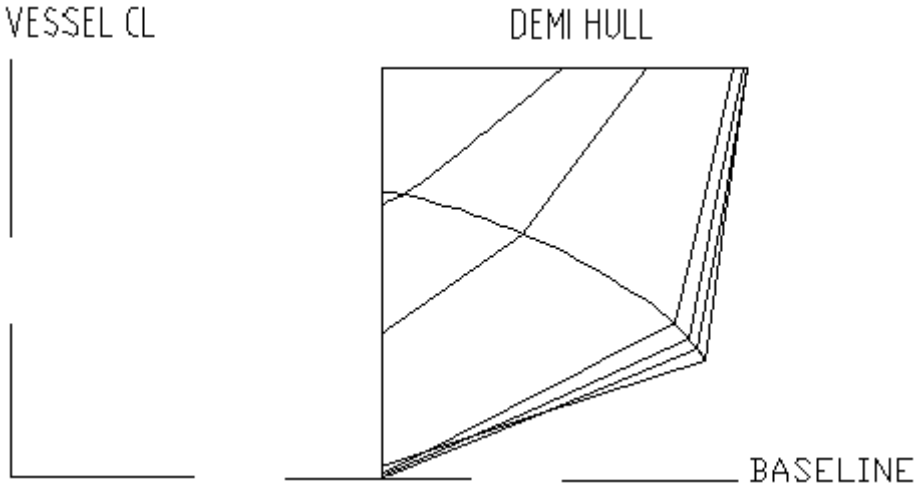

Figure A.8 Model 00-03, Catamaran, Hull #12

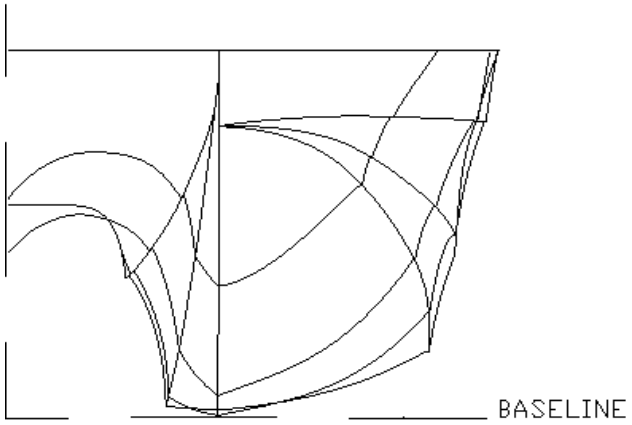

Figure A.9 Model 93-07, Catamaran, Hull #13

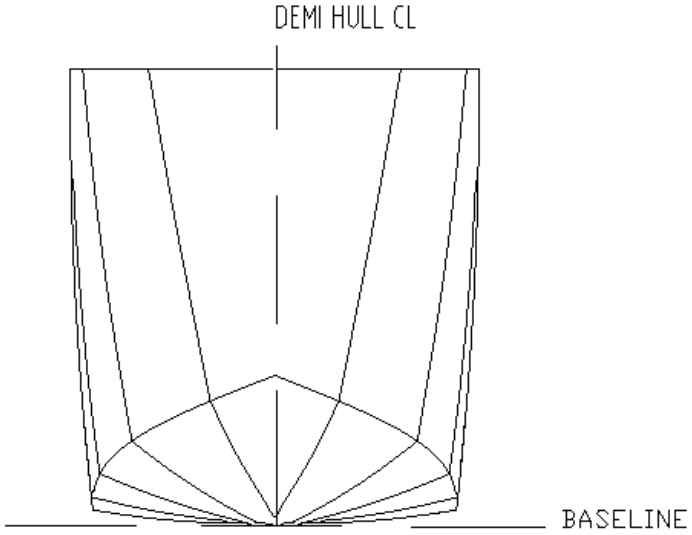

Figure A.10 Model AMC 99-01, Catamaran, Hull #14

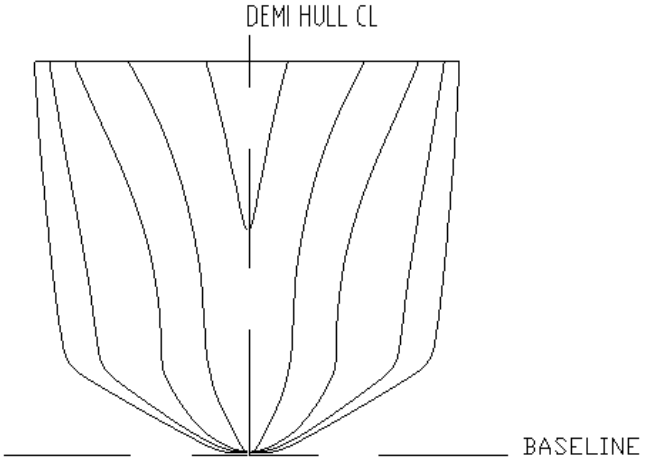

Figure A.11 Model AMC 99-27, Catamaran, Hull #15

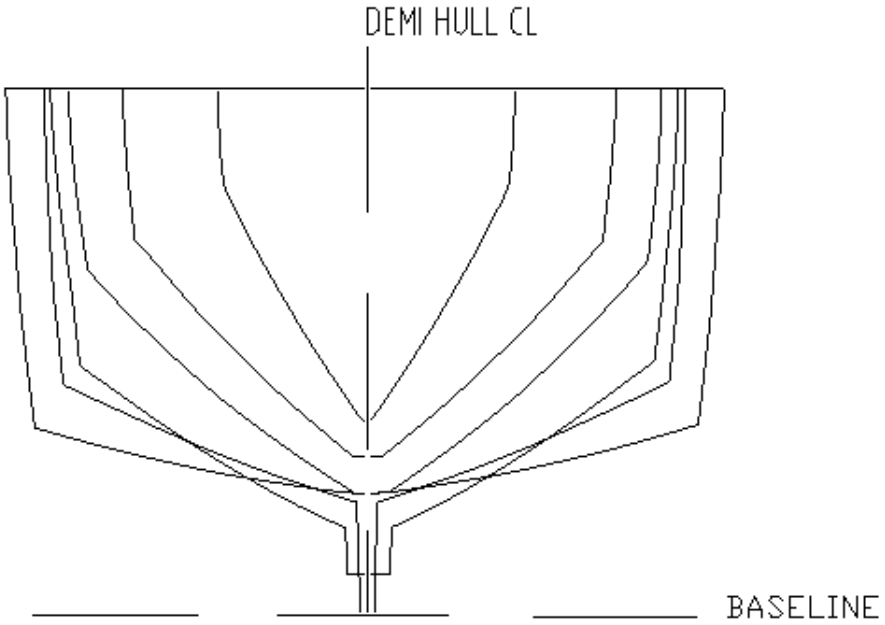

Figure A.12 Model AMC 93-03, Catamaran, Hull #16, #17

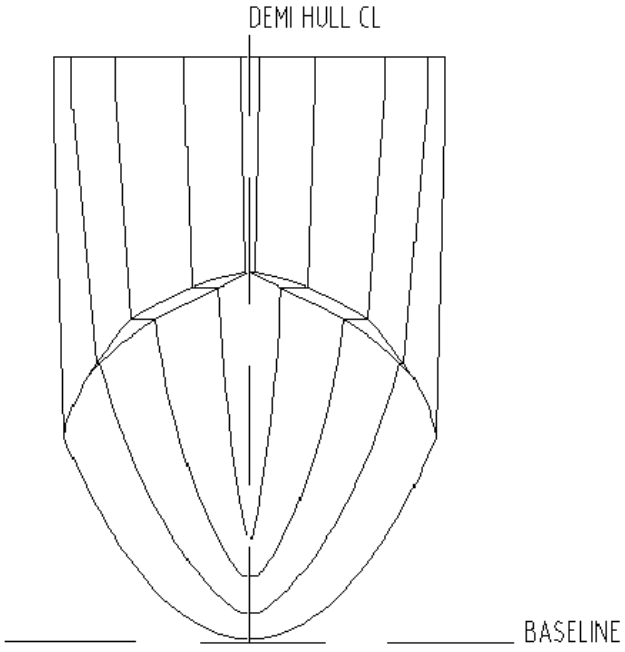

Figure A.13 Model AMC 98-16, Catamaran, Hull #18, #19

Appendix B

Typical Vessel Operations in Australian Sheltered Waterways

A study of typical vessel operations in several key Australian sheltered waterways was conducted, primarily to determine certain parameters from which to design the series of physical scale model experiments. This included knowledge about the principal dimensions of specific marine craft currently and previously in operation, and information about the waterways in which they operate(d), such as water depths. A summary of these details are provided in Table B.1. Note that the author has access to full scale wave wake trials data for about 90% of the vessels listed.

No.	Location	Nominal h (m)	Vessel Description	L_{OA} (m)	L (m)	Δ (kg)	$L/\nabla^{1/3}$	Vessel Speeds		Fr_L		Fr_h		h/L
								Min. (knots)	Max. (knots)	Min.	Max.	Min.	Max.	
1	Gordon River, TAS	13	29 m Cruise Vessel (catamaran) - Adventurer	29	25.36	69600	6.22	4	8	0.13	0.26	0.18	0.36	0.51
2	Gordon River, TAS	13	Yacht - Wraith of Hamble	16.2	14.6	18300	5.59	5	8	0.21	0.34	0.23	0.36	0.89
3	Gordon River, TAS	13	Round bilge displacement hull - Heritage Wanderer	20	18.3	38000	5.49	5	8	0.19	0.31	0.23	0.36	0.71
4	Gordon River, TAS	13	Light catamaran hull form - Mach II	8.4	7.6	2200	5.89	5	8	0.30	0.48	0.23	0.36	1.71
5	Gordon River, TAS	13	Light catamaran hull form - Pilara II	8.4	7.5	2200	5.81	5	8	0.30	0.48	0.23	0.36	1.73
6	Gordon River, TAS	13	Hard-chine semi-displacement monohull - James Kelly II	27.5	23.5	48000	6.52	5	8	0.17	0.27	0.23	0.36	0.55
7	Gordon River, TAS	13	Hard-chine semi-displacement monohull - Wilderness Seeker	19.95	18.2	26000	6.19	5	8	0.19	0.31	0.23	0.36	0.71
8	Gordon River, TAS	13	Hard-chine semi-displacement monohull - Gordon Explorer	32.3	27.75	55000	7.36	5	8	0.16	0.25	0.23	0.36	0.47
9	Gordon River, TAS	13	Steel ketch - Stormbreaker	20	16.8	44000	4.80	3	7	0.12	0.28	0.14	0.32	0.77
10	Gordon River, TAS	13	Seaplane - Wilderness Air	10	5.94	1500	5.23	3	45	0.20	3.03	0.14	2.05	2.19
11	Gordon River, TAS	13	DevilCat catamaran hull (Tas PWS Shearwater)	8.1	7	2700	5.07	3	34	0.19	2.11	0.14	1.55	1.86
12	Gordon River, TAS	13	Cougar Catamaran (Federal Hotels charter vessel) - Sophia	10.5	9.13	5640	5.17	4	10	0.22	0.54	0.18	0.46	1.42
13	Gordon River, TAS	13	Catamaran charter vessel - Second Nature	11.6	10.3	8100	5.17	4	10	0.20	0.51	0.18	0.46	1.26
14	Gordon River, TAS	13	Catamaran cruise vessel - Soracha	17.5	15.74	30000	5.11	4	22	0.17	0.91	0.18	1.00	0.83
15	Macquarie Harbour, TAS	12	24 m Catamaran Cruise Vessel - Wanderer II	24	21.71	55000	5.76	6	28	0.21	0.99	0.28	1.33	0.55
16	Tamar River, TAS	3.3	Cougar Catamaran - Tamar Odyssey	14.9	13.8	18500	5.26	4	22	0.18	0.97	0.36	1.99	0.24
17	Noosa River, QLD	6	Luxury Afloat Houseboat - Amberjack	13.1	11.5	15500	4.65	4	5	0.19	0.24	0.27	0.34	0.52
18	Noosa River, QLD	6	12' Aluminium Dinghy	3.65	3.35	285	5.13	4	11	0.36	0.99	0.27	0.74	1.79
19	Noosa River, QLD	6	Everglades Water Bus Co.	9.3	8.2	3900	5.25	7	27	0.40	1.55	0.47	1.81	0.73
20	Noosa River, QLD	6	Aluminium tinnie (EPA vessel)	5.7	4.9	1100	4.79	5	28	0.37	2.08	0.34	1.88	1.22
21	Brisbane River, QLD	6	Pacific 7.75 m Centre Console	7.75	6.75	2480	5.03	6	33	0.38	2.09	0.40	2.21	0.89
22	Brisbane River, QLD	6	Ski Boat (6.36 m L_{OA} - Inboard)	6.36	5.3	1445	4.73	7	36	0.50	2.57	0.47	2.41	1.13
23	Brisbane River, QLD	6	Ski Boat (5.5 m L_{OA} - Outboard)	5.5	4.6	1027	4.60	7	35	0.54	2.68	0.47	2.35	1.30
24	Brisbane River, QLD	5.4	Jet Ski - Waverunner XL 800	3.16	2.7	457	3.53	5	42	0.50	4.20	0.35	2.97	2.00
25	Brisbane River, QLD	6	Clark 16' Survey Vessel	4.8	4.45	510	5.62	7	22	0.54	1.71	0.47	1.48	1.35
26	Brisbane River, QLD	10	CityCat catamaran passenger ferry	25	24	24000	8.39	5	25	0.17	0.84	0.26	1.30	0.42
27	Maroochy River, QLD	4.1	Ski Boat "Protege" (6.3 m L_{OA} - Inboard) Light Load	6.3	5.5	1340	5.03	10	25	0.70	1.75	0.81	2.03	0.75
28	Maroochy River, QLD	4.1	Ski Boat "Protege" (6.3 m L_{OA} - Inboard) Heavy Load	6.3	5.5	1550	4.79	10	23	0.70	1.61	0.81	1.87	0.75
29	Swan River, WA	2.5	Bayliner 375	8.4	7.8	2700	5.65	5	12	0.29	0.71	0.52	1.25	0.32
30	Swan River, WA	2.5	Haines Hunter Patriot 680	6.8	6	2100	4.72	6	15	0.40	1.01	0.62	1.56	0.42
31	Swan River, WA	2.5	Quintrex Freedom Sport 470	4.7	4.3	740	4.79	5	13	0.40	1.03	0.52	1.35	0.58
32	Swan River, WA	2.5	Quintrex Freedom Sport 570	5.7	5.2	1000	5.24	5	25	0.36	1.80	0.52	2.60	0.48
33	Swan River, WA	2.5	Captain Cook River Lady	24.9	24	60000	6.18	6	8	0.20	0.27	0.62	0.83	0.10
34	Swan River, WA	4	Haines Hunter Patriot 680	6.8	6	2100	4.72	6	20	0.40	1.34	0.49	1.64	0.67
35	Swan River, WA	4	Star Flyte Express	38.9	34	85300	7.79	9	24	0.25	0.68	0.74	1.97	0.12
36	Swan River, WA	4	LeisureCat Mako 9000	9	7.9	3000	5.52	6	20	0.35	1.17	0.49	1.64	0.51
37	Swan River, WA	2	Monohull workboat (Swan River Trust) - Noel Robins	8.5	7.6	3500	5.05	5	15	0.30	0.89	0.58	1.74	0.26
38	Sydney Harbour, NSW	12	HarbourCat 28 m Catamaran Passenger Ferries	27.1	26.7	35460	8.19	6	26	0.19	0.83	0.28	1.23	0.45
39	Sydney Harbour, NSW	13.5	First Fleet Catamaran Ferries	24.85	24	83000	5.55	4	13	0.13	0.44	0.18	0.58	0.56
40	Sydney Harbour, NSW	13.5	JetCat Catamaran Ferries	34.8	32	70000	7.83	9	31	0.26	0.90	0.40	1.39	0.42
41	Sydney Harbour, NSW	13.5	Rodriquez RHS-140 Hydrofoil	28.7	25	129000	4.99	6	37	0.20	1.22	0.27	1.65	0.54
42	Sydney Harbour, NSW	20	Lady Class Manly Ferries	44	41	370000	5.76	5	13	0.13	0.33	0.18	0.48	0.49
43	Sydney Harbour, NSW	20	Freshwater Class Manly Ferries	70.4	62	1140000	5.98	5	16	0.10	0.33	0.18	0.59	0.32
44	Sydney Harbour, NSW	3.5	RiverCat 35 m Catamaran Passenger Ferries	36.8	35	46500	9.81	5	10	0.14	0.28	0.44	0.88	0.10
45	Hawksbury River, NSW	3.5	Ski Boat (small, outboard)	4	3.7	250	5.92	4	26	0.34	2.22	0.35	2.28	0.95
46	Hawksbury River, NSW	3.5	Ski Boat (inboard)	4.6	4	600	4.78	5	26	0.41	2.14	0.44	2.28	0.88

Table B.1 List of typical vessel operations in Australian sheltered waterways

Appendix C

Use of Spectral Analysis

Several comparisons were undertaken between the resultant wave spectra from an FFT analysis and the primary output from the analysis process used in this thesis. Three examples from a single ship model are presented in Figures C.1, C.2 and C.3 for the speeds of Fr_h = 0.60, 0.95 and 1.29 respectively. In each of these figures the wave spectra are plotted as functions of wave frequency, f, as are the wave height constants for each of the three key waves (γ_A, γ_B and γ_C).

For the sub-critical speed of Fr_h = 0.60 (Figure C.1), it is clear that the vast bulk of the wave energy is concentrated within a single packet, with wave frequencies in the approximate range of 0.75 to 1.75 Hz. As can be seen, the three key waves all occur within this frequency range, with the longest wave, Wave A, occurring at a frequency that coincides very closely with the first (and only) major peak in the spectra (~1.0 Hz).

For the example at Fr_h = 0.95 (close to critical speed) in Figure C.2, there is clearly some wave energy at low frequency, around 0.3 to 0.6 Hz, which represents the energy of the leading wave (Wave A). As expected, this occurs at a significantly lower frequency than was found for the sub-critical case (Figure C.1). The frequency of Wave B occurs close to the two significant peaks in the spectra approximately centred around 0.75 Hz. There has been little change in frequency for Wave C between Fr_h of 0.60 and 0.95.

It is a similar case at the super-critical speed of Fr_h = 1.29, Figure C.3, in that there are three distinct packets of waves (i.e. a leading wave of long period, followed by two other packets possessing higher, but shorter period waves), although in this case each packet has become more pronounced.

A similar comparison was undertaken for several other ship models, at different ratios of h/L, with very comparable results. It is believed that these results support the use of the analysis technique adopted, as it highlights that up to three key waves are often generated, especially at super-critical speeds. It has also shown that each key wave is representative of each of these packets of waves identified using spectral analysis.

There were a couple of additional reasons for not pursuing the spectral option more thoroughly, including:

- Most of the key stakeholders are not familiar with this form of analysis and have difficulty visualising these concepts and measures. From experience, the use of measures that can be relatively easily visualised is critical because if they are complicated (or costly to collect and assess) regulatory authorities can be reluctant to pursue a path of boating management through scientific understanding.
- The adopted method is consistent with earlier work by the author and many others who have published in this field.

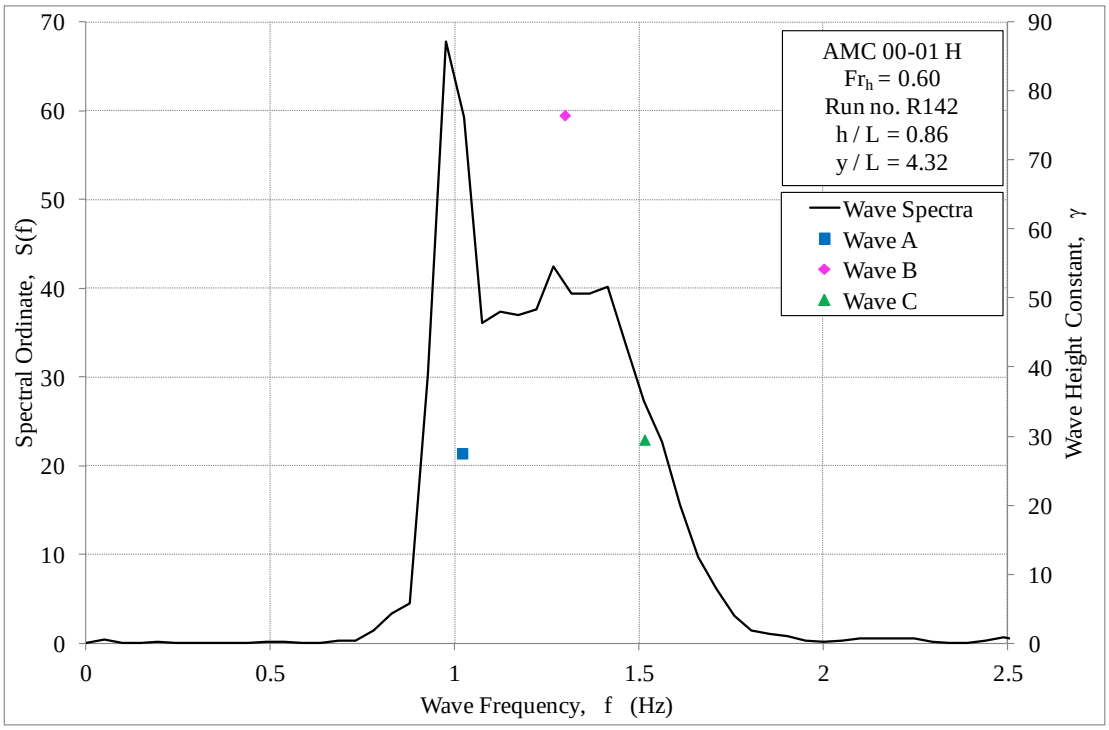

Figure C.1 Comparison with FFT analysis: $Fr_h = 0.60$

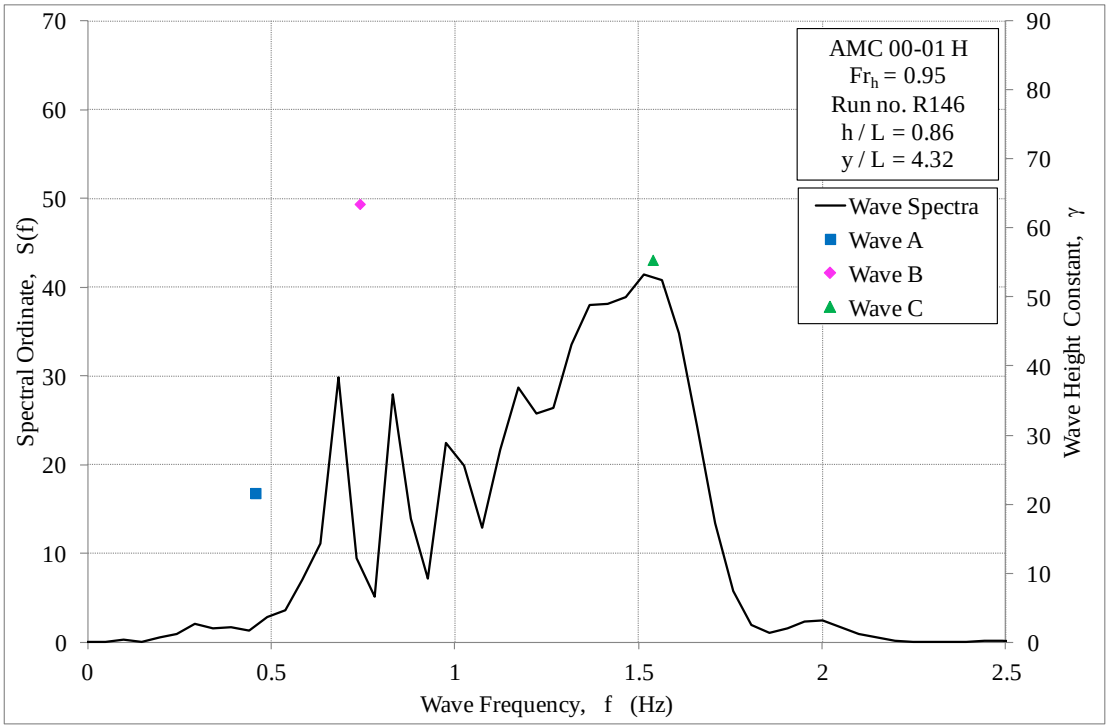

Figure C.2 Comparison with FFT analysis: $Fr_h = 0.95$

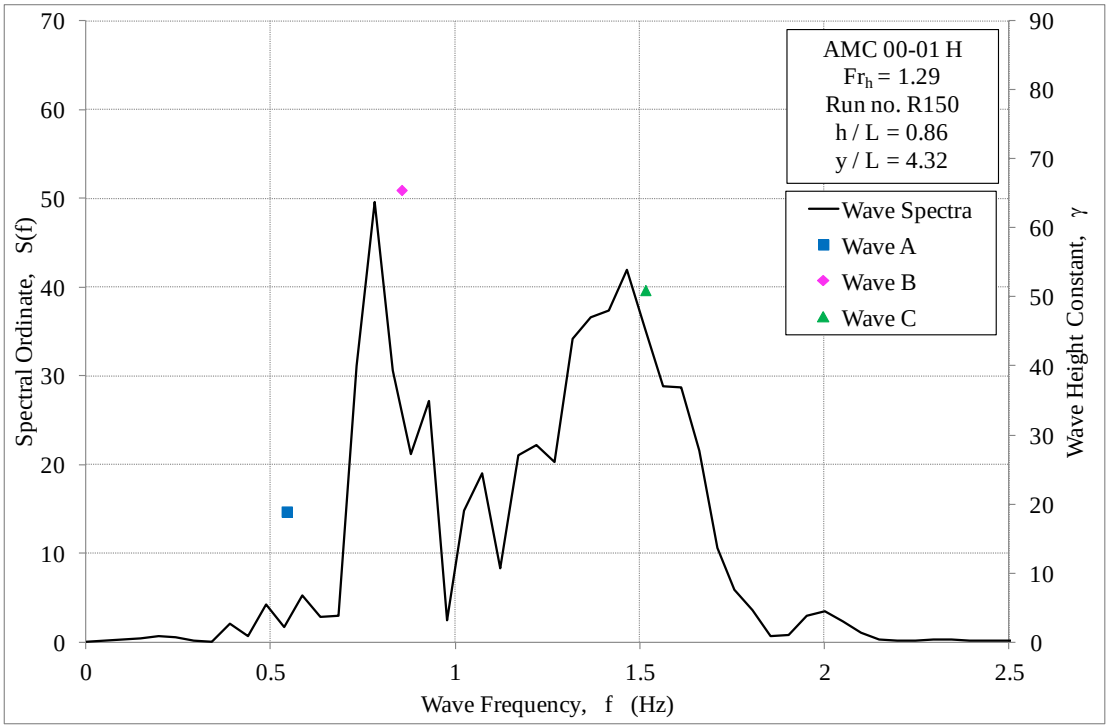

Figure C.3 Comparison with FFT analysis: $Fr_h = 1.29$

Appendix D

Uncertainty Analysis

The uncertainty analysis methodology and procedures are based on the 95% confidence, large-sample approach for assessing random uncertainty, as recommended by the AIAA (1999) and ASME (1998).

Surface wave elevations were measured using resistance type wave probes (refer Section 5.3.2), from which wave heights were determined (refer Section 3.3). The data reduction equation for wave height has been taken as:

$$H = f\left(\frac{C_{wp}V_{wp}}{Fr_h^2 L}\right) \tag{D.1}$$

Where:
C_{wp} = wave probe calibration factor.
V_{wp} = wave probe voltage.

For estimation purposes it was assumed that the uncertainty on the wave elevation measurements arose from four sources: wave probe calibration factor; voltage measurement; speed measurement and water depth measurement. Appropriate uncertainty estimates for each of these sources were used to find the uncertainty in each wave elevation measurement.

Uncertainty sources that were smaller than 1/4th or 1/5th of the largest sources were considered negligible (Longo and Stern 2005). Therefore the uncertainty due to acceleration due to gravity and the accuracy of model geometry were considered negligible.

The standard uncertainty in a typical wave elevation measurement is calculated using Equation D.2 (Barlow *et al*. 1999).

$$\sigma^2 H = \left(\frac{\partial_H}{\partial C_{wp}}\sigma_{C_{wp}}\right)^2 + \left(\frac{\partial_H}{\partial V_{wp}}\sigma_{V_{wp}}\right)^2 + \left(\frac{\partial_H}{\partial u}\sigma_u\right)^2 + \left(\frac{\partial_H}{\partial h}\sigma_h\right)^2 \tag{D.2}$$

Where:

$$\frac{\partial_H}{\partial C_{wp}} = \frac{ghV_{wp}H}{u^2 L} \tag{D.3}$$

$$\frac{\partial_H}{\partial V_{wp}} = \frac{ghC_{wp}H}{u^2L} \quad (D.4)$$

$$\frac{\partial_H}{\partial u} = \frac{ghC_{wp}V_{wp}H}{u^3L} \quad (D.5)$$

$$\frac{\partial_H}{\partial h} = \frac{gC_{wp}V_{wp}H}{u^2L} \quad (D.6)$$

Typical uncertainties for each variable for experiments conducted within the semi-controlled environment of the AMC model test basin are:
σ_{Cwp} = 0.5% of the calibration factor.
σ_{Vwp} = 4.5 mV, based on accuracy of the A/D board where typical range of measurement was +/- 3.0 V.
σ_u = 0.01 m/s.
σ_h = 0.010 m.

Typical uncertainties for each variable for full scale experiments conducted in the field are:
σ_{Cwp} = 1.0% of the calibration factor.
σ_{Vwp} = 5.5 mV, based on accuracy of the A/D board where typical range of measurement was +/- 3.5 V.
σ_u = 0.025 m/s.
σ_h = 0.10 m.

A similar process was undertaken to determine the uncertainty for the measurement of wave period, although in this case the voltage and calibration factor of the wave probe were irrelevant as period is purely related to the time-step between data samples, which is a function of the analogue-to-digital converter card and computer.